Regulation of iron acquisition by an iron starvation sigma factor system in *Burkholderia cenocepacia*

By:

Saeedah H Aljadani

A thesis submitted in partial fulfilment of the requirements for the degree of Doctor of Philosophy

Supervisor:

Dr. Mark S. Thomas

The University of Sheffield

Faculty of Medicine, Dentistry and Health

Department of Infection, Immunity & Cardiovascular Disease

7th May 2018

Acknowledgements

First and foremost, I would like to thank my supervisor Dr Mark Thomas who has supported me during my project with his guidance, support and knowledge. I really appreciate Dr Thomas's efforts in increasing my scientific knowledge and making me very passionate about my project.

I would also like to thank all my colleagues in LU103 lab in the past and present who have supported me and encouraged me to gain lab experience.

I am grateful for God who gave me very supportive family and friends. Also, I would like to express my sincere appreciations to my husband Mr Waeel Aldour for his love and support he has given me throughout my PhD. This work is dedicated to my parents for their endless support.

Abstract

Burkholderia cenocepacia is a human opportunistic pathogen which causes severe respiratory infections in immunocompromised individuals who have been diagnosed with cystic fibrosis. In low iron conditions, *Burkholderia cenocepacia* can colonize inside the lungs of CF patients. This bacterium possesses several iron uptake systems in order to survive during iron starvation conditions. In iron-limited conditions this bacterium can biosynthesize two small iron-chelating siderophores and it can also utilize other exogenous siderophores for iron uptake. One of the systems for uptake of exogenous siderophores, the Flr system, provides a convenient model system for the study of signal transduction in Gram-negative bacteria by TonB-dependent transducers (TBDTs). TBDTs are composed of a three-component trans-envelope signal transduction pathway (the siderophore receptor located in the outer-membrane, an anti-sigma factor inserted in the cytoplasmic membrane, and a sigma factor of the iron starvation subclass). Binding of an iron-siderophore complex to the FlrA receptor is predicted to induce the anti-sigma factor FlrR to either release or activate the cytoplasmically located sigma factor FlrS.

By using a bacterial two-hybrid system and pull-down assay, we present evidence that the N-terminal domain of FlrR interacts with the C-terminal domain of FlrS, and the C-terminal domain of FlrR interacts with the N-terminal domain of FlrA. Data from this study confirms the presence of an FlrS-dependent promoter located in the intergenic region between *flrR* and *flrA*. Measurement of the activity of this promoter (P_{flrA}) indicates that FlrS is activated by FlrR through its N-terminal cytoplasmic domain. This result suggests that FlrR has critical dual role in the Flr system. With reference to P_{flrA}, we determined the sequences of the -10 and -35 regions in the P_{flrA} promoter that are recognized by FlrS sigma factor. We have also identified a promoter region upstream of FlrS known as P_{flrS}. This promoter is iron-regulated and it can be repressed by the Fur protein in the presence of iron. Finally, a siderophore-deficient *Burkholderia cenocepacia* strain was used in an attempt to identify the role of FlrA in utilising xenosiderophores. Xenosiderophores tested in this study can be utilised by this strain. However, no evidence was obtained to confirm that FlrA is TonB-dependent receptor that is involved in the uptake of xenosiderophores used in this study.

Table of Contents

List of Tables

List of Figures

List of abbreviations

°C	Centigrade
µg	Microgram
µl	Micro litre
µ	Micro (10^{-6})
ABC	ATP binding cassette
ATP	Adenosine triphosphate
BACTH	Bacterial adenylate cyclase two-hybrid
B. cenocepacia	*Burkholderia cenocepacia*
Bcc	Burkholderia cepacia complex
BHI	Brain heart infusion
BLAST	Protein Basic Alignment Search Tool
bp	Base pair
cAMP	Cyclic adenosine 3', 5'-monophosphate
CRP	cAMP receptor protein
CTD	C-terminal domain
CF	Cystic fibrosis
CAA	Casamino acids
$CaCl_2$	Calcium chloride
Da	Daltons
Δ	Deletion
ddH_2O	HPLC grade sterile water
DMSO	Dimethyl sulfoxide
DNA	Deoxyribonucleic acid
DNAse	Deoxyribonuclease
dNTP	Deoxyribonucleoside triphosphate
E. coli	*Escherichia coli*
EDDHA	Ethylenediamine-N,N'-bis(2-hydroxyphenylacetic acid)
EDTA	Ethylenediaminetetraacetic acid
Fur	Ferric Uptake Regulator
Fe^{+3}	Ferric iron

Fe^{+2}	Ferrous iron
HDTMA	Hexadecyltrimethylammonium bromide
HRP	Horseradish peroxidase
g	Grams
× *g*	Gravitational accelaration
HCl	Hydrochloric acid
H_2O	Water
IgA	Immunoglobulin A
IgG	Immunoglobulin G
IgM	Immunoglobulin M
IPTG	Isopropyl β-D-1-thiogalactopyranoside
IMAC	Immobilised metal ion affinity chromatography
IST	Iso-sensitest
IS	Iron starvation
Kb	Kilobase
kDa	Kilodalton
KCl	Potassium chloride
LB	Lysogeny broth
LPS	Lipopolysaccharide
MBP	Maltose binding protein
MCS	Multiple cloning sites
M	Molar
m	Milli (10^{-3})
ml-1	Per milli litre
mol	Moles
M9	Minimal salts
Mu	Miller units
MW	Molecular weight
mRNA	Messenger RNA
$MgSO_4$	Magnesium sulphate
NaOH	Sodium chloride
NMWL	Nominal molecular weight limit
NCR	Non-conserved residues

NRPS	Non-ribosomal peptide synthetase
NTD	N-terminal domain
ONPG	O-nitrophenyl-β-D-galactoside
Oligo	Oligodeoxyribonucleotide
OD	Optical density
OD_{600}	Optical density at 600 nm
OM	Outer membrane
ORF	Open reading frame
P. aeruginosa	*Pseudomonas aeruginosa*
PCR	Polymerase chain reaction
PAGE	Polyacrylamide gel electrophoresis
PVDF	Polyvinylidene fluoride
psi	Pounds per square inch
P	Promoter
RNA	Ribonucleic acid
RNAP	RNA polymerase
RNAse	Ribonuclease
R.p.m	Revolutions per minute
σ	Sigma
CSS	Cell-surface signaling
SDS	Sodium dodecyl sulphate
TAE	Tris/acetate/EDTA
TBDR	TonB-dependent receptor
TBDT	TonB-dependent transducer
TGED	TGED, Tris/glycerol/EDTA/DTT buffer
TE	Tris HCl/EDTA
TEMED	N, N, N', N'-tetramethylethylenediamine
Tm	Melting temperature
TMD	Transmembrane domains
Tris	Tri (hydroxymethyl) methylamine
TSS	Transcriptional start site
V	Volts
VSVg	G glycoprotein of the vesicular stomatitis virus

UV	Ultra Violet
v/v	Volume/volume
w/v	Weight/volume
X-Gal	5-bromo-4-chloro-3-indolyl-β-d-galactopyranoside

Chapter 1 Introduction

1.1 The *Burkholderia cepacia* complex

Burkholderia cenocepacia is a rod-shaped Gram-negative bacterium belonging to the β-subgroup of proteobacteria (Vandamme *et al.*, 2003; Mahenthiralingam *et al.*, 2005; Valvano *et al.*, 2005). This bacterium is a member of a group of closely related species or 'genomovars' known as the *Burkholderia cepacia* complex (Bcc) (Burkholder, 1950). *B. cepacia* was the first isolate identified from the Bcc and was described as a plant pathogen that causes onion rot (Vandamme *et al*., 1997). Originally, it was named *Pseudomonas cepacia* because of its phenotypic relationship to *Pseudomonads*, in common with several other *Burkholderia* species that were also classified in the *Pseudomonas* genus. In 1973, the species within this genus were divided into five distinct groups depending on their 16S ribosomal RNA homology (Palleroni *et al.*, 1973). In 1992, the species within one of these 16S rRNA homology groups were assigned to a new *Burkholderia* genus in the β subdivision of the proteobacteria, based on their 16S rRNA sequences, cellular lipid and fatty acid composition, DNA-DNA homology values and phenotypic characteristics (Yabuuchi *et al*., 1992). In 1997, it became clear that one of these species, *B. cepacia*, was composed of five distinct genomovars (I-V) and these were assigned as the species: *B. cepacia*, *B. multivorans, B. cenocepacia*, *B. stabilis* and *B. vietnamiensis* (Table 1.1) (Vandamme *et al*., 1997; Coenye *et al*., 2001). Recently, it has been found that Bcc consists of 18 distinct, but closely related (approximately 99% identical 16S rRNA), bacterial species (Coenye *et al*., 2001; Vandamme and Dawyndt, 2011; Peeters *et al*., 2013). The isolates of Bcc species can be distinguished from other Bcc species by using a polyphasic method. This requires several tests such as rRNA typing DNA sequence analysis using amplified fragment length polymorphism (AFLP) (Vandamme *et al*., 2003).

Bcc species are mainly found in the soil specifically in the rhizosphere of some plants. The first plant infection recognised to be caused by Bcc species was observed in onions wounded during harvesting (Burkholder, 1950). The bacteria can enter the scale of onions through the soil or irrigation water causing an infection known as sour skin. The infection changes the onion tissue turning it yellow and brown and causing softness in the rot (Burkholder, 1950). Not all Bcc species cause infections, however, and indeed some species are highly beneficial since they can protect plants from

infection caused by certain fungi and from diseases such as damping-off disease, caused by *Pythium* species and *Rhizoctonia solani*. These biological control properties of Bcc species are attributed to the production of siderophores and antimicrobials (Yoshihisa *et al*., 1989; Parke and Gurian-Sherman, 2001). There are a number of antimicrobials produced by members of the Bcc including cepacin (Parker *et al*., 1984), and this group produces four siderophores (Park and Gurian-Sherman, 2001; Thomas, 2007). It has been found that Bcc species can also increase the growth of commercial crops, such as rice, maize and wheat through the production of the plant growth hormone known as IAA (indole-3-acetic acid) (Parke and Gurian-Sherman, 2001). Some members of Bcc have another beneficial feature namely the ability to degrade pollutants. This is due to their capacity to use a wide variety of carbon sources including pollutants of ground water and chlorinated aromatic compounds that are found in pesticides and herbicides (Parke and Gurian-Sherman, 2001; Mahenthiralingam *et al.*, 2005).

1.2 The Bcc as a human pathogen

The association of the Bcc with human infection has been increasingly recognised over the years. They were first recognised as opportunistic human pathogens in immunocompromised patients who suffer from chronic granulomatous disease (CGD) and cystic fibrosis (CF) (Mahenthiralingam *et al*., 2001; LiPuma *et al*., 2001). *B. cenocepacia* is responsible for 70% of Bcc infections in CF, while *B. multivorans* is the second major pathogen among these species commonly found in CF patients in the USA and UK (Mahenthiralingam *et al*., 2008).

Table 1-1: *B. cepacia* complex species and their habitat[a]

Name	Habitat	Reference
B. cepacia	Human (CF and non-CF), soil, rhizosphere soil, plant, water.	Vandamme *et al*., 1997
B. multivorans	Human (CF and non-CF), soil, rhizosphere soil, plant material, water, industrial.	Vandamme *et al*., 1997
B. cenocepacia	Human (CF and non-CF), animals, soil, rhizosphere soil, plant, water, industrial contaminants.	Vandamme *et al*., 2003
B. stabilis	Human (CF and non-CF), rhizosphere soil, hospital equipment.	Coenye *et al*., 2001
B. vietnamiensis	Human (CF and non-CF), soil, rhizosphere soil, plant material, animal.	Coenye *et al*., 2001
B. dolosa	Human (CF), plant material, rhizosphere soil.	Vermis *et al*., 2004
B. ambifaria	Human (CF), soil, rhizosphere soil	Coenye *et al*., 2001
B. anthina	Human (CF), animals, soil, rhizosphere soil, river water	Vandamme *et al*., 2002
B. pyrrocinia	Human (CF and non-CF), soil, rhizosphere soil, water	Vandamme *et al*., 2002
B. ubonensis	Human (non-CF), soil	Yabuuchi *et al*., 2000
B. latens	Human (CF)	Vanlaere *et al*., 2008
B. diffusa	Human (CF and non-CF), soil, hospital equipment	Vanlaere *et al*., 2008
B. arboris	Human (CF and non-CF), soil, rhizosphere soil, water, industrial contaminant	Vanlaere *et al*., 2008
B. seminalis	Human (CF and non-CF), plant material, rhizosphere soil	Vanlaere *et al*., 2008
B. metallica	Human (CF)	Vanlaere *et al*., 2008
B. contaminans	Human (CF and non-CF), soil, animal, hospital equipment	Vanlaere *et al*., 2009
B. lata	Human (CF and non-CF), soil, plant material, water	Vanlaere *et al*., 2009
B. acidipaludis	Environment	Aizawa *et al*., 2010
B. pseudomultivorans	Human, plant	Peeters *et al*., 2014
B. stagnalis	Environmental and human (CF) sources	De Smet *et al*., 2015
B. territorii	Environmental and human (CF) sources	De Smet *et al*., 2015

Modified from Sousa *et al*., 2011.

1.2.1 Bcc infections in patients with chronic granulomatous disease (CGD)

Chronic granulomatous disease (CGD) is a genetically determined disorder. Most cases of CGD are inherited as X-linked defects. The disease affects approximately one in 250,000 live births (Van den Berg *et al*., 2009) and occurs because phagocytic cells have lost their ability to kill certain bacteria and fungi after ingesting them, which leads to formation of tissue granulomas. It has been found that there are four structural genes encoding NADPH oxidase that are mutated in 65% of CGD of cases (Segal *et al.*, 2000). The commonly cultured microorganisms from CGD patients are *Staphylococcus aureus, Aspergillus spp* and *Salmonella spp* while *Pseudomonas spp* and *B. cenocepacia* are less common in CGD patients (Van den Berg *et al.*, 2009).

1.2.2 Bcc infection in CF patients

The term cystic fibrosis refers to the formation of scars that appear on the lungs, pancreas and others organs of CF patients. In the 1930s, the condition was recognised in the pancreas for the first time (Andersen DH, 1938). The incidence of CF is 1 in 2,750 live births in Caucasians. Typical symptoms associated with CF are chronic respiratory infections and gastrointestinal abnormalities that cause malabsorption and nutritional deficits (Stern, 1997).

The genetics of CF are well-characterized; CF arises from mutations in the gene encoding the cystic fibrosis transmembrane conductance regulator (CFTR). The defective gene causes major medical issues for the patient (Lyczak *et al.*, 2002). It is responsible for the thick pulmonary mucus associated with this disease which decreases the ability of respiratory function (Saldias and Valvano, 2009). Two functional (wild type, WT) alleles of the *CFTR* gene are present in most individuals and only one intact copy is sufficient to prevent CF. Having a *CFTR* mutation in both alleles causes CF, therefore it is an autosomal recessive genetic disorder (Davis, 2006; Drumm *et al*., 2012). The *CFTR* gene encodes a 168-kD protein that is an ATP-binding cassette (ABC) transporter. This is responsible for regulating chloride ion transport in the epithelial cell membranes and acting as a channel under the control of cAMP (Carson *et al*., 1995). Another function of this gene is to regulate or transport HCO_3^- through the epithelial cell membrane (Ratjen, 2009).

More than 500 putative mutations have been reported in the *CFTR* gene since 1989. ΔF508 is the most common mutation, causing a deletion of one amino acid, phenylalanine (F), located at position 508. This single amino acid change is responsible for about 70% of defective CF alleles in northern Europe (N. Morral *et al*., 1994). This mutation affects secretion of cAMP-dependent Cl^- and HCO_3^- and causes excessive absorption of ENaC-mediated Na^+ in epithelial cells, which results in a dehydrated mucus (Boucher, 2007). Infection and inflammation in the airways of CF patients could be a direct result of the dehydrated epithelial cell surfaces and abnormal electrolyte composition, making them a suitable environment for bacterial infections (Ratjen, 2009).

The number of bacterial pathogens that might cause the infection in CF patients are limited. The pathogens of CF are *Pseudomonas aeruginosa*, *Staphylococcus aureus*, *Haemophilus influenzae*, Bcc and *Stenotrophomonas maltophilia.* The most common pathogen observed in CF patients responsible for about 90% of lung infections is *P. aeruginosa* (Mahenthiralingam and Vandamme, 2005). The Bcc species were recognised in the 1980s as opportunistic pathogens associated with CF in immunocompromised patients (Isles *et al*., 1984). In CF patients, Bcc clinical infections induce inflammatory responses that can rapidly affect the lung function. For example, *B. cenocepacia* is the cause of what is known as Cepacia syndrome, which leads to fatal necrotising pneumonia in CF patients. Moreover, *B. cenocepacia* is associated with dysregulated inflammatory responses (Gavrilin *et al*., 2012; Rosales-Reyes *et al*., 2012).

1.3 Resistance to antibiotics

The most problematic phenotype of Bcc bacteria is their high resistance to antibiotics. This high resistance to antimicrobial drugs is the main cause of mortality in CF patients following infection by Bcc bacteria (LiPuma *et al*., 2001). Bcc is resistant to aminoglycosides, but also have other multiple mechanisms for resistance to other types of antibiotics (LiPuma *et al*., 1998). For example, members of Bcc are known to be resistant to chloramphenicol, quinolones and trimethoprim, possible due to the activity of a specific efflux pump (Burns *et al.*, 1996). Bcc mechanisms of resistance

involve changes in the structure of lipopolysaccharide, inducible chromosomal β-lactamases, efflux pumps and their ability to alter their penicillin-binding proteins. The presence of drug efflux pump systems in Bcc is the most common cause of antibiotic resistance as it decreases antibiotic access (LiPuma *et al.*, 1998). Combination of antibiotic treatments are usually used in the case of severe Bcc infection (Speert, 2002).

1.4 Virulence factors of the Bcc

1.4.1 Exopolysaccharides (EPS)

The production of secreted carbohydrate polymers (EPS) is important for the physiology and pathogenesis of many bacteria. *P. aeruginosa* produces at least three EPS: alginate, Psl and Pel (Ryder *et al*., 2007). Hypersecretion of alginate EPS is responsible for *P. aeruginosa* mucoid colonies. In the case of chronic infections of CF patients, the mucoid phenotype of *P. aeruginosa* contributes to poor lung function, increased anti-EPS antibody titres and poor patient outcomes (Govan and Deretic, 1996; Wozniak *et al*., 2003; Billings *et al*., 2013). Alongside the alginate EPS of *P. aeruginosa* the production of non-alginate EPS seems to be important for adaptation in the CF lung. The non-alginate EPS, Psl, for example, is as important as the alginate EPS with its production increasing in the first 40,000 generations during infection (Huse *et al*., 2013). Bcc clinical and environmental isolates produced six different polymers, one of which is Cepacian, which forms double-stranded aggregates in dilute aqueous solutions and a network of polymer in concentrated systems (Herasimenka *et al*., 2008). The second EPS consists of three galactose residues and one 3-deoxy-D-manno-oct-2-ulosonic acid (Cescutti *et al*., 2003), and the third EPS is composed of one glucose and one galactose residue (Herasimenka *et al*., 2007). The other three EPS molecules are neutral polysaccharides which are always synthesised in a single strain in the presence of any of the EPS reported above (Herasimenka *et al*., 2007). The study of the structural properties of EPS from Bcc species indicates that Cepacian is the most common EPS produced by Bcc isolates (Herasimenka *et al*., 2007).

1.4.2 Lipopolysaccharide (LPS)

Lipopolysaccharide (LPS) is a major component of the outer membrane of Gram-negative bacteria. It is a large molecule divided into three parts: lipid A, core polysaccharide and O-antigen repeats. The lipid A component is considered to be responsible for the toxic effect associated with infections caused by some species of these bacteria (Kleine *et al.*, 1985). LPS has been identified as a pathogen-associated molecular pattern (PAMP) since it can be recognised by host pathogen-recognition receptors, thereby inducing a marked inflammatory response via TLR4/MD2-mediated signalling pathways (Zhang *et al.*, 2009). A study using a 2-Dimensional Difference Gel Electrophoresis (2-D DIGE) quantitative proteomic approach showed that the production of O-antigen is diminished in *B. cenocepacia* clinical isolates, and at later stages of CF infection, both *P. aeruginosa* and *B. cenocepacia* showed reductions in O-antigen and lipid A production (Madeira *et al.*, 2013). Whole Bcc bacteria are not toxic to outbred mice or guinea pigs, unless the animals are injected with large doses of bacteria (Straus *et al*., 1988; Jonsson, 1970). However, an extracellular toxic complex (ETC) made from supernatants of liquid Bcc cultures was lethal when injected into mice. Furthermore, ETC induced pulmonary pathology in rats, even in the absence of an active Bcc infection. Later studies by the same group demonstrated that the toxic component of ETC was LPS (Straus *et al*., 1989; Straus *et al*., 1990). In human cell lines, the production of LPS induces the pro-inflammatory cytokines TNFα and IL-6, and long-term stimulation of TNFα and IL-6 by LPS causes inflammation and tissue damage in the lungs of CF patients, due to the consequent production of reactive oxygen species as a result of the individual's inflammatory response (Bamford *et al*., 2007; Silipo *et al*., 2007).

1.4.3 Proteases

Proteases are one of the factors that have been implicated in *B. cenocepacia* virulence. The importance of proteases comes from their ability to aid bacteria in various activities. In particular, exotoxic secreted proteases are associated with bacterial virulence (Gingues *et al*., 2005). There are two extracellular proteases that have been found to be produced by *B. cenocepacia* and by at least four other Bcc species: ZmpA and ZmpB. Even though these two proteases are present in the same Bcc species, there is no genetic link between them (Gingues *et al*., 2005; Kooi *et al.*, 2006). They cause

degradation of some substrates involved in the integrity of tissues and host defences such as type IV collagen, fibronectin, neutrophil α 1-proteinase inhibitor and α 2-macroglobulin. ZmpA cleaves gamma interferon (IFN-γ) and ZmpB degrades transferrin, lactoferrin, and human IgA, IgG and IgM immunoglobulins (Kooi *et al.*, 2005; 2006). A study by Gingues *et al*. (2005) showed that a mutation in either of the *zmp* genes in the *B. cenocepacia* strain K56-2 results in a reduced ability to persist in chronic lung infection model, causing a reduction in lung pathology when compared to the parent strain.

HtrA is another protease found to be present in Gram-negative bacteria. It is a periplasmic serine protease that is highly conserved in bacteria, plants and mammals. Under normal conditions, it acts as a chaperone, but when periplasmic proteins are misfolded due to heat shock response it can act as a protease (Strauch *et al*., 1989; Danese *et al*., 1995; Kim and Kim, 2005). *B. cenocepacia* is able to use HtrA when growing under osmotic and thermal stress conditions in order to survive *in vivo* (Flannagan *et al*., 2007).

1.4.4 Biofilm formation

Medical devices or damaged tissue can become encased in a hydrated matrix of polysaccharide and protein, forming a layer known as bacterial biofilm (Flemming, 1993). Bcc can colonise medical devices such as catheters causing hospital-acquired infections (Costerton *et al*., 1999; Orsi *et al*., 2006). Bacterial biofilms are well known for their high level of antibiotic resistance, and the promotion of bacterial biofilm formation is the main factor contributing to chronicity of infections, especially those associated with implanted medical devices (Stewart and Costerton, 2001).

1.4.5 Motility

The flagellum is an important virulence factor that has more than one function. It allows motility in some bacterial species and is involved in the process of adhesion and invasion of host cells (Tomich *et al*., 2002). The flagellum is composed of approximately 50 different proteins. The outer part of the flagellar filament consists of flagellin (FliC) and has been found to be the major factor responsible for inducing

inflammatory responses (Eaves-Pyles *et al*., 2001). *B. cenocepacia* is a motile pathogen whose motility is facilitated by polar flagella (Burkholder, 1950). The study of flagellar morphology in *B. pseudomallei* and *B. cenocepacia* indicates that they have one single polar flagellum that is linked to their virulence (Chua *et al*., 2003; Urban *et al*., 2004). It is not clear yet, whether flagellar gene upregulation can cause any change in the structure and function of the flagellum (Correa *et al*., 2005; Murray and Kazmierczak, 2006). Recently, the flagellin expression and flagellar morphology of *B. cenocepacia* grown in CF conditions has been investigated and compared with a sample grown in a minimal medium. Data from this study suggested that the nutritional conditions induce expression of cell surface flagella in the CF lung. In *B. cenocepacia*, the putative GTPase FlhF is a positive regulator of motility, flagellin expression, and flagellar biosynthesis (Kumar and Cardona, 2016), and has also been found to be responsible for flagellar localisation and biosynthesis in other bacteria (Correa *et al*., 2005; Murray and Kazmierczak, 2006).

1.4.6 Pili (fimbriae)

Adherence is an essential process in pathogenicity for many bacterial species. It is also associated with the colonisation and infection caused by the Bcc members in the respiratory tract of CF patients (Goldstein *et al*., 1995). The potential factor used by *B. cenocepacia* to colonise host cells is the expression of surface pili. Electron microscopy observations indicate that at least five types of pili are produced by Bcc strains (Goldstein *et al.,* 1995). It has been found that there is only one type of pilus of Bcc involved in the infection of CF (Goldstein *et al.,* 1995). It has also been shown that there is an association between pili and 22-kDa adhesin in *B. cenocepacia* that contributes to pathogenesis through adherence to host airway epithelial cells (Sajjan and Forstner, 1993; Sajjan *et al*., 2002; Urban *et al*., 2005).

1.4.7 Quorum sensing systems

A number of bacterial pathogens are able to utilise cell-cell communication systems known as quorum sensing (QS). These systems allow bacteria to communicate with neighbouring cells of the same species, but the signal may also be recognised by other species. This system is used to produce and sense chemical signals that alter the

expression of genes and phenotypes and can be used to increase their pathogenicity (Ng and Bassler, 2009). Most of the well-studied quorum sensing systems of Gram-negative bacteria are involved the production of *N*-acyl-homoserine lactones (AHLs) by synthases of the LuxI protein family (Ryan and Dow, 2008; Ng and Bassler, 2009). AHLs are released into the surrounding medium during bacterial growth, with high cell densities resulting in relatively high concentrations of AHLs. It has been found that if there are sufficient numbers of AHL molecules inside the bacterial cells, they bind reversibly to cognate transcriptional regulators of the LuxR protein family. The binding of AHL causes a conformational change that activates the transcriptional regulator. The LuxR proteins in the AHL-bound or unbound state are able to dictate the activation or repression of transcription (Fuqua *et al*., 1996; Subramoni and Venturi, 2009).

Two quorum sensing systems have been identified in two clinical strains of *B. cenocepacia*: CciIR system and CepIR system. The most common system used by Bcc is the CepIR system. The CepI AHL synthase is responsible for N-octanoyl-homoserine lactone (OHL) and N-hexanoyl-homoserine lactone synthesis. The CepR transcriptional regulator can exert both positive and negative regulatory effects and seems to be responsible for regulating the extracellular expression of swarming motility, biofilm production and proteases (Lewenza *et al*., 1999; Huber *et al*., 2001; Lewenza *et al*., 2002). It has been shown that CepR has a negative regulatory effect on its own expression and on the biosynthesis of the siderophore ornibactin (Lewenza and Sokol, 2001; Riedel *et al*., 2003).

It has been demonstrated that QS mutations only rarely occur in the airways of chronically infected CF patients when studied over isolate collection times of 2-16 years. Mutations resulting in loss of function were observed in only one out of 45 sequential isolates from 22 CF patients (12 infected with *B. cenocepacia* and 10 with *B. multivorans*). This isolate came from a patient with a *B. cenocepacia* strain who was known to have had isolates with functional QS genes for at least 10 years previously and the loss of QS activity resulted from the combination of mutations in both *ccpR* and *cciR* (McKeon *et al*., 2011). Directed mutations in either QS system of *B. cenocepacia* resulted in the loss of QS function but were associated with either no or a negative growth advantage over wild-type strains *in vitro* (growth in synthetic CF

sputum medium) or *in vivo* (a rat agar bead respiratory infection model) (McKeon *et al*., 2011).

This indicates a competitive advantage for strains with QS systems, hence suggesting QS regulation of virulence factors is important in chronic Bcc infections. The relative stability/low propensity to mutation of the QS function furthermore indicates that the QS function might be an appropriate target for antimicrobial treatments, and in fact there is some experimental evidence for therapeutic benefit in targeting this system. A triple knock-out mutant in J2315 of *cepI*, *cciR* and the gene encoding the enzyme required for synthesis of *Burkholderia* diffusible signal factor showed a reduction in biofilm formation, lower resistance to antibiotics and lower virulence towards *C. elegans* when compared with the WT (Udine *et al*., 2013; Cullen and McClean, 2015).

1.4.8 The *Burkholderia cepacia* epidemic strain marker (BCESM)

The BCESM of *B. cenocepacia* was identified during RAPD (random amplified polymorphic DNA) typing and is 1.4 kb in size. It is a conserved amplification product in otherwise distinct strain fingerprints of *B. cenocepacia* isolates from CF patients (Mahenthiralingam *et al*., in 1997). This is very commonly used as a marker to identify any increased risk associated with the spread of infection from patient-to-patient in CF. It encodes a single CDS for a putative negative transcriptional regulator designated as EsmR (Mahenthiralingam *et al.*, 1997). Approximately 77% of III-A genomovar (*B. cenocepacia*) were found to have BCESM while it was found to be absent in III-B isolates (Mahenthiralingam *et al*., 2001; Manno *et al*., 2004). Currently, BCESM is considered a part of a unique genomic island that is specific for *B. cenocepacia*, known as the Cenocepacia Island (cci). Genes belonging to this island have been found to be associated with virulence and metabolism in the bacteria (Baldwin *et al*., 2004). BCESM-positive strains were reported to exhibit increased transmissibility and virulence, giving rise to high levels of mortality in infected patients (Mahenthiralingam *et al*., 2001; Speert, 2002).

1.4.9 Siderophores

The term siderophores is derived from the Greek: iron carriers. Siderophores are iron-chelating compounds of low molecular weight (200-2000 Da), and are synthesised by many bacteria, fungi and plants (Schwyn and Neilands, 1987; Neilands, 1995; Chu *et al*., 2010; Hider and Kong, 2010; Saha *et al*., 2013). Siderophore production is recognised as the most common mechanism employed by bacteria to acquire iron. Siderophores have the ability to deliver iron to bacterial cells because of their high affinity for Fe^{3+} and the existence of high affinity uptake systems for iron-siderophore complexes (Saha *et al*., 2013). Pyoverdine is a well-studied siderophore produced by *P. aeruginosa* and is considered as a virulence factor of this bacterium. Ornibactin, meanwhile, is a siderophore produced by members of Bcc that seems to increase the virulence of strains associated with CF infection (Sokol *et al*., 1999). A recent study showed that siderophores not only bind to iron but also to other metals with different affinities. For example, pyochelin and pyoverdine from *P. aeruginosa* are able to bind to 16 different metals (Braud *et al*., 2009; 2010), although pyoverdine is more efficient at sequestrating heavy metals outside the bacterial cells than pyochelin (Braud *et al*., 2010). In the environment, siderophores can also form complexes with other elements that are essential for bacterial cells such as Co, Ni, Mn and Mo (Kraepiel *et al*., 2009; Braud *et al*., 2009a; 2009b). Most siderophores have the ability to increase the mobility and solubility of a wide range of metals, i.e. Cd, Cu, Ni, Pb, Zn, and the actinides Th (IV), U (IV) and Pu (IV) (Schalk *et al*., 2011).

Types and structures of siderophores

The structural features of siderophores are very diverse. Nevertheless, the ability of siderophores to form six-coordinate complexes with Fe^{3+} has been demonstrated as a feature of many siderophores. However, more than one siderophore molecule may ligand to a single iron atom and water can be coordinated when there are less than six donor atoms in a siderophore (Miethke and Marahiel, 2007). Siderophores with three bidentate ligands per molecules are very powerful in forming a hexadentate complex (Roosenberg *et al.*, 2000). The classification of siderophores depends on the ligands that can be used to chelate the ferric iron. Based on this, there are three main chemical groups involved in chelating iron: α-hydroxycarboxylic acid, hydroxamic acid and

catechol (Miethke and Marahiel, 2007). Examples of siderophores that contain these groups are ornibactin, which consists of two types of iron-chelating groups (two hydroxamates and an α-hydroxycarboxylate) whereas enterobactin contains three catecholate groups. Many siderophores are synthesized by non-ribosomal peptide synthetases (NRPSs); however, some like aerobactin and rhizobactin are synthesized independently of NRPs, which termed as the NIS (NRPs-independent siderophore) pathways (Challis, 2005).

1.5 The importance of iron for bacterial growth

Iron is an essential nutrient for bacterial cells as there are many cellular processes, such as, DNA biosynthesis, methanogenesis, H_2 production and consumption, N2 fixation, respiration and the tricarboxylic acid (TCA) cycle are dependent on iron. Almost all of the biological roles of iron depend on its ability to be incorporated into proteins, which can be as a mono- or binuclear species or in a more complex form as part of iron-sulphur clusters or haem groups (Andrews *et al*., 2003).

Although iron is generally abundant in nature, it cannot readily be found in its preferred form. Iron is present essentially in two oxidation forms: ferrous iron (Fe^{2+}) and ferric iron (Fe^{3+}). Fe^{3+}, the oxidised form, occurs when oxygen is highly concentrated in the environment and is the most prevalent form of the metal. In the presence of water and oxygen, Fe^{3+} forms insoluble ferric oxide hydrate complexes which are very stable and result in an available free Fe^{3+} concentration of about 10^{-9} to 10^{-18} M (Wandersman and Delepelaire, 2004; Miethke and Marahiel, 2007). Due to the low solubility of Fe^{3+}, it is not available to be used by microorganisms (Guerinot, 1994; Ratledge and Dover, 2000). The Fe^{2+} form has much higher solubility in water but this form can only be found at low pH levels or under anoxic conditions (Chu *et al.*, 2010).

Due to the low solubility of ferric iron under aerobic conditions and at neutral pH, the acquisition of iron in nature has become a complicated process. In animal hosts, bacterial pathogens also face iron-restricted conditions as iron at the intracellular level is sequestered in haem-containing proteins or in fluids by high affinity iron-binding proteins such as transferrin and lactoferrin (Bagg and Neilands, 1987; Neilands, 1995).

In poor iron environments, the survival of organisms within the host depends on using iron acquisition mechanisms. These allow the bacteria to scavenge iron from the surrounding environment or from the host iron-binding proteins (Whitby *et al*., 2006). Bacteria to acquire iron use two principal methods: (i) direct capture of iron from transferrin, lactoferrin or direct binding to the haem at the bacterial cell membrane: (ii) through synthesis by siderophores which are capable of acquiring iron from iron-binding proteins (Wandersman and Delepelaire, 2004; Krewulak and Vogel, 2008).

In respect to the first of these methods, lactoferrin is a protein that is structurally similar to transferrin. Both proteins are monomeric glycoproteins composed of two similar lobes that are involved in iron binding. The two proteins are able to bind to two Fe (III) ions for each monomer (Baker and Baker, 2004). Both proteins are able to chelate iron found in the lung in order to avoid iron-oxygen reaction damage (Whitby *et al.,* 2006: Pi *et al.,* 2012). Ferritin is considered the main iron storage protein in host cells. It is a hollow, roughly spherical protein, which is able to hold around 4,500 Fe^{3+} atoms (Barnes *et al*., 2002). It has been found that the level of Ferritin in the CF lung is significantly higher (a 70-fold increase) compared to the lungs of healthy humans while transferrin levels remained constant (Whitby *et al*., 2006).

1.6 Siderophores and iron uptake

Catalases, superoxide dismutases and peroxidases are antioxidant enzymes in which iron is an important component. Low iron levels will therefore not only affect the growth and the metabolism process of bacteria but will also decrease the oxidative defences which will lead to oxidative injury (Crosa, 1997; Byers and Arceneaux, 1998). For these reasons, bacteria require unique and carefully controlled systems for iron acquisition. High affinity iron uptake systems used by Gram-negative bacteria include various components; outer membrane receptor proteins, periplasmic binding proteins, ATP-dependent ABC-type transporters, the TonB-ExbB-ExbD protein complex and in many cases, siderophores. All these components are important for a functional iron transport system (Ferguson *et al*., 1998; Andrews *et al*., 2003). Bacteria can use one or more siderophores for iron uptake: many of them produce more than

one type of siderophores (either two or three) and some can use siderophores produced by other bacteria, fungi and plants (xenosiderophores) (Matzanke *et al*., 1997).

Another iron uptake system recently reported is the FtrABCD system. This system has been described in *Bordetella sp, Brucella abortus* and *B. cenocepacia* (Brickman and Armstrong, 2012; Elhassanny *et al*., 2013; Mathew *et al*., 2014). The FtrABCD system is similar to the EfeUOB system described in *E. coli* (Cao *et al*., 2007). This system consists of four proteins: FtrA is an aperiplasmic Fe^{2+} binding protein, FtrB is a periplasmic protein responsible for oxidisation of Fe^{2+} to Fe^{3+} and integral cytoplasmic membrane proteins, FtrC which is an iron permease protein and FtrD which is a ferredoxin (Brickman and Armstrong, 2012; Elhassanny *et al*., 2013). The mechanism of this iron uptake system involves internalisation of Fe^{2+} through the OM porin channels resulting in the binding between Fe^{2+} and homodimeric FtrA. Fe^{2+} is oxidised to Fe^{3+} through the copper ion within the cupredoxin-like domain of FtrB and Fe^{3+} is transferred to FtrC permease subsequently in order to be transported across the CM. In the CM, electrons liberated by ferroxidation activity are transferred to ferredoxin which allows them to pass to an electron acceptor causing reoxidisation of the ferroxidase activity of FtrB (Figure 1.1) (Brickman and Armstrong, 2012; Elhassanny *et al*., 2013). In addition, in several pathogens more than one ferrous uptake system has been recognised, such as the YfeABCD, FeoABC and EfeUOB systems described in *Yersinia pestis* (Bobrov *et al*., 2015).

On the other hand, Gram-positive bacteria use slightly different mechanisms for iron uptake. These bacteria have no outer-membrane and their cell wall consists of carbohydrates, murein, teichoic acid and proteins which separate the bacterial cytoplasm from its environment (Krewulak and Vogel, 2008). They can uptake iron through membrane-anchored binding proteins which are similar to PBPs in Gram-negative bacteria and ABC transporters. The mechanism of iron uptake relies on binding to the lipoprotein solute-binding proteins (SBPs) that are found in the CM which then transport the iron complex through the ABC system. This system is composed of a lipoprotein substrate receptor, transmembrane permease proteins and ATPase. *Staphylococcus* species have SitABC, SirABC and SstABCD as examples of ABC transporters (Sebulsky and Heinrichs, 2001; Brown and Holden, 2002).

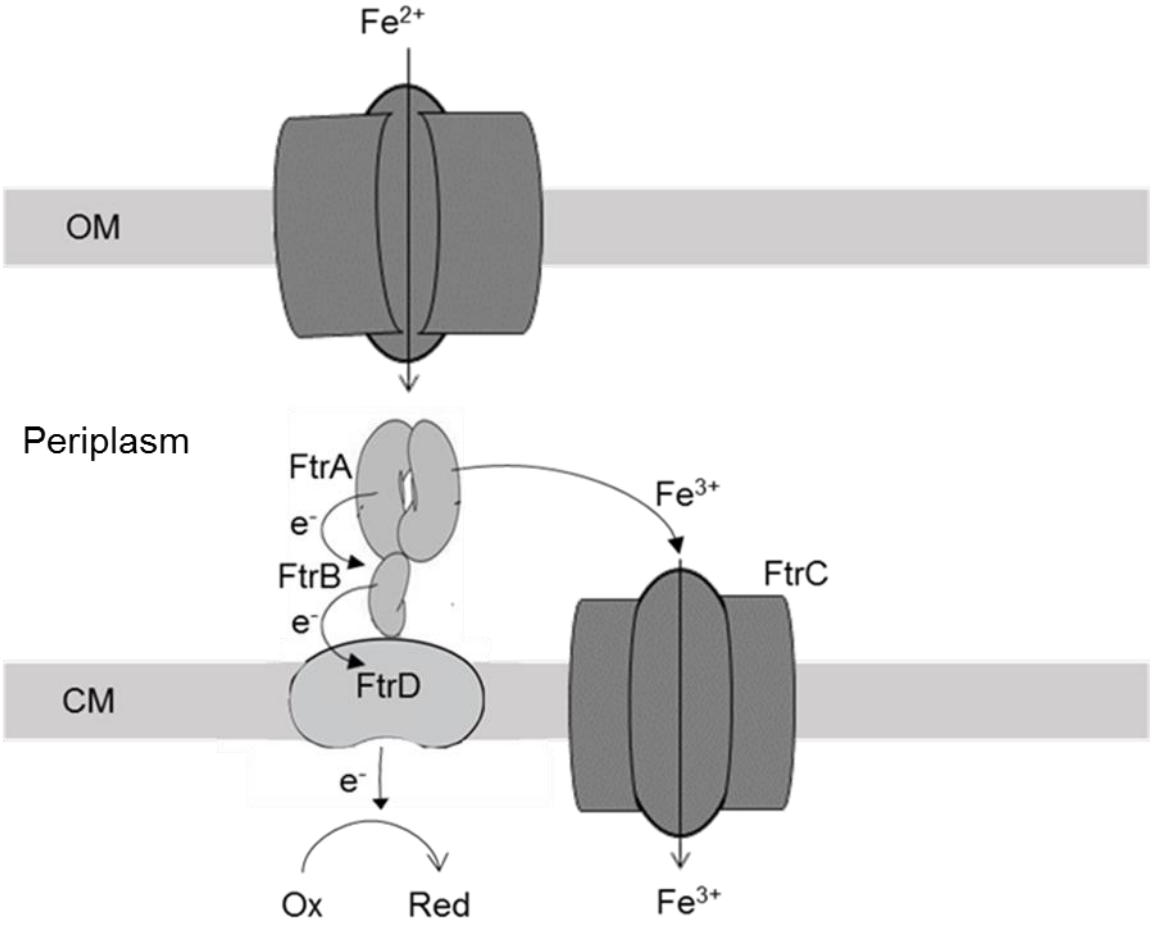

Figure 1-1: Model of FtrABCD system-dependent ferrous iron utilisation.

Ferrous iron (Fe^{2+}) internalised through porin channels located in the outer-membrane (OM) which result in the binding between Fe^{2+} and homodimeric FtrA in the periplasm. A copper site within the cupredoxin-like protein FtrB is responsible for the oxidation of Fe^{2+}. The ferric iron is transferred to the FtrC permease for translocation across the cytoplasmic membrane (CM). As a result of ferrous iron oxidation, electrons are released and passed from the FtrB to the FtrD 4Fe-4S cluster polyferredoxin in the CM, allowing them to pass to an electron acceptor. Modified from Brickman and Armstrong, 2012.

1.7 Haem uptake

Like iron, most organisms require haem for important cellular processes. This is a porphyrin (tetrapyrrole) ring that serves as a redox active moiety (cofactor) required for cellular protein functions. Haem acts as an electron shuttle in enzymes of the electron transport chain and is required for cellular respiration. A wide range of conserved enzymes in cells such as catalase and nitric oxide synthase rely on haem for their proper functioning. Moreover, haem is associated with diverse cellular functions: signalling, gas sensing, microRNA processing and cellular differentiation (Bonyhady *et al*., 1982; Shelver *et al*., 1997; Faller *et al*., 2007). Many bacteria are capable of taking up haem as a source of iron (Wandersman and Delepelaire, 2004). Haem uptake systems in bacteria scavenge exogenous haem or protein-bound haem as an iron source. Unlike siderophores, haem uptake can involve the use of secreted proteins called haemophores that scavenge free exogenous haem (Letoffe *et al*., 1994). Haem uptake systems in bacteria extract haem from haem-albumin, haemopexin, haemoglobin and haptoglobin.

In Gram-negative bacteria, haem is transported from the outer-membrane through the TBDRs or haem-binding proteins. Once in the periplasm, haem binds to a haem transport protein (HTP). The haem-HTP complex is delivered to the ABC transporters located in the inner membrane where it is then transported to the cytoplasm in an ATP-dependent process. The iron is released from the haem-HTP complex by degradation using haem oxygenases (HOs) and then the porphyrin ring can be recycled again. Haem uptake mechanisms are used by various bacterial pathogens such as *P. aeruginosa* and *V. cholerae* (Anzaldi and Skaar, 2010; Smith and Wilks, 2015; Abi-Khalil *et al*., 2015).

The haem uptake system in Gram-positive bacteria is similar to the one used by Gram-negative bacteria as both of them require a cell surface receptor for haem. The chaperone proteins located in the bacterial cell wall facilitate the internalisation of haem. ABC transporters are involved in haem translocation. HtaA is a cell surface exposed protein that is able to bind to haemoglobin and transfers haem to HtaB. Inside the cell, a protein called HmuT transports haem. Once in the cytoplasm, the ATP transporter and the haem oxygenase, Hmuo, are able to extract the iron (Wilks and

Schmitt, 1998; Drazek *et al*., 2000; Allen and Schmitt, 2009). The HtaAB-HmuOTUV haem uptake system is illustrated in *C. diphtheriae* (Allen and Schmitt, 2009).

1.8 Siderophores of *B. cenocepacia*

The severity of the infection caused by *B. cenocepacia* differs between CF patients, possible as a result of the different virulence factors produced among strains associated with this disease. Siderophores are one of the key virulence factors implicated in the pathogenesis of *B. cenocepacia* infections. Members of the Bcc often produce up to four siderophores; cepabactin, cepaciachelin, pyochelin and ornibactin (Darling *et al*., 1998; Sokol *et al*., 1999), with the latter two being predominant in *B. cenocepacia* strains. Salicylic acid, a precursor of pyochelin (as well as several other siderophores), is also widely produced by clinical isolates, and has been classified as a siderophore in *Pseudomonas fluorescens* (Meyer *et al*., 1992). The iron-binding constant of salicylate is too low to allow it to compete effectively with ions such as phosphate present within the blood, which causes free iron to precipitate. Salicylate has been shown to have little effect on the concentration of soluble Fe^{3+} *in vitro*, and furthermore cannot sequester iron from a complex with chrome azurol sulphonate (CAS). This suggests that salicylate does not act as a siderophore (Ratledge and Dover, 2000; Chipperfield and Ratledge, 2000).

Pyochelin

All clinical isolates of *P. aeruginosa* produce pyochelin and it was the first siderophore produced by *P. aeruginosa* to be isolated from CF (Sokol, 1986). Furthermore, the virulence of *P. aeruginosa* in respiratory infections of CF patients is correlated with the production of pyochelin (Sokol, 1986). Pyochelin is not only produced by *P. aeruginosa* but also by some species of Bcc, the second most common CF isolate. On the other hand, approximately half of the clinical isolates of Bcc from CF patients produce little or no pyochelin (Sokol, 1986; Darling *et al*., 1998), showing that while this siderophore is common amongst pathogenic strains, it does not seem to confer a competitive growth advantage in infection of the CF lung. Consistent with this, in a rat agar bead model, there was a little difference in persistence observed between a

pyochelin negative mutant of a CF clinical isolate of *B. cenocepacia* inh comparison to its parent strain (Visser *et al*., 2004).

In 1981, the structure of pyochelin was determined to be 2-(2-*o*-hydroxyphenol-2-thiazolin-4-yl)-3-methylthiazolidine-carboxylic acid (Cox *et al*., 1981). Pyochelin has a unique structure compared to most other siderophores and belongs to the phenolate class (Figure 1.2A) (Cox and Graham, 1979). It has low solubility in water (Visca *et al*., 2002) but its ferric complex is very stable and soluble in water unlike the iron-free form. Thus, pyochelin-ferric iron 2:1 complexes occur in solution. The octahedral coordination is asymmetrical, with one pyochelin molecule acting as a tetradentate ligand whereas the other behaves as a bidentate ligand (Figure 1.2A) (Ankenbauer *et al*., 1988; Tseng *et al*., 2006). Pyochelin can be detected under ultra-violet light and is easily recognised by its fluorescent yellow-green colour (Cox and Graham, 1979).

Ornibactin

Ornibactin is produced by most clinical isolates of *B. cenocepacia* (Stephan *et al.*, 1993). The peptide structure of ornibactin is quite similar to the pyoverdines, produced by the fluorescent *pseudomonads*. Bcc species that are known to produce ornibactin under iron-limited conditions are *B. cenocepacia, B. vietnamiensis, B. multivorans* and *B. ambifaria* (Meyer *et al*., 1995; Thomas, 2007; Asghar *et al*., 2011; Denman *et al*., 2014). In contrast to pyoverdines, the structure of ornibactin lacks a chromophore. It has been demonstrated to have a tetrapeptide backbone consisting of L-ornithine–D-hydroxyaspartate–L-serine–L-ornithine**.** The N-terminal ornithine residue is modified at the amino group (N^5) by hydroxylation and the addition of a hydroxy acid via an amide linkage (Figure 1.2B). The C-terminal is modified with formic acid and the carboxyl group is modified with putrescine (Stephan *et al.*, 1993; Thomas, 2007). There are three types of ornibactin categorised by their acyl chain lengths: ornibactin-C4, ornibactin-C6 and ornibactin-C8 (Stephan *et al.*, 1993). These are different from each other at the N-terminus of the tetrapeptide according to the carbon chain length of the 3-hydroxy acid (Stephan *et al*., 1993).

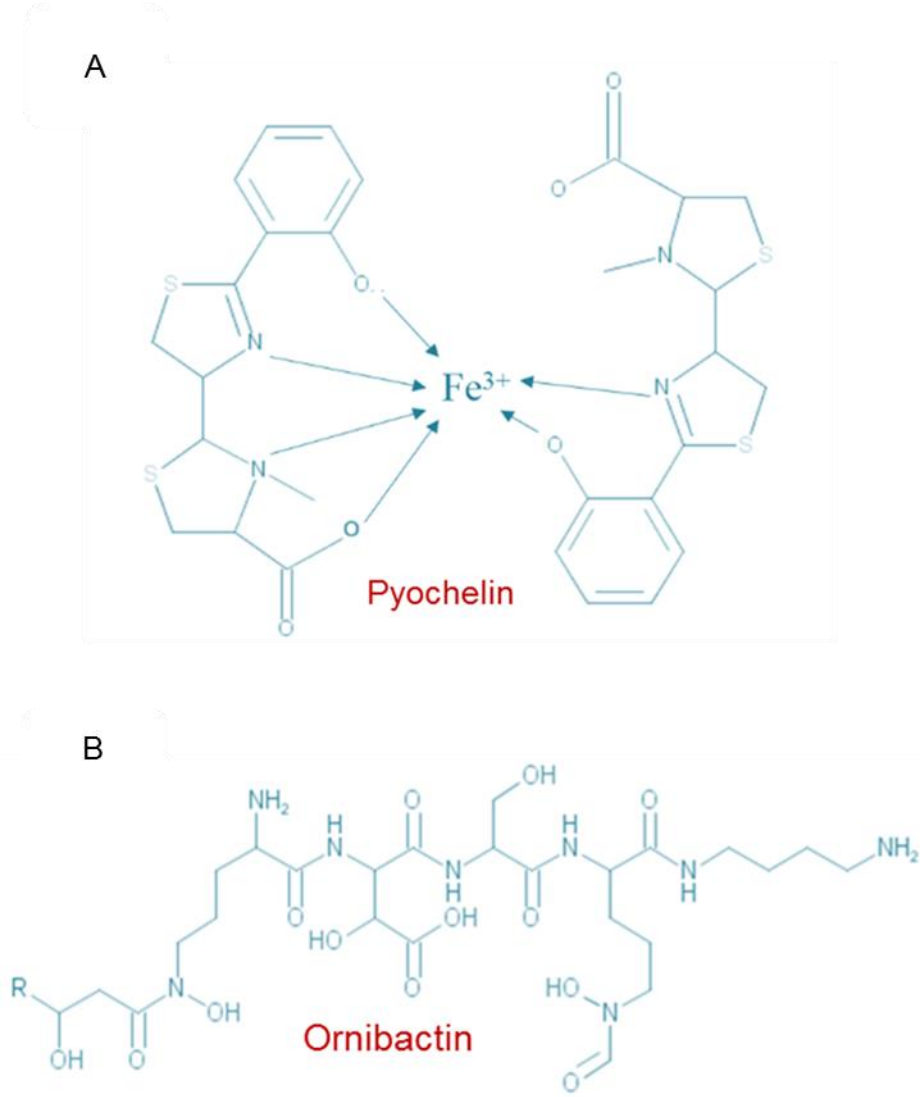

Figure 1-2: Structure of the siderophores pyochelin and ornibactin.

A. Structure of the siderophore pyochelin. Two pyochelin molecules coordinate with one ferric iron atom to form the pyochelin-Fe (III) complex.

B. Structure of the siderophore ornibactin. The ornibactin siderophore structure contains an α-hydroxycarboxylic acid and two hydroxamic acid groups for binding to iron. Generated using the Accelrys JDraw 1.1 SP2 Program.

Cepabactin

Cepabactin belongs to the cyclic hydroxamate group of siderophores and has the structure of 1-hydroxy-5-methoxy-6-methyl-2 (1H)-pyridinone (Figure 1.3A) (Meyer *et al*., 1989). It is produced by *Pseudomonas alcaligenes* and the *Pseudomonas* strain BN227 as a metal-binding antibiotic. Cepabactin has the characteristics of a siderophore: it is biosynthesised under low iron conditions and stimulates growth when added to a low iron media and it assists in iron uptake (Meyer *et al*., 1989). There is no *in vivo* evidence to indicate that cepabactin functions as a siderophore. Binding between cepabactin and ferric iron forms an orange complex that consists of three bidentate molecules of cepabactin per metal ion (Klumpp *et al*., 2005). The presence of pyochelin causes the formation of a purple-coloured complex that includes pyochelin, cepabactin and ferric iron in a 1:1:1 ratio; two coordinating groups are provided by cepabactin and four are provided by pyochelin (Klumpp *et al*., 2005). Although *B. cenocepacia* strains such as K56-2 and 715j are unable to produce cepabactin (Darling *et al*., 1998) it is possible that members of Bcc are able to utilise cepabactin and produce this siderophore (Meyer *et al.,* 1989). For example, adding cepabactin to a culture of the *P. aeruginosa* strain PAO1 facilitated iron uptake. This suggests that there is a receptor specific for this siderophore in this species (Meyer, 1992; Mislin *et al*., 2006).

Cepaciachelin

Cepaciachelin is a catecholate siderophore. It was first isolated from the supernatant of a *B. ambifaria* strain. The structure of cepaciachelin was determined by using mass spectrometry and ^{1}H and ^{13}C NMR as 1-N-[2-N',6-N'-di(2,3-dihydroxybenzoyl)-L-lysyl]-1,4-diaminobutane (Figure 1.3B) (Barelmann *et al*., 1996). It consists of a single molecule of lysine derivatised with 2,3-dihydroxybenzoic acid (DHBA) on the α and ε amino groups, and with diaminobutane (putrescine) on the carboxyl group. In terms of its structure, cepaciachelin shares similarities with protochelin. The role of cepaciachelin as a siderophore promoting iron uptake has not been determined (Thomas, 2007).

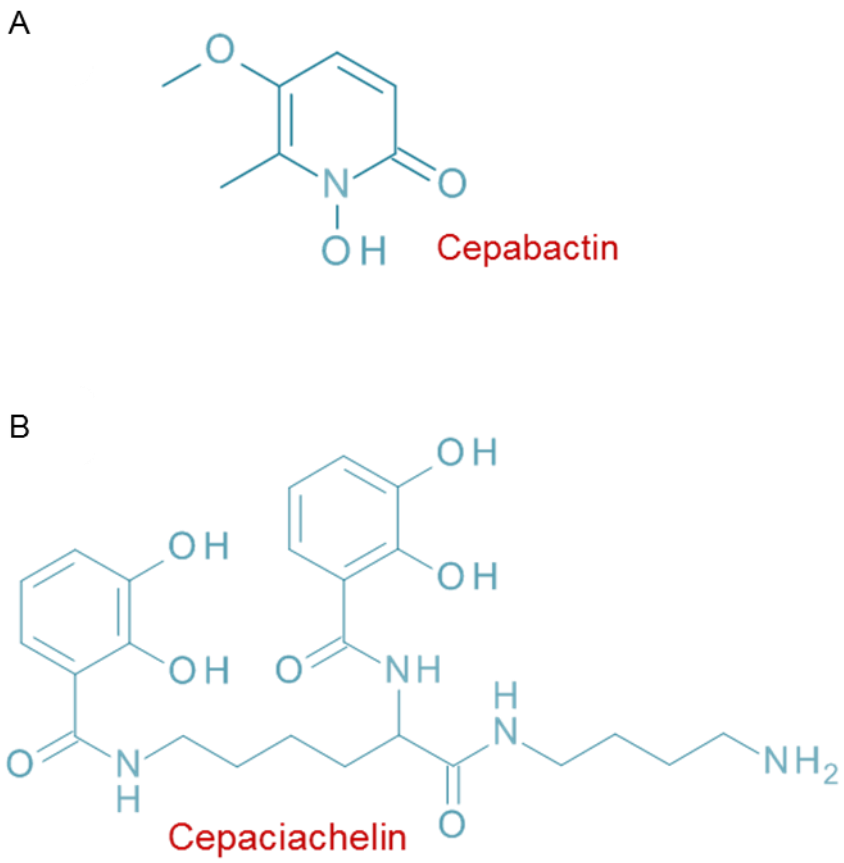

Figure 1-3: Structure of the siderophores cepabactin and cepaciachelin.

A. Structure of the siderophore cepabactin.

B. Structure of the siderophore cepaciachelin. Generated using the Accelrys JDraw 1.1 SP2 Program.

1.9 Siderophore outer-membrane receptor proteins

The Gram-negative bacteria cell envelope consists of an inner and outer membrane separated by the periplasmic space. Specialised outer-membrane receptors are required to transport the ferric-siderophore complex into the periplasm. These receptors have been demonstrated to be gated porin channels and are referred to as TonB-dependent receptors (TBDRs) (Chimento *et al*., 2005). The functions of the TBDR include recognition, binding and transporting of ferric-siderophore complexes into the periplasm.

The structures of the four originally identified TBDRs were determined by Chimento *et al*. (2005). TBDRs consist of two important domains: a 22-stranded antiparallel ß-barrel domain and a globular N-terminal "plug" domain of about 140 residues that is located within the ß-barrel (Figure 1.4). The residues on the extracellular side of the plug domain are responsible for forming the ligand binding sites (Figure 1.5A). A structure-based sequence alignment of the plug and barrel revealed that there are conserved motifs in the plug and barrel (Noinaj *et al*., 2010). TBDRs belong to a sub-family known as TonB-dependent transducers (TBDTs). TBDTs are involved in signal transduction and have a unique N-terminal extension of 70-80 amino acids that permit it to interact with the regulatory anti-σ factor (Figure 1.5B) (Noinaj *et al.*, 2010; Hartney *et al.*, 2011).

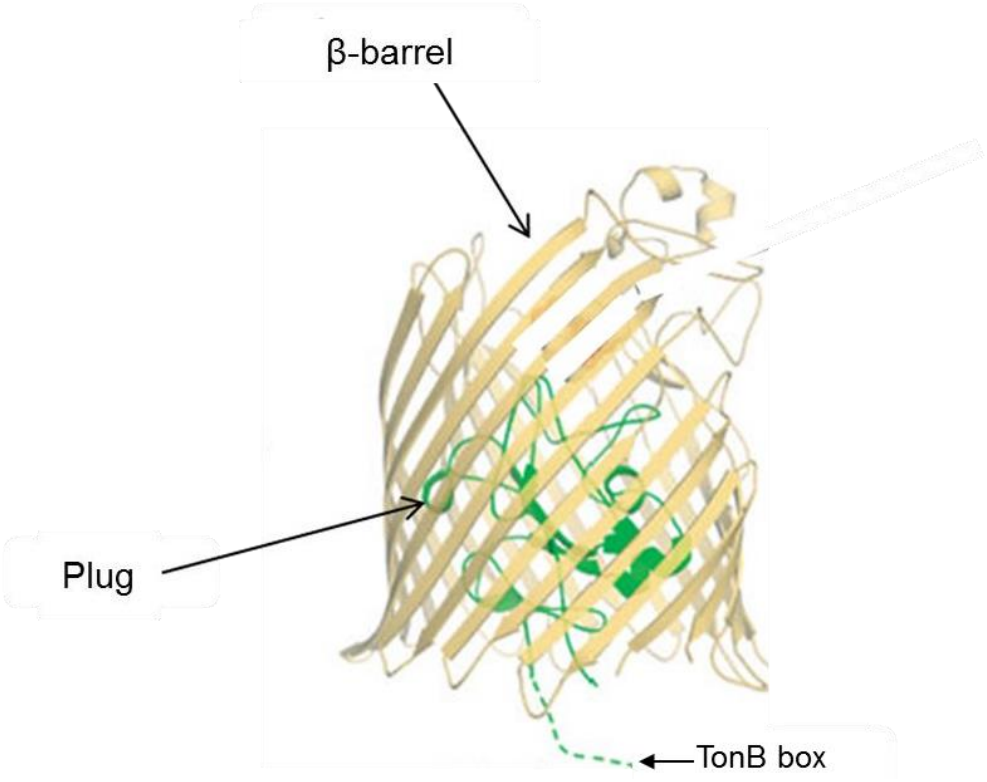

Figure 1-4: Structure of a TBDR.

The structure of the β-barrel and plug domain of the FhuA and FepA TBDR are shown in yellow and green colour, respectively. The plug domain is located inside the C-terminal 22-stranded β-barrel domain. The conserved TonB box sequence is located near the N-terminus of the plug domain facing the periplasm (Noinaj *et al*., 2010).

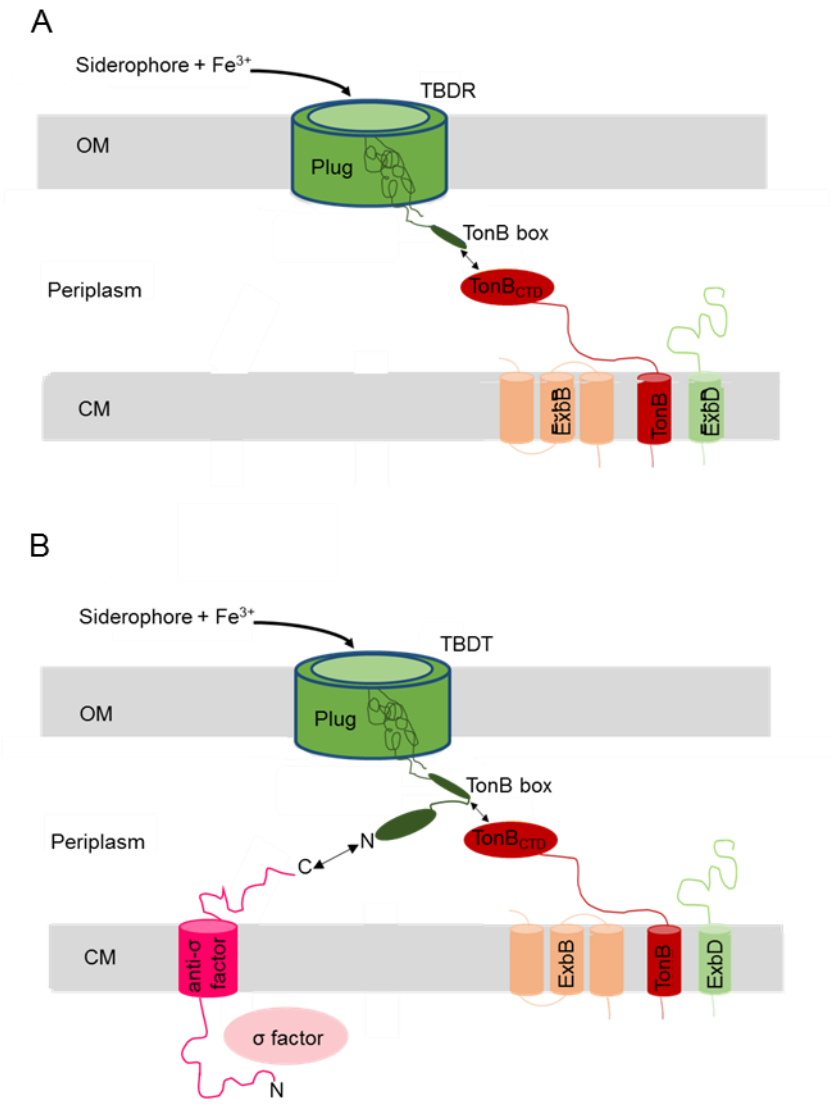

Figure 1-5: Mechanism of action of a TonB-dependent receptor and TonB-dependent transducers.

A. Mechanism of action of a TonB-dependent receptor (TBDR). The TBDR located in the outer membrane contains a TonB box sequence near its N-terminus that interacts with the energising TonB protein complex which consists of three cytoplasmic membrane proteins, TonB, ExbB and ExbD.

B. Mechanism of action of a TonB-dependent transducer (TBDT). The TBDT is a TBDR that has a unique N-terminal extension that interacts with an anti-σ factor. The binding of a ferric-siderophore complex to the TBDT activates the iron starvation σ factor through a signal transportation system involving the anti-σ factor. The σ factor eventually activates transcription of the TBDT gene.

1.9.1 The TonB box

The TonB box is an essential conserved sequence of about seven residues that is located at the N-terminus of the plug domain. It can be found extended into the periplasm or, in some structures, tucked up into the plug domain inside the barrel. In some cases, it might be located in a disordered region and is therefore not visible in the structures. The TonB box plays an important role in activating TBDRs which is required for the transport of ferric-siderophore complexes from the extracellular medium into the periplasm (Wiener, 2005; Noinaj *et al*., 2010). Once a ferric-siderophore complex binds to its outer-membrane receptor, a signal is transduced across the outer membrane resulting in the TonB box disordering or unfolding causing interaction with the TonB protein within the periplasm. The translocation of the iron-siderophore complex across the outer-membrane depends on the TonB protein complex (Section 1.9.2) (Eisenhauer *et al.*, 2005; Wiener, 2005; Noinaj *et al.*, 2010). More is known about the interaction between the TonB box and the TonB CTD as they have been analysed at structural level.

1.9.2 TonB-ExbB-ExbD complex

In Gram-negative bacteria, there is no energy source at the outer membrane and these bacteria have therefore evolved the Ton system to overcome this deficiency (Krewulak and Vogel, 2011; Celia *et al*., 2016). The Ton system mediates the uptake of metals, carbohydrates, ferric-siderophore complexes and many bacteriocins (Cadieux *et al*., 2007; Noinaj *et al.*, 2010). The TonB protein is located in the cytoplasmic membrane and is responsible for transducing the energy from the proton motive force generated at the cytoplasmic membrane to the outer membrane ferric-siderophore receptor in order to activate it. It has been demonstrated that the TonB protein functions as part of an energy transduction complex with two other cytoplasmic membrane proteins, ExbB and ExbD (Wandersman and Delepelaire, 2004). Periplasmic TonB is attached to the cytoplasmic membrane by a single anchor, which allows it to interact with the outer-membrane proteins, as a result TonB spans the periplasmic space (Letain and Postle, 1997; Braun *et al*., 2003; Noinaj *et al*., 2010). Once the ferric-siderophore is in the periplasm it can be transported across the inner membrane to the cytoplasm by ABC transporters or permeases.

1.9.3 Periplasmic binding proteins

In order for the ferric-siderophore complex to be transported to the inner membrane, periplasmic binding proteins are required (Crowley *et al*., 1991). FhuD is an example of a periplasmic binding protein that has the ability to recognise and bind to hydroxamate siderophore-iron complexes (Crowley *et al*., 1991; Schryvers and Stojiljkovic**,** 1999).

1.9.4 ABC transporters

ABC (ATP-binding cassette) transporters are found in prokaryotes and eukaryotes. These are members of the most active conserved family of transporters called the super family of ABC transporters which are highly active in transporting a variety of ferric-siderophores (Schneider and Hunke, 1998). ABC transporters consist of two identical transmembrane domains (TMDs) embedded in the cytoplasmic membrane bilayer and two ABC domains (also designated as the nucleotide binding domains (NBDs)) located in the cytoplasm (Biemans-Oldehinkel *et al*., 2006). The two domains are formed by a series of α-helices spanning the membrane. Energy generated by the hydrolysis of ATP is used by these proteins to drive transport (Koster, 2001; Borths *et al*., 2002). ABC transporters in bacteria utilise periplasmic binding proteins in order to transport substrates to the cytoplasm (Borths *et al*., 2002).

1.9.5 TonB-dependent mechanism of iron uptake

In iron-limited environments, the ferric-siderophore complex is recognised by the outer-membrane receptor (TBDR). A conformational change occurs in the β barrel structure of the receptor and the globular domain in the plug resulting in high affinity binding between the ferric-siderophore complex and the receptor ligand binding site (Noinaj *et al*., 2010). In the cytoplasmic membrane, ExbB and ExbD couple energy in the form of proton motive force in order to transduce energy to the TonB protein (Ollis *et al.*, 2012). After energisation, the TonB undergoes conformational changes and this increases the interaction of the TonB box and the C-terminal domain of TonB which is located in the periplasmic space (Ollis *et al.*, 2012; Ollis and Postle, 2012). This interaction causes strand pairing which facilitates energy transfer and the transport of the ferric-siderophore complex via the outer-membrane receptor (Noinaj *et al*., 2010).

In the periplasm, the ferric-siderophore complex binds to a specific periplasmic binding protein which enables the complex to be transferred across the cytoplasmic membrane using an ABC transporter. This allows the complex to be transported through the permease proteins that span the cytoplasmic membrane. Once the complex is in the cytoplasm, the ferrous ion is released for use and the siderophore might be degraded or recycled (Matzanke *et al*., 2004; Miethke and Marahiel, 2007).

1.10 Transcription in bacteria

Initiation of transcription in bacteria is a multi-step process requiring several components: RNA polymerase (RNAP) holoenzyme, a specific DNA sequence that acts as a promoter, σ factor and transcription factors (TF_S) (McClure, 1985).

1.10.1 RNA polymerase (RNAP) holoenzyme

In all bacterial species, the main checkpoint for controlling gene regulation is the transcription of DNA into RNA via RNAP. RNAP is a key enzyme in all living cells and is required for transcription and gene regulation. Bacterial core RNAP is composed of five subunits: two α subunits, single β, β' and ω subunits (Paget and Helmann, 2003). Binding between core RNAP and a σ factor forms RNAP holoenzyme, which is obligatory for transcription initiation due to the fact that the σ factor is required for promoter recognition and DNA strand separation.

1.10.2 σ factors

There are two distinct σ factor families, known as the σ^{54} and σ^{70} families based on their respective amino acid sequence similarity (Helmann, 2002), although there is no sequence similarity between σ^{70} and σ^{54} (Gruber and Gross, 2003). Furthermore, the σ^{70} family is divided into five sub-groups based on phylogenetic homology and functions (Figure 1.6) (Gruber and Gross, 2003; Paget and Helmann, 2003; Kazmierczak *et al.*, 2005). Group 1 includes the essential primary σ factor present in most bacterial species; σ^{70} of *E. coli* is the most-studied example of this group. Almost all bacteria have only a single primary σ factor from group 1, whereas the numbers of σ factors from the other groups can be higher (Paget and Helmann, 2003). The primary

σ factor varies between 40 to 70 kDa in size and consists of four conserved sequence regions known as regions 1 to 4 (Lonetto *et al*., 1992; Gross *et al*, 1998). These σ factors are able to recognise at least two specific promoter regions of consensus sequence TTGaca located near position -35 and TAtaaT located near position -10 relative to the transcription site (upper case letters indicated the most important, i.e. conserved positions) (Helmann, 2002).

Group 2 proteins are most closely related to the primary σ factor proteins but are not required for cell growth. They are nonessential alternative σ factors that are highly similar in sequence to members belonging to group 1 (Gross *et al.*, 1998). RpoS is an example of a σ factor of group 2 (Mulvey and Loewen, 1989). Group 3 consists of proteins distantly related to σ^{70} and they are functionally related since they respond to a certain signal such as heat shock (Paget and Helmann, 2003). Finally, Group 4 is a collection of highly diversified σ factors and this group is termed the extracytoplasmic function (ECF) subfamily. Almost all members of this subfamily respond to signals from the extracytoplasmic environment (Paget and Helmann, 2003). Group 4 is the largest group of σ factors and they are present in most bacteria. There is also another group of proteins which appears to form a fifth group of σ factors. This group consists of TxeR of *Clostridium difficile* which is a σ factor that controls toxin gene expression in this bacterium (Gruber and Gross, 2003).

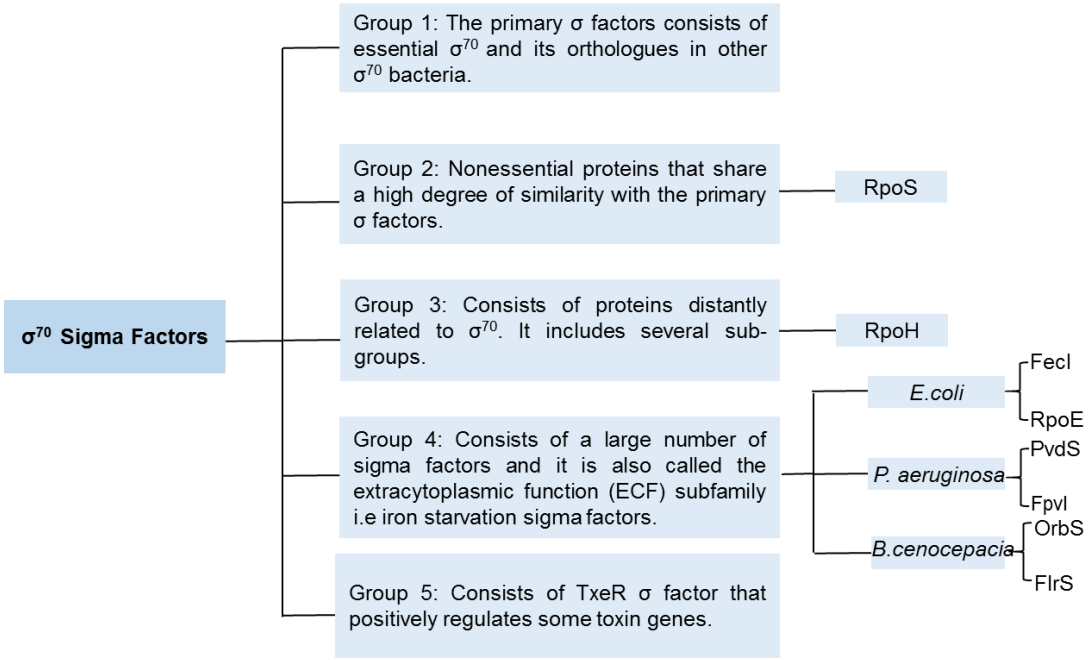

Figure 1-6: Classification of the σ^{70} family.

Group 4 is the largest group of the σ^{70} family sub-groups which are also referred to as ECF σ factors. It consists of the iron starvation σ factors. Some examples of iron starvation σ factors from different bacterial species are shown in this Figure.

1.10.3 Promoter recognition

During holoenzyme formation, conformational changes occur in core RNAP. These allow the σ factor to recognise promoter DNA, specifically sequences in the -10 region and -35 region (Burgess *et al*., 1969; Gross *et al*., 1998; Campbell *et al*., 2002a; Kuznedelov *et al*., 2002). The three-dimensional structure of σ^{70} of *E. coli*, σ^{R} of *S. coelicolor* and σ^{A} of *Thermus thermophilus* indicates that σ^{70} has at least three domains, σ_2, σ_3 and σ_4, that broadly correspond to three of the conserved regions; region 2, region 3 and region 4, respectively. σ_2 contains region 1.2 and 2.4 a stretch of non-conserved residues (NCR) between regions 1.2-2.1. Region 2.1 has a critical role in transcription initiation. It interacts with the non-template strand downstream of the -10 region in order to aid the function of σ_2 by stabilising its conformation and thus supporting the process of promoter binding and melting of DNA (Haugen *et al*., 2008; Bochkareva and Zenkin, 2013). Region 2.2 is an important region within σ^{70} since it is the most conserved region and is essential for RNAP binding (Young *et al*., 2001). Region 2.3 is crucial for promoter melting and for interaction with the -10 region (Young *et al*., 2004; Feklistov and Darst, 2011). Region 2.4 interacts with the -10 region and is responsible for ensuring a strong interaction between RNAP and the promoter (Lonetto *et al*., 1992). σ_3 consists of regions 3.0 and 3.1 and forms three helices, one of which is able to interact with the extended -10 region present in some promoters corresponding to a TG at positions -15 and -14. This conserved sequence element was previously known as region 2.4 but was renamed later as region 3.0 (Murakami *et al*., 2002; Murakami and Darst, 2003). σ_4 consists of four helices. Part of σ_4, region 4.2, interacts with the promoter sequence of the -35 region, resulting in strong RNAP binding (Figure 1.7) (Lonetto *et al*., 1992; Campbell *et al*., 2002b). σ_4 is conected to σ_3 through a link corresponding to region 3.2. Recently, region 1.1 corresponds to $\sigma_{1.1}$ was shown for the first time in the context of an entire *E. coli* RNAP in an X-ray structure study. This domain ($\sigma_{1.1}$) was found to be located at the RNAP DNA-binding channel where it prevented DNA from entering the RNAP active site (Murakami, 2013). Not all of the conserved regions of the σ factor proteins can be found in all σ^{70} members (Gruber and Gross, 2003). Region 1.1 is present in group 1 and 2 σ factors but it seems to be absent in group 4. In addition, region 3 appears to be missing from ECF σ factors (Campbell *et al*., 2003).

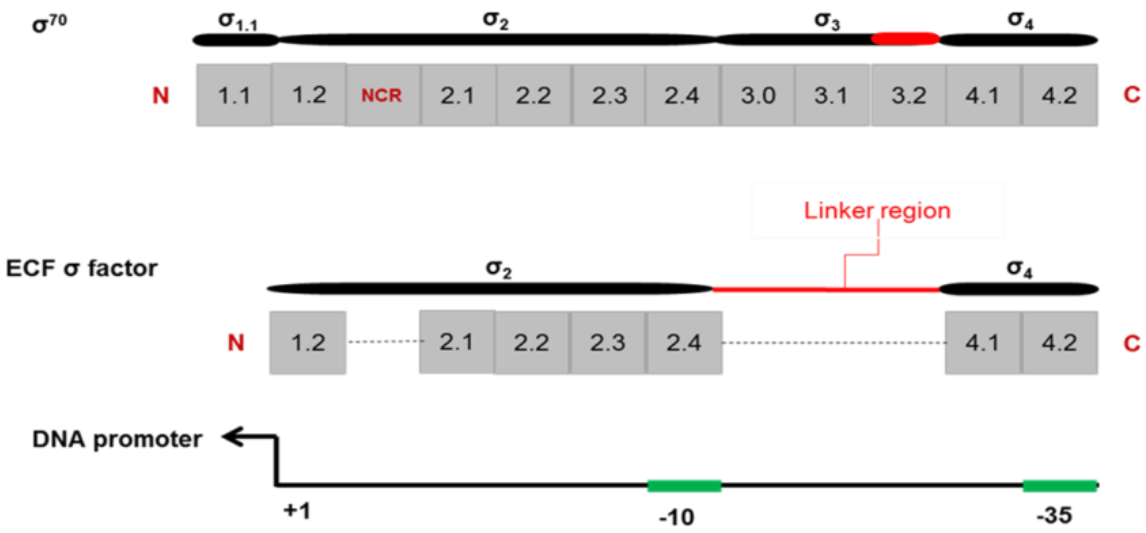

Figure 1-7: The functional regions of σ^{70}.

Structural differences between σ^{70} and ECF σ factors. σ^{70} consists of four domains ($\sigma_{1.1}$, σ_2, σ_3 and σ_4) that are subdivided into conserved regions apart from the non-conserved region (NCR) in σ_2 and region 3.2 in σ_3. ECF σ factors do not have $\sigma_{1.1}$ and lack almost all of σ_3. The NCR is also missing in ECF σ factors.

1.10.4 Initiation of transcription

The transcription process starts by the binding of RNAP holoenzyme to DNA sequences located at -35 and -10 regions using the σ factor. Once the binding between RNAP and the promoter region occurs a closed promoter complex is formed at the transcriptional start site (TSS). Binding between holoenzyme and a promoter form a 'closed' promoter complex, which becomes an 'open' complex following melting of the DNA at the -10 region (Helmann and deHaseth, 1999; Murakami and Darst, 2003; Browning and Busby, 2004; Hook-Barnard and Hinton, 2007). Transcription starts when a complementary nucleoside triphosphate (NTP) base pairs with the nucleotide located at the +1 region in the template strand. The next important step in transcription, is the elongation step. The formation of the first ~12 nucleotides of RNA causes displacement of the σ factor loop ($\sigma_{3.2}$). This disturbs the interaction between σ_4 and the β flap domain of the β subunit and σ_4 is released from the β flap. This destabilises interaction between σ_4 and the -35 element where RNAP 'lets go' of the promoter. When the RNAP escapes from the promoter the σ factor is generally released (Murakami and Darst, 2003).

The final step is the termination of transcription which occurs when RNAP encounters a transcriptional terminator. Broadly, two different mechanisms are used by bacteria; intrinsic and factor-dependent termination. Intrinsic termination occurs when a segment of DNA is transcribed into RNA that forms a hairpin structure (stem-loop) followed by several U residues. This mechanism does not require the involvement of protein factors. The initial role of hairpin formation is to serve as a transcription pause signal, allowing the nascent RNA to be removed from the base paring with the template DNA. RNA is released from the complex because the hydrogen bonding between A and U residues is very weak (Yarnell and Roberts, 1999; Borukhov and Nudler, 2003; Murakami and Darst, 2003).

On the other hand, factor dependent termination depends on a protein called Rho (p) protein. Rho is an RNA-DNA helicase that actively releases nascent mRNAs from paused transcription complexes (Das, 1993). This process is initiated upstream of the termination sites within regions of mRNA that are unstructured and untranslated. In these regions, Rho interacts with the RNA chain that contains at least 60 nt which is very low in the secondary structure (Guerin *et al.*, 1998).

1.11 Extra-cytoplasmic function (ECF) σ factors

ECF σ factors are regulatory proteins in bacteria that belong to group 4 of the σ^{70} family. Although they are the largest and most diverse subfamily within the σ^{70} proteins, the σ factors belonging to this group are the smallest σ factors in terms of their size consisting of only two domains, σ_2 and σ_4. The ECF σ factor in region 2, however, seems to possess a distinct structure in comparison to non-ECF σ factors (Gross *et al*., 1989; Leoni *et al.*, 2000; Lonetto *et al*., 1992).

Another feature that distinguishes most ECF σ factors from the other groups of σ factors is the presence of cognate cytoplasmic membrane anti-σ factors. Most anti-σ factors consist of two domains, an N-terminal cytoplasmic domain and a C-terminal periplasmic domain which are separated by a single transmembrane segment. Under normal conditions, σ factors appear to bind to their corresponding anti-σ factor leading to inactivation of the σ factor. The activation of this system is thought to occur through the C-terminal domain (CTD) of the anti-σ factor but the exact mechanism is unknown, although it might be caused by the interaction of the CTD with regulatory proteins localised in the cell envelope. As a result, the anti-σ factor becomes inactive thereby causing the release of the σ factor into the cytoplasm where it can bind to core RNAP and initiate transcription of the target genes (Raivio and Silhavy, 2001). Genes encoding group 4 σ factors are usually co-transcribed along with the gene encoding their transmembrane anti-σ factor with an extracytoplasmic sensory domain and an intracellular inhibitory domain (Gross *et al*., 1989; Leoni *et al.*, 2000).

E. coli σ^E was the first σ factor to be identified within this group and was initially regarded as a second heat shock σ factor (Wang and Kaguni, 1989). σ^E, however, is usually activated in response to a variety of periplasmic signals including intense heat shock as well as other stimuli resulting in conformational change of the outer-membrane proteins. It also has the ability to control the expression of proteases and folding catalysts that are usually active in the periplasm (Alba *et al.,* 2001).

There are a set of adjacent genes that are responsible for regulating the σ^E gene (*rpoE*): *rseA, rseB* and *rseC*. RseA is a transmembrane protein that functions as an anti-σ factor. RseB is a periplasmic protein that enhances the action of RseA (Alba *et al.*, 2001).

In unstressed cells, the RseA anti-σ factor sequesters σ^E. The high affinity between RseA and σ^E prevents the interaction of σ^E with RNAP (Campbell *et al*., 2003). σ^E is released from RseA as a result of a proteolytic cascade caused by the accumulation of unfolded peptides in the periplasm. There are two proteases involved in the proteolytic cascade process, DegS and RseP which act sequentially (Kanehara *et al*., 2002). The activity of DegS is induced by a signal released due to the presence of unfolded outer-membrane proteins located in the periplasm. The PDZ domain is cleaved from the periplasmic region of RseA by DegS as a result of the binding between the C-terminal peptides of the porins OmpC or OmpF and the PDZ domain. The tight binding between RseA and the periplasmic protein RseB protects RseA from proteolytic degradation (Cezairliyan and Sauer, 2007). It has therefore been reported that RseB can function as an LPS sensor; it can detect the mislocalised LPS which is accumulated in the periplasm (Lima *et al*., 2013). The LPS binding molecules cause the release of RseB from RseA making it susceptible to cleavage by DegS, first cleavage (site-1). The transmembrane segment (site-2) of RseA is then also cleaved by RseP. As a result, the cytoplasmic domain of RseA is released from σ^E. Subsequently, the cytoplasmic domain of RseA is degraded by cytoplasmic proteases of the CIpXP complex. Following this, free σ^E is able to interact with the core RNAP in order to start the transcription of σ^E regulon genes (Figure 1.8) (Flynn *et al*., 2003; 2004). Other ECF σ factors appear to have the ability to regulate virulence genes and virulence associated genes in different species of bacteria (Bashyam and Hasnain, 2004).

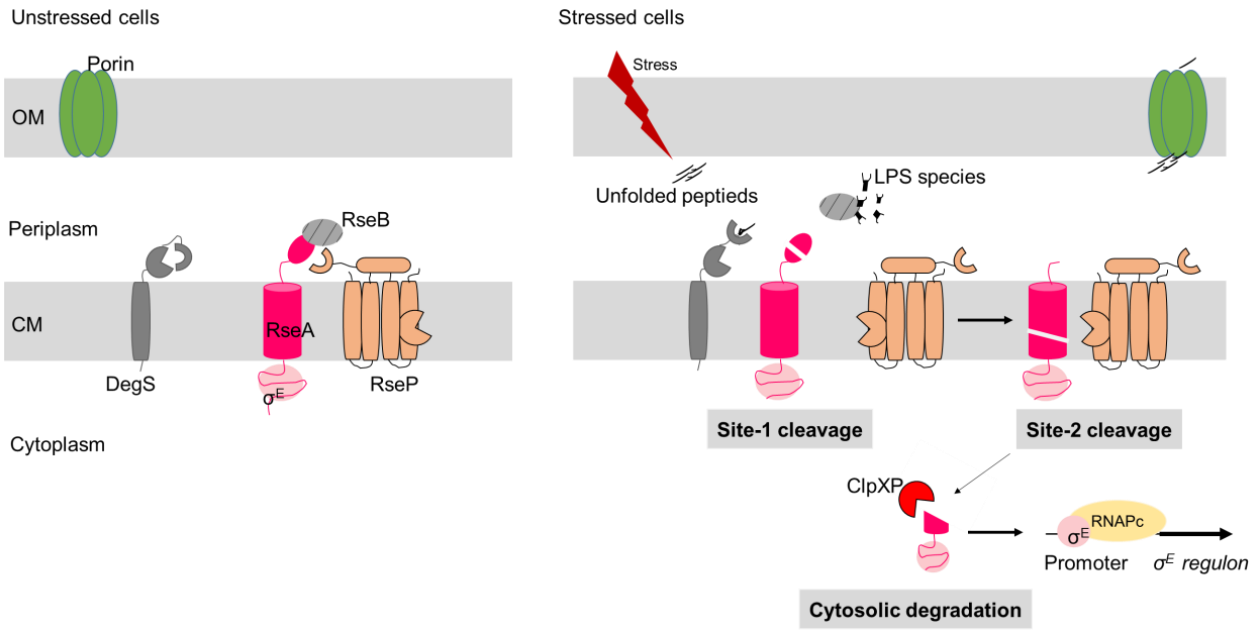

Figure 1-8: Activation of the *E. coli* ECF σ factor σ^E (RpoE) by cell envelope stress.

In unstressed cells, the binding between σ^E and RseA anti-σ factor inhibits the activity of σ^E. The DegS and RseP proteases are not active because of inhibitory interactions associated with their respective PDZ domains, the RseB protein and a glutamine-rich region of RseA. In stressed cells, however, the accumulation of unfolded proteins in the periplasm activates the DegS protease by binding to its PDZ domain. In the periplasm, the mislocalised LPS species displaces RseB from the RseA protein which allows cleavage of the periplasmic domain of the anti-σ factor by DegS (site-1 cleavage). RsePs then cleaves the transmembrane region of RseA (site-2 cleavage). The remaining cytoplasmic region of RseA is degraded by ClpXP proteases and σ^E is released in order to interact with the RNAP core enzyme and direct transcription of its target genes.

1.12 Bacterial ferric uptake regulator (Fur) protein and other metal dependent regulatory proteins

Iron uptake mechanisms are tightly regulated in order to prevent them from causing excessive accumulation of Fe^{2+} which would harm the cell, since it is able to produce toxic oxygen radicals through the Fenton reaction (Bagg and Neilands, 1987; Crosa, 1997). This regulation mostly occurs at the transcriptional level, and commonly involves an iron responsive transcription regulator protein. The ferric uptake regulator protein (Fur) is a global transcriptional regulator that responds to intracellular iron concentration in Gram-negative and Gram-positive bacteria. The Fur protein is 15-17 kDa in size with a high degree of amino acid sequence conservation. Fur protein binds to a single ferrous iron atom, dimerises and binds to the Fur box where it functions as a repressor that inhibits transcription of many iron-regulated genes (Gao *et al.*, 2008; Butcher *et al.*, 2011; Yu and Genco, 2012). The Fur box is a specific well conserved consensus sequence located in the promoter region of the target gene. The Fur protein binding at the Fur box blocks the binding of RNA polymerase (RNAP) and therefore represses transcription of the genes (Figure 1.9). Also, in some cases it has been found that Fur has the ability to repress gene transcription in the absence of a ferrous iron cofactor and this process is known as apo-Fur-mediated regulation (Gao *et al.*, 2008; Butcher *et al.*, 2011; Yu and Genco, 2012). Bfr is a ferritin-like protein containing both haem and iron (Quail *et al*., 1996). Fur binds to the bfr promoter and represses the expression of iron-storage proteins that have been shown to be directly regulated by apo-Fur (Delany *et al.*, 2001; Ernst *et al.*, 2005).

Moreover, in iron-replete conditions, a subset of genes is found to be upregulated, suggesting the ability of Fur to function as a transcriptional activator (Yu and Genco, 2012). It has been found, however, that Fur activates some genes indirectly through inhibition of a gene encoding a post-transcriptional repressor. Such a mechanism is found to be used by organisms such as *E. coli*, *P. aeruginosa* and *V. cholerae* (Masse *et al.*, 2003). The indirect positive regulation by Fur is often mediated by Fur-dependent repression of a small non-coding RNA (sRNA), RyhB. RyhB regulates gene expression by base pairing with mRNAs to trigger their degradation via RNase E and RNase III. In many bacteria, RyhB is involved in regulating various essential

cellular roles such as resistance to oxidative stress, TCA cycle activity and iron homeostasis in *E. coli* (Masse *et al.*, 2003; Huang *et al.*, 2012).

Moreover, genes encoding some activator proteins and iron starvation σ factors are regulated by Fur. For example, PchR is a Fur-regulated transcription activator protein that is required for the expression of pyochelin biosynthesis and transport genes in *P. aeruginosa* and *Burkholderia* species in iron-limited conditions (Heinrichs *et al*., 1991; Heinrichs and Poole, 1996). In the presence of iron-loaded pyochelin, PchR induces the Fur-regulated pyochelin receptor gene, *fptA* and the two Fur-regulated biosynthetic operons, *pchDCBA* and *pchEFGHI* (Reimmann *et al*., 1998; 2001). Fur indirectly causes transcription of iron-regulated genes in the absence of iron by this mechanism. The first description of the *E. coli* DNA binding consensus sequence for Fur (GATAATGATAATCATTATC) provided a greater understanding of the iron regulation mechanism associated with this protein and due to the high sequence conservation of the Fur protein, the 19 bp consensus sequence became the gold standard when comparing the Fur regulatory mechanism across all bacteria (Carpenter *et al.*, 2009).

Sheikh and Taylor. (2009) determined the crystal structure of Fur from *V. cholerae*. Fur proteins are composed of two domains, an N-terminal DNA-binding domain and a C-terminal dimerisation domain. The DNA-binding domain consists of four helices followed by a two-stranded antiparallel β-sheet. The C-terminal dimerisation domain of each Fur monomer is composed of α/β-domain in which three antiparallel β-strands cover one long α-helix, and importantly, they are associated with the formation of the functional protein dimer. The three-dimensional structure indicates two zinc ion (Zn^{2+}) binding sites per monomer (Figure 1.10) (Pohl *et al.*, 2003). The same study by Pohl *et al.* (2003) suggested that the binding sites (Zn1) and (Zn2) in *P. aeruginosa* Fur serve as the regulatory site and structural site, respectively. Under iron sufficient conditions, Fe^{2+} binds to the regulatory site. The *V. cholerae* Fur structure study, however, proposed that the Zn2 site is the regulatory iron binding site with the Zn1 site having a subsidiary role (Sheikh and Taylor, 2009). An *in vitro* study has suggested that, in addition to Fe^{2+}, there are a number of other divalent cations that can bind the regulatory metal binding site and inhibit the binding between Fur and DNA such as Zn (II) and Mn (II) (Bagg and Neilands, 1987; Mills and Marletta, 2005).

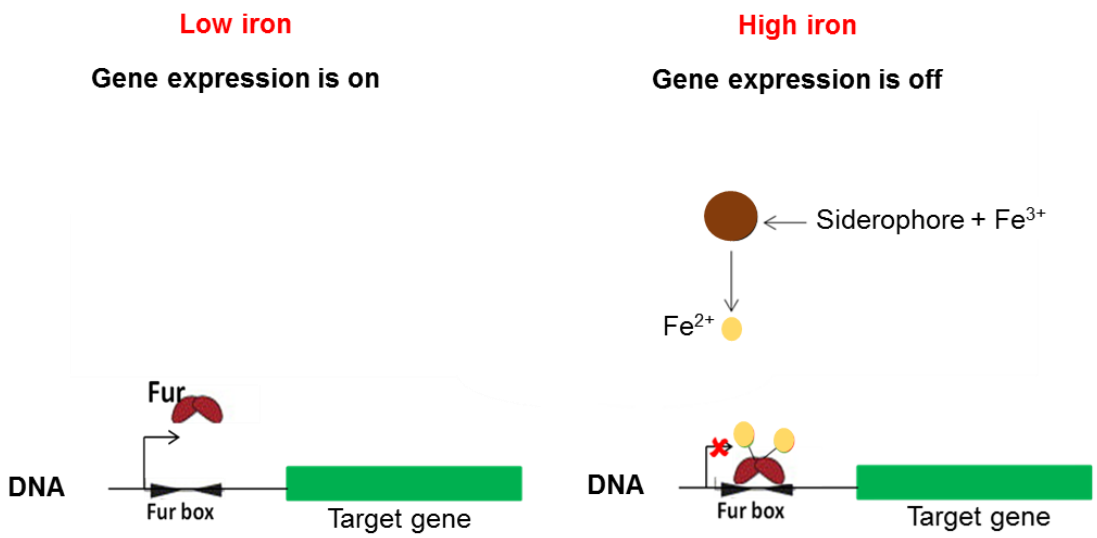

Figure 1-9:Mechanism of Fur (ferric uptake regulator) iron-dependent regulation.

In iron-limited conditions Fur is in the apo-form (not bound to iron) and cannot bind to a specific operator sequence known as the Fur box, located overlapping or downstream of the iron-regulated promoter. As a result, the target is actively transcribed (‘derepression’). When there is a high level of iron, however, the Fur dimer binds Fe^{2+} and then binds to the Fur box.

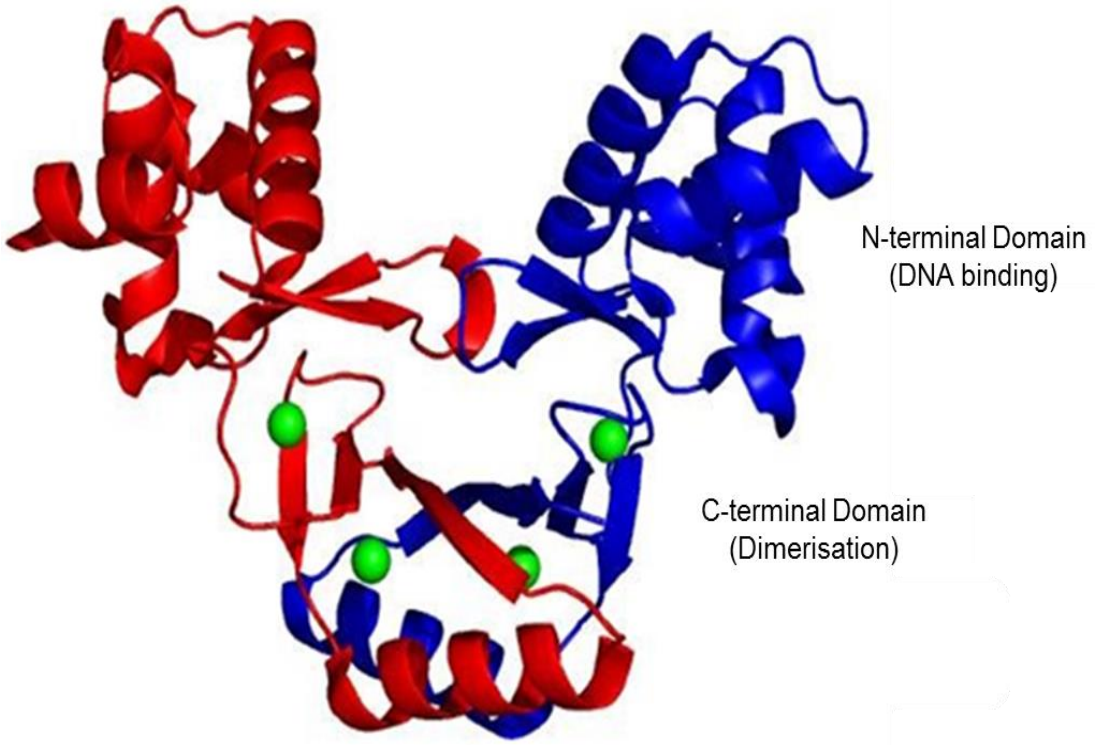

Figure 1-10:The three-dimensional structure of Fur from *V. cholerae*.

The Fur dimer crystal structure bound to four metal zinc ions are represented by green spheres. The image was generated using the PyMOL® Molecular Graphics System, Version 1.2r3pre, Schrödinger, LLC.

1.13 The iron starvation subgroup of ECF σ factors

Iron is an essential element that is required by bacteria to colonise and grow in any environment. Even when the free iron concentration in the host environment is very low, bacteria are capable of acquiring iron by high affinity iron-uptake systems. It has been mentioned previously that the most common mechanism that bacteria employ is utilisation of siderophores (Visca *et al*., 2002). Siderophores bind to iron outside the bacterium in order to transport it through an outer-membrane receptor into the Gram-negative bacteria cell. As discussed in Section 1.12, the Fur repressor regulates iron starvation σ factors which in turn regulate the iron acquisition system. Iron starvation σ factors systems are different from those of other ECF σ factors as the former require a TBDT (Section 1.9) to respond to a signal detected at the cell surface rather than periplasmic stress signals (Braun *et al*., 2003). For this reason, they are also referred to as cell surface signalling (CSS) systems (Breidenstein *et al*., 2006). *P. aeruginosa* (PvdS) and *E. coli* K-12 (FecI) are the most-studied examples of iron starvation ECF σ factors, although there are many others, some of which are discussed in more detail below.

1.13.1 *E. coli* FecI σ factor

Iron uptake in *E. coli* occurs through a variety of processes, including at least one siderophore which makes enterobactin and several xenosiderophores. One of the latter is citrate. Two molecules of citrate contain three ligands for ferric iron and give rise to an octahedral complex with a single iron atom to form ferric-dicitrate. The regulation of ferric citrate uptake is a well-studied example of a system involving an iron starvation σ factor (Braun *et al.*, 2003). Regulation of the ferric citrate transport system of *E. coli* K-12 is mediated by a σ factor known as FecI. In order for ferric citrate to be transported into the cell, FecA, an outer-membrane protein, is required. FecA transmits the signal from the outer-membrane to FecR located in the inner membrane. The *fecBCDE* genes encode an ABC transporter periplasmic binding protein system for translocation of ferric-citrate across the cytoplasmic membrane (Braun *et al.*, 2003). Through the TonB-ExbB-ExbD complex, FecA has the ability to derive energy for internalisation of ferric-citrate. The contact between FecA and TonB

occurs at the heptapeptide TonB-box sequence near the N-terminus of the TBDR and allows FecA to behave as an active transporter (Braun *et al.*, 2003).

FecR is a regulatory protein in the cytoplasmic membrane that binds to the FecI σ factor in order to regulate its activity. FecR has two domains: The N-terminal domain (NTD) and the C-terminal domain (CTD) located in the cytoplasm and periplasm, respectively. These two domains are highly conserved regions. The N-terminal region of FecA in the periplasm interacts with the C-terminal region of FecR. FecR contains a CTD leucine zipper sequence, and it has been suggested that this sequence plays a role in aiding the interaction between FecR and FecA. Due to the conformational and structural changes that occur in FecA the signal is transferred to FecR (Braun *et al.*, 2003; Breidenstein *et al.*, 2006). Through the C-terminal region of FecR, the information is transmitted by some unknown mechanism through the inner membrane to the NTD which consequently affects FecI. FecI is then activated to recruit RNA polymerase and bind to the *fecABCDE* operon, thus increasing the expression of the iron-citrate uptake genes. In normal conditions, however, FecR will inhibit FecI activity, and it will only activate it if ferric citrate binds to FecA (Ferguson *et al.*, 2002; Braun *et al.*, 2003).

The *fecI* and *fecR* regulatory genes are located upstream of the *fecABCDE* genes, and their regulation depends on the intracellular concentration of iron. Fur protein with Fe^{2+} loaded is able to bind to the *fecI* and *fecA* promoters and inhibit their expression. Under iron-limited conditions, the FecI and FecR proteins are synthesised. The *fecABCDE* genes will not be transcribed unless FecI is also activated by the presence of ferric citrate that binds to FecA (Figure 1.11) (Braun *et al.*, 2003).

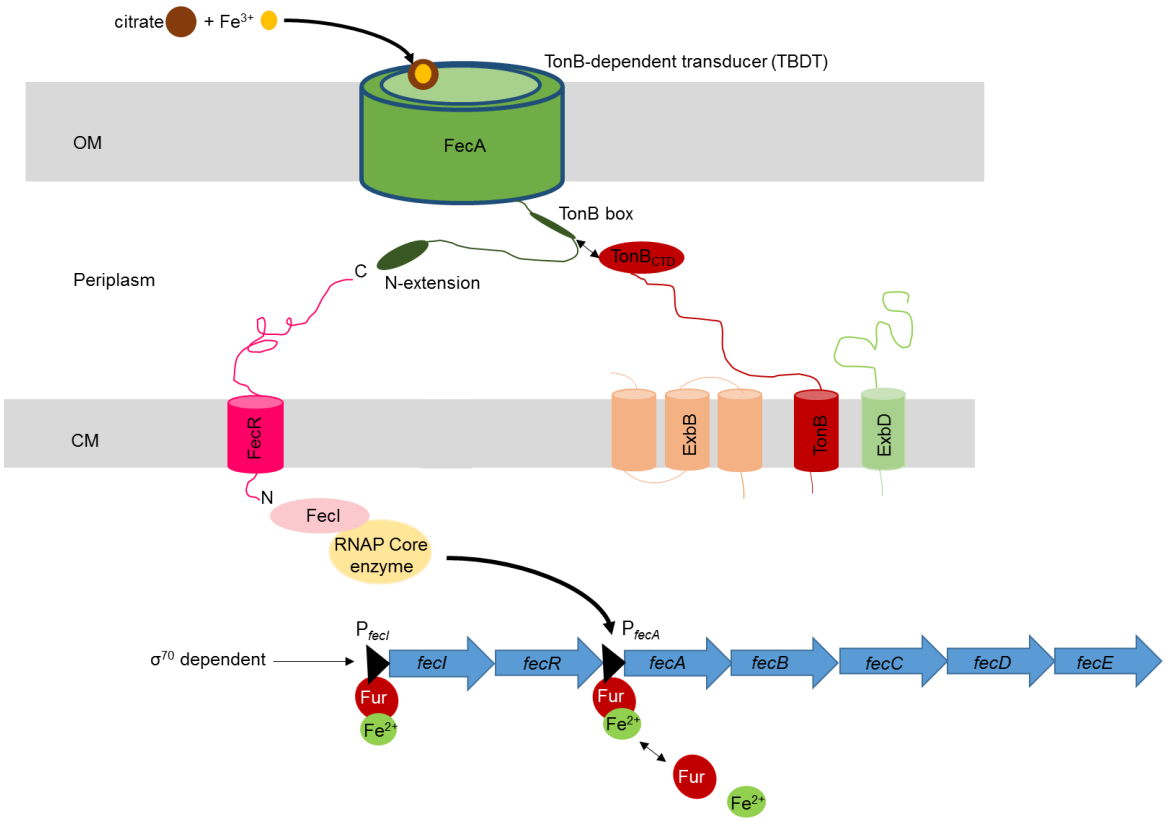

Figure 1-11: Regulatory model of the FecI system in *E. coli*.

The binding between FecA and ferric citrate stimulates the transcription of genes by the activation of the FecI σ factor by FecR. *fecI* and *fecR* are transcribed in the absence of iron but *fecABCDE* will only be transcribed in the absence of iron together with the presence of ferric-dicitrate.

1.13.2 *P. aeruginosa* σ factor PvdS

P. aeruginosa is a human pathogenic bacterium that produces a large number of virulence factors including siderophores. One of these siderophores is pyoverdine (PVD). PVD is a critical siderophore since it is an iron carrier and a bacterial signal molecule of virulence-related genes (Holloway, 1969; Visca *et al*., 2007). PVD is utilised by *P. aeruginosa* as the primary mechanism for acquiring iron. Synthesis of PVD is stimulated under low iron conditions. Negative control of PVD synthesis is regulated by the global regulator, Fur. PVD is repressed by Fur under high iron conditions (Ochsner *et al.,* 2002). PVD synthesis is also regulated by the siderophore PvdS which regulates the expression of *pvd* genes as well as the production of exotoxin A and the extracellular protease PrpL (Ochsner and Vasil, 1996; Wilderman *et al.*, 2001; Lamont *et al*., 2002). The *P. aeruginosa* genome includes three clusters of genes that are associated with pyoverdine biosynthesis, and a large number of these genes are *pvd* genes (Miyazaki *et al.,* 1995; Stintzi *et al.,* 1999; Ochsner *et al.,* 2002). PvdS, FpvI, FpvA and FpvR are regulatory proteins involved in the pyoverdine signal transduction pathway. FpvA is the ferric-pyoverdine receptor that has the N-terminal extension present in TBDTs (Leoni *et al.,* 2000). The anti-σ factor FpvR is responsible for controlling the activity of two σ factors, PvdS and FpvI, that are responsible for the transcription of pyoverdine biosynthetic genes and the gene encoding the ferric pyoverdine receptor, *fpvA*, respectively (Figure 1.12) (Redly and Poole, 2005).

The binding between PVD and ferric iron at the cell surface enhances the expression of *pvd* genes. The TBDT FpvA recognises the siderophore-iron complex. The signal is transmitted from the cell surface to the cytoplasm through the N-terminal extension of FpvA coming into contact with the periplasmic CTD of FpvR. The activation of FpvR subsequently causes the NTD to release PvdS which, in turn, binds to core RNA polymerase and directs it to the *pvdA* promoter and other *pvd* promoters (Shen *et al.*, 2002).

PvdS also activates transcription of the regulatory gene, *ptxR*. PtxR activates the *pvc* genes that are required for biosynthesis of the PVD chromophore. PvdS therefore indirectly activates some genes by activating transcription of an intermediary transcription activator (Stintzi *et al*., 1999; Visca *et al.,* 2002).

A study by Spencer *et al*. (2008) investigated the regulation of PvdS activity by the anti-σ factor FpvR. The data obtained from this study indicated that the reduction of PvdS levels in bacterial strains lacking PVD or FpvA is not because of the reduction of *pvdS* gene expression. It has been suggested that an increase in the proteolysis of PvdS following binding by FpvR is more likely to be the reason for the decrease in PvdS concentration. Recently, the signal transduction mechanism that is triggered by the binding of PVD to FpvA has been investigated (Draper *et al.*, 2011). It has been found that, in the presence of PVD, the anti-σ factor FpvR undergoes complete proteolysis that causes activation of the two σ factors PvdS and FpvI and this result in increased of gene expression for PVD synthesis and uptake. When there is no pyoverdine present the FpvR subfragments inhibit binding of PvdS and FpvI to core RNAP (Spencer *et al.*, 2008; Draper *et al.*, 2011).

1.13.3 The Fiu and Fox CSS systems

P. aeruginosa dose not only have the Fpv system, it also has twelve CSS systems, a large number of which are responsible for regulation of heterologous siderophore (xenosiderophore) uptake. Two examples of CSS systems used by *P. aeruginosa* are the Fox and Fiu CSS pathways (Llamas and Bitter, 2010; Llamas *et al*., 2014). The synthesis of the *P. aeruginosa* CSS receptors Fox and Fiu was found to be induced by the xenosiderophores ferrioxamine B (produced by *Streptomyces* species) and ferrichrome (produced by fungi), respectively (Llamas *et al*., 2006). The mechanism of these two systems shows many similarities to the Fec system of *E. coli*. σ^{FiuI} mediates expression of the *fiuA* receptor gene in response to ferrichrome and σ^{FoxI} mediates expression of the *foxA* receptor gene in response to ferrioxamine B (Llamas *et al*., 2006). The σ^{FoxI} and σ^{FiuI} genes are co-transcribed with those of their respective anti-σ factors FoxR and FiuR, respectively, and the expression of their genes is regulated by iron through Fur (Llamas *et al*., 2006). The function of *P. aeruginosa* FoxR and FiuR is similar to *E. coli* FecR; they act as a σ factor regulator that not only inhibit but are also required for σ factor activity (Mettrick and Lamont, 2009). The anti-σ factors of these CSS systems: FoxR, FiuR and FpvR are processed prior to the perception of the inducing signal in order to produce an N-terminal domain of ∼21 kDa and a C-terminal domain of ∼15 kDa. A protease seems to be responsible for this process which is known as initial cleavage. It is not yet clear how the two domains of

the anti-σ factor are separated. In the case of FoxR, the initial cleavage process occurs because of RseP protease which generates the N-terminal tail of FoxR (Llamas *et al*., 2006; Draper *et al*., 2011; Bastiaansen *et al*., 2015).

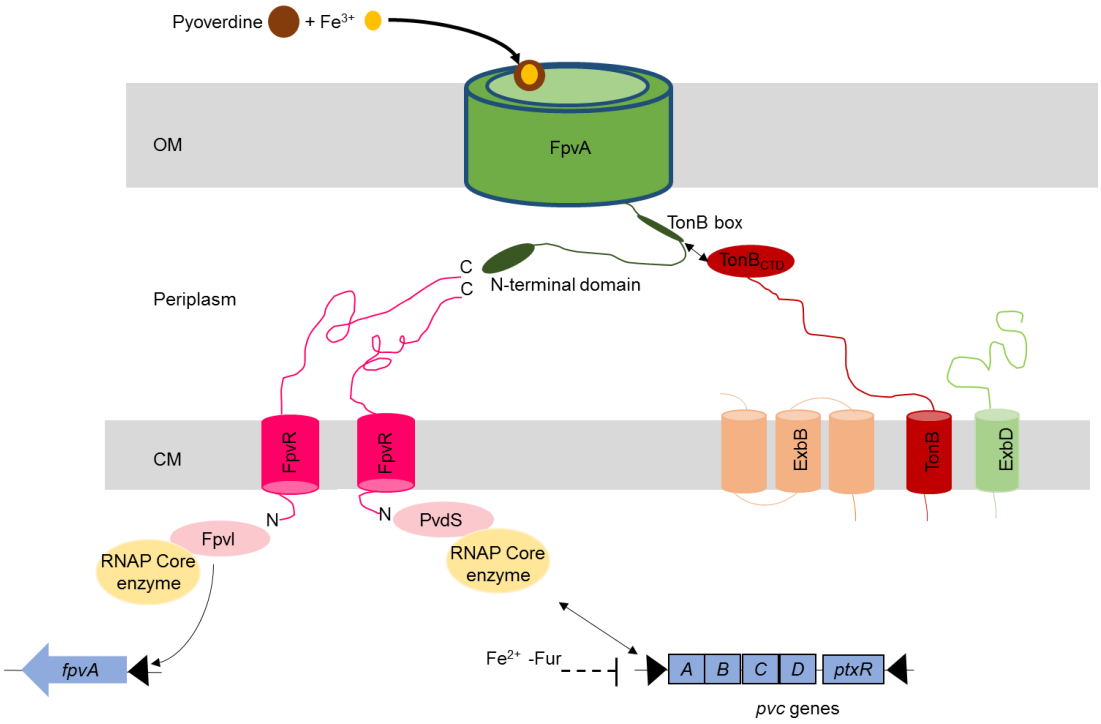

Figure 1-12: Structure of the pyoverdine regulatory system in *P. aeruginosa*.

The periplasmic domain of the FpvR anti-σ factor interacts with the N-terminal extension of the outer-membrane PVD receptor, FpvA, whereas the cytoplasmic domain of FpvR interacts with the σ factors PvdS and FpvI. FpvA also interacts with the TonB protein via its TonB box. FpvI activates the *fpvA* gene whereas PvdS activates *pvc* genes and *ptxR*.

1.13.4 The Flr system of *B. cenocepacia*

B. cenocepacia encodes 13 ECF σ factors, two of which are in the iron starvation subclass and involved in iron acquisition (Thomas, unpublished results; Menard *et al*., 2007). OrbS is one of these σ factors and is required for transcription of genes required for synthesis and transport of the siderophore ornibactin. This σ factor is unusual as it does not have an anti-σ factor or N-terminal extension. The other iron starvation σ factor is known as FlrS (Thomas, unpublished results). The *flr* operon of *B. cenocepacia* consists of four genes, *flrS, flrR, flrA* and *flrX* (Figure 1.13). *flrR* is located downstream of *flrS* and is predicted to encode an anti-σ factor. Downstream of *flrR* is *flrA* which codes for a TBDT for an unknown siderophore. The function of the *flrX* gene product has not been determined. The Flr system is analogous to the FecI system of *E. coli* but has no ABC transporter gene homologues downstream of *flrS, flrR* and *flrA*. This organisation is usually associated with the utilisation of a xenosiderophore, a siderophore produced by other microorganisms (Braun *et al.*, 2003). By analogy to the Fec system and other systems regulated by iron starvation σ factors, *B. cenocepacia* is proposed to use σ factor FlrS to regulate *flrA* and *flrX* genes (Thomas, unpublished results) (Figure 1.13). FlrA is predicted to be a TBDT since it has the characteristic N-terminal extension. Once a xenosiderophore binds to FlrA, FlrA transmits a signal across the outer membrane to FlrR, thus allowing the signal to pass to the σ factor FlrS which binds to core RNAP, forming the $E\sigma^{FlrS}$ RNAP holoenzyme that causes the activation of the *flrA* promoter (P_{flrA}) located between *flrR* and *flrA* (Figure 1.13). FlrR protein is hypothesised (from a BLAST search) to encode an anti-σ factor. Thus, FlrR would be expected to interact with FlrS. Normally, the group 4 σ factor C-terminal domain interacts with the anti-σ factor N-terminal cytoplasmic domain, meaning that an interaction between FlrR and FlrS and FlrR and FlrA would be expected. In the absence of a siderophore, FlrR might inhibit the σ factor by sequestering it or inducing its proteolysis. When the xenosiderophore binds to FlrA the σ factor may be released by FlrR. Alternatively, the presence of the siderophore may cause FlrR to activate FlrS, as occurs in some iron starvation σ factor systems.

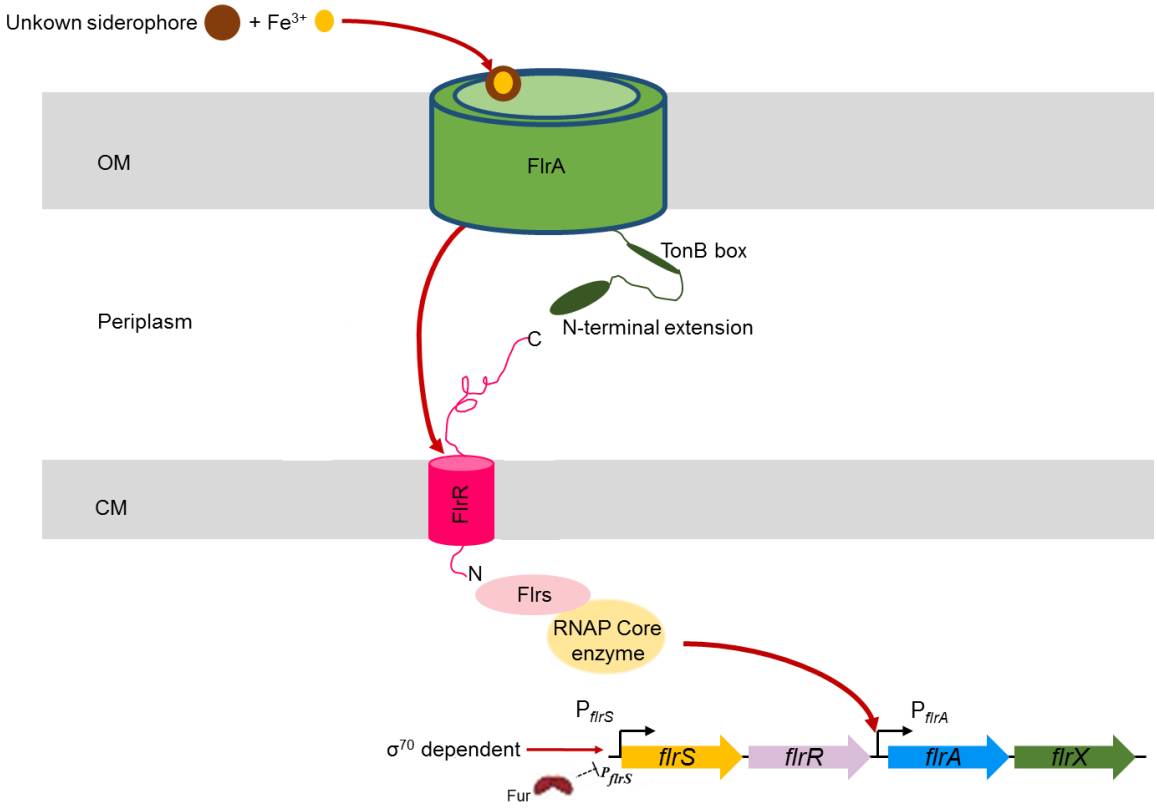

Figure 1-13: Model of the Flr system of *B. cenocepacia*.

FlrA is an outer-membrane receptor for an unknown siderophore complexed with iron. Upon ferric-siderophore binding, FlrA is predicted to transduce a signal to the anti-σ factor FlrR. This signal causes the activation or the release of σ factor FlrS by an unknown mechanism. FlrS is predicted to be required for the transcription of *flrA* and *flrX*. The red arrows indicate unknown mechanisms of regulation in the Flr system.

Hypothesis

- FlrA is a TBDT that is requestable for the uptake of a xenosiderophore complex with iron.

- FlrR regulates FlrS in response to the binding of an unknown ferric-siderophore complex to FlrA. Therefore, FlrR interacts with FlrA and FlrS.

- σ^{70} and putative σ^{FlrS} recognise a specific promoter sequence located upstream of *flrS* and *flrA* respectively.

- FlrS orthologues in *P. aeruginosa* and *P. syringae* are proposed to have switched their roles. *flrS*, *PA3899* of *P. aeruginosa* and *PSPTO1209* of *P. syringae* encoded homologous σ factors and therefore their predicted promoters P_{flrA}, P_{PA3901} and $P_{PSPTO1207}$ are predicted to be recognized by these σ factors. However, the adjacent TBDT genes are non-orthologous.

Aims

- To investigate the interaction between the σ factor FlrS and the anti-σ factor FlrR. Particularly, to investigate the interaction between the C-terminal domain of FlrS and the N-terminal domain of the putative anti-σ factor FlrR.

- To show FlrR interaction with FlrA.

- To investigate the role of FlrR in regulating the σ factor FlrS, i.e. FlrR is required to activate FlrS under inducing conditions.

- Determine the location and DNA sequence elements in the P_{flrA} promoter that are recognized by FlrS.

- Investigate the functional equivalence of FlrS and homologous σ factors from *Pseudomonas* species.

- To determine the location of P_{flrS} promoter.

- To investigate whether the activity of P_{flrS} is regulated by Fur.

- Attempt to identify the xenosiderophore that is transported by FlrA, i.e. to demonstrate that FlrA is a TBDT and establish the inducing signal.

Chapter 2 Materials and Methods

2.1 Bacterial strains and plasmids

Table 2-1: Bacterial strains used in this study

Bacterial strains	Description	Reference
E. coli		
JM83	F$^-$*ara Δ (lac-proAB) rpsL ϕ80dlacZΔM15* (Sm^R)	Yanisch-Perron *et al*., 1985
MC1061	*hsdR araD139 Δ(ara-leu)7697 ΔlacX74 galUgalK rpsL* (Sm^R)	Casadaban and Cohen, 1979
BTH101	F$^-$, *cya-99 araD139 galE15 galK16 rpsL1* (Tc^R) *hsdR2 mcrA1 mcrB1*	Karimova *et al.,* 1998
CC118(*λpir*)	*araD139 Δ (ara-leu) 7697 ΔlacX74galEgalK phoA20 thi-1rpsE argE*(am) *recA1 λpir rpoB* (Rf^R)	Timmis *et al*., 1990
SM10(*λpir*)	*thi-1 thr leu tonA lacY supE recA* RP4-2- Tc: Mu (Km^R) (*λ pir*)	Simon *et al*., 1983
S17-1(*λpir*)	S17-1 lysogenized with *λpir*	Miller, 1972
BL21(λDE3)	F$^-$*ompT hsd*S$_B$ ($r_B^- m_B^+$) *dcmgal*λ(DE3)	Moffatt *et al*., 1986
C41(λDE3)	Spontaneous mutants of BL21(λDE3)	Miroux *et al*., 1996
C43(λDE3)	Spontaneous mutants of BL21(λDE3)	Miroux *et al*., 1996
QC1732	F$^-$Δ(*argF-lac*) *U169rpsL*Δ*fur*::*kan* (Sm^R Km^R)	Touati *et al*., 1995
H1717	*aroB fhuF*:λp*lac*Mu53	Hantke, 1987
B. cenocepacia		
H111	CF isolate, prototroph (Orb$^+$ Pch$^+$)	Huber *et al*., 2001
715j	CF isolate, prototroph	McKevitt *et al*., 1989; Darling *et al*., 1998
AHA27	715j *pobA* mutant	Asghar *et al*., 2011

AHA27-*flrA*::Tp	AHA27 containing Tp^R cassette inserted in *flrA* (Orb^-Pch^-)	Sofoluwe, 2017
H111Δ*pobA*	H111 containing in-frame deletion within *pobA* (Orb^- Pch^-)	Huessin, 2017
H111Δ*pobA*/*flrA*::Tp	H111Δ*pobA* containing Tp^R cassette inserted in *flrA*	This Study
H111Δ*pobA*/*flrA*::Tp/*BCAL2339*::Cm	H111Δ*pobA* containing Tp^R cassette inserted in *flrA* and Cm^R cassette inserted in *BCAL2339*	This Study
HIIIΔ*fur*::Tp	HIIIΔ*fur* with Tp^R cassette inserted in *fur*	Aaron Butt
P. aeruginosa		
P. aeruginosa PAO1	Prototroph, WT isolate	Stover *et al*., 2000

Table 2-2: Plasmids used in this study

Plasmid	Description	Reference
pBBR1MCS2	Mobilisable broad host-range cloning vector (Km^R)	Kovach *et al*., 1994
pKAGd4	Broad host-range *lacZ* transcriptional fusion vector (Cm^R, Ap^R)	Agnoli *et al*., 2006
pBBR2-FlrSR	pBBR1MCS2 carrying *B. cenocepacia flrS* and *flrR* genes in same orientation as *lacZ* promoter	Paleja, 2007
pBBR2-$FlrR_{NTD}$	pBBR2 carrying *B. cenocepacia flrR* gene encoding N-terminal domain in same orientation as *lacZ* promoter	This study
pBBR2-$FlrSR_{NTD}$	pBBR1MCS2 carrying segment of *B. cenocepacia flrS* gene and segment of *flrR* gene encoding N-terminal domain in same orientation as *lacZ* promoter	This study
pBBR2-PA3899	pBBR1MCS2 carrying *P. aeruginosa PA3899* gene	Yunrui, 2010
pBBR2-PA0149	pBBR1MCS2 carrying *P. aeruginosa PA0149* gene	This study
pKAGd4-P_{PA0151}	pKAGd4 carrying *P. aeruginosa* promoter PA0151(Cm^R, Ap^R)	Yunrui, 2010
pKAGd4-P_{PA3901}	pKAGd4 carrying *P. aeruginosa* promoter PA3901(Cm^R, Ap^R)	Yunrui, 2010
pKAGd4-$P_{PSPTO1207}$	pKAGd4 carrying *P. syringae* promoter 1207 (Cm^R, Ap^R)	This study
pKAGd4-P_{flrA}	pKAGd4 carrying *B. cenocepacia* promoter P_{flrA} (Cm^R, Ap^R)	Yunrui, 2010
pBBR2-FlrS	pBBR1MCS2 carrying *B. cenocepacia flrS* gene in same orientation as *lacZ* promoter	Mohanlal, 2007
pKT25	Vector for generating N-terminal CyaA T25 fusions to the protein of interest, ori p15A (Km^R)	Karimova *et al.,* 2001
pKNT25	Vector for generating C-terminal CyaA T25 fusions to the protein of interest, ori p15A (Km^R)	Karimova *et al.,* 2001

pUT18	Vector for generating C-terminal CyaA T18 fusions to the protein of interest, ori ColE1 (Ap^R)	Karimova *et al.,* 2001
pUT18C	Vector for generating N-terminal CyaA T18 fusions to the protein of interest, ori ColE1 (Ap^R)	Karimova *et al.,* 2001
pKT25-*Zip*	A derivative of pKT25 in which the leucine zipper is genetically fused in-frame to the T25 fragment (Km^R)	Karimova *et al.,* 2001
pUT18C-*Zip*	A derivative of pUT18C in which the leucine zipper of GCN4 is genetically fused in-frame to the T18 fragment (Ap^R)	Karimova *et al.,* 2001
pUT18-$FlrS_{CTD}$	pUT18 *B. cenocepacia* encoding C-terminal domain of FlrS	Haldipurkar, 2012
pUT18-$FlrR_{NTD}$	pUT18 *B. cenocepacia* encoding N-terminal domain of FlrR	Haldipurkar, 2012
pUT18C-$FlrS_{CTD}$	pUT18C *B. cenocepacia* encoding C-terminal domain of FlrS	This study
pUT18C-$FlrR_{NTD}$	pUT18C *B. cenocepacia* encoding N-terminal domain of FlrR	This study
pKT25-$FlrS_{CTD}$	pKT25 *B. cenocepacia* encoding C-terminal domain of FlrS	Haldipurkar, 2012
pKT25-$FlrR_{NTD}$	pKT25 *B. cenocepacia* encoding N-terminal domain of FlrR	This study
pKNT25-$FlrS_{CTD}$	pKNT25 *B. cenocepacia* encoding C-terminal domain of FlrS	Haldipurkar, 2012
pKNT25-$FlrR_{NTD}$	pKNT25 *B. cenocepacia* encoding N-terminal domain of FlrR	Haldipurkar, 2012
pKT25-$FlrR_{CTD}$	pKT25 *B. cenocepacia* encoding C-terminal domain of FlrR	This study
pKNT25-$FlrR_{CTD}$	pKNT25 *B. cenocepacia* encoding C-terminal domain of FlrR	This study
pUT18-$FlrR_{CTD}$	pUT18 *B. cenocepacia* encoding C-terminal domain of FlrR	This study
pUT18C-$FlrR_{CTD}$	pUT18C *B. cenocepacia* encoding C-terminal domain of FlrR	This study
pKT25-$FlrA_{NTD}$	pKT25 *B. cenocepacia* encoding N-terminal domain of FlrA	This study

pKNT25-FrA_{NTD}	pKNT25 *B. cenocepacia* encoding N-terminal domain of FlrA	This study
pUT18-$FlrA_{NTD}$	pUT18 *B. cenocepacia* encoding N-terminal domain of FlrA	This study
pUT18C-$FlrA_{NTD}$	pUT18C *B. cenocepacia* encoding N-terminal domain of FlrA	This study
pKT25-FlrR	pKT25 *B. cenocepacia* encoding the full length *flrR*	This study
pUT18C-FlrR	pUT18C *B. cenocepacia* encoding the full length *flrR*	This study
pSHAFT2-*flrR*::Tp	pSHAFT2 containing *B. cenocepacia flrR* gene inactivated with a Tp^R cassette	This study
pSHAFT2	Mobilisable suicide vector derived from pUT, ori_{R6K} (Ap^R Cm^R)	Shastri, 2010
pKAGd4-P_{flrA}ds1	pKAGd4 containing 44 bp *flrA* promoter	Paleja, 2009
pKAGd4-P_{flrA}ds2-ds11	pKAGd4-P_{flrA}ds1 with single base pair substitutions at positions 2-10, respectively	Paleja, 2009
pKAGd4-P_{flrA}ds12-ds45	pKAGd4-P_{flrA}ds1 with single base pair substitutions at positions 11-44, respectively	Yunrui, 2010
pKAGd4-P_{flrA}UP	pKAGd4 containing UP element of P_{flrA}-*lacZ* fusion (Cm^R)	Paleja, 2009
pKAGd4-P_{flrA} intermediate	pKAGd4 containing intermediate element of P_{flrA}-*lacZ* fusion (Cm^R)	Paleja, 2009
pKAGd4-P_{flrA}short	pKAGd4 containing short element of P_{flrA}-*lacZ* fusion (Cm^R)	Paleja, 2009
pKAGd4-P_{flrA}vshort	pKAGd4 containing very short P_{flrA}-*lacZ* fusion (Cm^R)	Paleja, 2009
pKAGd4-P_{flrA}v.vshort	pKAGd4 containing very. very short element of P_{flrA}-*lacZ* fusion (Cm^R)	Paleja, 2009
pKAGd4-P_{flrA}core	pKAGd4 containing core element of P_{flrA}-*lacZ* fusion (Cm^R)	Paleja, 2009
pACYCDuet-1	Expression vector containing two MCS each proceeded by a T7 promoter/lac operator and RBS. p15A origin of replication	Novagen
pACYCDuet-1-His_6-$FlrS_{CTD}$	pACYCDuet-1 containing $FlrS_{CTD}$ with an N-terminal His tag cloned between the *Pst*I and *Bam*HI sites (Cm^R)	This study

pACYCDuet-1-His_6-$FlrR_{CTD}$	pACYCDuet-1 containing DNA fragment encoding $FlrR_{CTD}$ cloned between the *Bam*HI and *Pst*I sites (Cm^R)	This study
pACYCDuet1-1-$FlrR_{NTD}$-VSVg	pACYCDuet-1 containing DNA fragment encoding $FlrR_{NTD}$ with a C-terminal VSVg tag cloned between the *Nde*I and *Bgl*II sites (Cm^R)	This study
PACYCDuet-1-VSVg-$FlrA_{NTD}$	pACYCDuet-1 containing DNA fragment encoding $FlrA_{NTD}$ with an N-terminal VSVg tag cloned between the *Nde*I and *Bgl*II sites (Cm^R)	This study
pACYCDuet-1-His_6-Full-length FlrS	pACYCDuet-1 containing DNA fragment encoding full-length FlrS with an N-terminal His tag cloned between the *Bam*HI and *Hin*dIII sites (Cm^R)	This study
pETDuet -1	*E. coli* T7 expression vector, pBR322-derived ColE1 replicon, two T7 promoter/lac operator regions proceeding two MCS, lacI. (Ap^R)	Novagen
pETDuet-1-His_6-$FlrR_{NTD}$	pETDuet-1 containing DNA fragment encoding $FlrR_{NTD}$ with a C-terminal His tag cloned between the *Noc*I and *Bgl*II sites (Cm^R)	This study
pMALc5X	*E. coli* vector containing ampicillin resistance genes (*bla*) and *malE* gene (encoding MBP) under control of the tac promoter (Ap^R)	New England Biolabs
pMALc5X-$FlrR_{NTD}$-VSVg	pMALe5x containing DNA fragment encoding $FlrR_{NTD}$ with an N-terminal VSVg tag cloned between the *Nde*I and *Bam*HI sites (Ap^R)	This study
pMALc5X-$FlrA_{NTD}$-VSVg	pMALe5x containing DNA fragment encoding $FlrA_{NTD}$ with an N-terminal VSVg tag cloned between the *Nde*I and *Bam*HI sites (Ap^R)	This study
pMALc5X.His_6-$FlrR_{NTD}$	pMALe5x containing DNA fragment encoding $FlrR_{NTD}$ with an N-terminal His tag cloned between the *Nde*I and *Bam*HI sites (Ap^R)	This study
pKAGd4-$P_{flrSlong}$	pKAGd4 containing $P_{flrSlong}$ *lacZ* fusion (Cm^R)	Jithu, 2007

pKAGd4-$P_{flrSintermediate}$	pKAGd4 containing $P_{flrSinter}$ *lacZ* fusion (Cm^R)	Jithu, 2007
pKAGd4-$P_{flrSshort}$	pKAGd4 containing $P_{flrSshort}$ *lacZ* fusion (Cm^R)	Jithu, 2007
pKAGd4-$P_{flrSvshort-11G}$	pKAGd4 containing $P_{flrSveryshort-11G}$ *lacZ* fusion (Cm^R)	This study
pKAGd4-$P_{flrSveryshort}$	pKAGd4 containing $P_{flrSveryshort}$ *lacZ* fusion (Cm^R)	This study
pKAGd4-P_{flrA}triT1	pKAGd4 containing P_{flrA}triT1 *lacZ* fusion (Cm^R)	This study
pKAGd4-P_{flrA}triT2	pKAGd4 containing P_{flrA}triT2 *lacZ* fusion (Cm^R)	This study
pKAGd4-P_{flrA}triT3	pKAGd4 containing P_{flrA}triT3 *lacZ* fusion (Cm^R)	This study
pKAGd4-P_{flrA}triTX	pKAGd4 containing P_{flrA}triTX *lacZ* fusion (Cm^R)	This study
pKAGd4-P_{flrA}triTXSP	pKAGd4 containing P_{flrA}triTXSP *lacZ* fusion (Cm^R)	This study
pKAGd4-P_{flrA}triTSP	pKAGd4 containing P_{flrA}triTSP *lacZ* fusion (Cm^R)	This study
pBluescript II KS	*E. coli* specific cloning vector (Ap^R)	Alting-Mees and Short, 1989
pBluescript II KS-$P_{flrSvshort}$	pBluescript II KS containing DNA fragment encoding $P_{flrSvshort}$ promoter	This study
p3ZFBS	pGEM3Z containing consensus *E. coli* Fur binding site (Ap^R)	Vanderpool and Armstrong, 2001
pRLG770	*E. coli* vector, *rrnB* terminator, Ap^R, used for *in vitro* transcription analysis	Ross W *et al.,* 1990
pRLG770-P_{flrA}	pRLG770 containing DNA fragment encoding P_{flrA} promoter cloned between the *Bam*HI and *Hin*dIII sites (Ap^R)	This study
pSHAFT.GFP-*flrA*::Tp	pSHAFT-GFP containing Tp^R cassette inserted into *flrA* of *B. cenocepacia*	Sofoluwe, 2014
pSHAFT.GFP-*BCAM2439*	pSHAFT-GFP containing *BCAM2439* of *B. cenocepacia*	Sofoluwe, 2014
pSHAFT.GFP-*BCAL2439*::Cm	pSHAFT-GFP containing *BCAL2439* of *B. cenocepacia* with Cm cassette inserted into the *Zra*I site	This study

p34E-Cm2	p34E-Km derivative containing *cat* gene with synthetic promoter cloned between *Eco*RI site. (Ap^R, Cm^R)	Shastri, 2011

Cm^R, chloramphenicol resistance; Km^R, kanamycin resistance; Rf^R, rifampicin resistant; SmR, streptomycin resistant; Ap^R; Ampicillin resistance; Tp^R, trimethoprim; Pch, pyochelin phenotype; Orb, ornibactin phenotype.

2.2 Bacteriological Media

For the cultivation of bacteria in this study, the following types of Media were used. Sigma, Melford or Oxoid supplied the chemicals.

2.2.1 Luria-Bertani (LB) broth and agar

10 g tryptone, 5 g yeast extract and 10 g sodium chloride, were dissolved in 1 litre of distilled water. The mixture was then sterilized by autoclaving for 20 minutes at 120^{o}C/16 psi and stored at room temperature.

2.2.2 LB agar

15 g agar was added to 1 litre of prepared LB before autoclaving for 20 minutes at 120^{o}C/16 psi. After autoclaving, the mixture was allowed to cool to 55-60°C whereupon the antibiotics were added when required. The LB agar was poured into Petri dishes. The dishes were kept on the bench to allow the agar to solidify and then dried before use.

2.2.3 MacConkey-maltose agar

To make MacConkey agar, 43 g of MacConkey Agar Base powder (Difco) was added to 1 litre of distilled water and then mixed well to dissolve all the powder. The mixture was then sterilized by autoclaving for 20 minutes at 120^{o}C/16 psi. After the mixture had cooled down to ~ 60°C maltose was added to final concentration of 1% (w/v).

2.2.4 IST broth and IST agar

To make IST broth, 23.4 g of Oxoid Iso-sensitest was added to 1 litre distilled water. The solution was mixed well to ensure that all the powder dissolved. The mixture was then autoclaved for 20 minutes at 120^{o}C/16 psi. IST agar was made by solidifying IST broth with 1.5 % (w/v) agar (Oxoid). To prepare IST agar, 2.34 g of IST powder was added to 100 ml of H_2O, the solution was sterilized by autoclaving for 20 minutes at 120^{o}C/16 psi.

2.2.5 Brain-heart infusion (BHI) broth and agar

To make 1 litre of BHI broth, 43 g of BHI broth powder was added to 1 litre of distilled water. Aliquoted and sterilized by autoclaving for 20 minutes at 120^{o}C/16 psi. To make BHI agar plates, 15 g of BHI agar powder was added to 1 litre of BHI broth and sterilized by autoclaving for 20 minutes at 120^{o}C/16 psi.

2.2.6 M9-CAA agar

The M9 minimal salts medium was prepared by adding 0.2 g of casamino acids and 1.5 g agar to 90 ml of distilled water and then the mixture was autoclaved for 20 minutes at 120^{o}C/16 psi. The mixture was left to cool down to approximately 60°C and the following were added to the mixture:

10 ml 10× M9 salts

0.1 ml 1M $MgSO_4$

0.1 ml 0.1M $CaCl_2$

The 10× M9 salts were prepared in 1 litre of distilled water by adding the following components:

60 g Na_2HPO_4

30 g KH_2PO_4

5 g NaCl

10 g NH_4Cl

All the above components were autoclaved for 20 minutes at 120^{o}C/16 psi.

2.2.7 Auto-induction media

To prepare Auto-induction medium for testing protein expression the following components were added to 400 ml of H_2O: 2.4 g Na_2HPO_4, 1.2 g of $NHPO_4$, 8 g tryptone, 2 g yeast extract and 2 g NaCl. The mixture was autoclaved for 20 minutes at 120^{o}C/16 psi. After the mixture cool down the following components were added; 4 ml of 60% glycerol, 2 ml of 10% glucose and 10 ml of 8% lactose.

2.3 Antibiotics

All antibiotics used in this study are listed below:

Ampicillin was made to a concentration of 100 mg/ml in distilled water; filter sterilized and stored at -20°C.

Chloramphenicol was made to a concentration of 25 mg/ml in 100% ethanol and stored at -20°C.

Kanamycin was made to a concentration of 25 mg/ml in distilled water; filter sterilized and stored at -20°C.

Trimethoprim was made to a concentration of 25 mg/ml in DMSO and stored at -20°C.

Tetracycline (Tc) Tc powder was dissolved in water to make a concentration of 40 mg/ml. To make the final concentration 20 mg/ml, an equal amount of absolute ethanol was added and the stock solution stored at -20°C.

Table 2-3: Antibiotic concentrations used in this study

Antibiotics	**Concentration in media (µg/ml)**	
	E. coli	***B. cenocepacia***
Ampicillin	100	n/a
Chloramphenicol	25	25
Kanamycin	50	n/a
Trimethoprim	25	25

2.4 Media supplements

2,2'-dipyridyl a 0.1 M solution was made by dissolving 0.16 g 2,2'-dipyridyl in 10 ml of absolute ethanol.

0.1M Ferric chloride 0.162 g of $Fecl_3$ powder was dissolved in 10 ml of 10 mM hydrochloric acid to make a concentration of 0.1 M of $Fecl_3$. The solution was filter sterilized and stored in a dark place at room temperature.

IPTG a 0.1 M solution was made by dissolving 0.24 g IPTG in 10 ml distilled water and filter sterilized using a 0.22 μm syringe filter.

X-gal a 20 mg/ml solution was made by dissolving 20 mg of X-gal powder in 1 ml of DMSO.

Ethylenediaminedi (o-hydroxyphenylacetic) acid (EDDHA)

EDDHA powder was dissolved in 1 M NaOH to make concentration of the stock solution 30 mg/ml. The stock stored at 4°C.

Table 2-4: Supplement concentrations used in this study

Supplement	Concentration in media	
	E. coli	***B. cenocepacia***
2,2'-dipyridyl	175 μM	n/a
IPTG	0.1 mM	n/a
X-gal	25 μg/ml	n/a

2.5 Recombinant DNA techniques

2.5.1 Plasmid DNA isolation

Two methods were used to prepare small amounts of plasmid DNA in this study. The most commonly used technique was a phenol-chloroform method. Plasmids that were to be sequenced were isolated by a Mini-column method.

Plasmid DNA preparation: alkaline lysis with phenol-chloroform method

Bacterial cultures were inoculated from a fresh colony growing on agar in 2 ml of suitable medium with an appropriate antibiotic. The bacterial culture was incubated overnight at 37°C with aeration. The following day, 1.5 ml of overnight bacterial culture was transferred into a sterile 1.5 ml micro-centrifuge tube; the bacterial pellet was harvested by centrifugation at 13,000 x *g* for 5 minutes. The supernatant was gently aspirated out of the tube and discarded. The cell pellet was resuspended in 100 µl ice cold Solution I and then kept on ice for 10 minutes. 200 µl of Solution II was added and the contents were gently mixed by inverting the tubes, the tubes were stored on ice for a further 5 minutes. 150 µl of Solution III was added to the mixture and mixed immediately, forming a white precipitate. The tubes were left on ice for a further 5 minutes, after which the tubes were centrifuged at 13,000 x *g* for 5 minutes. The supernatant was transferred carefully to a new 1.5 ml micro-centrifuge tube. 400 µl of phenol-chloroform was added to the supernatant and the mixture was vortexed. The solution was then centrifuged at maximum speed for 3 minutes. The top layer was carefully transferred into a new 1.5 ml micro-centrifuge tube. Two volumes (800 µl) of 100% ethanol were added to the supernatant and mixed briefly. The tubes were then incubated at room temperature for 30 minutes to allow nucleic acids to precipitate. Following this, the solutions were centrifuged at maximum speed for 5 minutes at room temperature. The supernatant was gently aspirated off and discarded.1 ml of 70% ethanol added and the solution was mixed by pipetting several times. The contents were centrifuged at maximum speed for 5 minutes at room temperature, the supernatant was completely removed and the pellet was air-dried for 60 minutes. The pellet was resuspend in 50 µl of sterile distilled water. The DNA was stored at -20°C.

Solution I

50 mM glucose

25 mM Tris-HCl (pH 8)

10 mM EDTA (pH 8)

The above components were mixed together and autoclaved and stored at 4°C. This solution was prepared by preparing these solutions as separate stocks; 1 M TrisHCl, pH 8.0 and 0.5 M EDTA, pH to 8.0. This solution was diluted to the require concentration and autoclaved.

Solution II

0.2 M NaOH

1% (w/v) SDS

The solution stored at room temperature without autoclaving.

Solution III

60 ml of 5 M potassium acetate

11.5 ml of Glacial acetic acid

28.5 ml of distilled water

The mixture autoclaved and stored at 4°C.

Mini-column method

The QIAprep Miniprep kit was used according to the manufacturer's instruction. To determined nucleotide sequence integrity, the plasmid was sequenced by the Core Genomics Facility, University of Sheffield.

2.5.2 Agarose gel electrophoresis

Agarose gels were prepared depending on the DNA sample size. In order to prepare an agarose gel, 0.8-1 g of agarose powder was mixed in 100 ml of TAE buffer. The mixture was heated in the microwave oven until boiling and completely melted. The agarose mixture was poured into a gel tray and the comb was placed to form wells, allowing the gel to solidify at room temperature. The comb was then removed and the tray was placed into an electrophoresis tank containing TAE buffer, the gel was completely submerged in the buffer. The samples were loaded into the wells and ran at 100 volts for 1 hour or until the loading dye migrated to 75% of the gel. The gel was incubated in ethidium bromide solution (0.5 µg/ml) for 30 minutes, with agitation. Excess ethidium bromide was removed by washing the gel three times in water. The DNA bands were then visualized on a UV transilluminator and the gel image was taken using a gel capturing system (Kodak).

Preparing TAE buffer

In order to prepare (50×) stock solution of TAE buffer the following were combined:
242 g Tris base
57.1 ml glacial acetic acid
100 ml of 0.5 M EDTA (pH 8.0)
All components were dissolved in milliQ water and the final volume was made up to 1 litre. The solution was kept at room temperature. 1× TAE was made by diluting the solution 50× with milliQ water.

2.5.3 DNA ladders used in this study

Supercoiled DNA ladder (1µl) (Biolabs) was used for determining the size of plasmid DNA, and Qstep4 DNA ladder (5 µl) (York Biosciences) was used for linear DNA.

2.5.4 Polymerase chain reaction (DNA amplification) for cloning:

KOD polymerase

In order to amplify a required region of DNA, KOD polymerase was used due to its proofreading activity. The resulting products were used for further cloning purposes. The following components were combined:

Table 2-5: PCR components for reactions using KOD polymerase

Component	Amount (µl)
Template DNA	3.0 µl
10× KOD buffer	5.0 µl
DMSO	2.4 µl
50 mM $MgSO_4$	2.0 µl
10 µM Forward primer	3.0 µl
10 µM Reverse primer	3.0 µl
KOD polymerase	0.5 µl
ddH_2O	Total volume up to 50 µl

A G-STORM GS1 thermal cycler (Gene technologies) was used for subsequent amplification of the DNA. Initiation of the program began with a "hot start" step for 2 minutes at 95°C to heat the lid. The KOD polymerase was the last component to be added thus the program was paused and 0.5 µl KOD polymerase was added to each tube. The program was resumed to start the reaction of 30 cycles. The 30 thermal cycles comprised of a denaturation temperature step at 95°C for 30 seconds, then an annealing step for 30 seconds where the temperature was based on the primer composition and calculated using the formula below. The final step was an elongation step at 70°C for 30 seconds per 500 bp of DNA being amplified.

Formula used to calculate the annealing temperature:
$Tm = [4(G+C) + 2(A+T)] – 5^oC$.

Q5 DNA polymerase

PCR was also performed with Q5 polymerase (NEB) instated of KOD polymerase as it is ideal for difficult DNA templates. The PCR was carried out as in the case of KOD polymerase with the exception of the extension temperature 72^oC.

Table 2-6: PCR components for reactions using Q5 DNA polymerase

Component	**Amount (µl)**
Template DNA	3.0 µl
Q5 5× Reaction Buffer	10.0 µl
Q5 GC enhancer	10.0 µl
dNTP mixture (2 mM each dNTP)	5.0 µl
10 µM Forward primer	2.4 µl
10 µM Reverse primer	2.4 µl
Q5 High-Fidelity DNA Polymerase (2 units/ml)	0.5 µl
ddH_2O	Total volume up to 50 µl

PCR Screening of recombinant plasmids in *E. coli* (Colony PCR)

In order to determine the correct clone, the gene of interest was amplified using high-fidelity replication GoTaq polymerase (Promega). PCR screening is the easiest way to confirm the size of a small fragment of the DNA. Transformation colonies were touched with a sterile toothpick in order to be resuspended inside of the PCR tubes. PCR reaction ingredients were added to each tube. The components used for PCR screening were as followed:

Table 2-7: PCR components for reactions using GoTaq DNA polymerase

Component	**Amount (µl)**
Template DNA	3.0 µl
dNTP mixture (10 mM each dNTP)	1.0 µl
DMSO	2.4 µl
$MgCl_2$ (25 mM)	4.0 µl
10 µM Forward primer	3.0 µl
10 µM Reverse primer	3.0 µl
GoTaq polymerase (5 units/µl)	0.25 µl
ddH_2O	Total volume up to 50 µl

The PCR was carried out as described in Section 2.5.4.

PCR screening of candidate *B. cenocepacia flrR*::Tp mutants

A loopful of each colony was suspended in 200 µl of TE buffer in a screw capped Eppendorf tube. The tube was left in a boiling water bath for 10 minutes, centrifuged at 13,200 x *g* for 2 minutes to remove the cell debris. The resulting supernatant was used as DNA template. The PCR was carried out as described in Section 2.5.4.

2.5.5 DNA gel extraction

The desired DNA fragment was excised from an agarose gel and purified using a gel extraction kit (Qiagen) according to the manufacturer's instructions.

2.5.6 DNA purification

DNA purification was carried out to remove the remaining restriction enzymes by using the QIAquick spin PCR purification kit (Qiagen) according to manufacturer's instructions.

2.5.7 Restriction Digestion

Desired DNA fragments were digested by adding the following components into a 1.5 ml micro-centrifuge tube:

DNA	100-1000 ng of DNA
10× restriction buffer	5.0 µl
Restriction enzyme	1.0 µl

The total volume was made up to 50 µl by adding sterile milliQ water. The appropriate restriction enzymes were used with the suitable reaction buffer. The mixture was incubated at 37^{o}C water bath for 2 hours and purified using the QIAquick spin PCR purification kit.

2.5.8 Ligation

Depending on the DNA concentration, 5 to 15 µl of linearised plasmid DNA was used for the ligation procedure to be cloned into the plasmid. 3 µl of 10× ligase buffer was added to three tubes, ligation, ligation control and vector control. For the ligation 3 µl of T4 DNA ligase (Promega) was added to the ligation and ligation control tubes and gently mixed. The ligase enzyme was the last component to be added. Deionized water was added to make the final volume up to 30 µl. The ligation tubes were then incubated at room temperature overnight to allow the ligation to occur. The resulting ligation samples were then transformed into the appropriate competent cells.

2.5.9 Oligonucleotide annealing for cloning

To produce double-stranded fragments, 45 µl of each oligonucleotide at 100 µM were transformed into PCR tube with 10 µl of annealing buffer (10 mM $MgCl_2$, 200 mM Tris-Cl (pH 8.0) in >18 MΩ H_2O). The mixture was incubated for 10 minutes at 90°C in a thermal block. After that, the mixtures were kept on the bench-top to cool down for 1 hour.

2.5.10 DNA sequencing

Mutation can occur in the amplified DNA sequence when using DNA polymerase. All constructed plasmids containing PCR amplified fragment were checked by sequencing using specific primers. This was to confirm the integrity of the entire sequence of inserted DNA fragment. All constructs made in this study were checked by sequencing. The sequencing was carried out by Lark technologies at the University of Sheffield at Medical School Core Sequencing Facility.

2.6 RNA extraction

RNA was extracted by using Thermo Scientific kit. The start culture of HIII *B. cenocepacia* was grown in LB medium at 37°C for overnight. The following day, the bacterial culture was used to set up sub-culture; the culture was diluted at 100 fold in 10 ml in same medium supplemented with 100 μM 2'2-dipyridyl in order to grow the cell under iron-limited conditions. The resulting solution was treated with DNAse, and the extraction process was carried out as per the manufacturer's instructions.

2.7 Identification of transcription start site

To identify the transcription start site, a method called ARF-TSS (alternative for identification transcription start site) was used. This method was described by Wang *et al*. (2012). The method was carried out using self-ligation cDNA obtained by using bacterial RNA growing under iron-limited conditions.

2.7.1 First-strand synthesis of cDNA

First-strand cDNA carried out using Promega protocol. 1 μg of RNA and 0.5 μg of gene specific primers were added in a sterile RNase-free microcentrifuge, the tube incubated at 70°C for 5 minutes to melt the secondary structure and then left on ice immediately to prevent the secondary structure from forming again. The following components were added to the annealed primer and template mixture:

Table 2-8: Components for First-strand synthesis of cDNA

Component	Amount (µl)
M-MLV 5× Reaction Buffer	5.0 µl
dNTP mixture (10 mM each dNTP)	1.25 µl
DMSO	2.4 µl
Recombinant RNasin ® Ribonuclease Inhibitor	1.0 µl
M-MLV RT	1.0 µl
Nuclease-Free Water to final volume	9.5 µl

The tube was mix gently by flicking and incubated for 50 minutes at 70°C. To activate the reaction, the tube was incubated for 15 minutes at 70°C.

2.7.2 Ligation of single strand cDNA

First strand cDNA was ligated by adding the following components:

Table 2-9: Components for ligation of single strand cDNA

Component	Amount (µl)
First strand cDNA	15.0 µl
10× T4 RNA ligase buffer	2.0 µl
10 Mm ATP	2.0 µl
50% PEG8000	5.10 µl
RNase inhibitor	1.0 µl
T4 RNA ligase enzyme	1.0 µl
Nuclease-free water	20.0 µl

The ligation mixture incubated at 37°C for 30 minutes, the ligation was used for PCR amplification. The ligated PCR products were confirmed by electrophoresis on 1% agarose gel.

2.8 Reverse transcription PCR (RT-PCR)

RT-PCR was carried out using extracted RNA as described in Section 2.6. The cDNA was prepared from RNA as described in Section 2.7.1. For each reaction 5 µl of cDNA was used as a template. To determine the optimum annealing temperatures for each primer pair the standard PCR was performed. The reaction was carried out according to the manufacturer's instructions. As *B. cenocepacia* DNA is G+C rich, 2.4 µl of DMSO was added to each 50 µl reaction. Same experiment was carried out without RT enzyme as a control to make sure mRNA is not contaminated with DNA. The resulting products from RT-PCR were analysed on 1.6% agarose gel.

2.9 Bacterial Transformation

2.9.1 Preparation of competent cells for transformation (Hanahan's method)

The Hanahan method (Hanahan, 1983) was used to prepare competent cells which were stored at -80°C in order to be maintained for a long period of time. Bacterial strains required for transformation were inoculated from a fresh colony growing on an agar plate in 5 ml of LB medium. Cells were grown overnight at 37°C with aeration. The following day, 50 ml of LB was inoculated with 0.5 ml of the overnight culture and cells were incubated at 37°C with aeration until the cells had reached exponential phase (OD_{600} 0.3-0.5). Once the cells reached the required OD the cells were chilled on ice for 15 minutes. The cells were harvested by centrifugation at 4,000 x *g* for 10 minutes at 4^{o}C. The supernatant was discarded and the cell pellets were gently resuspended in 16 ml of cold RF1 solution. The cell suspensions were incubated on ice for 30 minutes, followed by centrifugation at 4,000 x *g* for 10 minutes at 4^{o}C. The supernatant was discarded and the cell pellets were resuspended again in 4 ml of RF2 solution. The competent cells were incubated on ice for a further 15 minutes. Cell were then distributed into 1.5 ml microcentrifuge tubes as 400 µl aliquots and then stored at -80°C to be used when required**.**

RF1 Solution

9.90 g $MnCl_2.4H_2O$

7.46 g KCl

1.50 g $CaCl_2.2H_2O$

2.84 g potassium acetate

150 ml glycerol

The above components were dissolved in 750 ml distilled water. The solution was adjusted to pH 5.8 using 0.2 M acetic acid (glacial acetic acid is 17.4 M). The solution was then autoclaved and stored at 4°C.

RF2 Solution

To make RF2 solution, two solutions A and B were made.

Solution A: 0.5 M MOPS, pH 6.8

Solution B: 10 mM KCl, 75 mM $CaCl_2.2H_2O$ and 15% (w/v) glycerol.

RF2 solution was made by mixing 2 ml of solution A and 98 ml of solution B. All solutions were stored at 4°C.

2.9.2 Transformation

15 µl of each ligation reaction was mixed with 100 µl ice-cold competent cells. The tubes were then kept on ice for 30 minutes and the tubes were flicked every 5 minutes, preventing the cells to settle in the bottoms of the tubes. The tubes were then transferred in a 42°C water bath for 2 minutes and then returned on ice for 5 minutes.1 ml of LB broth was added to each tube and then incubated at 37°C for 1 hour. 100 µl of the transformation mixture was plated onto a selection plate containing the appropriate antibiotics. The plates were then incubated overnight at 37°C.

2.9.3 Electroporation

The donor and recipient strains were grown overnight in 6 ml LB and incubated at 37°C. Next day, each 6 ml of overnight culture were distributed into four 1.5 ml microcentrifuge tubes. The cell harvested by centrifugation for 2 minutes at room temperature, and the supernatant was discard. The cell pellet of each tube was resuspend in 1 ml of autoclaved 300 mM sucrose by pipetting up and down, centrifuge again at 16,000 x *g* for 1 minutes. The supernatant was discard and the pellet was

resuspend again by repeating the same procedure and then centrifuge for 2 minutes. The four tubes containing four cell pellets were resuspend in 100 µl of 300 mM sucrose, each cell pellet was sequentially resuspending in the same 100 µl of 300 mM sucrose and then transferred the suspension to the next tube. 500 ng of desire DNA was mixed with 100 µl of competent cell, the bacterial cells were transferred into a 2 mm-gap width electroporation cuvette. Pulse was applied using Bio-Rad gene pulser (25 µF, 200 Ω, 2.4 kV) which is automated setting for bacteria. The cuvette opened in the microbiological safety cabinet in order to add 1 ml of LB broth to the mixture. The mixture was then transferred into a sterile universal tube and incubated at 37°C for 2 hours with shaking. After incubation the bacterial culture was plated onto selection plates.

2.9.4 Conjugation to transfer plasmid DNA to *B. cenocepacia*

Bacterial strains (donor and recipient strain) were inoculated in 5 ml of LB containing the appropriate antibiotics. The bacterial cultures were incubated overnight at 37°C with aeration. The next day, 1 ml of the overnight culture was harvested by centrifugation at 15,000 x *g* for 2 minutes. The cells were then resuspended in 100 µl of 0.85% saline. Using sterile forceps, a nitrocellulose filter was placed on LB agar plate for each mating, as well as for the donor and recipient controls. In a screw cap micro-centrifuge tube 25 µl of the donor and 25 µl of the recipient strains were mixed with 25 µl of saline. The mating and control mixtures were then spread onto the nitrocellulose filters on the LB agar plates using a p200 tip. All plates were incubated overnight at 37°C. The following day, the nitrocellulose filters were transferred to sterile universal tubes using sterile forceps which contained 3 ml of 0.85% saline. The universal tubes were vortexed to resuspend the bacteria. 10^{-1} dilutions were made of the bacterial suspensions. 100 µl of undiluted and diluted suspensions were then plated onto selective medium.

2.9.5 Bacterial strain maintenance

The bacterial strains used in this study were *E. coli, B. cenocepacia* and *P. aeruginosa*. To maintain the bacterial strain for long-term, strains were stored as glycerol stocks. For a short-term used *E. coli* and *P. aeruginosa* were stored on LB agar plates supplemented with appropriate antibiotics if required and kept at 4°C. The bacterial

strains were restreaked on LB fresh plates every four weeks and incubated at 37°C overnight before storage at 4°C. In the case of *B. cenocepacia,* it cannot be stored in rich medium, as it dies rapidly and it cannot be stored at 4°C because it loses viability. Therefore, it was stored as glycerol stocks or M9 agar plate at room temperature.

2.10 Bacterial adenylate cyclase two hybrid assay (BACTH)

The appropriate (pUT18C, pUT18) and (pKT25, pKNT25) based recombinant plasmids were transformed into a *E. coli cya*- strain, BTH101. Cells were then plated onto an indicator medium (MacConkey agar plates containing the appropriate antibiotics to select for both vectors) to evaluate the $Cya^{+/-}$ phenotype. The plates were then incubated at 30°C for 5 days to observe Mal phenotype.

2.11 β-galactosidase assay

The following experimental materials were prepared in advance.

Z-Buffer to prepare Z-buffer the following components are required.
16.1 g $Na_2HPO_4.7H_2O$
5.5 g $NaH_2PO_4.H_2O$
0.75 g KCl
0.246 g $MgSO_4.7H_2O$
All the components above were dissolved in 1 litre of sterile water. The Z-buffer was stored at 4°C. 0.27 ml of β-mercaptoethanol was added to 100 ml of Z-buffer on the day of the experiment.

1M Na_2CO_3 10.6 g of sodium carbonate was dissolved in 100 ml deionized water.

4 mg/ml ONPG on the day of the experiment, 40 mg of ONPG was added to 10 ml of Z-buffer containing β-mercaptoethanol.

0.1% SDS a 1% stock solution of SDS was made up and diluted 10× when required.

All bacterial strains required for β-galactosidase assay were inoculated from a fresh colony in 3 ml of LB supplemented with the appropriate antibiotics. The bacterial strains were incubated at 37°C overnight with aeration. After overnight incubation, 50 µl of each strain was added to 5 ml of LB supplemented with the appropriate antibiotics, 1 mM of IPTG and 175 µM 2,2'-dipyridyl were added when required. The bacterial cultures were incubated at 37°C in shaking incubator until the desired OD_{600} was reached. Once each strain reached the appropriate OD_{600}, they were transferred onto ice for 20 minutes to prevent further growth. After incubation on ice the following procedure was carried out. For each strain 6 glass test tubes were employed (each strain was assayed in triplicate and then duplicated). 950 µl of Z-buffer containing β-mercaptoethanol was added to each test tube and 30 µl of chloroform was then carefully added to the surface of the Z-buffer to prevent it evaporating. The required amount of bacterial culture (between 50 µl to 200 µl) was added carefully as to not disturb the chloroform layer. Then, 30 µl 0.1% SDS was added along the inside of each tube. All the tubes were then vortexed for 10 seconds, allowing the cells to be permeabilized. The following equation was then used to calculate the activity of β-galactosidase in Miller units. All tubes were transferred and incubated at 30°C water bath for 15 minutes. As a control, a sterile growth medium was used, it also used as the blank. To start the reactions, 200 µl of ONPG solution was added to each tube and interval of 30 seconds then the tube vortexed for 1 second, the tube was returned to the water bath. To stop the reactions, 0.5 ml of 1 M sodium carbonate solution was added to each tube and interval for 30 seconds, and then the tube was vortexed briefly. The starting and the stopping time were carefully noted. All the tubes were left for 10 minutes in order to allow the chloroform to settle. 1 ml of the reaction mixture was taken from each tube and transferred into a cuvette. The optical density at 420 nm was then measured to measure β-galactosidase and 550 nm to account for scattering by cell debris. Also, 600 nm was recorded to measure the cell density using a spectrophotometer.

$$\text{Miller Unit} = 1000 \times \frac{OD_{420} - (1.75 \times OD_{550})}{\text{Time} \times \text{Volume} \times OD_{600}}$$

Time: the reaction time (starting time-stopping time) in minutes.

Volume: the volume of bacterial culture used in the assay millilitres.

OD_{600}: cell density.

2.12 Siderophore assay

To study the ability for bacteria to utilize siderophores specific LB plates were prepared containing 200 μM EDDHA and appropriate antibiotics. The LB plates were prepared by using 0.65% agar in LB in order to get a soft LB agar. The sterilized soft LB agar was distributed into 3 ml aliquots in 20 ml universal glass and maintained at 42°C. To each universal tube 1 ml of overnight culture was added and then poured onto LB containing EDDHA. When the soft LB agar solidified, 10 mm sterile filter paper discs were placed on the soft agar and 20 μl of siderophore solution was added to each filter paper. As a negative control, Ultrapure water was used, the plates kept to dry for 30 minutes before incubating at 37°C.

Table 2-10: Preparation of siderophores

Siderophore	**Solvent**	**Concentration**
Ferrichrome	dH_2O	1 mM
Rhizoferrin	dH_2O	1 mM
Rhodotorulic acid	dH_2O	1 mM
Desferricoprogen	dH_2O	1 mM
Nicotianamine	dH_2O	1 mM
Enterobactin	DMSO	1 mM
Bacillibactin	DMSO	1 mM
Arthrobactin	dH_2O	1 mM
Schizokinen	dH_2O	1 mM

2.13 Fur titration assay (FURTA)

An *E. coli* strain called H1717 was used to carry out Fur titration assay. A high copy number plasmid called pBluescript IIKS was used to clone a desired DNA sequence into it which was analysed to demonstrate the presence of Fur binding sites. The transformation of the resulting clone was analysed on MacConkey agar (Section 2.2.3). When the MacConkey agar cools down the following components were added; 1% (w/v) maltose and 40 μM $Fe(NH_4)_2(SO_4)_2$. 40 μM $Fe(NH_4)_2(SO_4)_2$ was prepared from 30 mM filter sterilized $Fe(NH_4)_2(SO_4)_2$ stock solution which dissolved in H_2O. The agar plates were allowed to set. Cells to be analyzed were grown on LB plates at 37°C first and then were streaked on MacConkey agar using a sterile wire loop. The plates were incubated at 37°C to allow colony formation.

2.14 Protein overproduction and purification techniques

2.14.1 Growth of bacterial cultures and protein overproduction

For protein overproduction competent *E. coli* BL21(λDE3) cells were used. The cells contain plasmids that can express the cloned target genes. The cells were grown in LB broth containing an appropriate antibiotic at 37°C until they reached an OD_{600} of 0.5. 1 ml of the culture was taken in order to obtain uninduced sample before adding IPTG. The cells were left to grow for 3 hours. To induce the cloned gene expression, IPTG was added to culture with final concentration of 1 mM, the culture was kept in the incubator for further 3 hours. Uninduced and induced samples were taken to be analysed by SDS-PAGE. 100 μl of each sample was centrifuged at 13,200 x *g* for 20 minutes at 4°C. The supernatant of each sample was discarded and then the cells pellet was resuspended in 50 μl of 2× Laemmli buffer; the samples were then boiled for 10 minutes to allow the protein to denature and solubilise.

Laemmli sample buffer 2× recipe for (10 ml)

600 μl Tris-Cl (pH 6.8)	Final conc. 250 mM
2 ml sodium dodecyl sulphate (SDS)	Final conc. 10%
2 ml glycerol	Final conc. 20%
1 ml bromophenol blue	Final conc. 0.01%

The volume addup to 9 ml with H_2O. 900 µl aliquot of the solution were taken and 100 of β-mercaptoethanol to be added.

2.14.2 Protein solubility test

To test whether the protein was soluble or insoluble after overexpression, 100 to 200 ml of liquid culture of *E. coli* BL21(λDE3) competent cells containing an expression vector. The liquid culture was grown overnight to give a starting OD_{600} of 0.003. The second day the culture was incubated at 37°C until culture was reached an OD_{600} = 0.3-0.4. To induce the culture 1 mM of IPTG was added and incubate for further 3-4 hours at 37°C. After that the entire culture centrifuged at 12,500 x *g* for 20 minutes at 4ºC. The supernatant was discarded and the cell pellet was resuspended in 25 ml of wash buffer containing the following material:

Wash buffer

25 mM Tris-HCl (pH 7.5)

150 mM NaCl

2 mM EDTA

pH was adjusted with 1 M HCL and autoclaved for 20 minutes at 120ºC/16 psi. ddH_2O was added to make the volume up to 1 litre. The liquid culture was centrifuged again at 12,500 x *g* for 20 minutes at 4ºC, and supernatant was discarded.

Lysis buffer

50 mM Tris-HCl (pH 8.0)

2 mM EDTA

200 mM NaCl

5% glycerol

Adjust pH to 8.0 with 1 M HCl and make the volume up to 1 litre with ddH_2O.

Autoclaved for 20 minutes at 120ºC/16 psi.

Following this, sonication was performed using a SONICS Vibracell VCX750 Ultrasonic Cell Disrupter with a micro-tip probe. The bacterial cells were subjected for sonication 4-5 times for about 30 minutes and between each sonication the cells

were put on ice for 2 minutes. 50 µl crude protein sample was taken and boiled with 50 µl of 2× Laemmli buffer for 10 minutes at 95°C, and the rest of the solution was centrifuged at 20,000 x *g* for 30 minutes at 4°C. Four samples was obtained from this process; uninduced cell, induced cell, crude lysate and cleared lysate, all the samples were analysed by SDS PAGE at 120 V. To increase protein solubility, the resulting pellet were resuspended in TGED buffer containing N-Lauroylsarcosine sodium salt. The TGED buffer was prepared by adding the following material:

50 mM Tris-HCl
5% glycerol
0.1 mM EDTA
0.1 mM DTT
50 mM of NaCl
The final pH of TGED buffer was adjusted to 7.9.

2.14.3 His-tagged proteins purification by Nickel affinity column usingAKTA system

Following induction of protein production, the soluble cell lysate that contains the proteins of interest was prepared as described above. AKTA protein purification system was used in order to carry out the purification process by attaching a 1 ml Hi-Trap nickel column from GE Healthcare to the system. The column was equilibrated with 10 ml of lysis buffer. The lysed cell supernatant that contains the protein of interest was sterilised and filter through a 0.22 µm filter using 10 ml syringe, and then the supernatant applied to the nickel column, the flow rate was 1 ml/min. After the collection of the flow through, the column was washed with 20 ml of lysis buffer. 10 to 100 mM of imidazole gradient applied to elute the target protein from the column and collected in 1 ml fractions. 50 µl of each fraction was mixed with the same amount of 50 µl of 2× Laemmli buffer and boiled for 10 minutes at 95°C. 15 µl of each sample was loaded and analyzed by SDS-PAGE.

Elution buffer
50 mM Tris-HCl (pH 8.0)
200 mM NaCl

10 % glycerol

≥150 mM imidazole

Regenerating Ni-NTA resin column

In order to use the nickel column again, it was necessary to wash it with 10 ml of 20% ethanol after finishing the process of protein purification. The column was then stored at 4°C for short-term storage. To remove residual protein material completely from the column, the column was washed with 5 ml 50 mM EDTA (pH 8.0) and then 5 ml of 500 mM guanidine hydrochloride was added. By doing the last step, the column was completely striped and the nickel along with any residual proteins was removed. The last step was washing the column several times with water and re-charged with 5 ml of 100 mM NiCl.

2.14.4 Purification of MBP fusion protein

Maltose-binding fusion protein (MBP) purification was carried out by transforming the pMALc5X encoding the gene of interest into *E. coli* BL21(λDE3). The bacterial culture was processed as described in Section 2.14.1. In order to purify maltose-MBP fusion proteins, 12 ml of amylose resin was packed in micro bio-spin column (BioRad) and equilibrated with column buffer. Bacterial cell lysate was loaded onto the column under gravity and the flow-through was retained. To remove unbound proteins, the column was washed twice (2 column volumes). To elute the desire protein, 10 mM maltose was added to 3 column volumes of column buffer and then applied to the column under gravity. The eluted fractions were collected and analysed by SDS-PAGE.

Column buffer

20 mM Tris-HCl (pH 7.4)

200 mM NaCl

1.0 mM EDTA

1.0 mM sodium azide

11 mM β-mercaptoethanol

All the above components were dissolved in 800 ml of ddH_2O, ddH_2O was added to make the total volume up to 1 litre. The buffer autoclaved for 20 minutes at 120°C/16 psi.

Regenerating the amylose resin

For reusing the amylose column several washes were carried out using the following:
Water: 3× column volumes
0.1% SDS: 3× column volumes
Water: 1× column volume
Column buffer: 3× column volumes
The column was stored at 4°C.

2.15 Sodium dodecyl sulphate polyacrylamide gel electrophoresis (SDS-PAGE)

2.15.1 Preparation of SDS-PAGE gel

SDS polyacrylamide gel was prepared according to the procedure described by (Laemmli, 1970). Sufficient amount of the resolving gel was poured between two glasses allowing ~2 cm from the top of the plate for the stacking gel. A few drops of isopropanol were added to the surface of the resolving gel to maintain the surface level before solidified, the isopropanol on the top of the gel was washed with water. The stacking gel was poured after the resolving gel was polymerised, allow the gel to set for 20-30 minutes.

12% resolving gel (10 ml)

4.3 ml dH_2O
3 ml 40% acrylamide:bis-acrylamide (Fisher scientific)
2.4 ml 1.5 M Tris-HCl (pH 8.8)
100 µl 10% (w/v) SDS
100 µl 10% ammonium persulphate
5.0 µl TEMED (Sigma)

15% resolving gel (10 ml)

3.55 ml dH_2O

3.75 ml 40% acrylamide:bis-acrylamide (Fisher scientific)

2.4 ml 1.5 M Tris-HCl (pH 8.8)

100 µl 10% (w/v) SDS

100 µl 10% ammonium persulphate

5.0 µl TEMED (Sigma)

The stacking gel was immediately applied on the resolving gel and the comb was carefully placed to avoid bubbles. After polymerisation, the comb was carefully removed and the gel was placed into gel tank filled with 1× SDS running buffer.

5% stacking gel (5 ml)

3.645 ml dH_2O

625 µl 40% acrylamide: bis-acrylamide (Fisher scientific)

630 µl 1 M Tris-HCl (pH 6.8)

50 µl 10% (w/v) SDS

50 µl 10% ammonium persulphate

5.0 µl TEMED (Sigma)

10× SDS running buffer

30.3 g Tris base

144 g glycine

10 g SDS

Make the volume up to 1 litre with ddH_2O

2.15.2 Electrophoresis of the gel

The protein samples for SDS analysis were prepared as described above. 10-15 µl of samples were loaded in each well and a protein molecular weight marker was loaded in one well. Then the SDS-PA gel was electrophoresed at 120 V for approximately 2 hours (until the bromophenol blue dye was migrated to the bottom of the gel).

2.16 Pull-down assay

To perform pull-down assay, 200 µl of nickel resin was loaded into three micro-centrifuged tubes and centrifuged at 5,000 x *g* for 2 minutes. The supernatant was

discarded. 1 ml of low salt lysis buffer was added to each tube, the tubes were then mix gently and inverted several times before they were centrifuged again. Replaced the supernatant with 1 ml of fresh low salt lysis buffer and centrifuged again to remove the supernatant, this wash step was repeated twice to get resin pellet. His-tagged prey protein was added to nickel resin and then kept on a rotating wheel at room temperature for 2 hours. To pellet the resin, the samples were centrifuged at 5,000 x *g* for 2 minutes and supernatant was discarded. 500 µl of fresh lysis buffer was added to wash the beads and centrifuged at 5,000 x *g* for 2 minutes. The supernatant discarded and the wash step was repeated one more time. To elute bound proteins 100 µl lysis buffer containing 500 mM imidazole was added and the mixture was mixed gently on a rotating wheel at room temperature for 30 minutes. To collect the resulting supernatant, the samples were centrifuged at 5,000 x *g* for 2 minutes. The eluted protein samples were mixed with equal volume of 2× Laemmli buffer and boiled prior to be analysed by SDS-PAGE.

2.17 Western blotting

In order to perform Western blot polyvinylidene fluoride (PVDF) membrane (GE Healthcare: Amersham Hybond™-P) cut to the size of the gel. PVDF membrane was soaked in 100% methanol for 30-60 second to activate the membrane and washed with H_2O for 2 minutes. The PVDF membrane was kept in cold 1× transfer buffer for 15 minutes. Also, two pieces of filter paper (Whatman 3M) cut in same size of gel were kept in 1× transfer buffer for 15 minutes along with two sponge pads and the gel, after it had been washed with dH_2O to make sure that the salt had been removed. To assemble the Western blot stack, the sponge pads were placed first, followed by the two pieces of filter papers and then the gel was placed on the top of the filter paper and aligned. The blotting membrane was added on the top of the gel and air bubbles were excluded. The final step was to place the last two filter papers followed by last sponge pad. A transfer tank (BioRad) was prepared by adding 1× western transfer buffer with 10% methanol and an ice cassette was placed in the tank to keep it cool while it transferring. The stack was placed inside the tank and the transferring process was carried out at 100 V for 60 minutes. After the transferring process completed the membrane was blocked in Tris-buffered saline containing 0.05% (v/v) Tween® 20 (TBS-T) with 5% semi-skimmed milk powder at room temperature for 1 hour. The

membrane was then kept on the shaker and washed for 10 minutes using TBS-T, the washed step was repeated twice. The appropriate primary antibody diluted in the required amount of TBS-T containing 5% (w/v) semi-skimmed milk powder and then the membrane probed with the antibody. The membrane inserted with antibody in the tube and incubated overnight at 4°C with gentle agitation. The membrane was washed three times for 10 minutes at room temperature to move unbound antibody, the wash was performed by using TBS-T. After that, the appropriate secondary antibody was probed to the membrane at the required dilution using TBS-T containing 5% (w/v) semi-skimmed milk powder and kept for 1 hour in room temperature with gentle agitation. After 1 hour, the membrane washed with TBS-T for 10 minutes by gentle agitation and the wash was repeated twice. 1 ml of detection reagent (EZ-ECL) was made by combining 0.5 ml EZ-ECL solution A and 0.5 ml EZ-ECL solution B. This was applied to the PVDF membrane and incubated for 5 minutes at room temperature. The excess detection reagent was removed and the Western blot was imaged using the Bio-Rad molecular imager ChemiDoc™ XRS+.

10× TBS (pH 7.4)

15 g Tris-base

40 g NaCl

1.0 g KCl

H_2O (>18 MΩ) to 1 L

The final pH of 10× TBS was adjusted to 7.4 with HCl

10× western transfer buffer (pH 8.3)

30.3 g Tris base

144 g glycine

H_2O (>18 MΩ) to 1 L

The final pH of 10× transfer buffer was adjusted to 8.3.

Table 2-11: Antibodies used in this study

Antibody	**Source**	**Dilution**	**Company**
His-probe linked with HRP	Mouse	1:4,000	Thermo Scientific
Anti-VSVg polyclonal antibody	Rabbit	1:5,000	Sigma-Aldrich
Anti-His_6	Mouse	1:5,000	BioLegend
Anti-MBP linked with HRP	Mouse	1:5,000	Biolabs

Chapter 3 Investigation of protein-protein interactions within the Flr system

3.1 Introduction

Thirteen ECF σ factors have been identified in *B. cenocepacia*, two of which belong to the iron starvation (IS) group. One of these is the well-characterised σ factor, OrbS (Agnoli *et al*., 2006). In this study, we investigated the IS σ factor known as FlrS. FlrS is similar to the *E. coli* IS σ factor FecI. Three genes encode the Flr system: *flrSRA*, apparently functioning in a similar way to genes involved in the Fec system. Of these, *flrR* is predicted to encode an anti-σ factor while *flrA* is predicted to encode an outer-membrane receptor. The domain organisation of FlrS, FlrR and FlrA was predicted by amino acid sequence alignments that were compared with the orthologous Fec system (Figures 3.1, 3.2 and 3.3). This showed that FlrS and FecI share 55% amino acid sequence similarity, FlrR and FecR share 35% similarity and FlrA and FecA share a lower degree of similarity (~23%). The important of these domains will be investigated in this chapter in order to understand how they are involved in signal transduction within the Flr system. These domains are the N-terminus of the outer-membrane receptor, FlrA, the N-terminus of the anti-σ factor, FlrR and the C-terminal domain of the putative σ factor, FlrS which share about 22%, 52% and 37% similarity, respectively, with the orthologous domains of the Fec system (Figures 3.1, 3.2 and 3.3). To gain insights into the orthologous relationship between the *B. cenocepacia* ECF σ factor and ECF σ factors of other species, multiple alignments of the amino acid sequences of selected σ factors were carried out in order to create a phylogenetic tree. The analysis of this phylogenetic tree indicates that FlrS clusters with known iron starvation σ factors FiuI, FoxI and FecI (Figure 3.4).

The experiments outlined in this chapter focus on investigating the possible interaction between the putative anti-σ factor FlrR, in particular, the N-terminal region of FlrR and the C-terminal region of the respective σ factor FlrS. In addition, it is predicted that there is a possible interaction between the C-terminal region of FlrR and the N-terminal region of the outer-membrane receptor FlrA. This possible interaction will be investigated in this study using BACTH system and pull-down assay.

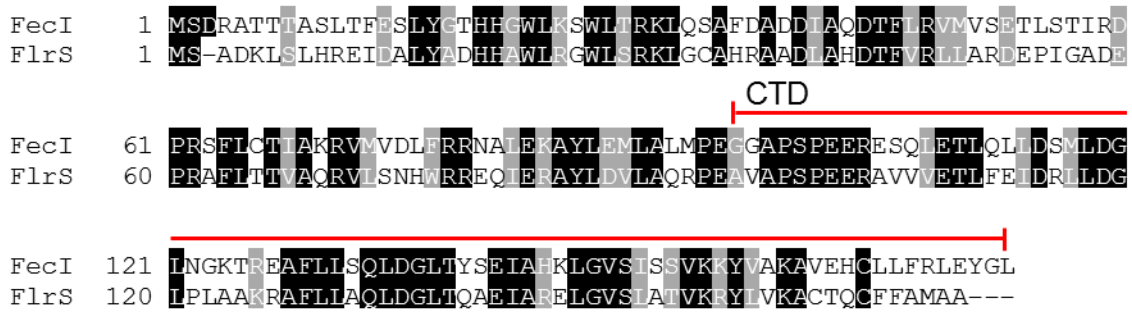

Figure 3-1: Alignment of FlrS with *E. coli* FecI.

An alignment was carried out between *B. cenocepacia* FlrS and *E. coli* FecI, using ClustalW2. Shading was applied using the BoxShade program. Amino acids identical or similar in both sequences are shown in white font and shaded by black or grey, respectively. The solid red line above the sequence revers to C-terminal domain of both σ factors.

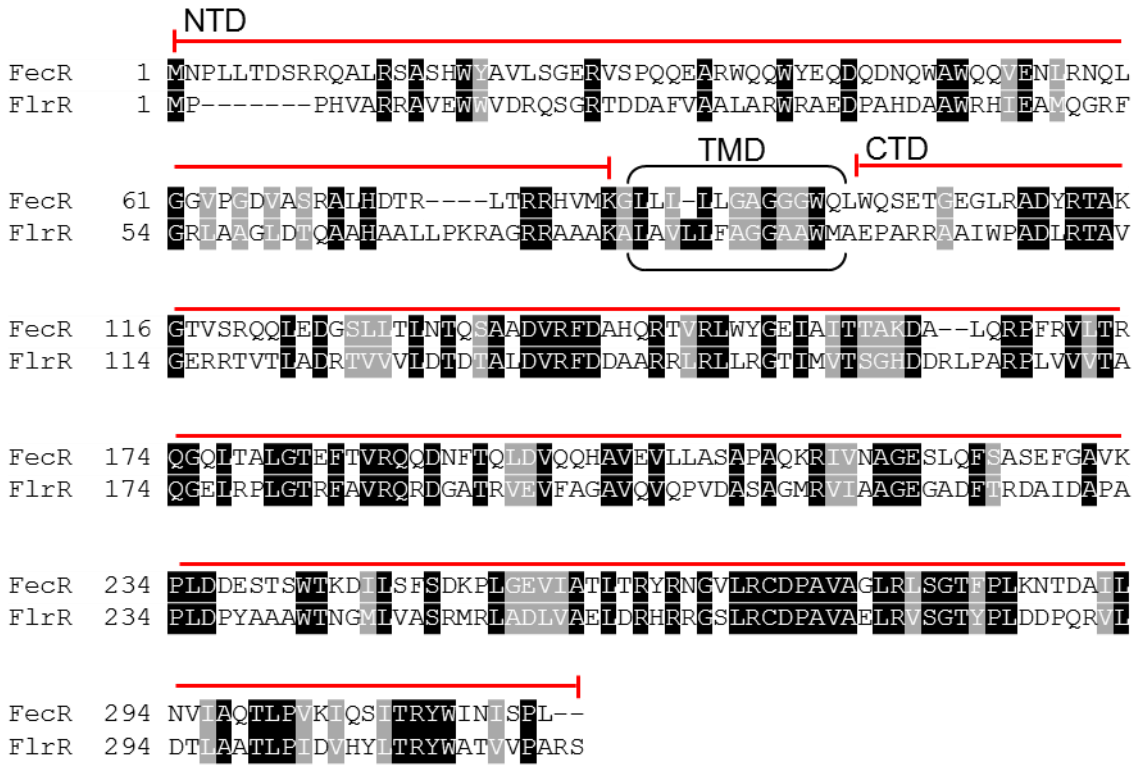

Figure 3-2: Alignment of FlrR with *E. coli* FecR.

An alignment was carried out between *B. cenocepacia* FlrR and *E. coli* FecR, using ClustalW2. Shading was applied using the BoxShade program. Amino acids identical or similar in both sequences are shown in white font and shaded by black or grey, respectively. The solid red line above the sequence revers to the N-terminal domain and the C-terminal domain of both anti-σ factors. The black bracket encloses the transmembrane domain sequence.

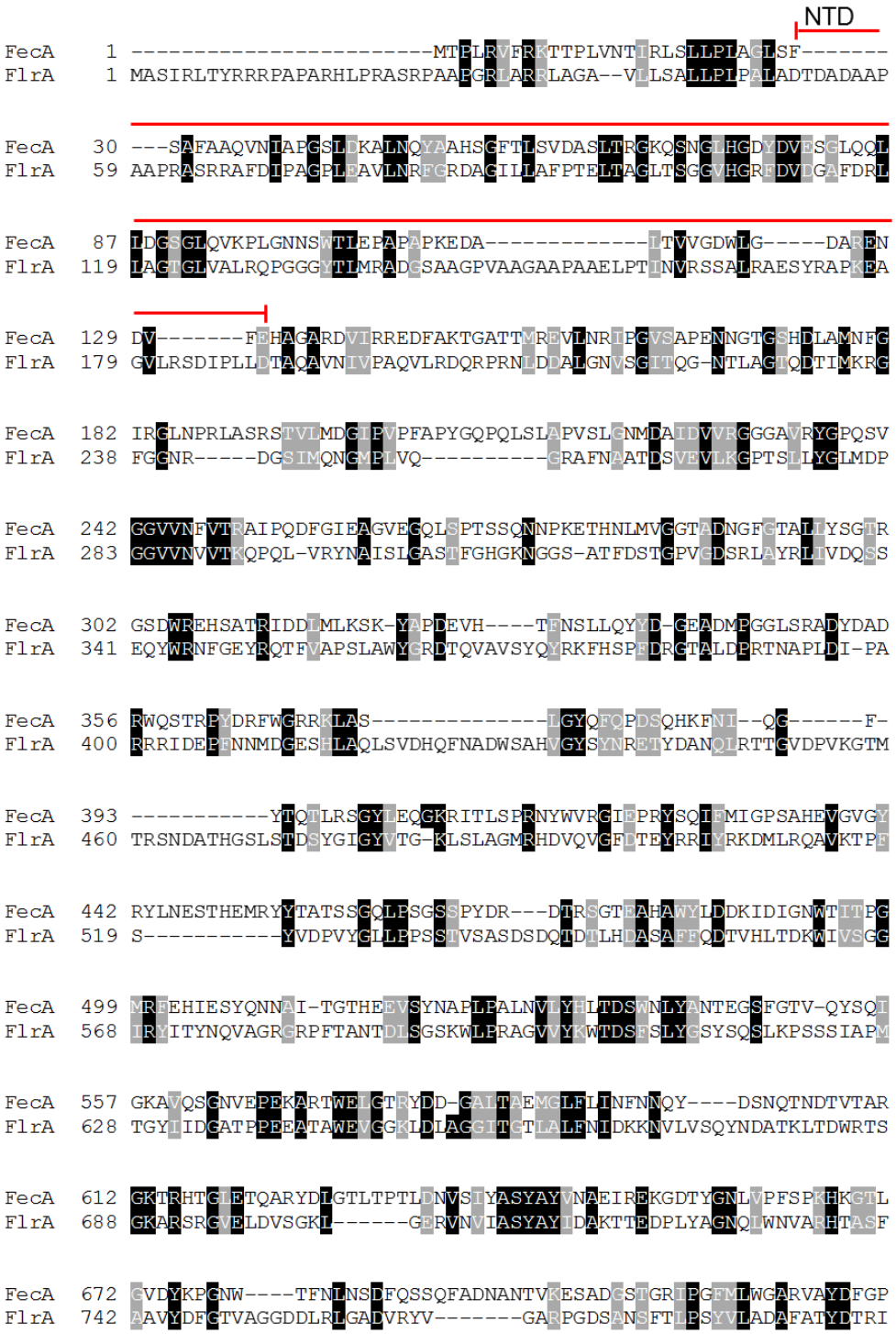

Figure 3-3: Alignment of FlrA with *E. coli* FecA.

An alignment was carried out between *B. cenocepacia* FlrA and *E. coli* FecA, using ClustalW2. Shading was applied using the BoxShade program. Amino acids identical or similar in both sequences are shown in white font and shaded by black or grey, respectively. The solid red line above the sequence revers to the N-terminal domain the outer-membrane receptors.

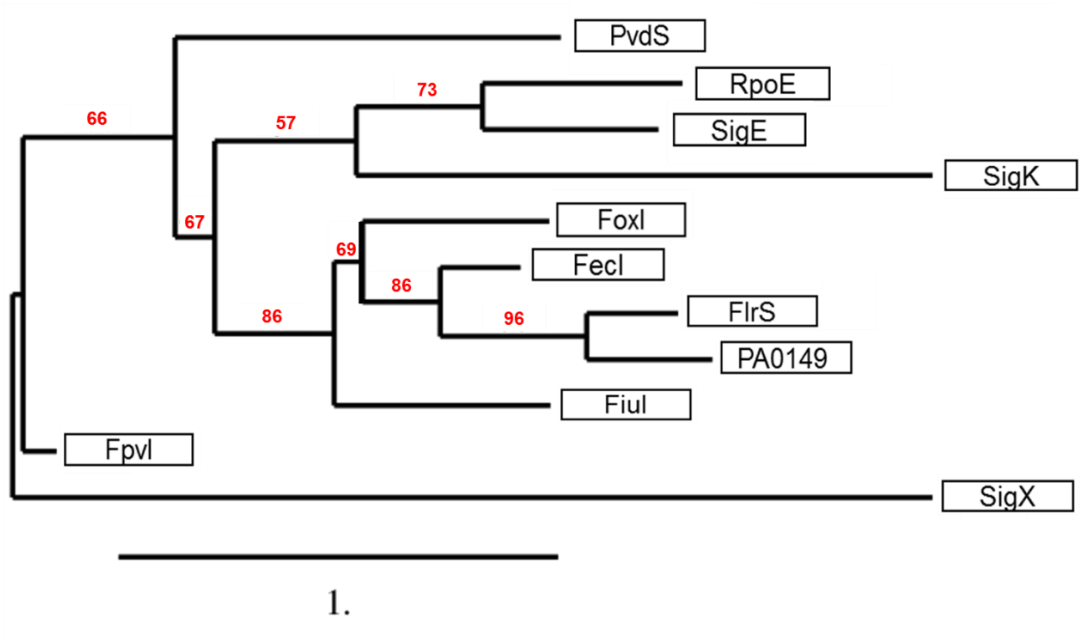

Figure 3-4: Phylogenetic tree of ECF σ factors.

Rooted phylogenetic tree with branch length (UPGMA) inferred from aligned ECF σ factor sequences of *B. cenocepacia* FlrS and ECF σ factors from *E. coli* (FecI and RpoE), *P. aeruginosa* (FoxI, FiuI, FpvI, PA0149 and PvdS), *M. tuberculosis* (SigE and SigK) and *B. subtilis* (SigX). Bootstrap values (in %) are indicated at the corresponding node for each cluster. The rooted phylogenetic tree was constructed from Phylogeny.fr.

3.1.1 Principles of the bacterial two-hybrid system (BACTH)

The BACTH system is based on the interaction-mediated reconstitution of bacterial adenylate cyclase activity in *E. coli*. In this system, the adenylate cyclase domain of the *Bordetella pertussis* CyaA protein is expressed as two complementary fragments, T25 and T18 (Karimova *et al*., 1998). When these two fragments are brought into close proximity, they lead to cAMP synthesis, while they become inactive when they are physically separated (Ladant, 1988; Ladant and Ullmann, 1999). An endogenously adenylate cyclase-deficient *E. coli* strain (Δ*cya*) is therefore used for this system. Once the T25 and T18 fragments are fused to interacting polypeptides, X and Y, the interaction of the T25 and T18 fragments with the X and Y polypeptides (i.e. hybrid proteins) results in the functional reconstitution of adenylate cyclase activity that causes synthesis of cAMP (Karimova *et al*., 2000).

The interaction of the hybrid proteins therefore causes the production of cAMP which binds to the *E. coli* cAMP receptor protein (CRP), also known as the catabolite activator protein (CAP), forming the cAMP/CAP complex. This complex has the ability to activate various gene promoters, including genes that are responsible for the metabolism of alternative carbon sources such as the *lac* and *mal* operons (Kuhnau *et al*., 1991). These are involved in lactose and maltose catabolism, respectively and thus function as reporter genes in the BACTH system, since the metabolism of these carbon sources used by bacteria can be easily detected on selective medium (Figure 3.5). The efficiency of the complementation between T25 and T18 can thus be quantified by measuring the β-galactosidase activities in liquid cultures.

The BACTH system employs two pairs of compatible vectors: (pKT25 and pKNT25) and (pUT18 and pUT18C). The multiple cloning sites (MCS) in both vectors were engineered either at the N-terminal or at the C-terminal coding sequences of each fragment: i.e. the N-terminus of the T25 fragment was engineered in pKNT25 while the C-terminus was engineered in pKT25 (Figure 3.6). In addition, like the T25 fragment, the MCS of the T18 fragment was engineered either at the N-terminus of the pUT18 or at the C-terminus of the pUT18C (Figure 3.7).

Having two compatible vectors is advantageous as it allows the protein of interest to be fused at the N-terminus or the C-terminus of the two CyaA fragments (T25 and T18). pKT25 and pKNT25 express kanamycin resistance, while pUT18 and pUT18C express ampicillin resistance (Figure 3.6 and 3.7). The BACTH plasmids (pKT25 and pKNT25) and (pUT18 and pUT18C) were derived from p15A and ColE1 respectively. The BACTH system also provides positive control plasmids: pKT25-*zip* and pUT18C-*zip* which encode the leucine zipper region of the yeast transcription regulatory protein GCN4 that self-interacts (Karimova *et al*., 1998). The dimerisation of the fused leucine zipper motifs causes an interaction between these two fusion proteins which gives a very strong Cya+ phenotype when they are co-transformed into a *Δcya E. coli* strain. There are two alternative *E. coli* reporter strains that can be used in this system: BTH101 and DHM1. The BACTH assay was used in this study as an *in vivo* screening mechanism to determine the interaction of all the proteins involved in the Flr system.

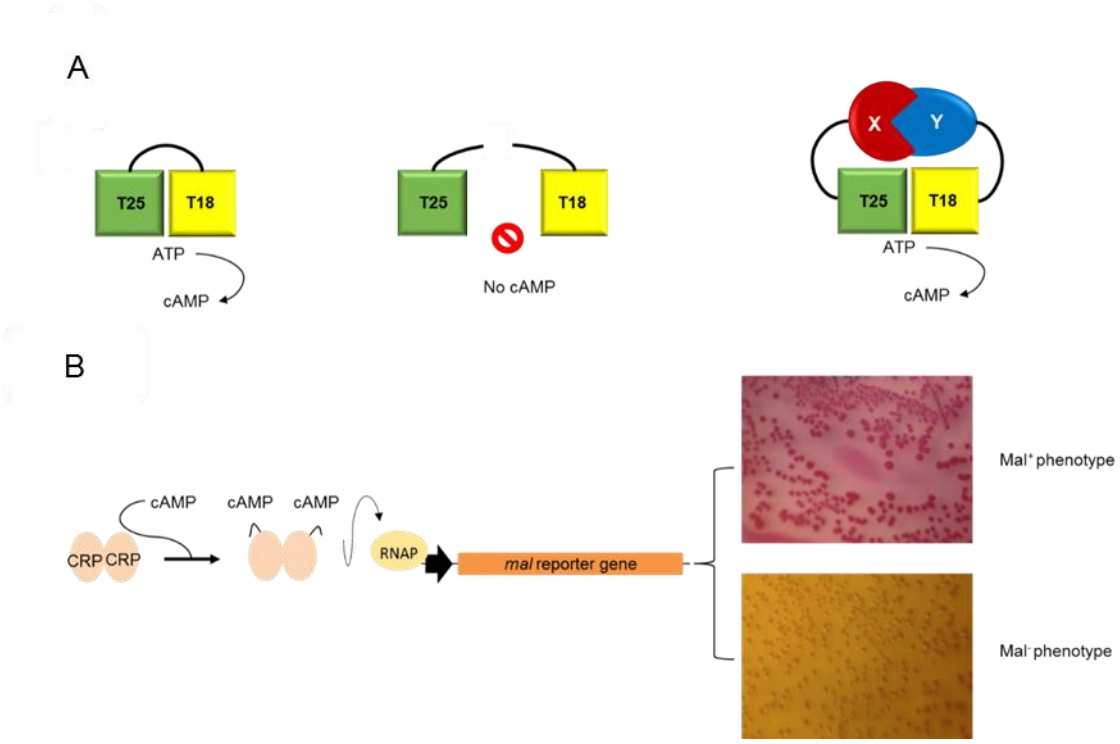

Figure 3-5: Mechanism of the BACTH system.

A. Separation of the T25 and T18 components results in no cAMP production. When the two interacting proteins (X and Y) are fused to the T25 or T18 components, however, they are brought into close proximity and interact with each other leading to the synthesis of cAMP.

B. The cAMP/CRP complex recognises specific promoters and activates the transcription of reporter genes such as the *mal* or *lacZ* genes. The Mal^+ phenotype image shows a strong positive maltose phenotype while the Mal^- phenotype image shows a weak negative maltose phenotype.

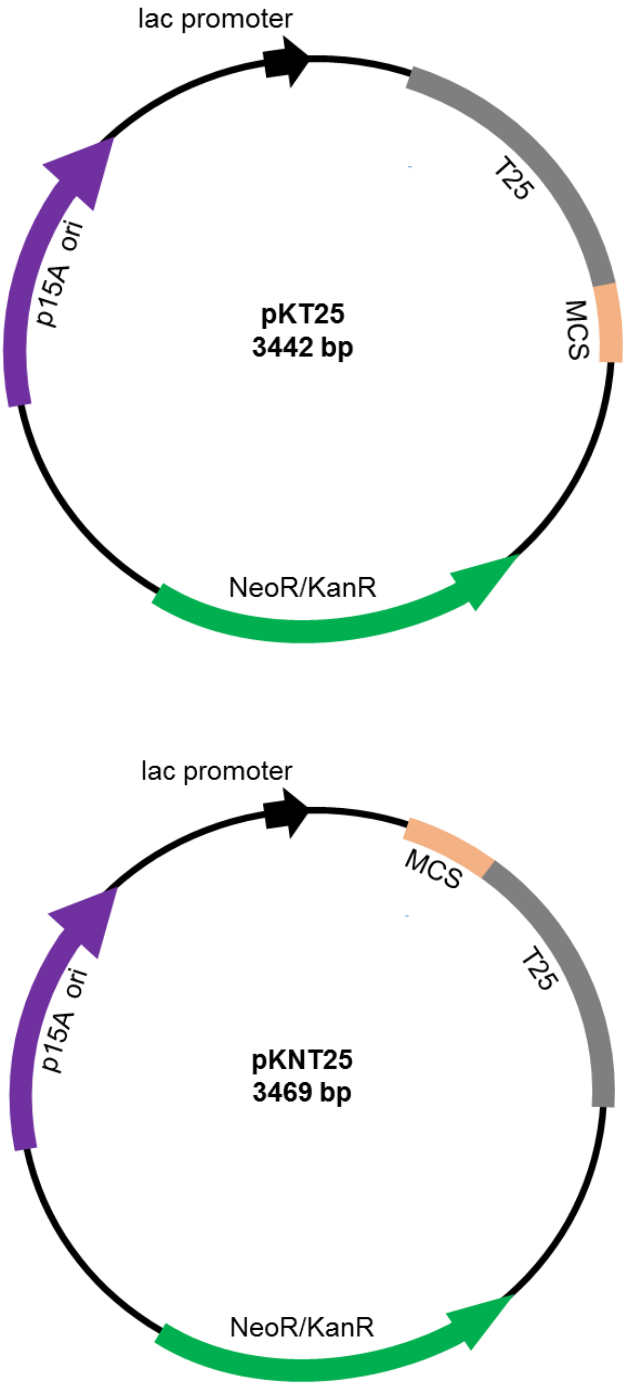

Figure 3-6: Schematic representation of the BACTH plasmids pKT25 and pKNT25.

The MCS is located at the C-terminus coding end of T25 and at the N-terminus coding end of T25, in pKT25 and pKNT25 respectively; shown in nude colour. ori p15A which is the origin of replication and both the kanamycin resistance gene Kan^R and the lac promoter are also shown.

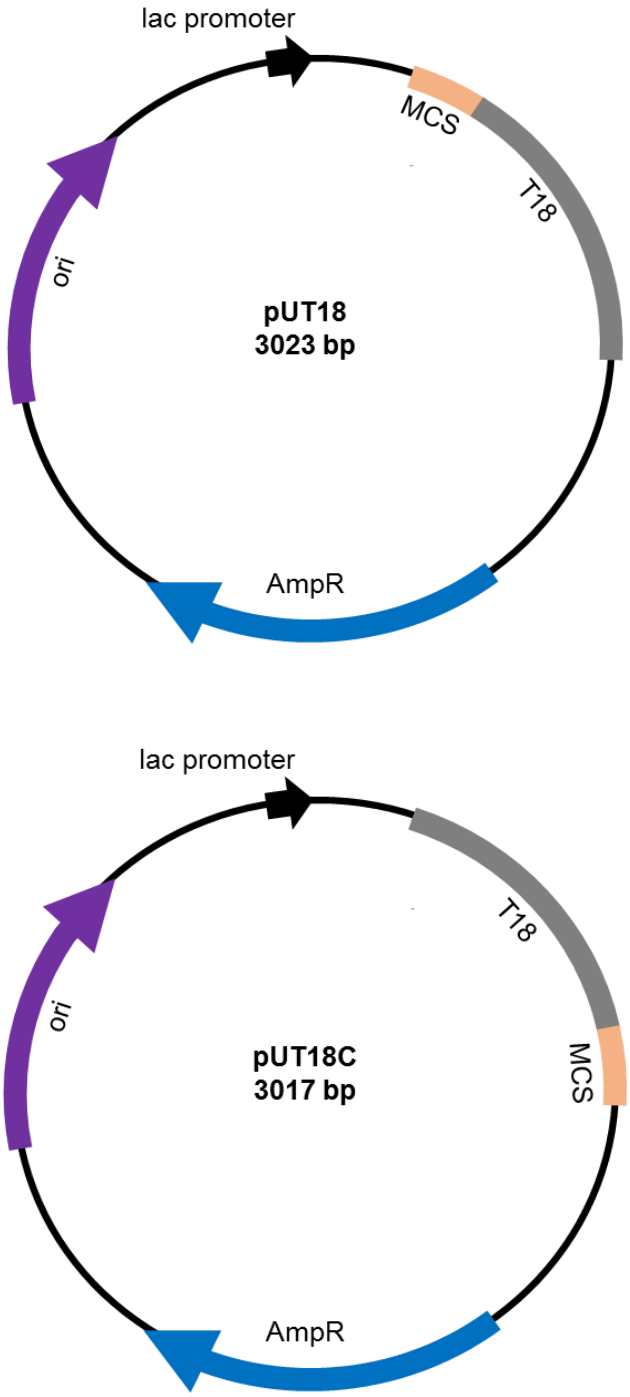

Figure 3-7: Schematic representation of the BACTH plasmids pUT18 and pUT18C.

The MCS is located at the N-terminus coding end of T18 and at the C-terminus coding end of T18, in pUT18 and pUT18C respectively; shown in nude colour. ori ColE1 which is the origin of replication and both the ampicillin resistance gene (Amp^R) and lac promoter are also shown.

3.1.2 Principle of the pull-down assay

The pull-down assay was originally described by Kaelin *et al*. (1991). The principle of the experiment is based on affinity purification of an unknown protein from a mixture of proteins in a soluble cell extract. In this study, proteins of interest were fused with a His-tag or VSVg tag. The fusion protein with a His-tag is termed the bait protein which is coupled to nickel agarose beads. The bait protein is able to compete with other proteins in the mixture for binding and interacts with the prey protein, i.e. interaction partners. The beads are centrifuged in order to allow the collection of the His-tagged fusion protein and any associated protein. Protein complexes are washed several times in order to remove any non-specific binding proteins. To elute the protein complexes from the beads a high concentration of imidazole was used (150-500 mM). Protein complexes can be eluted directly by boiling the samples in SDS loading buffer. Samples are resolved by SDS-PAGE for Coomassie blue staining or Western blotting, in which the prey protein can be detected by specific antibodies.

3.2 Objectives

- To investigate whether the N-terminal domain of the putative anti-σ factor FlrR interacts with the C-terminal domain of region (σ_4) of σ factor FlrS using the BACTH system.

- To establish whether the C-terminal domain of the putative anti-σ factor can interact with the N-terminal domain of the putative outer-membrane receptor FlrA using the BACTH system.

- To investigate any possible interaction between FlrR and FlrS and between FlrR and FlrA using pull-down assay.

3.3 FlrS-FlrR interaction using BACTH system

In other studied ECF σ factor systems such as the *E. coli* Fec system, it is known that the anti-σ factor N-terminal domain interacts with the C-terminal domain of the σ factor. The BACTH system is the most convenient technique to study protein-protein interactions. Thus, it was used in this study to investigate possible interactions between the σ factor, FlrS and the putative anti-σ factor, FlrR.

Construction of $FlrS_{CTD}$ and $FlrR_{NTD}$ into BACTH plasmids

The N-terminal domain of an anti-σ factor and the C-terminal domain of a σ factor interact with each other conventionally. In this study we are investigating two genes, *flrS* and *flrR* that are located upstream of *flrA*. A search in the GenBank database for homologous sequences revealed similarities between the FlrS-FlrR of the Flr system and the FecR-FecI of the Fec system (Section 3.1). Therefore, there is a possible interaction between regions encoding the N-terminal domain and the C-terminal domain of the predicted anti-σ factor FlrR and the putative σ factor FlrS. The interaction between these two domains were investigated in this study using the BACTH system.

Cloning *flrS* and *flrR* into pKNT25 and pUT18 results in the expression of a hybrid protein with its C-terminus fused to the N-terminus of T25 and T18, respectively. Using these two vectors required the removal of the stop codon of the gene encoding the test protein to allow the translation of T25 and T18 fragments. Cloning *flrS* and *flrR* into pKT25 and pUT18C results in the expression of a hybrid protein in which the N-terminus of the test protein is fused to the C-terminus of T25 and T18, respectively, and this result in eight combinations of $FlrS_{CTD}$ and $FlrR_{NTD}$. It is important that genes encoding $FlrS_{CTD}$ and $FlrR_{NTD}$ are inserted in-frame with the T25 or T18 ORF. Since five of eight required BACTH plasmids have been constructed previously (pKNT25-$FlrR_{NTD}$, pKNT25-$FlrS_{CTD}$, pKT25-$FlrS_{CTD}$, pUT18-$FlrR_{NTD}$ and pUT18-$FlrS_{CTD}$) (Haldipurkar, MSC dissertation, 2012). It was only necessary to construct pKT25-$FlrR_{NTD}$, pUT18C-$FlrR_{NTD}$ and pUT18C-$FlrS_{CTD}$. All these combinations were tested in order to find out the strongest interaction among them.

flrS and *flrR* were amplified using the proofreading enzyme, KOD Hot Start DNA polymerase. DNA encoding the N-terminal domain of the anti-σ factor $FlrR_{NTD}$ was amplified using two different pairs of primers, (flrRNTDKTfor and M13for) and ($FlrR_{NTD}$for2 and M13for). The first two primers were used to fuse $FlrR_{NTD}$ to T25 (pKT25) while the other two primers were used to fuse $FlrR_{NTD}$ to T18 (pUT18C). pBBR2-$FlrR_{NTD}$ was used as the template in both cases and the resulting PCR products gave the size of 328 bp (results not shown). The two PCR products, pKT25 and pUT18C vectors were digested with restriction enzymes *Pst*I and *Bam*HI. DNA encoding the C-terminal domain of the σ factor FlrS was amplified using these primers (FlrSCTDfor2 and FlrSCTDrev) and pBBR2-FlrSR was used as a DNA template. A PCR product of the expected size of 280 bp was obtained (results not shown). In order to clone the $FlrS_{CTD}$ PCR product into pUT18C, the PCR product and the vector were digested with restriction enzymes *Pst*I and *Bam*HI.

All digested PCR products were inserted into each vector using T4 DNA ligase. The ligation mixture was then transformed into *E. coli* JM83 or MC1061 competent cells. The transformation was plated on LB plates containing 50 mg/ml kanamycin when pKT25 and pKNT25 were used and 100 mg/ml ampicillin when pUT18 and pUT18C were used. The obtained colonies were screened by plasmid miniprep or by colony PCR in order to identify transformants containing plasmids harbouring the DNA fragment of interest. All positive clones of pKT25-$FlrR_{NTD}$, pUT18C-$FlrR_{NTD}$ and pUT18C-$FlrS_{CTD}$ gave the expected sizes of 3.77 kb, 3.345 kb and 3297 bp, respectively (results not shown).

3.3.1 FlrS-FlrR interaction

To perform the BACTH assay, *E. coli* BTH101 competent cells were co-transformed with compatible pairs of BACTH plasmids encoding fusions of $FlrR_{NTD}$ or $FlrS_{CTD}$. The interaction was investigated using all possible combinations of plasmids encoding fusions of $FlrR_{NTD}$ and $FlrS_{CTD}$ domains. In addition, the possible self-interaction of each domain was investigated (four pairwise combinations each).

Negative control plasmid combinations were included where one plasmid encoded a domain fusion and the other plasmid was an empty vector (eight combinations for each domain). Negative controls were included to ensure that the interactions are not due to non-specific interactions or as result of a protein's ability to induce a Cya^+ phenotype.

An additional negative control combination was included where no insert was present in either plasmid. In addition, a positive control plasmid combination of pUT18C-*zip* and pKT25-*zip* was included. It was observed on indicator MacConkey maltose agar plates that all possible combinations tested between the fusion proteins of $FlrR_{NTD}$ and $FlrS_{CTD}$ gave rise to a strong Mal^+ phenotype (Figure 3.8A). On MacConkey-maltose agar, the positive control resulted in a strong Mal^+ phenotype, whereas all possible combinations of $FlrR_{NTD}$ and $FlrS_{CTD}$ assayed with BACTH empty vectors (as negative controls) gave rise to a Mal^- phenotype (Figure 3.8B and C).

The interactions of BACTH plasmids encoding $FlrR_{NTD}$ and $FlrS_{CTD}$ fusions were quantified by measuring the β-galactosidase activities in cells growing in liquid culture (Karimova *et al*., 1998; 2005). The results of these β-galactosidase measurements confirmed the results obtained on MacConkey-maltose agar plates, i.e. all heterologous combinations of $FlrS_{CTD}$ and $FlrR_{NTD}$ hybrid proteins were associated with significantly high activity but the activities varied between all combinations. The highest activities were observed between the two combinations pUT18C-$FlrS_{CTD}$ and pKNT25-$FlrR_{NTD}$. Nonetheless, the activity was (2191 ± 30 Mu) less than the activity measured for the positive control pUT18C-*zip* and pKT25-*zip* (5867 ± 176 Mu). pUT18-$FlrS_{CTD}$ and pKNT25-$FlrR_{NTD}$ gave rise to a β-galactosidase activity which was slightly less than the activities observed for the first combinations. Two other combinations (pUT18C-$FlrS_{CTD}$ and pKT25-$FlrR_{NTD}$) and (pUT18-$FlrS_{CTD}$ and pKNT25-$FlrR_{NTD}$) gave rise to a roughly similar level of β-galactosidase activity (Figure 3.9A). All the negative controls gave rise to activities ranging between 66 and 70 Mu (Figure 3.9B).

A

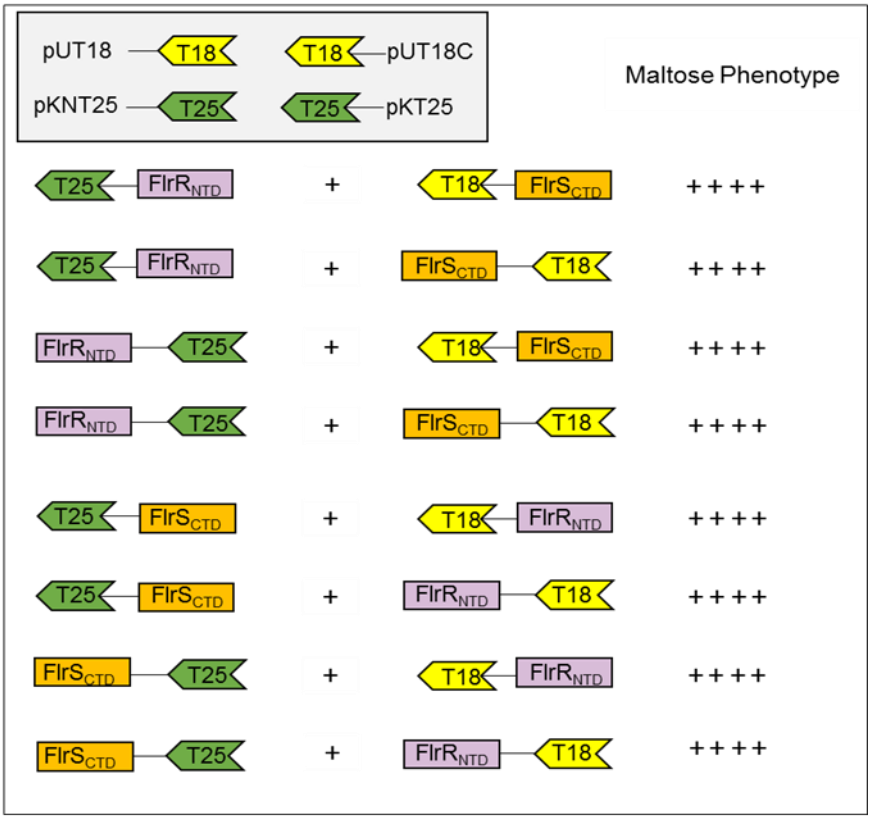
pUT18
T18
T18
pUT18C
pKNT25
T25
T25
pKT25
Maltose Phenotype
T25 FlrR$_{NTD}$ + T18 FlrS$_{CTD}$ ++++
T25 FlrR$_{NTD}$ + FlrS$_{CTD}$ T18 ++++
FlrR$_{NTD}$ T25 + T18 FlrS$_{CTD}$ ++++
FlrR$_{NTD}$ T25 + FlrS$_{CTD}$ T18 ++++
T25 FlrS$_{CTD}$ + T18 FlrR$_{NTD}$ ++++
T25 FlrS$_{CTD}$ + FlrR$_{NTD}$ T18 ++++
FlrS$_{CTD}$ T25 + T18 FlrR$_{NTD}$ ++++
FlrS$_{CTD}$ T25 + FlrR$_{NTD}$ T18 ++++

B

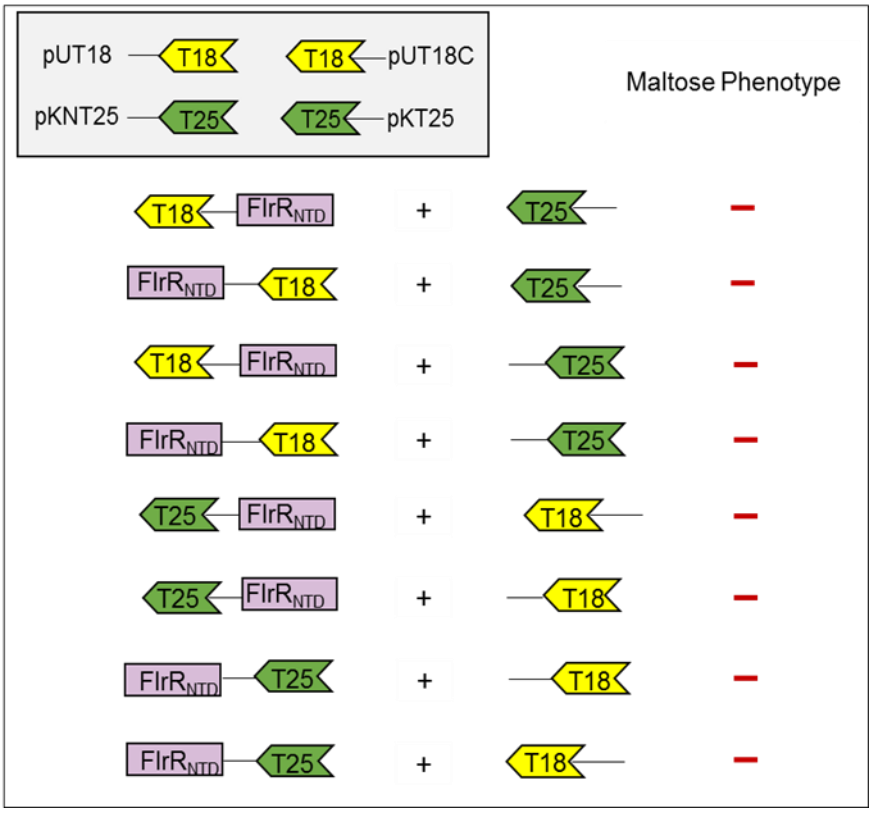
pUT18
T18
T18
pUT18C
pKNT25
T25
T25
pKT25
Maltose Phenotype
T18 FlrR$_{NTD}$ + T25 −
FlrR$_{NTD}$ T18 + T25 −
T18 FlrR$_{NTD}$ + T25 −
FlrR$_{NTD}$ T18 + T25 −
T25 FlrR$_{NTD}$ + T18 −
T25 FlrR$_{NTD}$ + T18 −
FlrR$_{NTD}$ T25 + T18 −
FlrR$_{NTD}$ T25 + T18 −

C

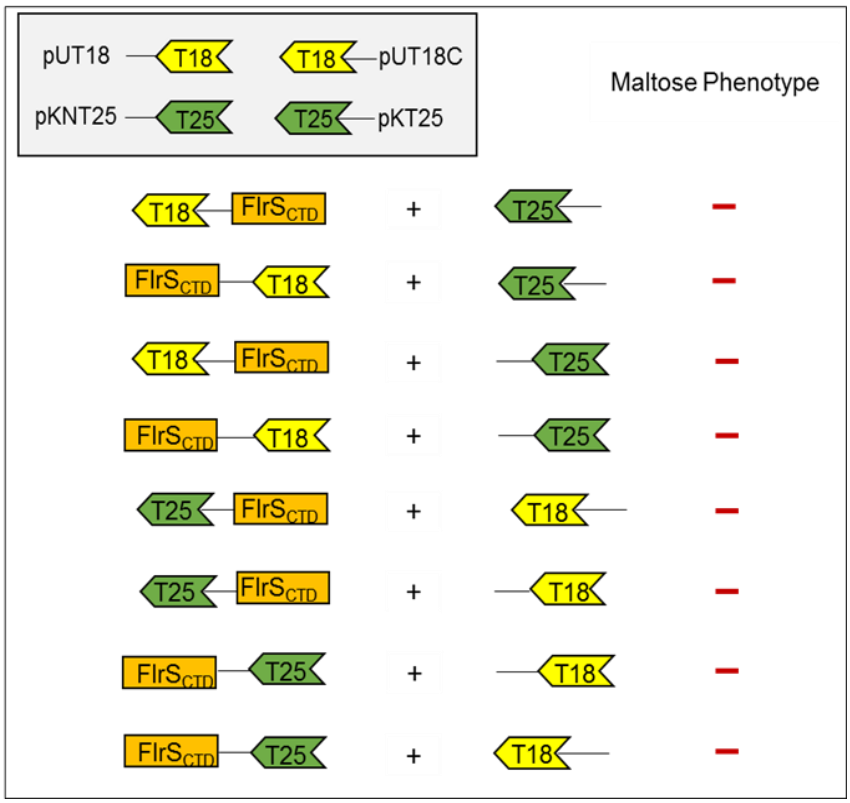

Figure 3-8: Investigation of $FlrS_{CTD}$ and $FlrR_{NTD}$ interaction using the BACTH system assay.

A. All possible combinations of $FlrR_{NTD}$ and $FlrS_{CTD}$ were fused to the N-terminal or C-terminal of *B. pertussis* adenylate cyclase T25 and T18 fragments.

B. All possible combinations of $FlrR_{NTD}$ and empty BACTH plasmids.

C. All possible combinations of $FlrS_{CTD}$ and empty BACTH plasmids.

All combinations were transformed into *E. coli* strain BTH101. Transformants were selected on MacConkey-maltose agar and scored for maltose phenotype after 5 days. The degree of the maltose phenotype is indicated next to the corresponding diagram. (++++) indicates strong Mal^+ phenotype and (−) Mal^- phenotype.

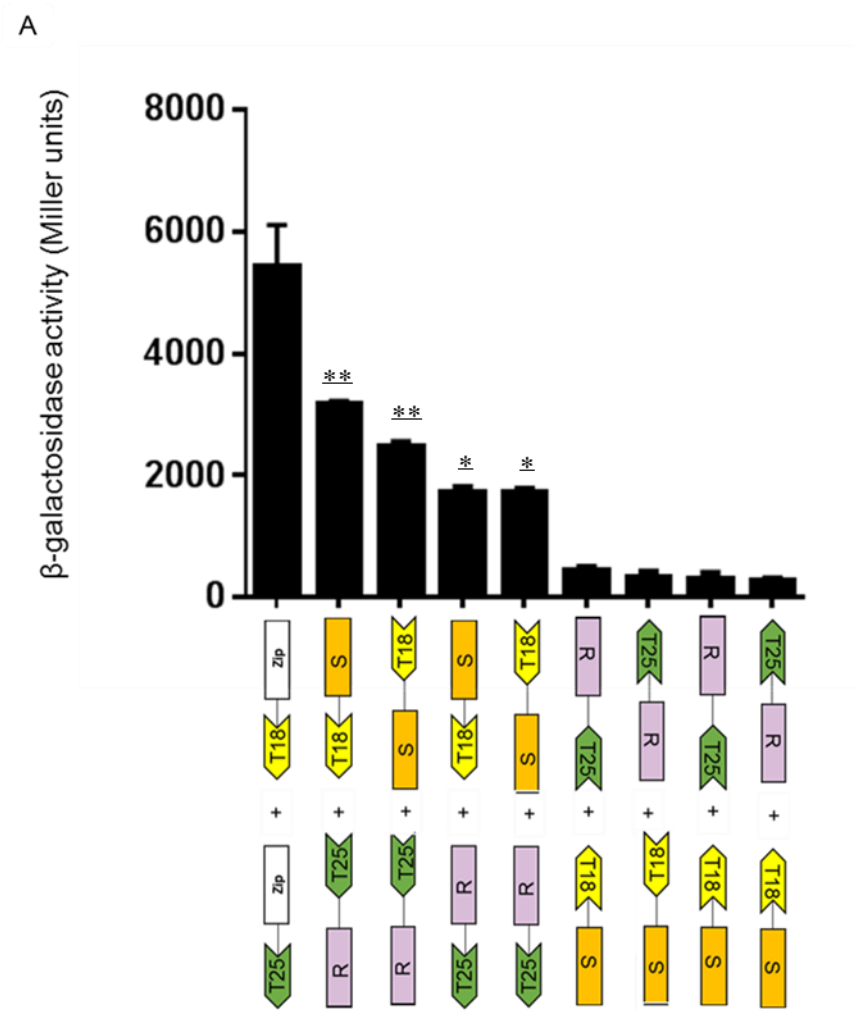
A
β-galactosidase activity (Miller units)
8000
6000
4000
2000
0
**
**
*
*
Zip
T18
+
Zip
T25
S
T18
+
T25
R
T18
S
+
T25
R
S
T18
+
R
T25
T18
S
+
R
T25
R
T25
+
T18
S
R
T25
+
T18
S
T25
R
+
T18
S

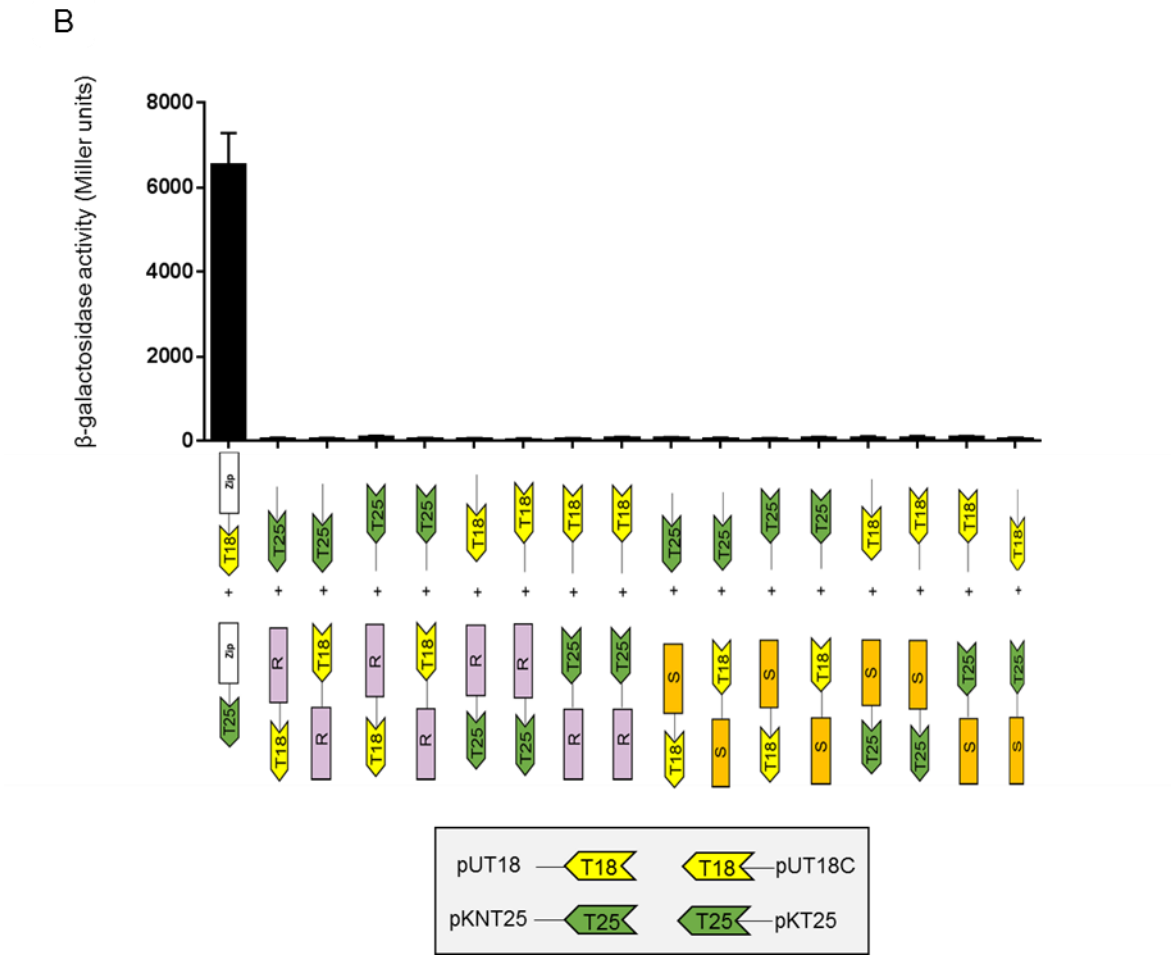

Figure 3-9: Quantification of $FlrR_{NTD}$ and $FlrS_{CTD}$ interaction using the BACTH system assay: β-galactosidase.

A. The efficiency of the functional complementation of CyaA due to $FlrR_{NTD}$-$FlrS_{CTD}$ interaction was quantitated by measuring β-galactosidase activity.

B. Analysis of interactions between all possible negative controls of $FlrR_{NTD}$ and $FlrS_{CTD}$ with BACTH empty vectors using β-galactosidase assay.

The efficiencies of functional complementation between $FlrR_{NTD}$ and $FlrS_{CTD}$ interactions with all empty BACTH plasmids (pKNT25-pKT25 and pUT18C-pUT18) were quantified by measuring β-galactosidase. A positive control, pUT18C-*zip* and pKT25-*zip* was included. R corresponds to $FlrR_{NTD}$ and S corresponds to $FlrS_{CTD}$. Error bars represent the standard deviation of three independent experiments. The background level of the β-galactosidase activity measured in the negative controls was 66-70 Mu. The results were analysed using T test ** $P < 0.01$, * $P < 0.05$.

3.3.2 Investigation of self-interaction of $FlrR_{NTD}$ and $FlrS_{CTD}$

The activities in cells harbouring all homologous pairwise combinations of the BACTH combinations of T25-$FlrR_{NTD}$ or T18-$FlrS_{CTD}$ (i.e. analysis of self-interactions) were investigated using BACTH assay. $FlrR_{NTD}$ or $FlrS_{CTD}$ fused at either end of T25 or T18 yielded a Mal^- phenotype indicating that self-interaction of $FlrR_{NTD}$ or $FlrS_{CTD}$ was not detected by the BACTH system (Figure 3.10A). pKT25-*zip* and pUT18C-*zip* were introduced in *E. coli* BTH101 as a positive control. Cells containing BACTH empty vectors in combination with a compatible plasmid expressing a fusion protein were used as negative controls (Figure 3.10B). The results for self-interactions of $FlrR_{NTD}$ and $FlrS_{CTD}$ showed that all homologous pairwise combinations of plasmids yielded low β-galactosidase activities which were similar to the level of β-galactosidase activities measured for the negative controls (Figure 3.11A and B).

A

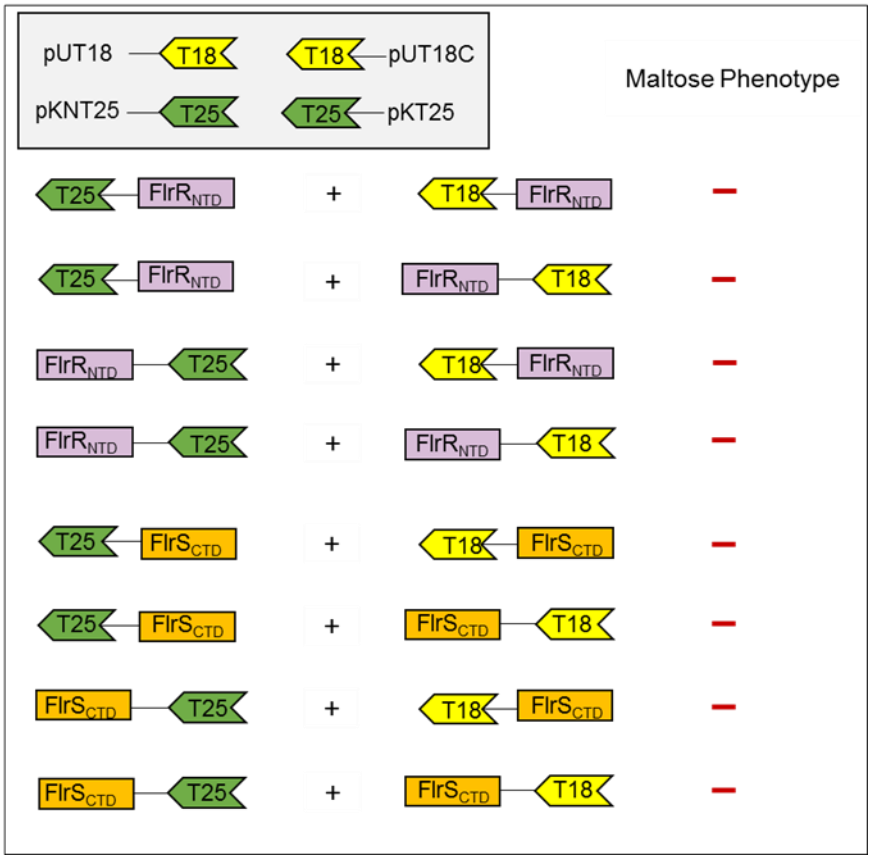

B

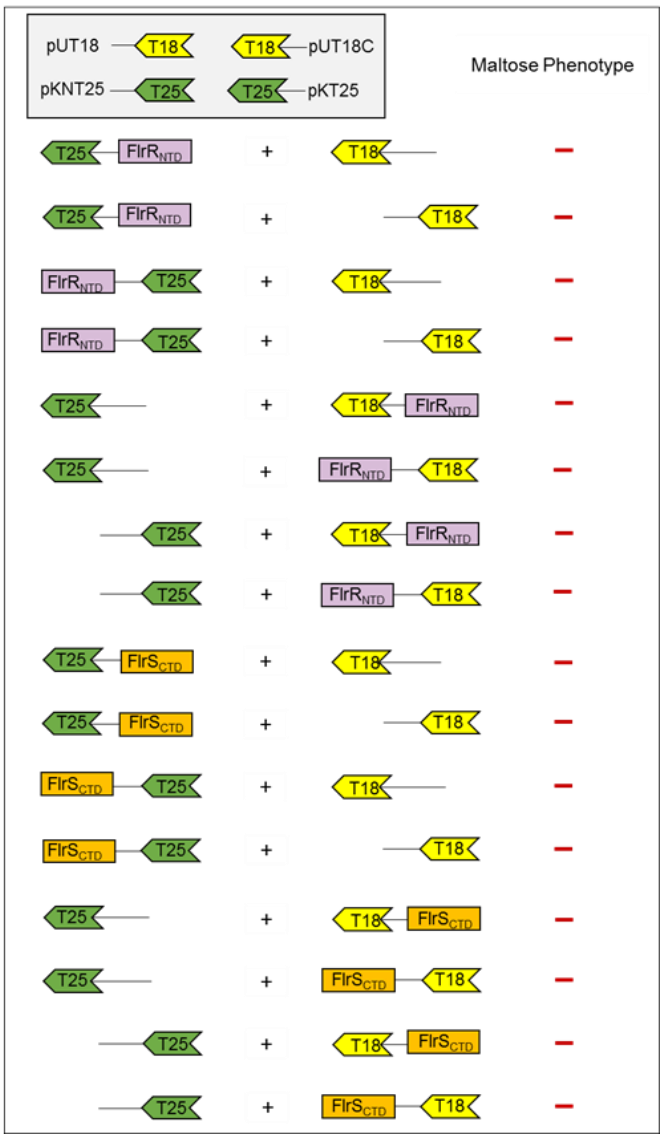

Figure 3-10: Investigation of $FlrR_{NTD}$ and $FlrS_{CTD}$ self-interaction using the BACTH system assay.

A. All possible combinations of $FlrR_{NTD}$ and $FlrS_{CTD}$ were fused to the N-terminal or C-terminal of *B. pertussis* adenylate cyclase T25 and T18 fragments.

B. Cells containing one empty vector in combination with a compatible plasmid expressing $FlrR_{NTD}$ and $FlrS_{CTD}$ were used as negative controls.

All combinations were transformed into *E. coli* strain BTH101. Transformants were selected on MacConkey-maltose agar plates and scored for the maltose phenotype after 5 days. (–) negative Mal^- phenotype. The degree of the maltose phenotype is indicated next to the corresponding diagram.

A

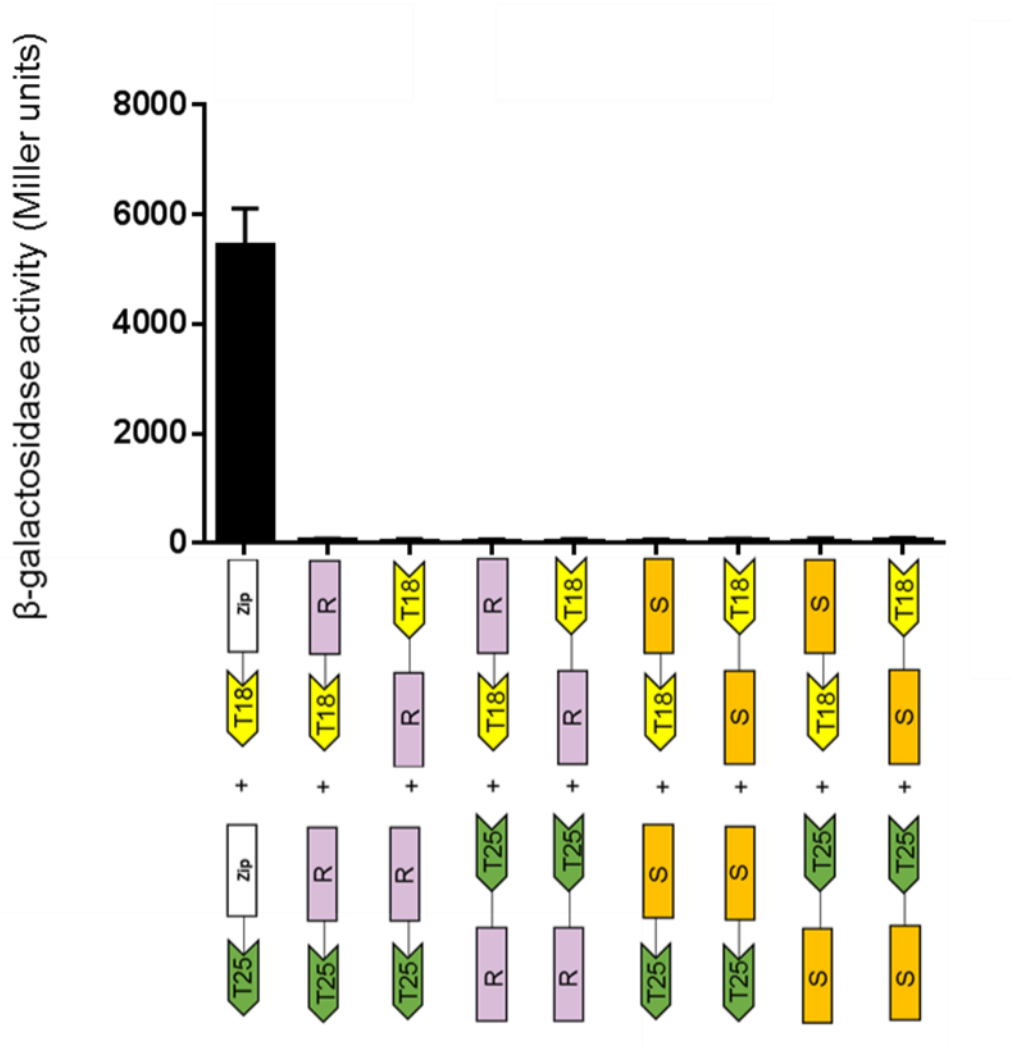
β-galactosidase activity (Miller units)
8000
6000
4000
2000
0
Zip
T18
R
T18
R
T18
S
T18
S
T18
+
Zip
T25
R
T25
R
T25
R
T25
R
T25
S
T25
S
T25
S
T25
S

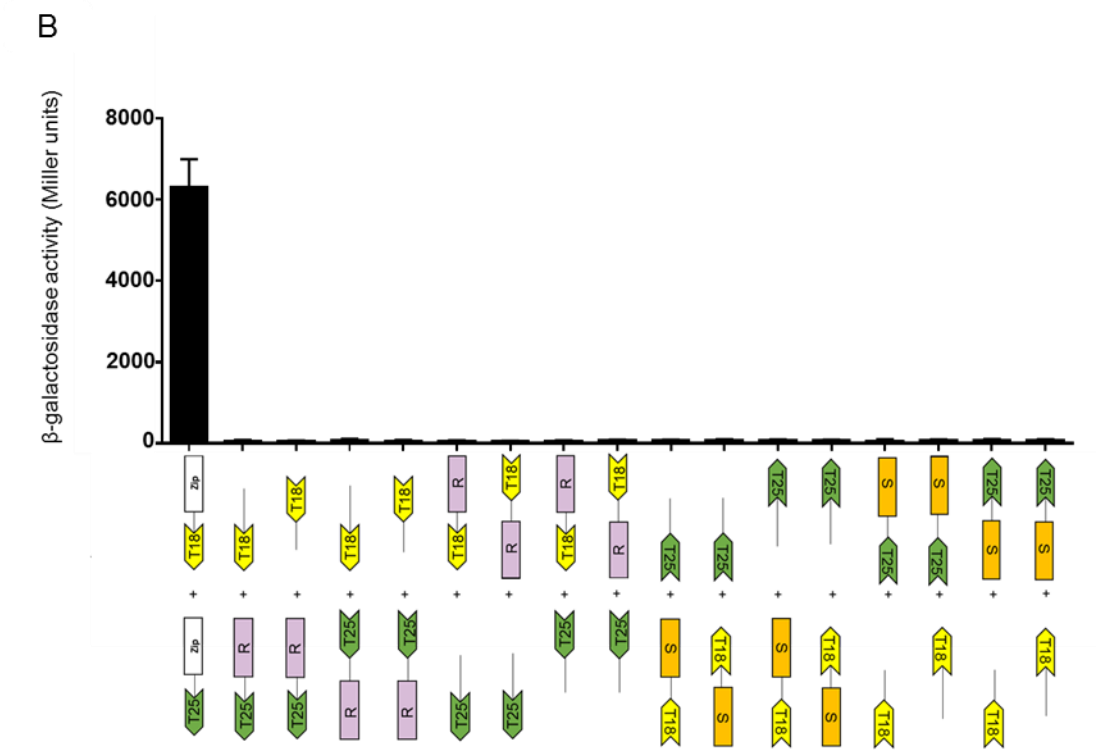

Figure 3-11: Quantification of $FlrR_{NTD}$ and $FlrS_{CTD}$ self-interaction using the BACTH system assay: β-galactosidase.

A. The possible self-interaction of $FlrR_{NTD}$ and $FlrS_{CTD}$ was investigated by measuring β-galactosidase activity in cells harbouring a combination of BACTH plasmids.

B. $FlrR_{NTD}$ and $FlrS_{CTD}$ with all possible empty BACTH vectors (negative controls) were investigated by measuring β-galactosidase activity in cells harbouring a combination of BACTH plasmids.

The efficiencies of functional complementation between $FlrR_{NTD}$ and $FlrS_{CTD}$ (self-interaction) and the negative controls interactions with all empty BACTH plasmids (pKNT25-pKT25 and pUT18C-pUT18) were quantified by measuring β-galactosidase. A positive control, pUT18C-*zip* and pKT25-*zip* was included. R corresponds to $FlrR_{NTD}$ and S corresponds to $FlrS_{CTD}$. Error bars represent the standard deviation of three independent experiments. The background level of the β-galactosidase activity measured in the negative controls was 66-70 Mu.

3.3.3 Investigation of Full-length FlrR self-interaction

The BACTH assay was performed to investigate the ability of the leucine zipper sequence within the FlrR to form a dimer and block the possible self-interaction of full-length FlrR. The Full-length FlrR was fused to pKNT25 and pUT18C in order to create in-frame fusions at the N-terminal of T25 and T18. To construct recombinant plasmids for this experiment, the Full-length *flrR* was amplified by PCR from the pBBR2-FlrSR plasmid. The corresponding primers used for amplification were fullFlrRFor and fullFlrRRev. To make in-frame fusions to the T25 and T18 fragment of the adenylate cyclase, the resulting PCR products were digested with *Bam*HI and *Pst*I and the DNA fragments were cloned into pKNT25 and pUT18C digested with the same enzymes (results not shown). MacConkey-maltose agar plate showed no interactions between pKNT25-FlrR and pUT18C-FlrR fusion proteins. Negative controls were also assayed and as expected they gave rise to a Mal^- phenotype (Figure 3.12). The β-galactosidase results were in agreement with the agar plate results, demonstrating that there were no activities observed between the fusion proteins of pKNT25-FlrR and pUT18C-FlrR. All possible controls were included (Figure 3.13).

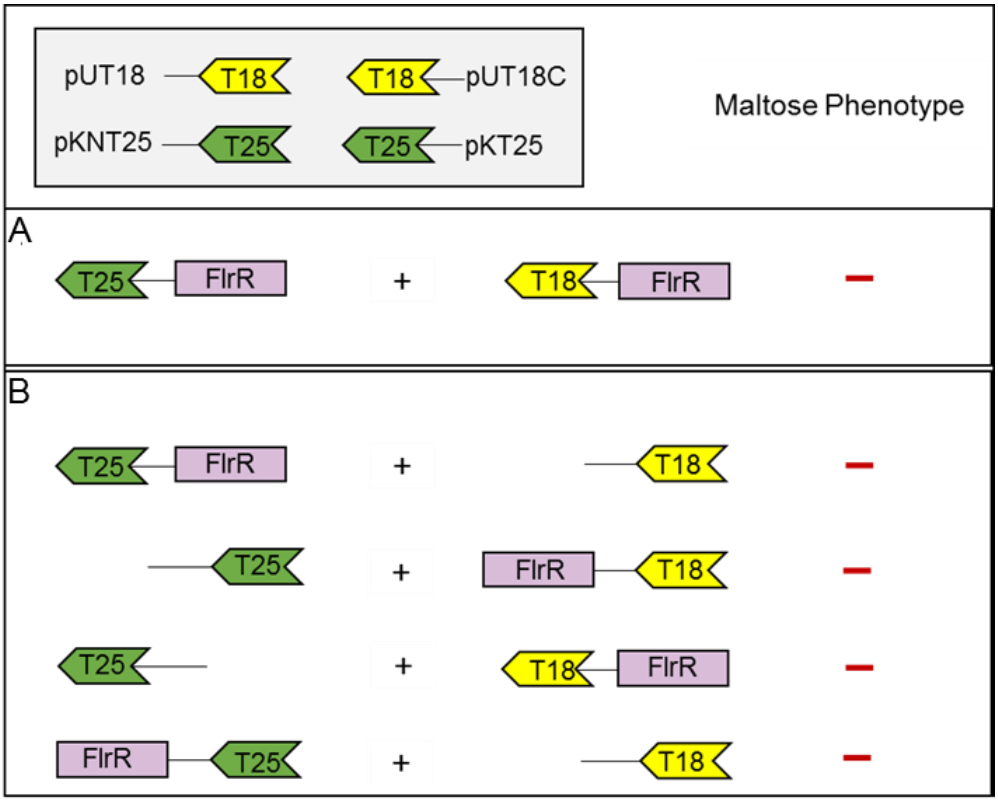

Figure 3-12: Investigation of full-length FlrR self-interaction using the BACTH system assay.

A. Full-length FlrR was fused to the N-terminal of *B. pertussis* adenylate cyclase T25 and T18 fragments.

B. Cells containing one empty vector in combination with a compatible plasmid expressing Full-length FlrR were used as negative controls.

All combinations were transformed into *E. coli* strain BTH101. Transformants were selected on MacConkey-maltose agar plates and scored for the maltose phenotype after 5 days. (–) Mal^- phenotype. The degree of the maltose phenotype is indicated next to the corresponding diagram.

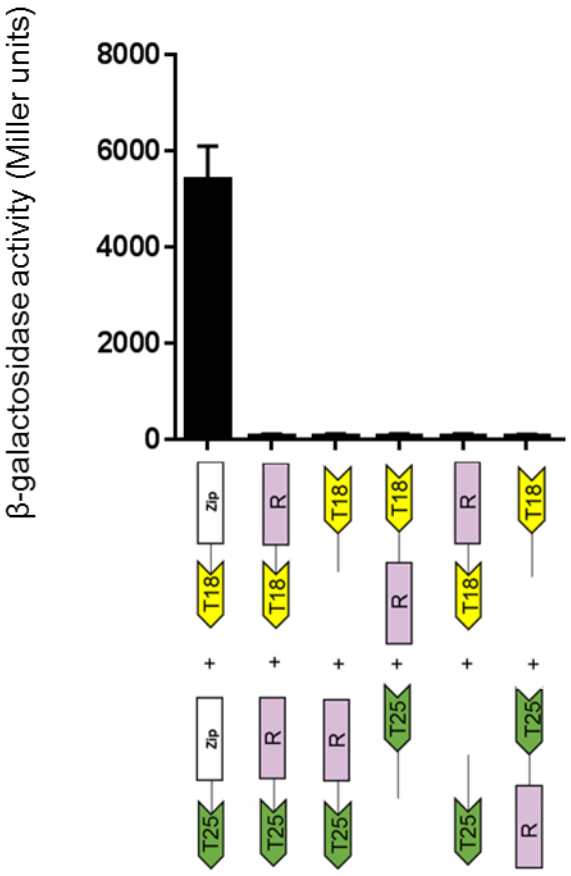

Figure 3-13: Quantification of full-length FlrR self-interaction using the BACTH system assay: β-galactosidase.

The possible self-interaction of full-length FlrR; pKNT25-FlrR and pUT18C-FlrR was investigated by measuring β-galactosidase activity in cells harbouring a combination of BACTH plasmids.

The efficiencies of functional complementation between pKNT25-FlrR and pUT18C-FlrR (self-interaction) and the negative controls interactions with all empty BACTH plasmids (pKNT25-pKT25 and pUT18C-pUT18) were quantified by measuring β-galactosidase. A positive control, pUT18C-*zip* and pKT25-*zip* was included. R corresponds to full-length FlrR. Error bars represent the standard deviation of three independent experiments. The background level of the β-galactosidase activity measured in the negative controls was 66-70 Mu.

3.3.4 Investigation of full-length FlrR and $FlrS_{CTD}$ interactions

Fusion proteins of the full-length FlrR were also used to investigate whether they can interact with pKNT25-$FlrS_{CTD}$ and pUT18C-$FlrS_{CTD}$ fusion BACTH plasmids encoding the C-terminal of σ factor FlrS. Combinations of pKNT25-FlrR and pUT18-FlrS fusion proteins yielded weak red/purple colonies on MacConkey maltose agar plates, the transformants were scored for their maltose phenotype on MacConkey-maltose agar after 5 days (Figure 3.14). The β-galactosidase results are consistent with the agar plates since they indicate that these combinations interact with each other. Positive control pKT25-*zip* and pUT18C-*zip* and all possible negative controls were included in both assays (Figure 3.15).

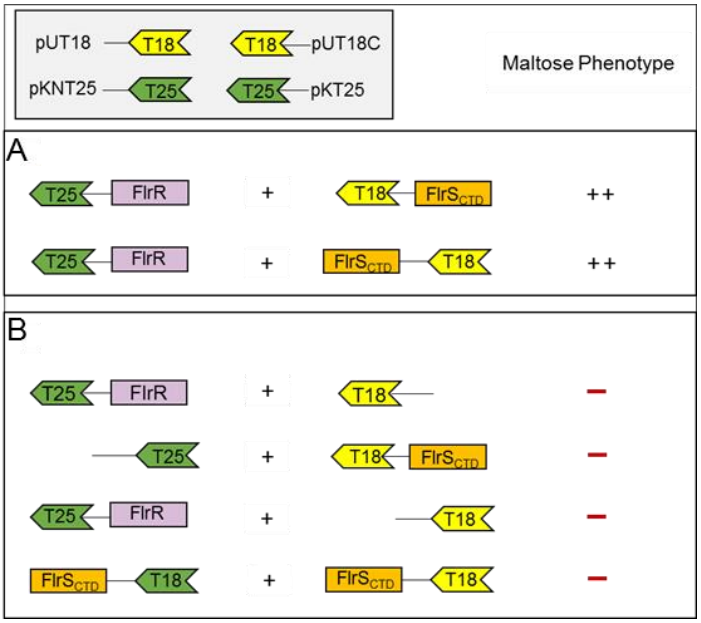

Figure 3-14: Investigation of full-length FlrR and $FlrS_{CTD}$ interaction using the BACTH system assay.

A. Full-length FlrR and $FlrS_{CTD}$ were fused to the N-terminal of *B. pertussis* adenylate cyclase T25 and T18 fragments.

B. Cells containing one empty vector in combination with a compatible plasmid expressing full-length FlrR and $FlrS_{CTD}$ were used as negative controls.

All combinations were transformed into *E. coli* strain BTH101. Transformants were selected on MacConkey-maltose agar plates and scored for the maltose phenotype after 5 days. (++) indicates Mal^+ phenotype and (−) Mal^- phenotype. The degree of the maltose phenotype is indicated next to the corresponding diagram.

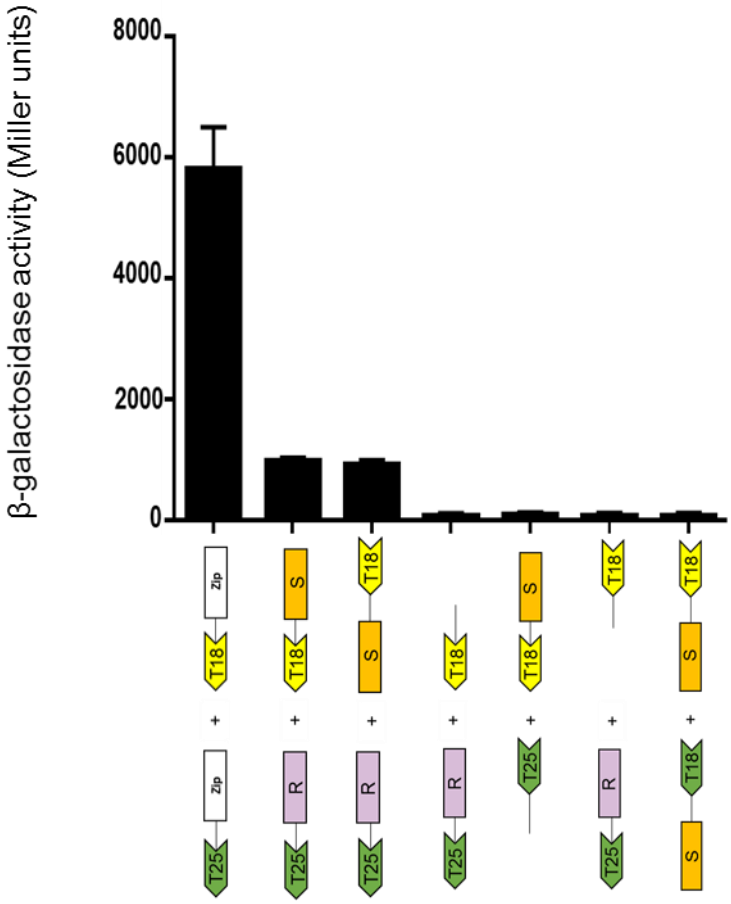

Figure 3-15: Quantification of full-length FlrR and $FlrS_{CTD}$ interaction using the BACTH system assay: β-galactosidase.

The possible interaction of full-length FlrR interaction with $FlrS_{CTD}$ was investigated by measuring β-galactosidase activity in cells harbouring a combination of BACTH plasmids.

The efficiencies of functional complementation between full-length FlrR interaction with $FlrS_{CTD}$ and the negative controls interactions with all empty BACTH plasmids (pKNT25-pKT25 and pUT18C-pUT18) were quantified by measuring β-galactosidase. A positive control, pUT18C-*zip* and pKT25-*zip* was included. R corresponds to full-length FlrR and S corresponds to $FlrS_{CTD}$. Error bars represent the standard deviation of three independent experiments. The background level of the β-galactosidase activity measured in the negative controls was 66-70 Mu.

3.4. Investigation of the interaction between $FlrR_{NTD}$ and $FlrS_{CTD}$ using pull-down assay

Pull-down assay will be used to investigate the interaction between $FlrR_{NTD}$ and $FlrS_{CTD}$ proteins as the BACTH system assay between $FlrR_{NTD}$ and $FlrS_{CTD}$ proteins gave a detectable positive maltose phenotype when they were fused to the T25 and T18 components of *B. pertussis* adenylate cyclase. It was therefore necessary to confirm this result using biochemical techniques such pull-down assay (Section 3.1.2), as the BACTH assay may give rise to false positive results.

Construction of pACYCDuet-$FlrR_{NTD}$-VSVg and pACYCDuet-His_6-$FlrS_{CTD}$

It was decided to clone the DNA sequence encoding $FlrR_{NTD}$ and $FlrS_{CTD}$ proteins into over-expression vector pACYCDuet-1. pACYCDuet-1 is an expression vector that has two multiple cloning sites (MCS), both located downstream of a T7 promoter/lac operator and ribosome-binding site (rbs). It carries the origin of replication of plasmid p15A and a chloramphenicol resistance gene (Figure 3.16).

$FlrS_{CTD}$ intend to be cloned into the first MCS of pACYCDuet-1 incorporating a His tag sequence at the N-terminal region of $FlrS_{CTD}$. Amplified $FlrS_{CTD}$ and pACYCDuet-1 plasmid were digested with *Bam*HI and *Pst*I restriction enzymes. The digested product was ligated and transformed into *E. coli* strain MC1061. Colony PCR was performed in order to screen for a positive clone that should give an expected DNA size of 280 bp for the insert (result not shown).

$FlrR_{NTD}$ to be cloned into pACYCDuet-1 at the second MCS of pACYCDuet-1 where the reverse primer added a VSVg tag at the C-terminal end of $FlrR_{NTD}$. Amplified $FlrR_{NTD}$ and pACYCDuet-1 plasmid were digested with *Nde*I and *Bgl*II. The digested DNA ligated and then transformed into *E. coli* MC1061 competent cell. The resulting colonies were PCR screened and the expected DNA size is 320 bp (result not shown).

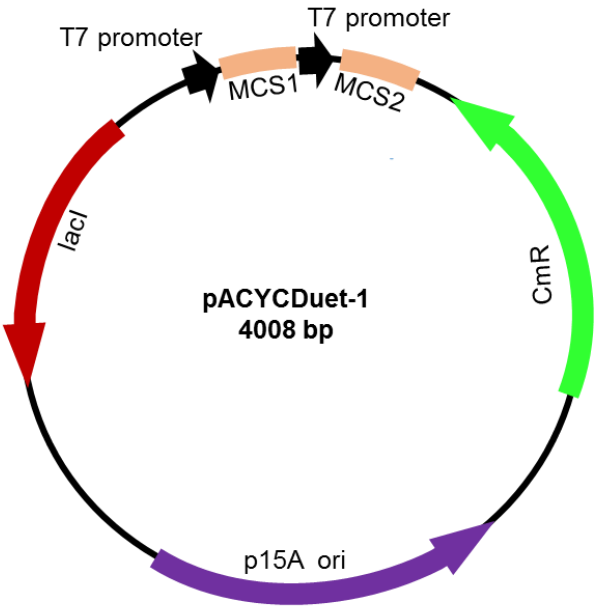

Figure 3-16: Diagrammatic illustration of the T7 expression vector pACYCDuet-1.

The purple colour represents the origin of p15A replication. The green colour is the chloramphenicol resistance gene. The two MCS sites of this overexpression vector are shown in nude colour. The lac operator is shown in red colour.

Overexpression of His_6-$FlrS_{CTD}$

To investigate His_6-$FlrS_{CTD}$ overexpression and solubility, pACYCDuet-His_6-$FlrS_{CTD}$ was introduced into *E. coli* BL21(λDE3) and subjected to 3 hours' induction with 1 mM IPTG at 37°C. Following induction, a smaller amount of His_6-$FlrS_{CTD}$ was produced for the corresponding molecular weight of 8.7 kDa and most of the protein remained insoluble (Figure 3.17A). A few attempts were made to increase and improve protein solubility by inducing His_6-$FlrS_{CTD}$ at lower temperatures and lower concentrations of 0.5 mM IPTG. Inductions were carried out at 30°C and 22°C, the cells were grown first at 37°C until they reached OD_{600} 0.5 and then shifted to the lower temperature before induction. Growing the cells at 30°C showed a slight improvement in the protein solubility (Figure 3.17B), but the solubility test of His_6-$FlrS_{CTD}$ at 22°C was unsuccessful (Figure 3.17C). This His_6-$FlrS_{CTD}$ solubility test was also performed at a higher temperature of 42°C for overnight induction but the attempt was unsuccessful (Figure 3.17D). For the subsequent experiments, therefore, it was decided to proceed to use the overproduced protein at 30°C, obtained from the insoluble fraction. Following the solubility test, Western blot with probed anti-His_6 antibody was performed in order to determine the corresponding size of the overproduced His_6-$FlrS_{CTD}$ (Figure 3.18).

Overproduction and solubility of $FlrR_{NTD}$-VSVg

To test $FlrR_{NTD}$-VSVg overexpression, pACYCDuet-$FlrR_{NTD}$-VSVg plasmid was introduced into *E. coli* BL21(λDE3). The expression of $FlrR_{NTD}$-VSVg was carried out by performing induction in *E. coli* BL21(λDE3) containing $FlrR_{NTD}$-VSVg. The cells were grown in LB with 1 mM IPTG for 3 hours at 37°C. The total protein from uninduced and induced cells were loaded and analysed by SDS-PAGE in order to confirm the size of overproduced $FlrR_{NTD}$-VSVg (10.03 kDa), but the stained gel showed no detectable expression of $FlrR_{NTD}$-VSVg (Figure 3.19). Different conditions were therefore used to induce the protein expression by growing the cells at a lower temperature and using a lower concentration of IPTG (results not shown) but still no protein expression was obtained. Attempts were therefore made to express $FlrR_{NTD}$-VSVg into different cells such as C41(λDE3) and C43(λDE3) (results not shown) but again, no protein at the predicted size of 10.03 kDa was expressed at any of these

conditions. It was therefore decided to clone the DNA fragment encoding $FlrR_{NTD}$-VSVg into a different expression vector, pMAL-c5X.

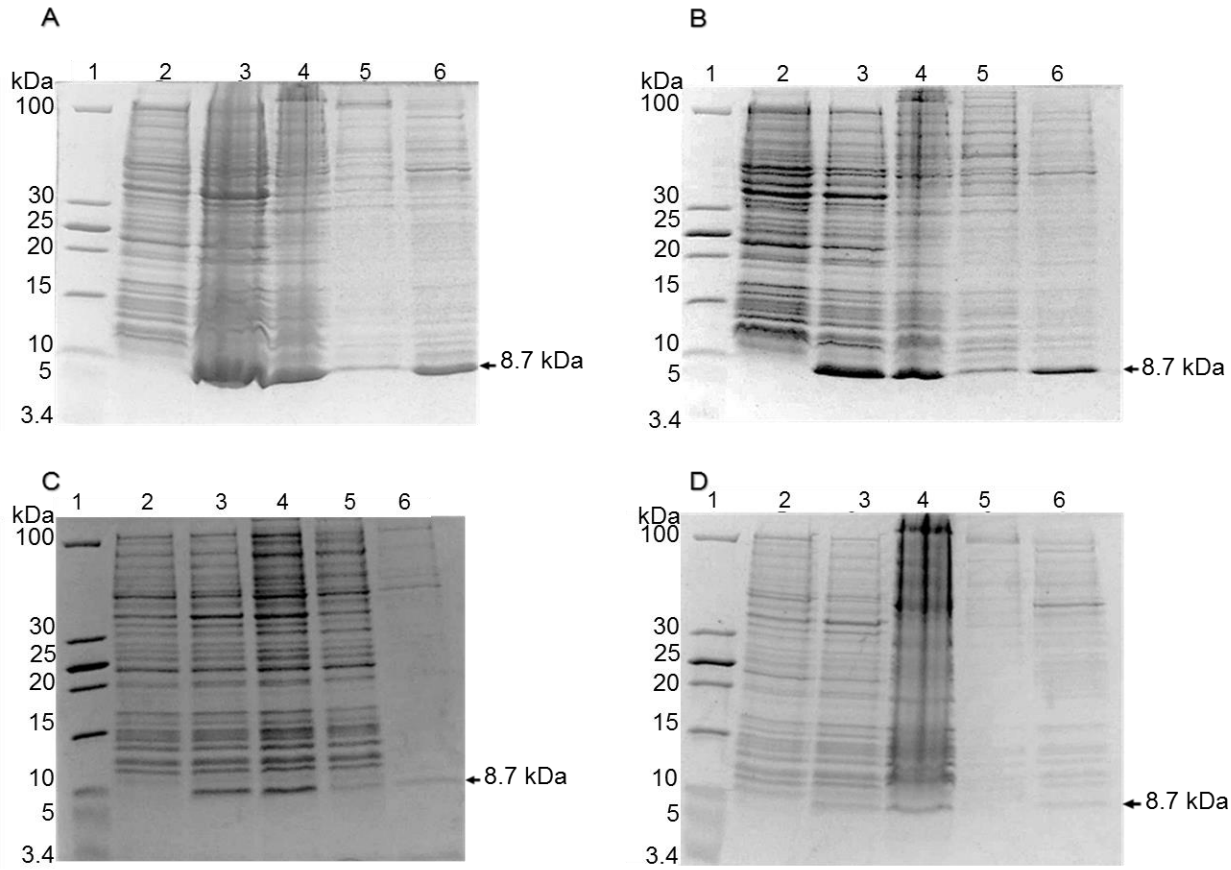

Figure 3-17: Analysis of His_6-$FlrS_{CTD}$ expression and solubility test.

A. His_6-$FlrS_{CTD}$ was overproduced in *E. coli* BL21(λDE3) at 37°C.

B. His_6-$FlrS_{CTD}$ was overproduced in *E. coli* BL21(λDE3) at 30°C.

C. His_6-$FlrS_{CTD}$ was overproduced in *E. coli* BL21(λDE3) at 22°C.

D. His_6-$FlrS_{CTD}$ was overproduced in *E. coli* BL21(λDE3) at 42°C.

E. coli BL21(λDE3) cells containing pACYCDuet-His_6-$FlrS_{CTD}$ were grown at 37°C in LB medium. Once it reached OD_{600} 0.5-0.7 protein expressions were induced at different temperatures and different concentrations of IPTG. 1 ml of bacterial cultures were taken as uninduced samples. The bacterial cultures were subjected to centrifugation and sonication in order to test for protein solubility. Lane 1, PageRuler Unstained Low Range Protein Ladder; lane 2, sample of uninduced *E. coli* BL21(λDE3) cells containing pACYCDuet-His_6-$FlrS_{CTD}$; lane 3, sample of induced BL21(λDE3) cells containing pACYCDuet-His_6-$FlrS_{CTD}$; lane 4, whole cell extracts, total; lane 5, soluble fraction; lane 6, insoluble fraction (A, B, C and D, respectively).

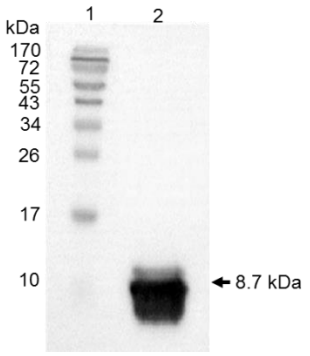

Figure 3-18: Detection of overproduced His_6-$FlrS_{CTD}$ in *E. coli*.

The insoluble fraction of *E. coli* BL21(λDE3) cells containing His_6-$FlrS_{CTD}$ was resolved on 15% SDS-PAGE. His_6-$FlrS_{CTD}$ was electro-blotted onto PVDF and probed with anti-His_6 antibody. Lane 1, EZ-Run Rec Protein Ladder; Lane 2, His_6-$FlrS_{CTD}$ detected at the expected size of 8.7 kDa.

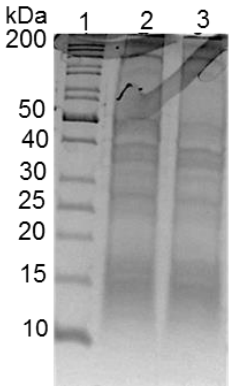

Figure 3-19: Analysis of $FlrR_{NTD}$-VSVg expression and solubility test.

Expression analysis of pACYCDuet-1 containing $FlrR_{NTD}$-VSVg in *E. coli* BL21(λDE3). The cells were grown in LB medium supplemented with 50 mg/ml chloramphenicol. The cells were allowed to grow until they reached OD_{600} 0.5 whereupon 1 ml of pre-induction sample was taken and 1 mM (final concentration) of IPTG was added to the rest of the culture. Protein expression of $FlrR_{NTD}$-VSVg was induced at 37°C for 3 hours. Lane 1, EZ-Run Rec unstained protein ladder; lane 2, uninduced sample of *E. coli* BL21(λDE3) containing pACYCDuet-$FlrR_{NTD}$-VSVg; lane 3, induced cells of pACYCDuet-$FlrR_{NTD}$-VSVg.

Construction of MBP-FlrR$_{NTD}$-VSVg

In a further attempt to overproduce FlrR$_{NTD}$, it was decided to fuse the N-terminal domains of FlrR$_{NTD}$ to the maltose binding protein (MBP). When comparing MBP to other protein tags, such as glutathione S-transferase (GST) and thioredoxin, it has been found that MBP has a better ability to enhance the solubility of a diverse group of otherwise aggregation-prone proteins (Kapust and Waugh, 1999). Moreover, MBP can serve as an affinity tag to allow purification of its fusion derivatives (Kapust and Waugh, 1999). The isolation of fusion proteins can be performed in one single chromatography step since MBP can bind to a cross-linked amylose matrix with high affinity and it is possible to release it from the matrix by adding 10 mM maltose. This purification step gives high degree of purity and a good protein yields as MBP itself does (Ferenci and Klotz, 1978; Kellerman and Ferenci, 1982). The affinity chromatography materials required for this process are inexpensive and it is easy to convert to a large-scale purification process.

The MBP expression vector, pMAL-c5X, was used to generate an N-terminal MBP tagged at the N-terminal of FlrR. The MCS of this vector is located downstream from the *E. coli* MBP coding sequence and is separated from the coding sequence by a sequence encoding a polyasparagine linker followed by a protease factor Xa recognition sequence (Figure 3.20).

Cloning DNA encoding FlrR$_{NTD}$ into pMAL-c5X was carried out using the pACYCDuet-FlrR$_{NTD}$-VSVg plasmid. pACYCDuet-FlrR$_{NTD}$-VSVg and pMAL-c5X was digested with (*Nde*I and *Bgl*II) and (*Bam*HI and *Bgl*II, produce compatible sticky ends), respectively. This results in a MBP-FlrR$_{NTD}$-VSVg (maltose binding protein) fusion. MBP-FlrR$_{NTD}$-VSVg expression and solubility was carried out in *E. coli* BL21(λDE3) cells grown at 37°C for 3 hours. To induce protein expression, the final concentration of 1 mM IPTG was added. The result showed a high abundance of MBP-FlrR$_{NTD}$-VSVg (Figure 3.21). The expected size for MBP-FlrR$_{NTD}$-VSVg is 52 kDa which was confirmed by Western blotting. The PVDF membrane was probed with anti-VSVg antibody (result not shown) and anti-MBP antibody (Figure 3.21).

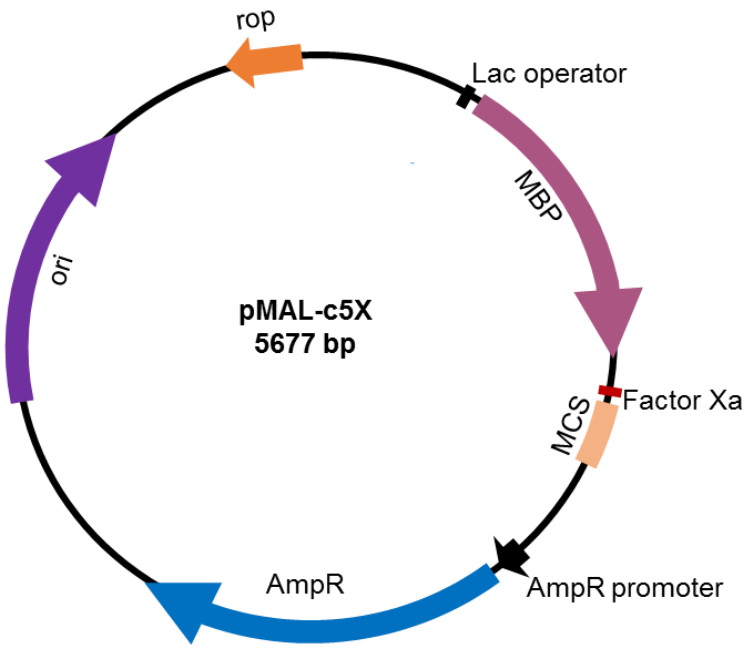

Figure 3-20: Schematic representation of overexpression vector pMAL-c5X.

pMAL-c5X diagram shows the repressor primer, rop, the ampicillin resistance gene, AmpR, the AmpR promoter and the multiple cloning site (MCS) (shown in nude colour). Factor Xa, the maltose-binding protein, MBP and the lac operator are shown in black and light purple colours, respectively.

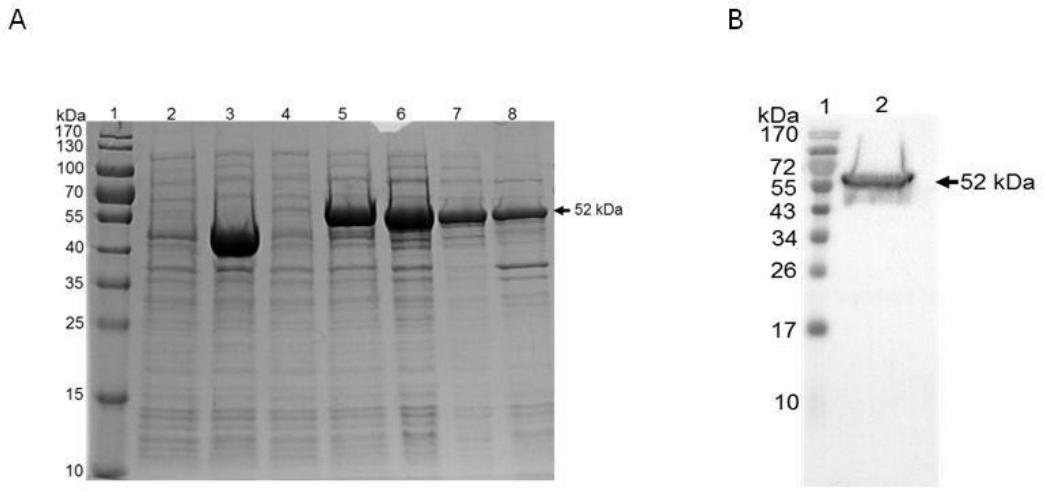

Figure 3-21: Overexpression, solubility test and Western blot detection of MBP-FlrR$_{NTD}$-VSVg.

A. *E. coli* BL21(λDE3) cells containing MBP (used as a control) and MBP-FlrR$_{NTD}$-VSVg were grown at 37°C in LB medium supplemented with 100 mg/ml ampicillin until it reached OD_{600} 0.5-0.7. Pre-induction, 1 ml of bacterial culture was taken as an uninduced protein sample and 1 mM IPTG was added to the induced protein expression. After 3 hours of induction, another 1 ml of culture was taken as an induced sample, and the two samples were analyzed using 15% SDS gel. Lane 1, EZ-Run Rec unstained protein ladder; lane 2, sample of uninduced BL21(λDE3) cells containing MBP empty vector; lane 3, sample of induced BL21(λDE3) cells containing MBP empty vector; lane 4, sample of uninduced BL21(λDE3) cells containing MBP-FlrR$_{NTD}$-VSVg; lane 5, sample of induced BL21(λDE3) cells containing MBP-FlrR$_{NTD}$-VSVg; lane 6, whole cell extracts, total; lane 7, soluble fraction; lane 8, insoluble fraction.

B. Western blot of MBP-FlrR$_{NTD}$-VSVg analyses in soluble fraction. On the transfer membrane, the soluble fraction of MBP-FlrR$_{NTD}$-VSVg protein was probed with anti-MBP antibody. Lane 1, EZ-Run Rec protein ladder; lane 2, soluble fraction of MBP-FlrR$_{NTD}$-VSVg.

Co-expression of MBP-FlrR$_{NTD}$-VSVg with His$_6$-FlrS$_{CTD}$

The co-expression of MBP-FlrR$_{NTD}$-VSVg and His$_6$-FlrS$_{CTD}$ was analysed by introducing MBP-FlrR$_{NTD}$-VSVg and His$_6$-FlrS$_{CTD}$ into *E. coli* BL21(λDE3) cells. The overproduction and solubility test were performed for both proteins as described in Section 2.14. The cells were allowed to grow until it reached OD_{600} 0.5-0.7. Once it reached the desired OD_{600}, the expressions of both proteins were induced by adding 1 mM IPTG, with the induction being carried out for 3 hours at 37°C. Following the induction, the cells were subjected to sonication, as described in Section 2.14. The co-expression result of MBP-FlrR$_{NTD}$-VSVg and His$_6$-FlrS$_{CTD}$ was overproduced and analysed by SDS-PAGE. A small amount of soluble His$_6$-FlrS$_{CTD}$ was produced compared to MBP-FlrR$_{NTD}$-VSVg (Figure 3.22). Both protein expressions were confirmed by Western blot using anti-VSVg antibody and anti-His$_6$ antibody (data not shown).

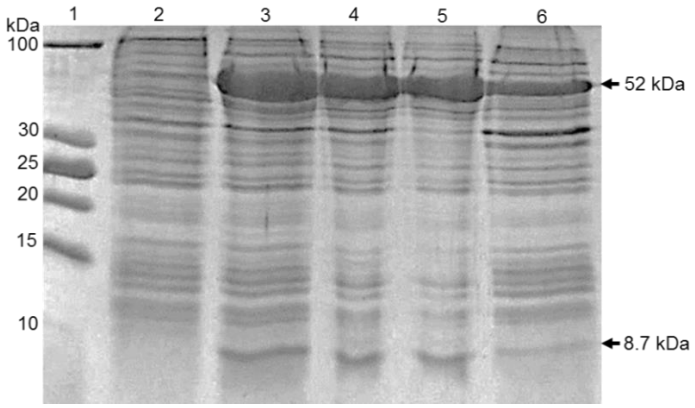

Figure 3-22: Co-expression of His_6-$FlrS_{CTD}$ and MBP-$FlrR_{NTD}$-VSVg proteins.

His_6-$FlrS_{CTD}$ and MBP-$FlrR_{NTD}$-VSVg were co-transformed into *E. coli* strain BL21(λDE3). The bacterial cell culture was grown in LB medium at 37°C and induced for 3 hours by adding 1 mM IPTG. All samples were analysed on 15% SDS-PAGE gel. Lane 1, PageRuler Unstained Low Range Protein Ladder; lane 2, sample of uninduced BL21(λDE3) cells containing His_6-$FlrS_{CTD}$ and MBP-$FlrR_{NTD}$-VSVg; lane 3, sample of induced BL21(λDE3) cells containing His_6-$FlrS_{CTD}$ and MBP-$FlrR_{NTD}$-VSVg; lane 4, whole cell extracts, total; lane 5, soluble fraction; lane 6, insoluble fraction.

Pull-down assay of His_6-$FlrS_{CTD}$ and MBP-$FlrR_{NTD}$-VSVg interaction

To confirm the interaction between $FlrS_{CTD}$ and $FlrR_{NTD}$ inferred from the BACTH assay, a pull-down assay was performed as described in Section 2.16. The pull-down was performed by overexpression of both prey and bait protein in the same cell. The two proteins were co-expressed. The cell lysate was obtained by centrifugation at 13,400 x *g* for 20 minutes. The resulting supernatants were incubated with Ni-agarose resin and left to be gently shaken on a wheel rotator for 2 hours. To remove non-specifically bound proteins, the resin was washed twice with wash buffer (50 mM Tris-HCl (pH 8.0), 200 mM NaCl, 10 mM imidazole and 5% glycerol). The final step was to elute the bound protein using elution buffer (50 mM Tris-HCl (pH 8.0), 200 mM NaCl, 150 mM imidazole, 5% glycerol). The eluted fractions were analysed by SDS-PAGE and visualised by Coomassie blue staining. Pull-down analysis using the co-expressed cell extract revealed that His_6-$FlrS_{CTD}$ did not bind to MBP. Although large amount of MBP bound to the column, the His_6 was neither able to bind to MBP nor the nickel affinity. Therefore, the pull-down assay using co-expression of both proteins in the same cell was unsuccessful.

The classical pull-down assay method was therefore carried out by overexpression of both proteins separately. It was decided to use this method in order to control the amount of His_6-$FlrS_{CTD}$ loaded on the column, as its expression was not sufficient to be used. To make the His_6-$FlrS_{CTD}$ more concentrated, an Amicon Ultra 4 ml centrifugal filter, ideal for the size of this protein, was applied (NMWL of 10 kDa). Cell lysate of His_6-$FlrS_{CTD}$ was applied to nickel affinity resin in order to allow immobilisation of His-tagged bait protein. After incubation with resin and washing, the cell lysate of the MBP-$FlrR_{NTD}$-VSVg 'prey' was applied to the resin in order to be incubated with the His_6-$FlrS_{CTD}$ bait protein for 2 hours. The His_6-$FlrS_{CTD}$ and MBP-$FlrR_{NTD}$-VSVg complex was washed with washing buffer containing 10 mM imidazole. The two proteins were eluted with elution buffer containing a high concentration of 500 mM imidazole. The pull-down assay confirmed the interaction between both proteins since His_6-$FlrS_{CTD}$ was successfully pulled-down to MBP-$FlrR_{NTD}$-VSVg. Immobilised His_6-$FlrS_{CTD}$ and MBP-$FlrR_{NTD}$-VSVg were included as controls (Figure 3.23).

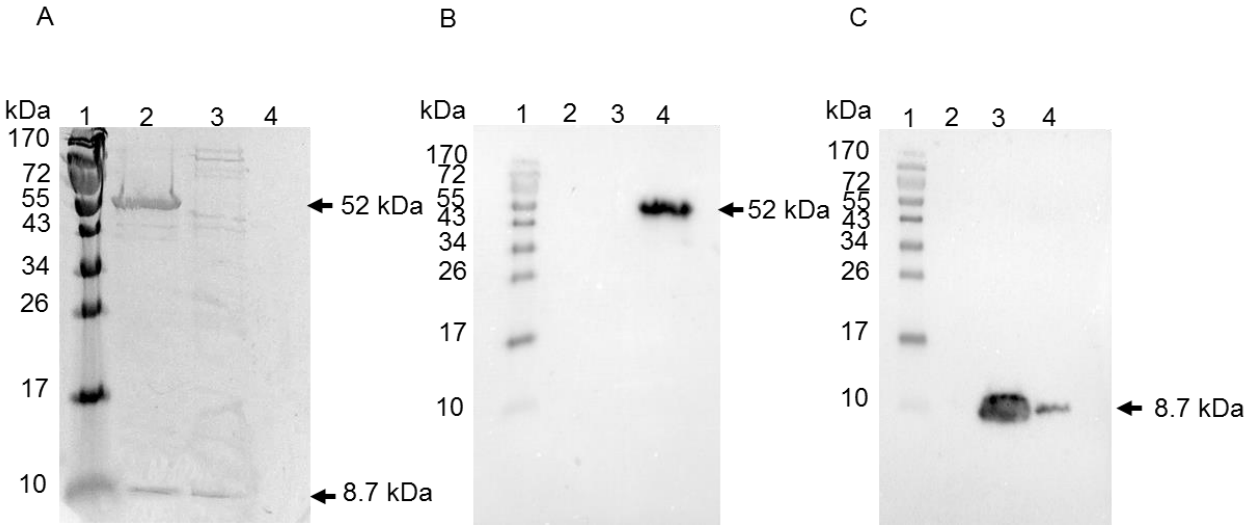

Figure 3-23: Demonstration of His_6-$FlrS_{CTD}$ and MBP-$FlrR_{NTD}$-VSVg interaction using pull-down assay.

His_6-$FlrS_{CTD}$ and MBP-$FlrR_{NTD}$-VSVg were overproduced in the *E. coli* strain BL21(λDE3) separately. The cell lysate of both induced proteins were applied to nickel affinity resin. The bound proteins were washed and eluted with 500 mM imidazole buffer. The eluted sample of the bound proteins was analyzed on 15% SDS-PAGE and visualised by Coomassie blue staining and by anti-His_6 antibody and anti-MBP antibody Western blotting. Immobilised His_6-$FlrS_{CTD}$ and MBP-$FlrR_{NTD}$-VSVg were included as controls.

A. Coomassie blue stain of His_6-$FlrS_{CTD}$ and MBP-$FlrR_{NTD}$-VSVg pull-down result.

B. Western blot of the eluted samples probed with anti-MBP antibody.

C. Western blot of eluted samples probed with anti-His_6 antibody.

A. Lane 1, EZ-Run Rec pre-stained protein ladder; lane 2, eluted His_6-$FlrS_{CTD}$ and MBP-$FlrR_{NTD}$-VSVg; lane 3, eluted His_6-$FlrS_{CTD}$; lane 4, eluted MBP-$FlrR_{NTD}$-VSVg.

B and C. Lane 1, EZ-Run Rec pre-stained protein ladder; lane 2, MBP-$FlrR_{NTD}$-VSVg; lane3, His_6-$FlrS_{CTD}$; lane 4, His_6-$FlrS_{CTD}$ and MBP-$FlrR_{NTD}$-VSVg.

3.5 FlrR and FlrA interaction using BACTH system

Constructing of $FlrR_{CTD}$ and $FlrA_{NTD}$ hybrid proteins

One of the hypotheses of this study is that the *flr* system is responsible for the uptake of xenosiderophore under iron-limiting conditions through the predicted FlrA which is homologous to siderophore receptors. A search for homologous sequences in the GenBank database revealed similarities between $FlrR_{CTD}$ and $FlrA_{NTD}$ and $FecR_{CTD}$ and $FecA_{NTD}$, and therefore it has been desided to investigate the interaction between the two predicted proteins using BACTH and pull-down assays in order to understand their involvement in signal transduction.

The coding sequences of the C-terminal region of FlrR and the N-terminal region of FlrA were cloned into BACTH vectors in order to investigate whether the two proteins interact with each other. BACTH plasmids encoding T25 or T18-$FlrR_{CTD}$ and T25 or T18-$FlrA_{NTD}$ were constructed by using these primers (FlrRCTDfor and FlrRCTDrev1), (FlrRCTDrev2 and FlrANTDfor) and (FlrANTDrev1 and FlrANTDrev2), respectively. The amplification and cloning of the two regions were carried as discussed in the previous Section 3.3.

In order to perform the BACTH assay between $FlrR_{CTD}$ and $FlrA_{NTD}$ the successful clones were co-transformed into *E. coli* strain BTH101. The transformants were plated onto 1% maltose-MacConkey agar plate containing 100 mg/ml ampicillin and 50 mg/ml kanamycin. It was observed that all combinations of $FlrR_{CTD}$ and $FlrA_{NTD}$ tested gave rise to a strong Mal^+ phenotype. The results were scored after 5 days' incubation at 30°C. The combination of pKT25-*zip* and pUT18C-*zip* was included in the assay as a positive control. All possible negative control combinations of BACTH plasmids encoding T18-T25 fusions to $FlrR_{CTD}$ or $FlrA_{NTD}$ with empty BACTH plasmids were included (Figure 3.24 A, B and C).

β-galactosidase activities for all compatible BACTH plasmids encoding T18-T25 fusions to $FlrR_{CTD}$ in combination with T18-T25 fusions to $FlrA_{NTD}$ were transformed into *E. coli* BTH101 in order to assay these fusion proteins in liquid cultures. The cells were grown in LB supplemented with appropriate antibiotics and 0.5 mM IPTG to induce protein expression. The β-galactosidase activity generated by these two combinations of pKTN25-$FlrR_{CTD}$ and pUT18-$FlrA_{NTD}$ indicates greater β-

galactosidase activity of 2513.3 ± 55 Mu. Overall, the β-galactosidase results of all combinations are in agreement with the BACTH plates assays (Figure 3.25A). Cells containing pKT25-*zip* and pUT18C-*zip* and possible negative controls were also included in this study (Figure 3.25B). As the BACTH assay show strong interaction between $FlrR_{CTD}$ and $FlrA_{NTD}$ it important to confirm this interaction using pull-down assay (Section 3.6).

A

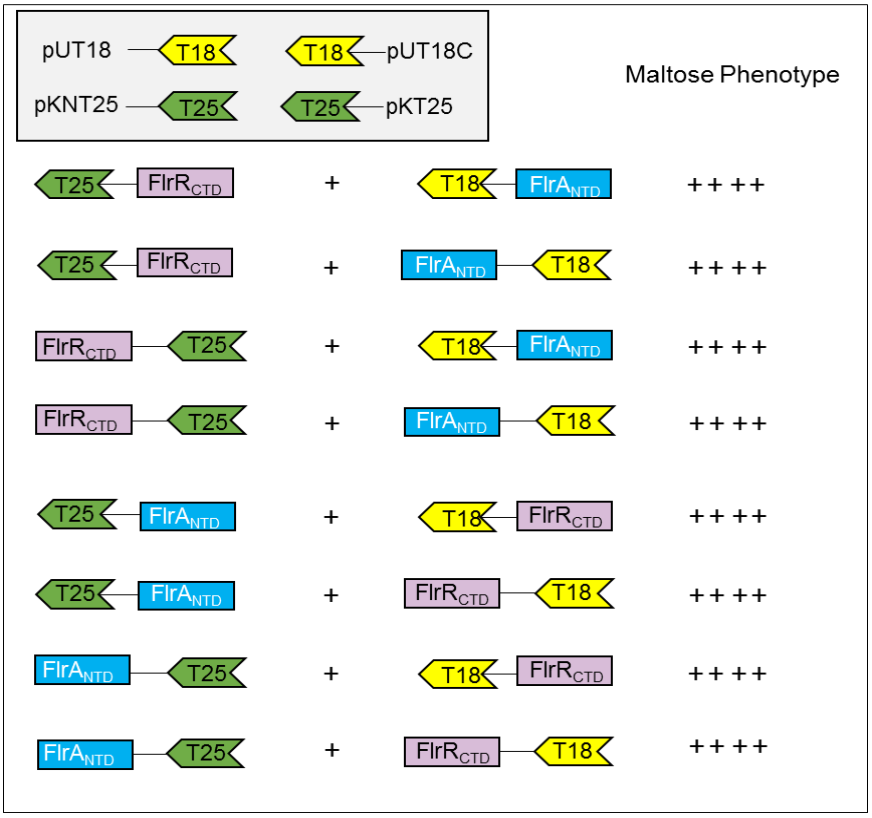
pUT18
T18
T18
pUT18C
pKNT25
T25
T25
pKT25
Maltose Phenotype
T25 FlrR$_{CTD}$ + T18 FlrA$_{NTD}$ ++++
T25 FlrR$_{CTD}$ + FlrA$_{NTD}$ T18 ++++
FlrR$_{CTD}$ T25 + T18 FlrA$_{NTD}$ ++++
FlrR$_{CTD}$ T25 + FlrA$_{NTD}$ T18 ++++
T25 FlrA$_{NTD}$ + T18 FlrR$_{CTD}$ ++++
T25 FlrA$_{NTD}$ + FlrR$_{CTD}$ T18 ++++
FlrA$_{NTD}$ T25 + T18 FlrR$_{CTD}$ ++++
FlrA$_{NTD}$ T25 + FlrR$_{CTD}$ T18 ++++

B

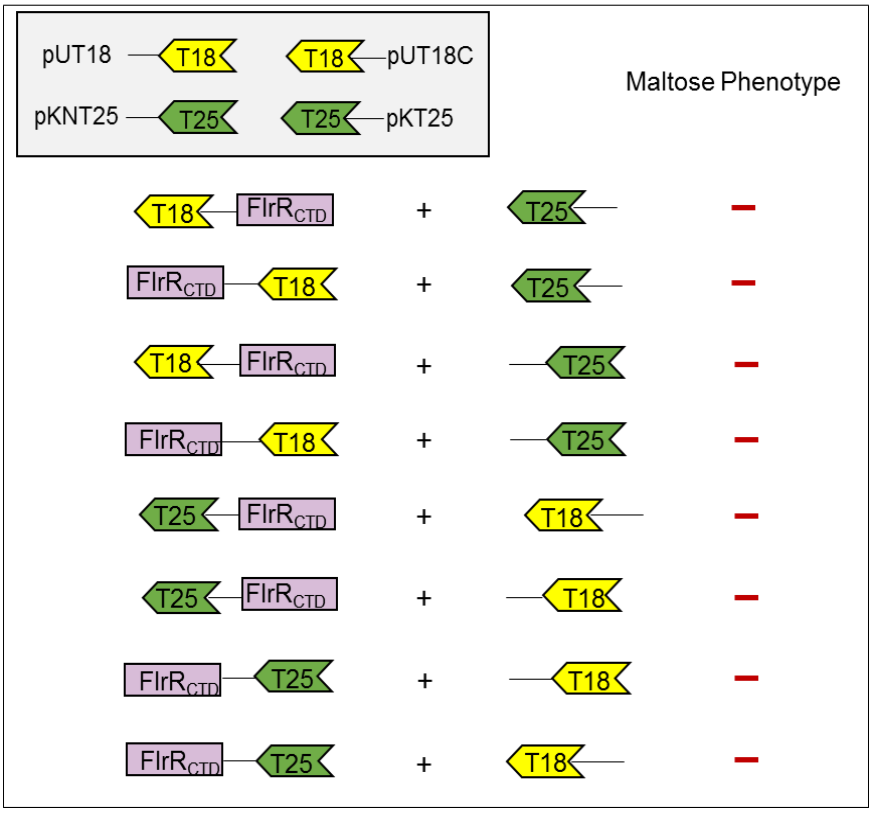
pUT18
T18
T18
pUT18C
pKNT25
T25
T25
pKT25
Maltose Phenotype
T18 FlrR$_{CTD}$ + T25 −
FlrR$_{CTD}$ T18 + T25 −
T18 FlrR$_{CTD}$ + T25 −
FlrR$_{CTD}$ T18 + T25 −
T25 FlrR$_{CTD}$ + T18 −
T25 FlrR$_{CTD}$ + T18 −
FlrR$_{CTD}$ T25 + T18 −
FlrR$_{CTD}$ T25 + T18 −

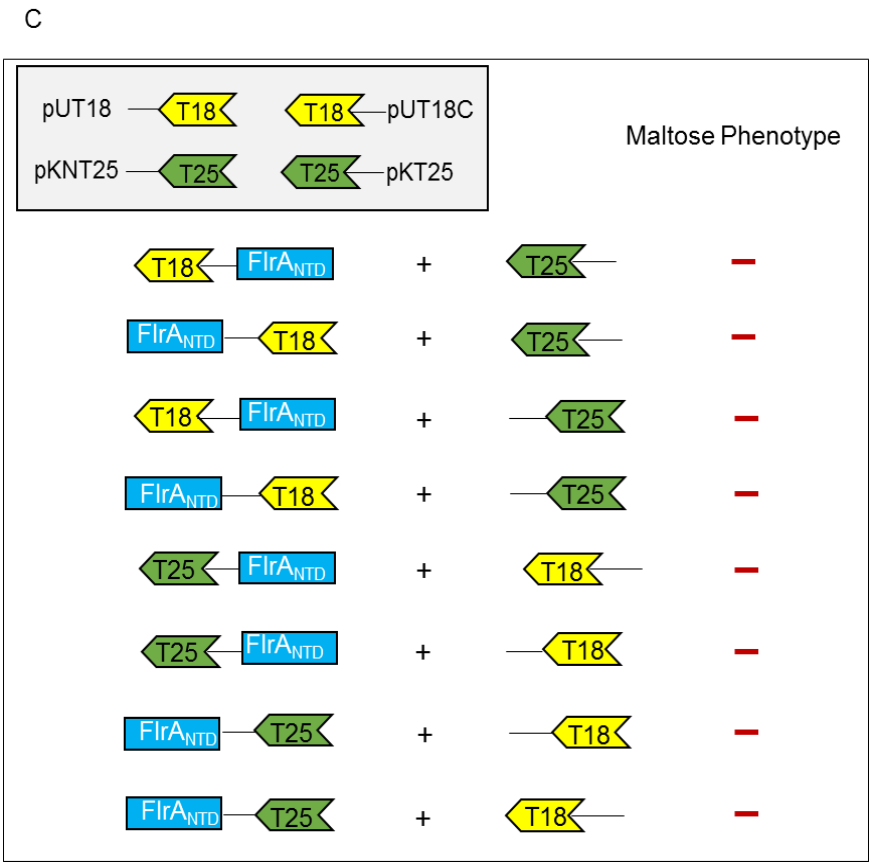

Figure 3-24: Investigation of $FlrR_{CTD}$ and $FlrA_{NTD}$ interaction using the BACTH system assay.

A. All possible combinations of $FlrR_{CTD}$ and $FlrA_{NTD}$ were fused to the N-terminal or C-terminal of *B. pertussis* adenylate cyclase T25 and T18 fragments.

B. All possible combinations of $FlrR_{CTD}$ and empty BACTH plasmids.

C. All possible combinations of $FlrA_{NTD}$ and empty BACTH plasmids.

All combinations were transformed into *E. coli* strsin BTH101. Transformants were selected on MacConkey-maltose agar plates and scored for the maltose phenotype after 5 days. (++++) indicates Mal^+ phenotype and (—) Mal^- phenotype. The degree of the maltose phenotype is indicated next to the corresponding diagram.

A

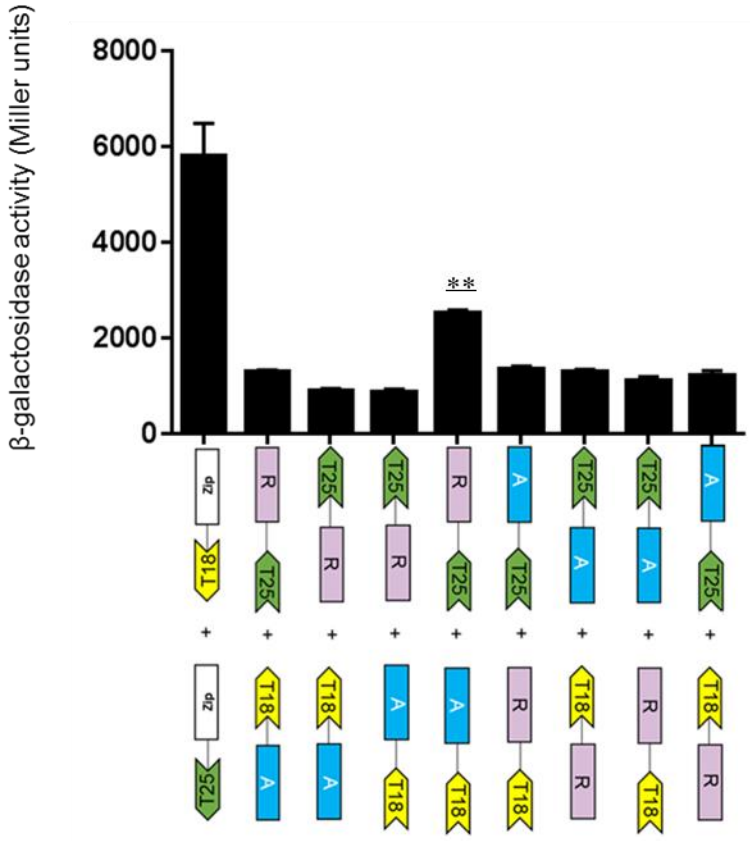
β-galactosidase activity (Miller units)
8000
6000
4000
2000
0
**
zip
T18
T25
R
A
+
zip
T25
T18
R
A

B

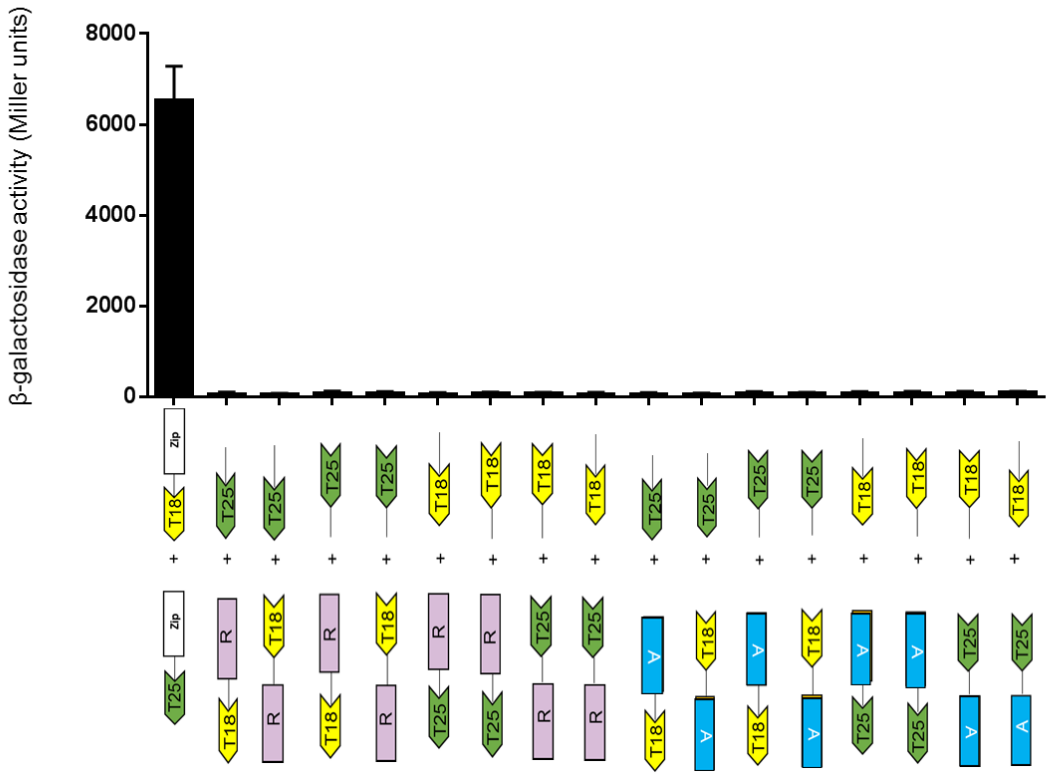

Figure 3-25: Quantification of $FlrR_{CTD}$ and $FlrA_{NTD}$ interaction using the BACTH system assay: β-galactosidase.

A. The efficiency of the functional complementation of CyaA due to $FlrR_{CTD}$-$FlrA_{NTD}$ interaction was quantitated by measuring β-galactosidase activity.

B. Analysis of interactions between all possible negative controls of $FlrR_{CTD}$ and $FlrA_{NTD}$ with BACTH empty vectors using β-galactosidase assay.

The efficiencies of functional complementation between $FlrR_{CTD}$ and $FlrA_{NTD}$ interactions with all empty BACTH plasmids (pKNT25-pKT25 and pUT18C-pUT18) were quantified by measuring β-galactosidase. A positive control, pUT18C-*zip* and pKT25-*zip* was included. R corresponds to $FlrR_{CTD}$ and A corresponds to $FlrA_{NTD}$. Error bars represent the standard deviation of three independent experiments. The background level of the β-galactosidase activity measured in the negative controls was 66-70 Mu. The results were analysed using T test ** $P < 0.01$.

3.5.1 Investigation $FlrR_{CTD}$ self-interaction

In this work, $FlrR_{CTD}$ self-interaction have been studied in order to confirm that the $FlrR_{CTD}$ itself might block the signal to pass to the σ factor under non-inducing conditions, where the activity might occur mainly through the C-terminal domain, since the full-length FlrR self-interaction showed Mal^- phenotype (Section 3.3.3). The self-interaction of $FlrR_{CTD}$ was analysed by using all possible combinations of $FlrR_{CTD}$ hybrid proteins constructed as described in this Section 3.3. Positive and negative controls were included. Two out of four combinations of the BACTH plasmid combinations encoding $FlrR_{CTD}$, (pKNT25-$FlrR_{CTD}$ and pUT18-$FlrR_{CTD}$) and (pKNT25-$FlrR_{CTD}$ and pUT18C-$FlrR_{CTD}$) showed a weak positive Mal^+ phenotype with moderate red/purple colonies; the other two combinations indicate Mal^- phenotype (Figure 3.26). The β-galactosidase assay results were consistent with the results observed on MacConkey-maltose agar plates. pUT18C-*zip* and pKT25-*zip* activity was assayed and all possible negative controls were included in both assays (Figure 3.27). These results indicate that FlrR might be responsible for blocking the signal and preventing the binding of $FlrR_{NTD}$ to the σ factor.

3.5.2 Investigation of $FlrA_{NTD}$ self-interaction

Self-interaction of $FlrA_{NTD}$ was analysed using the BACTH system. $FlrA_{NTD}$ protein was fused to the N-terminal of *B. pertussis* adenylate cyclase T25 and T18 fragments. Positive and negative controls were also included in the assay. All four combinations of $FlrA_{NTD}$ fusion proteins gave rise to Mal^- phenotype (Figure 3.28). β-galactosidase assays were performed to confirm the results which were consistent with those observed on MacConkey-maltose agar plates (Figure 3.29). The results indicate that the N-terminal region of the outer-membrane receptor does not self-interact.

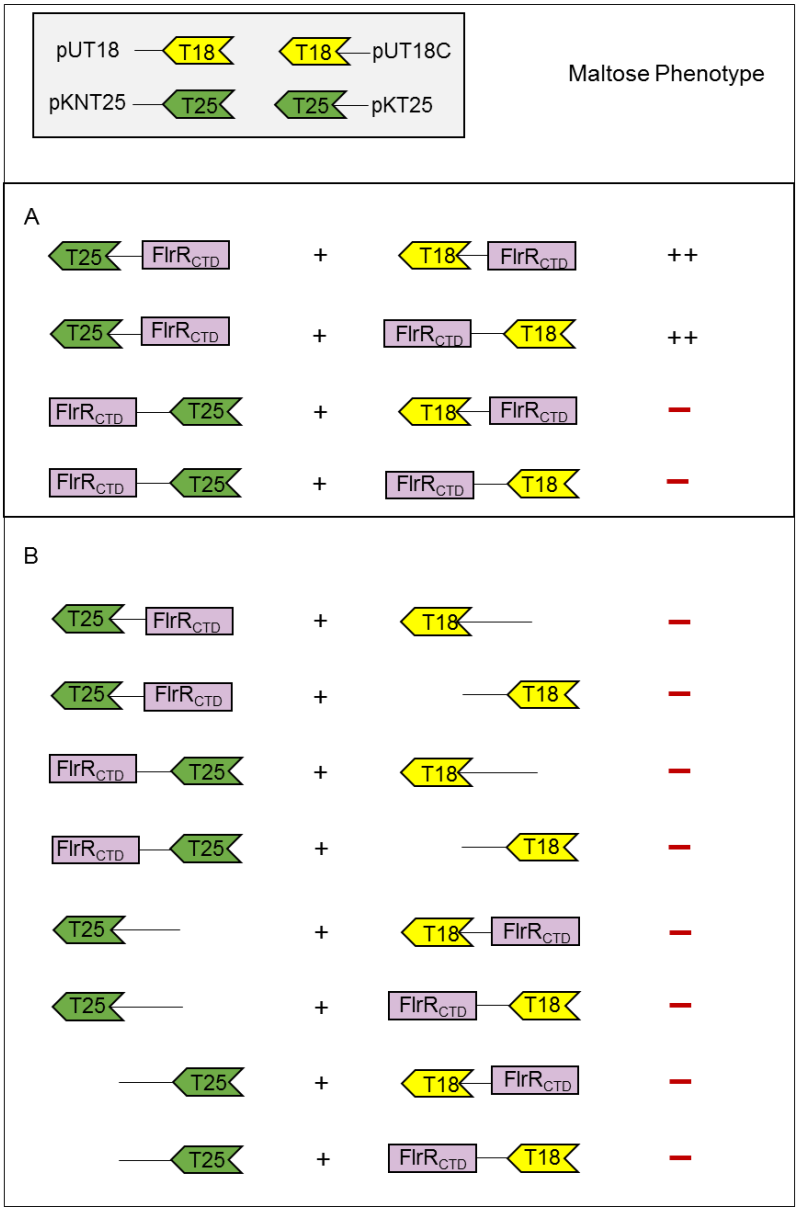

Figure 3-26: Investigation of $FlrR_{CTD}$ self-interaction using the BACTH system assay.

A. $FlrR_{CTD}$ proteins were fused to the C-terminal or N-terminal of *B. pertussis* adenylate cyclase T25 and T18 fragments.

B. All possible combinations of $FlrR_{CTD}$ and empty BACTH plasmids (as negative controls)

All combinations were transformed into *E. coli* strain BTH101. Transformants were selected on MacConkey-maltose agar plates and scored for the maltose phenotype after 5 days. (++) indicates Mal^+ phenotype and (−) Mal^- phenotype. The degree of the maltose phenotype is indicated next to the corresponding diagram.

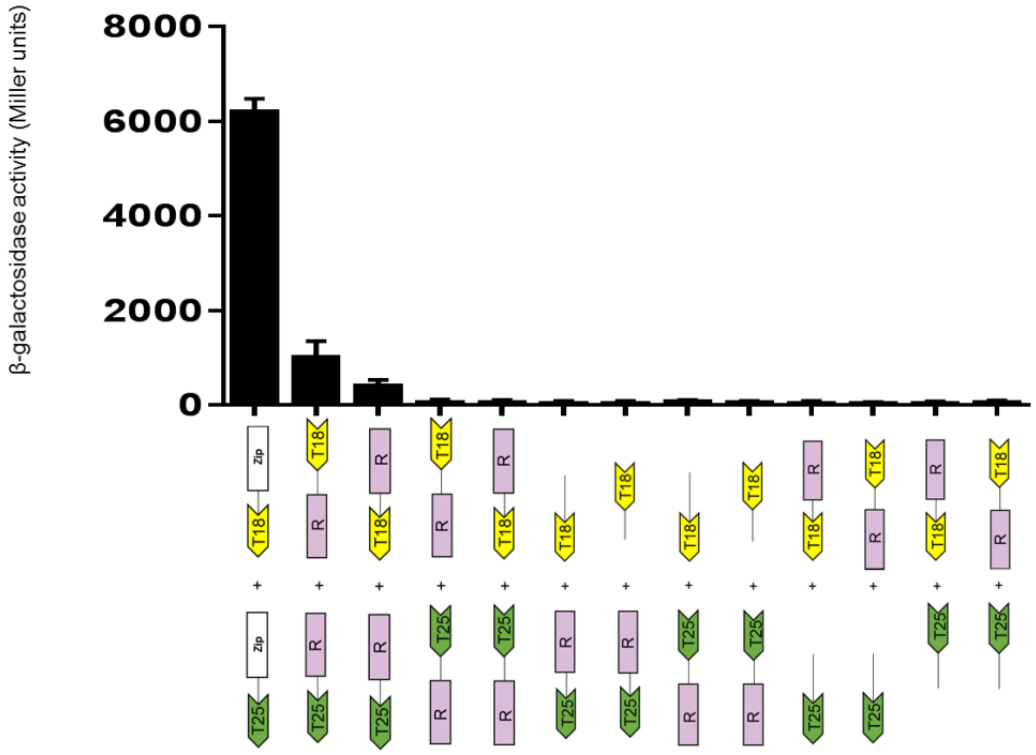

Figure 3-27: Quantification of $FlrR_{CTD}$ self-interaction using the BACTH system assay: β-galactosidase.

The possible self-interaction of $FlrR_{CTD}$ combinations (pKT25-$FlrR_{CTD}$ and pKNT25-$FlrR_{CTD}$) and (pUT18-$FlrR_{CTD}$ and pUT18C-$FlrR_{CTD}$) were investigated by measuring β-galactosidase activity in cells harbouring a combination of BACTH plasmids.

The efficiencies of functional complementation between $FlrR_{CTD}$ combinations and the negative controls interactions with all empty BACTH plasmids (pKNT25-pKT25 and pUT18C-pUT18) were quantified by measuring β-galactosidase. A positive control, pUT18C-*zip* and pKT25-*zip* was included. R corresponds to $FlrR_{CTD}$. Error bars represent the standard deviation of three independent experiments. The background level of the β-galactosidase activity measured in the negative controls was 66-70 Mu.

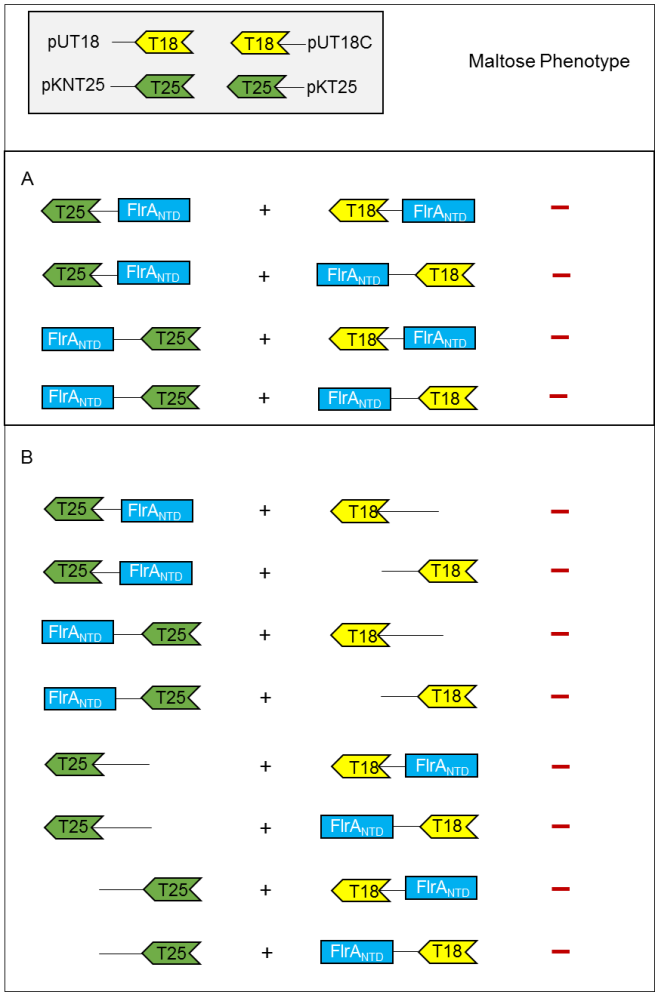

Figure 3-28: Investigation of FlrA$_{NTD}$ self-interaction using the BACTH system assay.

A. FlrA$_{NTD}$ proteins were fused to the C-terminal or N-terminal of *B. pertussis* adenylate cyclase T25 and T18 fragments.

B. All possible combinations of FlrA$_{NTD}$ and empty BACTH plasmids (negative controls) were assayed.

All combinations were transformed into *E. coli* strain BTH101. Cells containing pKT25-*zip* and pUT18C-*zip* were used as a positive control. All possible combinations of FlrA$_{NTD}$ and empty BACTH plasmids (as negative controls) were assayed. A corresponds to FlrA$_{NTD}$. (−) Mal$^-$ phenotype. The degree of the maltose phenotype is indicated next to the corresponding diagram.

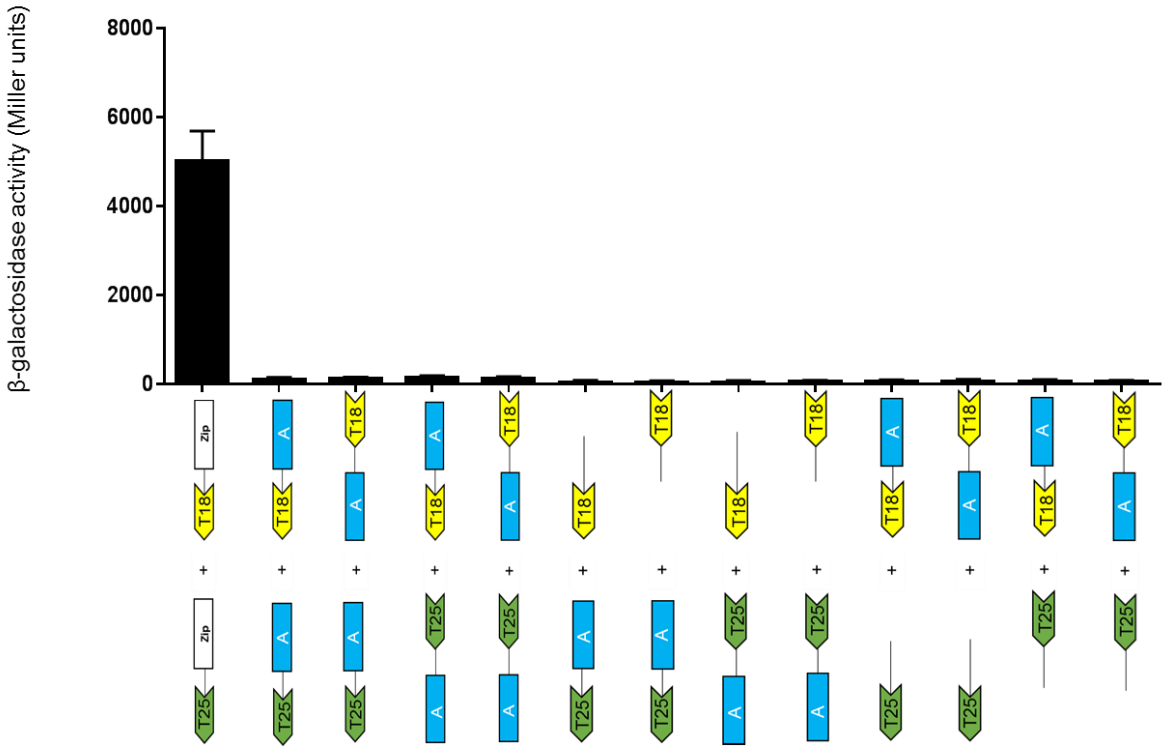

Figure 3-29: Quantification of $FlrA_{NTD}$ self-interaction using the BACTH system assay: β-galactosidase.

The possible self-interaction of $FlrA_{NTD}$ combinations (pKT25-$FlrA_{NTD}$ and pKNT25-$FlrA_{NTD}$) and (pUT18-$FlrA_{NTD}$ and pUT18C-$FlrA_{NTD}$) were investigated by measuring β-galactosidase activity in cells harbouring a combination of BACTH plasmids.

The efficiencies of functional complementation between $FlrA_{NTD}$ combinations and the negative controls interactions with all empty BACTH plasmids (pKNT25-pKT25 and pUT18C-pUT18) were quantified by measuring β-galactosidase. A positive control, pUT18C-*zip* and pKT25-*zip* was included. A corresponds to $FlrA_{NTD}$. Error bars represent the standard deviation of three independent experiments. The background level of the β-galactosidase activity measured in the negative controls was 66-70 Mu.

3.6 Investigation of the interaction between $FlrR_{CTD}$ and $FlrA_{NTD}$ using pull-down assay

Construction of pACYCDuet-His_6-$FlrR_{CTD}$ and pACYCDuet-$FlrA_{NTD}$-VSVg

Construction of His_6-$FlrR_{CTD}$ into pACYCDuet-1 was made by cloning the coding region of the C-terminus of FlrR into the first MCS of pACYCDuet-1 where a His tag sequence was added at the N-terminal region of $FlrR_{CTD}$. The N-terminal region of the outer-membrane receptor FlrA was cloned into pACYCDuet-1 as described in Section 3.4.

Overexpression and solubility test of His_6-$FlrR_{CTD}$

To determine expression of His_6-$FlrR_{CTD}$, the recombinant protein was introduced into *E. coli* BL21(λDE3). The bacterial cells containing pACYCDuet-His_6-$FlrR_{CTD}$ were grown in LB broth at 37°C until they reached the OD_{600} 0.3-0.7. The cell culture was divided into two tubes to collect uninduced and induced samples. The bacterial culture subjected for 3 hours' induction by adding 1 mM of IPTG. Following the induction, sonication was performed (Section 2.14) and all samples of overproduced and sonicated protein were separated by SDS-PAGE and visualised by Coomassie blue staining. The resulting overexpressed protein was present in the insoluble and soluble fraction which had the expected molecular weight of 13 kDa (Figure 3.30).

Purification of His_6-$FlrR_{CTD}$ by IMAC

Since a lot of the protein was expressed in the insoluble fraction, it was decided to prepare the protein from inclusion bodies in order to purify by Immobilised Metal Ion Affinity Chromatography (IMAC). To use the inclusion body to purify His_6-$FlrR_{CTD}$, a new culture was grown under the same conditions as described in Section 2.14.1. One way to increase protein solubility is to re-suspend the cell pellet in TGED buffer (50 mM Tris-HCl, 5% glycerol, 0.1 mM EDTA, 0.1 mM DTT (pH 7.9) and 50 mM NaCl) containing 0.25% of N-lauroylsarcosine. The purification method used was an

imidazole gradient elution that employs a GE Healthcare ÄKTAprimeplus system with a 1 ml His-trap Nickel affinity column. The samples of gradient elution (150 mM to 500 mM) were collected and were analysed by SDS-PAGE. Most of the protein was eluted successfully from the column with 500 mM imidazole (Figure 3.31). The purified protein was detected by Western blot using anti-His_6 antibody (Figure 3.32).

MBP-$FlrA_{NTD}$-VSVg overexpression and solubility test

Cloning of DNA encoding $FlrA_{NTD}$ into pMAL-c5X was carried out using the pACYCDuet-$FlrA_{NTD}$-VSVg plasmid. pACYCDuet-$FlrA_{NTD}$-VSVg and pMAL-c5X plasmid was constructed as described in Section 3.4. Overexpression and sonication of MBP-$FlrA_{NTD}$-VSVg was carried out as described in Section 2.14.1 and 2.14.2. MBP-$FlrA_{NTD}$-VSVg was successfully overexpressed in *E. coli* BL21(λDE3) after 3 hours of induction with 1 mM IPTG, and the expected size is 56 kDa. Protein samples were analysed in SDS-PAGE (Figure 3.33). The MBP-$FlrA_{NTD}$-VSVg protein was detected by Western blot using MBP-antibody (Figure 3.34).

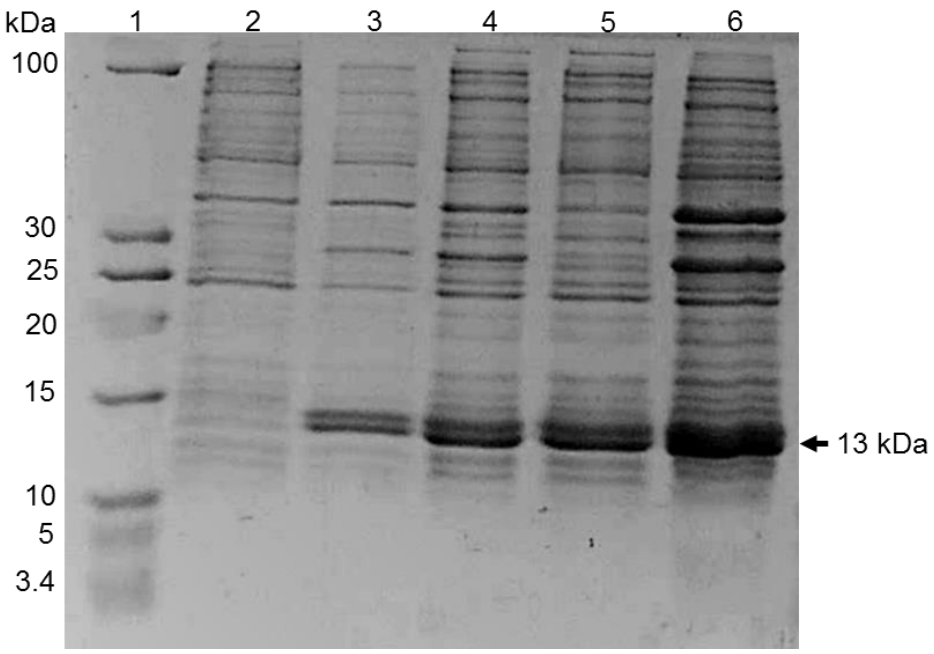

Figure 3-30: Analysis of His_6-$FlrR_{CTD}$ overexpression and solubility test.

E. coli BL21(λDE3) cells containing pACYCDuet-His_6-$FlrR_{CTD}$ were used to determine protein overexpression and solubility. The bacterial cells were grown at 37°C until the OD_{600} reached 0.5-0.7. 1 mM IPTG was added to induce protein expression, based on 3 hours' induction. Following the induction, sonication was performed. The samples were collected before and after the induction and analysed by SDS-PAGE using a 15% SDS-PAGE gel. Lane 1, PageRuler Unstained Low Range Protein Ladder; lane 2, sample of uninduced BL21(λDE3) cells containing pACYCDuet-His_6-$FlrR_{CTD}$; lane 3, sample of induced BL21(λDE3) cells containing pACYCDuet-His_6-$FlrR_{CTD}$; lane 4, whole cell extracts, total; lane 5, soluble fraction; lane 6, insoluble fraction. Expected size = 13 kDa

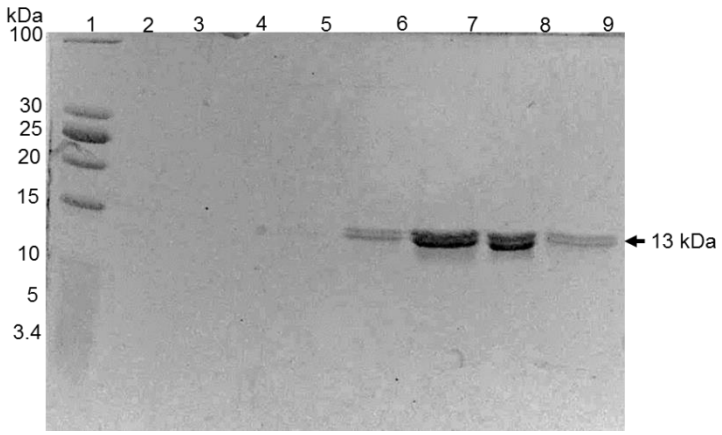

Figure 3-31: Purification of His_6-$FlrR_{CTD}$ using nickel affinity chromatography.

The insoluble fractions from *E. coli* BL21(λDE3) cells expressing pACYCDuet-His_6-$FlrR_{CTD}$. Cells were treated with N-lauroylsarcosine before being applied to a 1 ml GE Healthcare HisTrap HP column. His_6-$FlrR_{CTD}$ was eluted with 500 mM imidazole. Lanes 1, EZ-Run Rec pre-stained protein ladder; lane 2-9, gradient elution of His_6-$FlrR_{CTD}$.

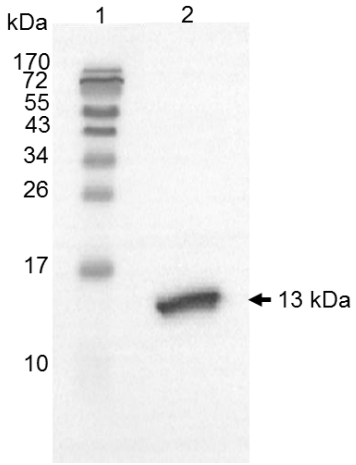

Figure 3-32: Detection of His_6-$FlrR_{CTD}$ by Western blot.

The insoluble fraction of His_6-$FlrR_{CTD}$ was blotted and transferred into PVDF membrane to be detected by anti-His_6 antibody. Lane 1, EZ-Run Rec pre-stained protein ladder; lane 2, insoluble fraction containing His_6-$FlrR_{CTD}$.

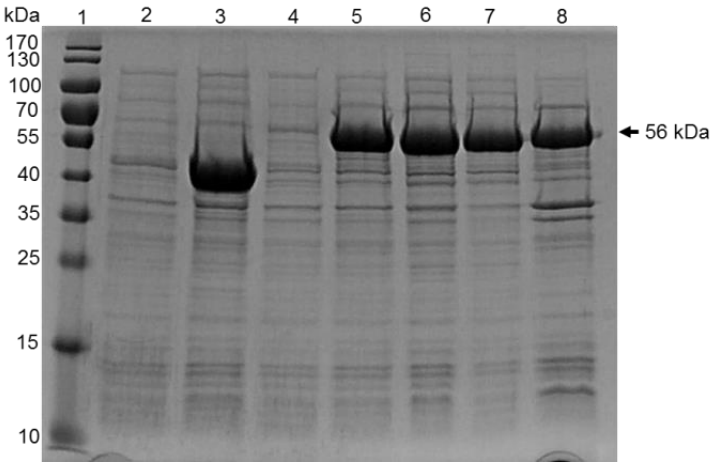

Figure 3-33: Analysis of MBP-FlrA$_{NTD}$-VSVg expression and solubility.

E. coli BL21(λDE3) cells containing pMALc5X (control) and MBP-FlrA$_{NTD}$-VSVg. The bacterial cells were grown at 37°C until OD_{600} reached 0.5-0.7. To induce protein expression, 1 mM IPTG was added for 3 hours' induction. Following the induction, sonication was performed. The samples were collected before and after the induction and analysed by SDS-PAGE using a 15% SDS-PAGE gel. Lane 1, PageRuler Unstained Low Range Protein Ladder; lane 2, sample of uninduced BL21(λDE3) cells containing pMALc5X; lane 3, sample of induced BL21(λDE3) cells containing pMALc5X; Lane 4, sample of uninduced BL21(λDE3) cells containing MBP-FlrA$_{NTD}$-VSVg; lane 5, sample of induced BL21(λDE3) cells containing MBP-FlrA$_{NTD}$-VSVg; lane 6, whole cell extracts, total; lane 7, soluble fraction; lane 8, insoluble fraction. Expected size = 56 kDa.

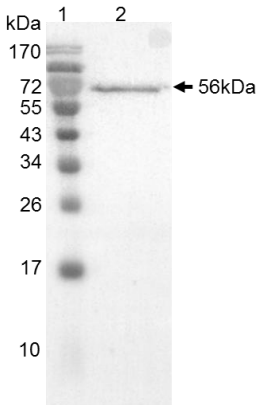

Figure 3-34: Western blot detection of MBP-FlrA$_{NTD}$-VSVg.

The soluble fraction of MBP-FlrA$_{NTD}$-VSVg was blotted and transferred into PVDF membrane to be detected by anti-MBP antibody. Lane 1, EZ-Run Rec pre-stained protein ladder; lane 2, soluble fraction of MBP-FlrA$_{NTD}$-VSVg.

Co-expression of His_6-$FlrR_{CTD}$ and MBP-$FlrA_{NTD}$-VSVg

The co-expression was analysed by introducing pACYCDuet-His_6-$FlrR_{CTD}$ and MBP-$FlrA_{NTD}$-VSVg together into *E. coli* BL21(λDE3). The bacterial cells were grown in LB medium supplemented with 50 mg/ml chloramphenicol and 100 mg/ml ampicillin. The cells were induced as described in Section 2.14.1. Following induction, the cells were subjected for sonication and solubility test (Section 2.14.2). Both proteins His_6-$FlrR_{CTD}$ and MBP-$FlrA_{NTD}$-VSVg were successfully co-overproduced and were also found to be insoluble in the same cells following cell lysis (Figure 3.35). Western blotting confirmed the expression of both proteins using anti-His_6 antibody and anti-MBP antibody (result not shown).

Interaction pACYCDuet-His_6-$FlrR_{CTD}$ and MBP-$FlrA_{NTD}$-VSVg by pull-down assay

The pull-down assay was carried out by growing the bacterial cells expressing both proteins in the same conditions. The clear lysate of bacteria expressing pACYCDuet-His_6-$FlrR_{CTD}$ and MBP-$FlrA_{NTD}$-VSVg were used in this assay. The pull-down assay was performed as described (Section 3.1.2). The pull-down result indicates a protein corresponding to the size of His_6-$FlrR_{CTD}$ (13 kDa) and MBP-$FlrA_{NTD}$-VSVg (56 kDa). His_6-$FlrR_{CTD}$ protein was eluted from the nickel column with 500 mM imidazole, the corresponding sizes of both proteins were observed on Coomassie blue stained SDS-PAGE gel and confirmed by Western blot (Figure 3.36). The pull-down for these two proteins His_6-$FlrR_{CTD}$ and MBP-$FlrA_{NTD}$-VSVg was carried out from both the single expression and co-expression, and it was also carried out using purified pACYCDuet-His_6-$FlrR_{CTD}$. Figure 3.36 shows the pull-down results from the single expression assay, but the other results are not shown. Immobilised His_6-$FlrR_{CTD}$ and MBP-$FlrA_{NTD}$-VSVg were included as controls (Figure 3.36).

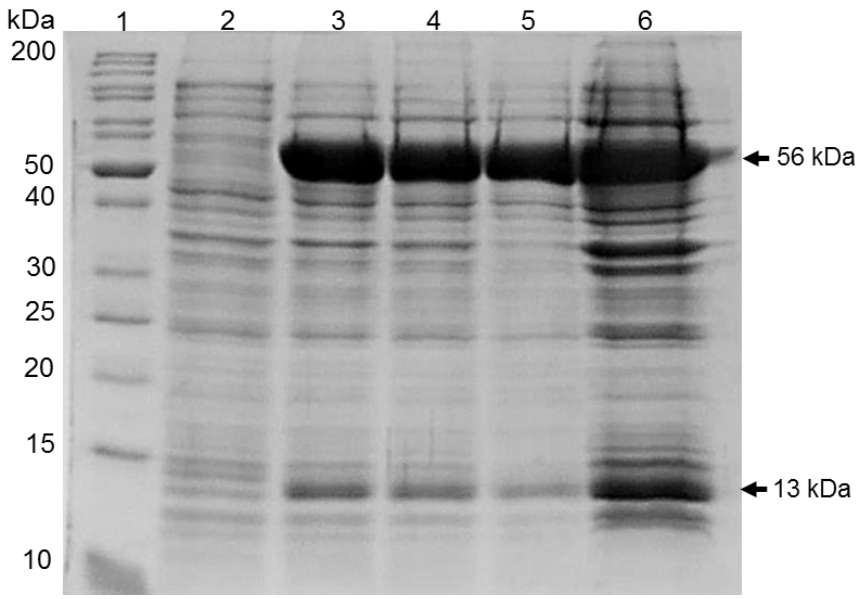

Figure 3-35: Co-expression of His_6-$FlrR_{CTD}$ and MBP-$FlrA_{NTD}$-VSVg.

pACYCDuet-His_6-$FlrR_{CTD}$ and MBP-$FlrA_{NTD}$-VSVg were co-transformed into *E. coli* strain BL21(λDE3). The bacterial cell culture was grown in LB medium at 37°C and induced for 3 hours' induction by adding 1 mM IPTG. All samples were analysed on 12% SDS-PAGE gel. Lane 1, EZ-Run Rec pre-stained protein ladder; lane 2, uninduced His_6-$FlrR_{CTD}$ and MBP-$FlrA_{NTD}$-VSVg, lane 3, induced His_6-$FlrR_{CTD}$ and MBP-$FlrA_{NTD}$-VSVg; lane 4, whole cell extracts, total; lane 5, soluble fraction; lane 6, insoluble fraction.

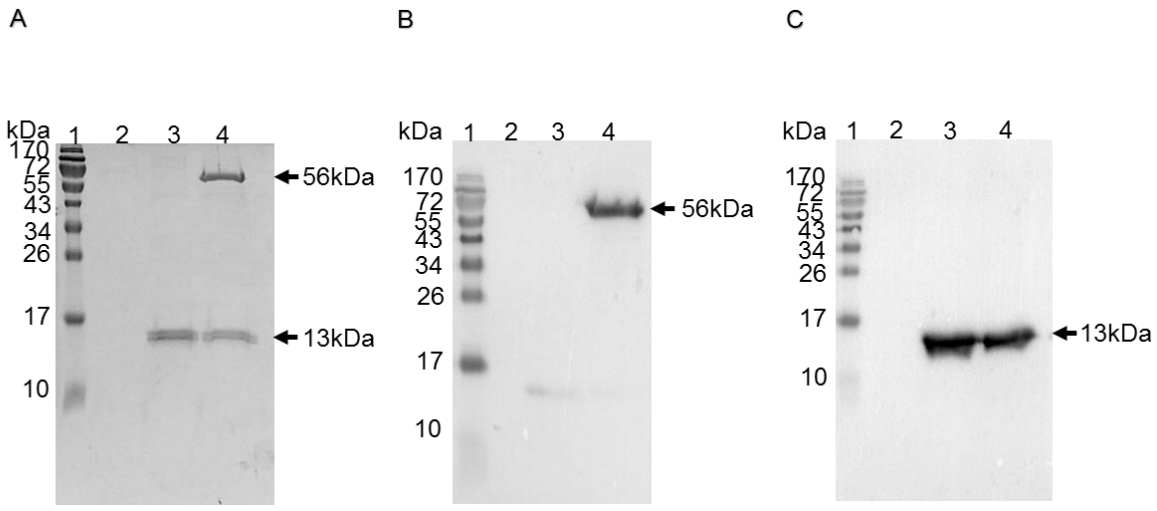

Figure 3-36: Demonstration of His_6-$FlrR_{CTD}$ and MBP-$FlrA_{NTD}$-VSVg interaction using pull-down assay.

pACYCDuet-His_6-$FlrR_{CTD}$ and MBP-$FlrA_{NTD}$-VSVg were overproduced in *E. coli* strain BL21(λDE3) separately. The cell lysate of both induced proteins was applied to nickel affinity resin. The bound proteins were washed and eluted with 500 mM imidazole buffer. The eluted samples of the bound proteins were analyzed on 15% SDS-PAGE and visualised by Coomassie blue stain and by Western blotting using anti-His_6 antibody and anti-MBP antibody. Immobilised His_6-$FlrR_{CTD}$ and MBP-$FlrA_{NTD}$-VSVg were included as controls.

A. Coomassie blue stain of His_6-$FlrR_{CTD}$ and MBP-$FlrA_{NTD}$-VSVg pull-down result.

B. Western blot of the eluted samples probed with anti-MBP antibody.

C. Western blot of eluted samples probed with anti-His_6 antibody.

A. Lane 1, EZ-Run Rec pre-stained protein ladder; lane 2, MBP-$FlrA_{NTD}$-VSVg; lane 3, His_6-$FlrR_{CTD}$; lane 4, His_6-$FlrR_{CTD}$ and MBP-$FlrA_{NTD}$-VSVg.

B and C. Lane 1, EZ-Run Rec pre-stained protein ladder; lane 2, MBP-$FlrA_{NTD}$-VSVg; lane 3, His_6-$FlrR_{CTD}$; lane 4, His_6-$FlrR_{CTD}$ and MBP-$FlrA_{NTD}$-VSVg. All the samples were eluted with 500 mM imidazole.

3.7 Discussion

This study has investigated the interaction between proteins involved in the Flr system of *B. cenocepacia* using two methods; the BACTH system as a first step, to identify the interaction between the putative iron starvation σ factor, FlrS, and its putative anti-σ factor, FlrR. Our hypothesis suggested that the cytoplasmic N-terminal domain of the anti-σ factor interacts with the σ factor's C-terminal domain. It also suggested that the C-terminal domain of the anti-σ factor interacts with the N-terminal domain of the outer-membrane receptor FlrA. Secondly, biochemical experiments, i.e. pull-down assay, were used to confirm the interaction between these domains' proteins.

The BACTH system is a very powerful and convenient technique that can be used to study protein-protein interaction. There are, however, a few restrictions involved in using the BACTH assay. In particular, it runs the risk of returning false positive interactions due to the ability of some proteins to interact non-specifically with other proteins. Also, since BACTH proteins are expressed either from high copy number plasmids (pUT18C and pUT18) or from low copy number plasmids (pKT25 and pKNT25) different amounts of protein may be produced corresponding to each BACTH plasmid (Battesti and Bouveret, 2012). Using BACTH assays alone, therefore, is not enough to confirm the interactions between proteins, and thus pull-down assays were included in this study to confirm the results of BACTH assays.

In this study, eight combinations, i.e. four fusion plasmids for each of the $FlrS_{CTD}$ and $FlrR_{NTD}$ domains were constructed and used to investigate protein-protein interactions. The strong M^+ phenotype that result from all eight combinations hybrid proteins is the first important finding in this study. This provided evidence that the cytoplasmic N-terminal domain of the anti-σ factor FlrR interacts strongly with the σ factor C-terminal domain of the FlrS. In this regard, it should be noted that the anti-σ factors serve to stabilise the σ factor in such a way that is no longer compatible with RNAP binding, achieving this by blocking the key RNAP binding determinants through bipartite interactions with σ_2 and σ_4 (Paget, 2015). It is possibe that FlrR may interact with $FlrS_{NTD}$ domain σ_2 of the σ factor but it has not been investigated in this study.

The involvement of the N-terminal region of the anti-σ factor is consistent with interactions demonstrated in other Gram-negative bacteria such as *E. coli* FecR and RseA (Campbell *et al*., 2003; Enz *et al*., 2000).

The possible self-interaction of each domain was also investigated, but no self-interactions were observed. This indicates that the domains are likely to remain as monomers rather than forming a dimer or oligomer. It is also consistent with the observation that σ factors do not self-interact. It should be noted that despite the fact that there might be an interaction between two proteins, their fusion to T25 and T18 domains might result in badly folded or unstable proteins, or simply inhibit the interaction with its partners. Therefore, these proteins cannot interact and produce cAMP, in which case the interaction may not be detected by the BACTH assay. Moreover, proteins with an intrinsic tendency to interact with any proteins known as sticky proteins, may give false positive results in the BACTH assay (Battesti and Bouveret, 2012).

In addition, the efficiency of the functional complementation between the interacting fusion proteins was quantified using β-galactosidase assays. It was expected that the T25-$FlrS_{CTD}$ and $FlrR_{NTD}$-T18, and T18-$FlrS_{CTD}$ and $FlrR_{NTD}$-T25 combinations would yield the highest level of β-galactosidase activity since $FlrS_{CTD}$ was located at the C-terminus of the fusion protein while $FlrR_{NTD}$ was located at the N-terminus of the fusion protein. In practice, however, the T18-$FlrS_{CTD}$ and T25-$FlrR_{NTD}$ combination gave the highest β-galactosidase activity. The enzyme assays confirmed the plate assay results in indicating that $FlrS_{CTD}$ and $FlrR_{NTD}$ probably do not self-interact since the level of β-galactosidase activities obtained were similar to those for the negative controls.

Testing for the self-interaction of full-length FlrR was studied in order to understand whether such an interaction might be involved in signal transduction. The BACTH assay results demonstrated that the full-length FlrR hyprid proteins gave rise to a M^- phenotype, suggesting that full-length FlrR does not self-associate. Also, the BACTH analysis suggested that full-length FlrR is able to interact with the C-terminal region of FlrS. However, the observed phenotypes were not as strong as the phenotypes

observed from the interaction between the N-terminal domain of FlrR and the C-terminal domain of FlrS.

One hypothesis suggested that the C-terminal domain of the anti-σ factor might self-interact, leading to dimerisation of the N-terminal domain which in turn may block the signal from being passed to the σ factor, thus not allowing the σ factor to bind to RNAP. Based on the mentioned theory, it was decided to study the self-interaction of $FlrR_{CTD}$ using the BACTH system, and the results of this analysis showed that $FlrR_{CTD}$ is capable of direct self-interaction as it gave rise to a weak positive maltose phenotype. This result suggests possible dimerization of the C-termanl domain that might be responsible for activation or inhabation of the FlrS activity, and thus affecting *flr* operon transcription. A cross-linking study on the RsbW anti-σ factor of *S. aureus* demonstrated that RsbW formed a dimer in solution; RsbW specifically inhibits the SigB σ factor that forms a monomer (Miyazaki *et al*., 1999). Also, SpoIIAB is an anti-σ factor of *B. subtilis* found to form a dimer (Miyazaki *et al*., 1999; Duncan and Losick, 1993).

FlrA has an N-terminal extention that is consreved in TBDRs that interact with σ factors regulatory proteins (Koebnik, 2005; Hartney *et al*., 2011). Screening for $FlrR_{CTD}$ interaction with $FlrA_{NTD}$ using the BACTH assay indicated that all possible $FlrR_{CTD}$ BACTH fusion proteins interact with all possible $FlrA_{NTD}$ BACTH fusions and gave rise to a strong M^+ phenotype. The results of the BACTH assay in this study therefore indicate that the N-terminal domain of FlrA interacts with the C-terminal domain, FlrR. A study on the Fec system in *E. coli* supported the binding of the periplasmic regions of FecA and FecR (Enz *et al*., 2003). FecA is a well-studied outer-membrane receptor, and the binding between FecA and ferric citrate has been shown to result in a structural change when it is compared to unoccupied FecA (Ferguson *et al*., 2002). A large movement in the periplasmic region of FecA has been observed to cause the interaction with FecR (Kim *et al*., 1997). The signal alters the structure of FecA and this causes the interaction with FecR, possibly involving a structural change of FecR (Mahren *et al*., 2002). Moreover, this data indicates that there is no physical self-interaction of $FlrA_{NTD.}$ The data obtained in this study supports the contention that FlrR is an anti-σ factor for FlrS and has a critical role in passing on signals from FlrA at the cell surface.

A pull-down experiment was designed as a confirmatory method for the interactions between $FlrR_{NTD}$ and $FlrS_{CTD}$ observed by BACTH assay. To do this, $FlrR_{NTD}$ and $FlrS_{CTD}$ were cloned and expressed with C-terminal VSVg and N-terminal His- respectively.

The N-terminally His-tagged $FlrS_{CTD}$ was successfully overproduced. The amount of $FlrS_{CTD}$ produced was not sufficient, however; although attempts were made to increase the protein production and solubility by expressing the protein at different temperatures and also by using different concentrations of IPTG. Our results suggest that most of $FlrS_{CTD}$ is in the insoluble fraction this phenomenon was previously been observed for other ECF σ factor. To increase protein solubility, therefore, the cell was induced at 22°C and 30°C, as a lower temperature reduces the rate of synthesis of the protein and this, in theory, gives it more time to fold properly. In our experiments, however, the protein seemed to be less soluble at the lower temperature, which is a surprising result. Therefore, it was decided to check the protein solubility at 42°C but this did not lead to an improvement. A further attempt to do pull-dwon assay was made using the insoluble materials of cells grown at 37°C.

$FlrS_{CTD}$ insolubility was not the only problem since it was not possibe to observe $FlrR_{NTD}$-VSVg expression from pACYCDuet-1 under any condition and thus the coding sequence was cloned into a vector encoding MBP. MBP is an important enhancer for protein solubility but the reason for this is not clear yet. One suggestion is that its ability to function as a general molecular chaperone protein occurs by transitory sequestration of aggregation-susceptible folding of intermediates of the fused protein that interferes with their self-association (Richarme and Caldas, 1997).

MBP-$FlrR_{NTD}$-VSVg was overproduced successfully and was soluble. However, using protein with the two tags might affect the interaction with $FlrS_{CTD}$ due to steric hindrance by MBP that's are tag. Since T25-$FlrR_{NTD}$ works well in a BACTH assay, however, it has a good chance of working because fusions at the N-terminus do not appear to inhibit the interaction.

In the pull-down experiments, although the expression of $FlrS_{CTD}$ was not ideal for protein interaction it was able to bind to $FlrR_{NTD}$. The association between both proteins was also confirmed by Western blotting. The cytoplasmic domain NTD of σ factor regulators detaches from the σ factor regulator following autoproteolysis. Presumably it remains attached to the σ factor and acts to stimulate their activities which in turn positively regulates gene transcription as in the case of *E. coli fec* and *P. aeruginosa* (Ochs *et al*., 1995; Draper *et al.*, 2011). Therefore, it was assumed that FlrR does likewise. In the *E. coli* Fec system, the activation of FecI is not necessarily due to a conformation change or chemical modification of FecI. Active FecR seems to be responsible for stabilising the active form of FecI. FecI bound to FecR would remain inactive until the transcription initiation signal is transmitted from the ferric citrate-loaded FecA. This allows the conformation change to occur in the cytoplasmic portion of FecR to which FecI remains bound (Stiefel *et al*., 2001).

Chapter 4 Characterization of the P_{flrA} promoter

4.1 Introduction

Bacterial σ factors are essential dissociable subunits of RNAP that are required for specific promoter recognition. The catalytic core of RNAP associates with different σ factors that are responsible for promoter recognition at different target consensus sequences. Therefore, the main function of the major σ factor, σ^{70}, is as the global regulator of transcription. Apart from the essential primary σ factor that directs transcription of most genes (mainly housekeeping genes), there are additional (mostly) non-essential σ factors (alternative σ factors) that recognize specific promoters for specific cell functions (Silar *et al*., 2016). One of the groups is known as Group 4 or ECF σ factors.

B. cenocepacia Flr ferric-siderophore uptake system is similar to *E. coli* Fec system that transports ferric-dicitrate into the cells (Section 1.13.1). Similarly, *flr* system is predicted to be regulated by two promoters; one promoter is regulated by σ^{70} and it is proposed to be responsible for transcription of *flrS* and *flrR*. The second promoter is located between *flrR* and *flrA* and is recognised by FlrS (σ^{FlrS}) in complex with RNAP. The work discussed in this chapter seeks to identify and characterise the promoter for transcription of *flrA* and *flrX*, namely P_{flrA}.

4.2 Objectives

- Demonstrate that a FlrS-dependent promoter is located between *flrR* and *flrA.*

- Investigate the role of FlrR in regulating the activity of FlrS, i.e. does FlrR release FlrS or does it activate FlrS under inducing conditions?

- Identify the -35 and -10 regions of the P_{flrA} promoter and other important features.
- Investigate the functional equivalence of FlrS and homologous σ factors from *Pseudomonas* species.

4.3 Identification of a FlrS-dependent promoter upstream of *flrA*

The sequence upstream of *flrA* was tested in order to determine it contains an FlrS-dependent promoter. To do this, a 166 bp DNA fragment containing *flrR-flrA* interginc region (102 bp) the 3' 5' bp of *flrR* and 3' 5' bp of *flrA* was cloned into, pKAGd4. This sequence, which is referred to as 'full-length P_{flrA}', was fused to the *lacZ* reporter gene in the transcription reporter plasmid pKAGd4. The promoter activity was intended to be measured in *E. coli* and *B. cenocepacia* WT strains in the presence of FlrS. Therefore, the *flrS* gene, together with its putative promoter, was cloned into plasmid pBBR1MCS2 downstream of *lacZ* promoter. pKAGd4-P_{flrA} and pBBR2-FlrS were transformed into *E. coli* MC1061 and the resulting transformants were grown on LB agar containing 100 mg/ml ampicillin and 50 mg/ml kanamycin. Also, they were introduced into *E. coli* S17-1(*λpir*) donor strain in order to sequentially conjugate them into *B. cenocepacia* strain HIII. The ex-conjugants were selected on M9 agar plates supplemented with 50 mg/ml chloramphenicol, 50 mg/ml kanamycin and 10 mg/ml tetracycline. The β-galactosidase assay was carried out on culture grown in LB medium containing 175 μM dipyridyl in order to measure P_{flrA} activity in both strains under iron-limited conditions.

The β-galactosidase assays in *E. coli* and *B. cenocepacia* indicated that the full-length P_{flrA} promoter fragment contained a FlrS-dependent promoter, as there was negligible promoter activity in the absence of pBBR2-FlrS, whereas in the presence of this plasmid an increased in β-galactosidase activity was measured (Figure 4.1). Although the activity of the full-length P_{flrA} was not high, it was decided to investigate the sequence upstream of *flrA* further as described in the following section.

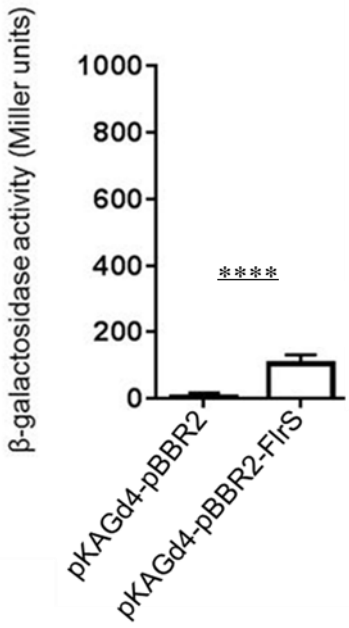

Figure 4-1: Activity of the full-length P_{flrA} promoter fragment in the presence of FlrS.

The full-length P_{flrA} promoter fragment was fused to *lacZ* in pKAGd4 and its activity was assayed in the presence of pBBR2-FlrS in *E. coli* strain MC1061. The activity of the control pBBR2-pKAGd4 was also measured. Error bars represent the standard deviation of three replicates assayed. The results were analysed using T-test ****$P < 0.0001$.

4.4 Effect of FlrR on the activity of FlrS at the full-length P_{flrA} promoter

The BACTH assay results discussed in the previous chapter suggest that the N-terminal domain (NTD) of the putative anti-σ factor FlrR interacts with the C-terminal domain (CTD) of the putative σ factor FlrS. These results indicate that FlrR could be the regulator of FlrS. In normal conditions (non-inducing conditions), anti-σ factors inhibit the activities of their partner σ factors. However, in some cases they also have a role in activating σ factors when required, as in the case of FecR *E. coli* (Section 1.13.1). As the activity of the full-length P_{flrA} promoter in the presence of FlrS is quite low it was decided to investigate the possibility that $FlrR_{NTD}$ could activate FlrS (as in the case in the orthologous Fec system) thereby improving the sensitivity of promoter scanning assays. Two bacterial host systems, *E. coli* and *B. cenocepacia*, were to be used to investigate the role of FlrR in regulating the σ factor FlrS. In each case, it was decided to employ two plasmid systems to assay the effect of FlrR and $FlrR_{NTD}$ on FlrS activity at P_{flrA}. For *E. coli* system one plasmid, pBBR1MCS-2 would express FlrS alone or together with FlrR or $FlrR_{NTD}$, and the other one is pKAGd4 carrying the full-length P_{flrA}. To assay the effect of FlrR on FlrS activity in *B. cenocepacia*, a strain lacking FlrR was to be used. Therefore, it was necessary to use *B. cenocepacia flrR* mutant as host species (Section 4.4.2). Furthermore, as *B. cenocepacia* harbours *flrS*, it was not necessary to employ a plasmid expressing FlrS, only FlrR or $FlrR_{NTD}$. The experiment set-up for the two-assay system is shown in Figure 4.2. Plasmids employed in these systems are pBBR2-FlrS, pBBR2-FlrSR' and pBBR2-FlrSR which were constructed in previous study (Haldipurkar, MSC dissertation, 2012), while pBBR2-$FlrR_{NTD}$ and pBBR2-$FlrSR_{NTD}$ were constructed in this study as described in Section 4.4.1.

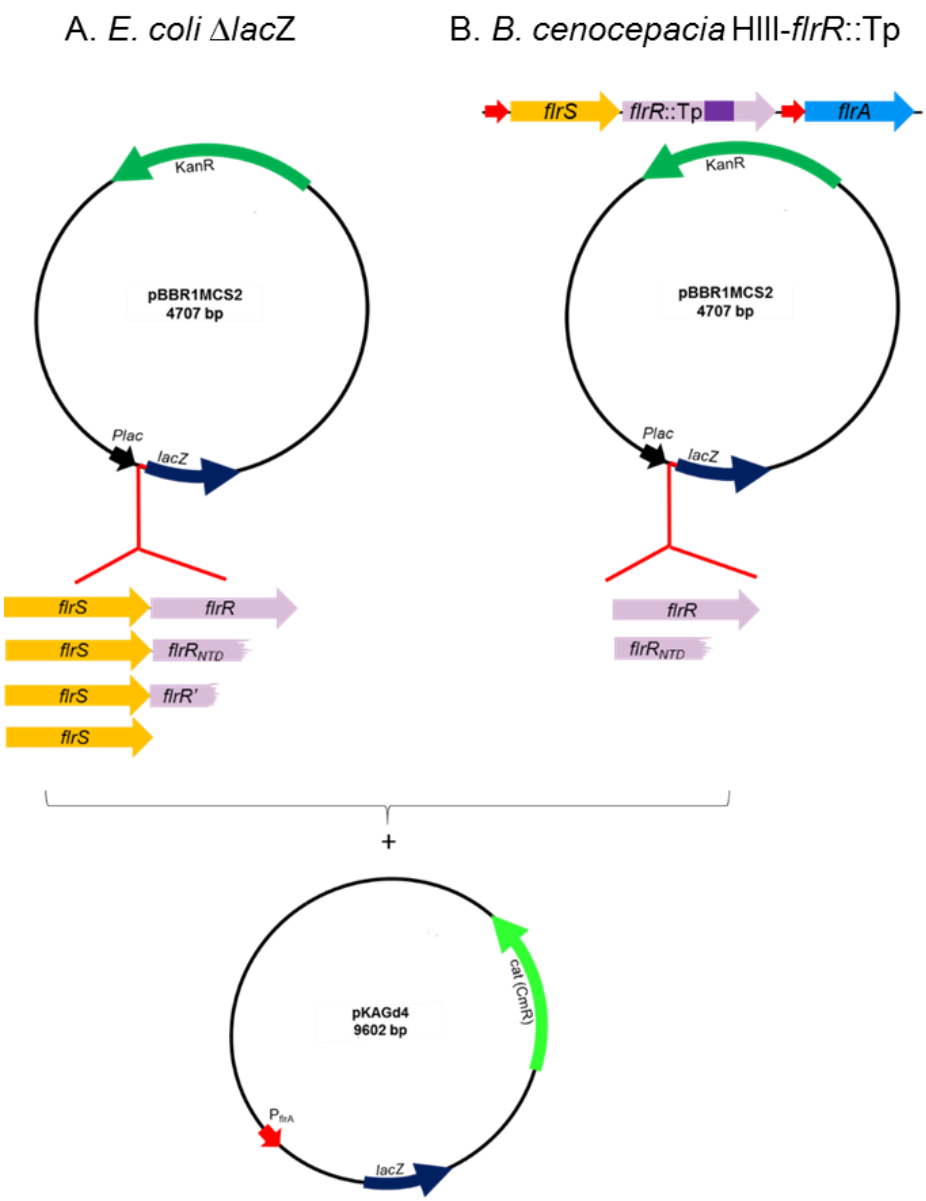

Figure 4-2: Host-vector system for investigating the role of FlrR on FlrS activity.

A. The activity of full-length P_{flrA} was measured in the *E. coli* Δ*lac*Z strain MC1061 using a P_{flrA}-*lac*Z reporter fusion plasmid (pKAGd4-P_{flrA}) and plasmids expressing FlrS alone (pBBR2-FlrS) or FlrS with FlrR (pBBR2-FlrSR), $FlrR_{NTD}$ (pBBR2-$FlrSR_{NTD}$) and a short fragment of FlrR (pBBR2-FlrSR'). pBBR2-$FlrSR_{NTD}$ encodes the N-terminal 48 amino acids of FlrR followed by 18 amino acids derived from pBBR1MCS-2 vector DNA flanking the flrSR' insert.

B. The activity of full-length P_{flrA} was measured in *B. cenocepacia* HIII-*flrR*::Tp using plasmids expressing FlrR (pBBR2-FlrR) and $FlrR_{NTD}$ (pBBR2-$FlrR_{NTD}$).

4.4.1 Effect of FlrR and $FlrR_{NTD}$ on FlrS activity in *E. coli*

Construction of pBBR2-$FlrR_{NTD}$

In a previous attempt to construct plasmid pBBR2-$FlrR_{NTD}$, pBBR2-FlrSR was used as template, and the $FlrR_{NTD}$ coding sequence (together with an introduced stop codon) was amplified using FlrRfor and FlrRNTDrev primers, following which, the PCR product and plasmid pBBR1MCS2 were cut with *Hin*dIII and *Bam*HI and ligated together. Following transformation of JM83, the obtained clones were sequenced and analysis of the sequence indicated that a deletion of 2 or 5 basepairs has occurred in the $FlrR_{NTD}$ coding sequence of each clone towards the stop codon, which resulted in addition of vector encoded amino acids to the C-terminus of $FlrR_{NTD}$. The deletion also resulted in loss of a naturally occurring *Not*I site in the $FlrR_{NTD}$ coding sequence and introduction of a *Sac*II site. Therefore, a double-stranded oligonucleotide was generated by annealing two single stranded oligonucleotides, FlrRstopfor2 and FlrRstoprev2, in order to rectify one of the clones (clone 2) (Appendix 8.6). Clone 2 was cut sequentially with restriction enzymes, *Sac*I and *Sac*II. The complementary oligonucleotides were designed to create compatible sticky ends for the *Sac*I site in the MCS downstream of $flrR_{NTD}$ and the *Sac*II site near the end of $flrR_{NTD}$. Clone 2 was ligated to the double stranded oligonucleotide and then transformed into *E. coli* MC1061 competent cells (Figure 4.3). Transformed cells were then plated on LB agar containing 50 µg/ml kanamycin. The plasmid DNA was isolated from a number of kanamycin-resistant transformants and candidate rectified clones were identified by agarose gel electrophoresis (result not shown).

Construction of pBBR2-$FlrSR_{NTD}$

In order to construct pBBR2-$FlrSR_{NTD}$, pBBR2-FlrSR and pBBR2-$FlrR_{NTD}$ were digested with restriction enzymes *Kpn*I and *Sma*I. Cutting pBBR2-FlrSR with these enzymes released *flrS* fragment which was gel purified in order to be ligated with pBBR2-$FlrR_{NTD}$ (Figure 4.4). The ligation reactions were transformed into *E. coli* MC1061 and the transformed cells were then plated on LB agar containing 50 µg/ml kanamycin. The obtained colonies were screened by plasmid miniprep to confirm the

size of the expected clone (6.16 kb) (result not shown). The DNA integrity of the correct clone was confirmed by sequencing using primers M13for and M13rev.

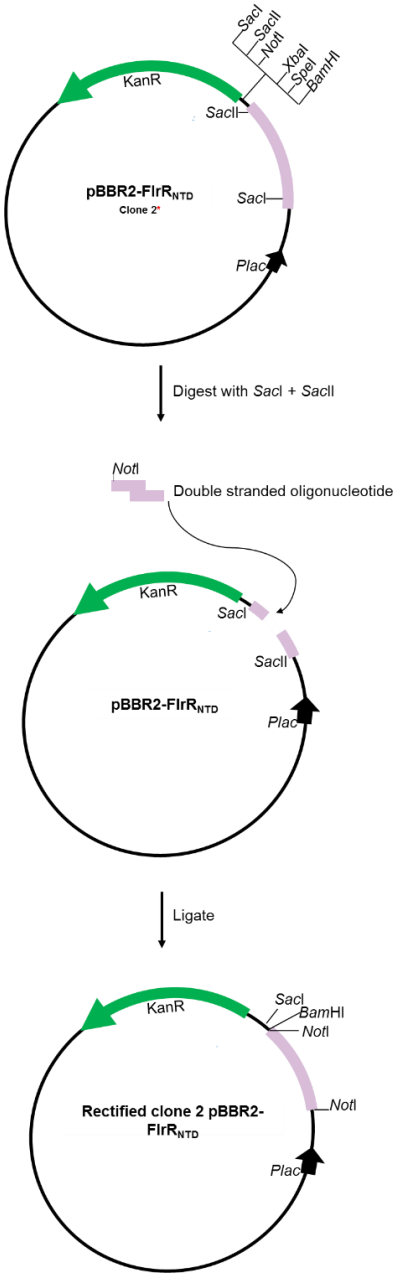

Figure 4-3: Construction of pBBR2-FlrR$_{NTD}$.

pBBR2-FlrR$_{NTD}$ clone 2, contains an out of frame deletion near the introduced stop codon and was rectified by inserting a double-stranded oligonucleotide between the *Sac*I and *Sac*II sites.

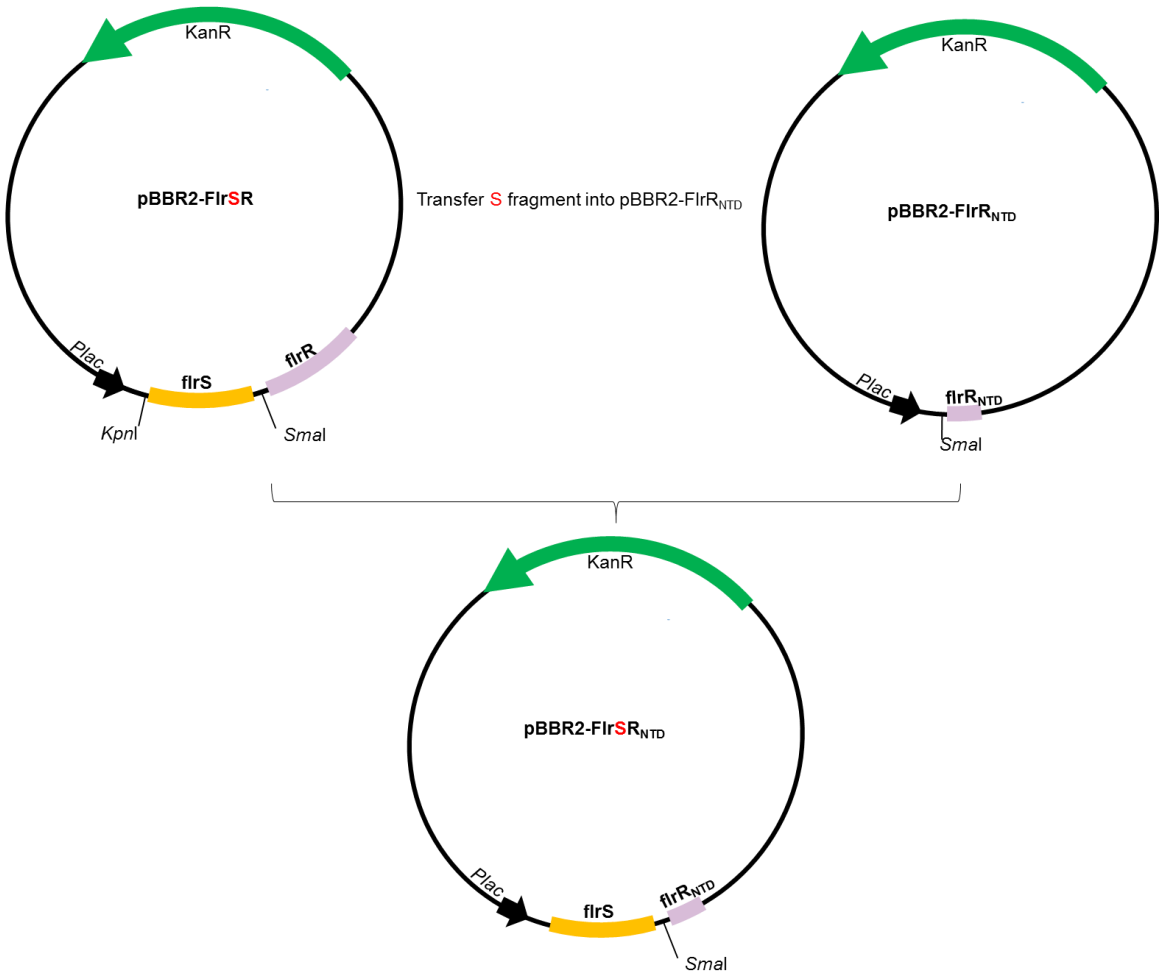

Figure 4-4: Construction of pBBR2-FlrSR$_{NTD}$.

flrS DNA fragment transferred from pBBR2-FlrSR into pBBR2-FlrR$_{NTD}$.

Effect of FlrR and $FlrR_{NTD}$ on FlrS activity in *E. coli*

β-galactosidase assays were performed to measure the activity of the full-length P_{flrA} promoter in cells growing under iron starvation conditions. In addition, the background β-galactosidase activity in cells containing pKAGd4 was measured for each pBBR1MCS-2 plasmid derivative and these basal activities were subtracted from the values measured in cells containing pKAGd4-P_{flrA}.

The results obtained from the β-galactosidase assays indicate that there is negligible P_{flrA} promoter activity in *E. coli* in the absence of FlrS (Figure 4.5). Introducing *flrS* on a plasmid led to a very low level of P_{flrA} promoter activity. When *flrR* was introduced along with *flrS* there was a ~2 fold increase in P_{flrA} promoter activity relative to the presence of FlrS alone. Introducing pBBR2-FlrSR' showed a similar low level of P_{flrA} promoter activity as when *flrS* was present alone. However, when introducing pBBR2-$FlrSR_{NTD}$, that expressed FlrS and $FlrR_{NTD}$, the P_{flrA} promoter activities increased by almost 20-fold relative to full-length FlrR (Figure 4.5). Therefore, it was decided to test the effect of $FlrR_{NTD}$ on FlrS in *B. cenocepacia.* The experiment demonstrated that $FlrR_{NTD}$ activists FlrS. For further experiments, it was decided to assay P_{flrA} promoter activity using the region encoding the N-terminal 48 amino acids of FlrR, in addition to FlrS,

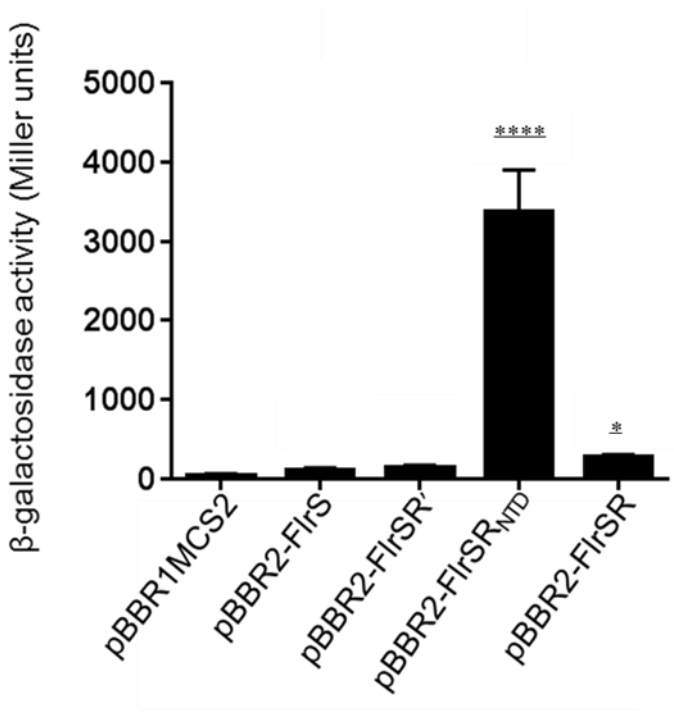

Figure 4-5: Effect of FlrR and FlrR$_{NTD}$ on FlrS activity in *E. coli*.

P_{flrA} promoter activity was assayed in *E. coli* MC1061 harbouring pKAGd4-P_{flrA} in the presence of the indicated plasmids. The activities shown are after the subtraction of pKAGd4 basal activity in cells containing the corresponding pBBR1MCS-2 (pBBR2) derivative. Error bars represent the standard deviation of three replicates assayed. The results were analysed using one-way analysis (ANOVA) ****$P < 0.0001$, *$P < 0.05$.

4.4.2 Effect of FlrR and $FlrSR_{NTD}$ on FlrS activity in *B. cenocepacia*

The experimental rationale for assaying the effect of FlrR and $FlrSR_{NTD}$ on FlrS activity in *B. cenocepacia* has been discussed in Section 4.4. *B. cenocepacia* strain HIII, that is sensitive to kanamycin, is required to investigate the role of FlrR and $FlrSR_{NTD}$ on FlrS activity. Therefore, an *flrR* knockout mutant of this strain was constructed as described in the following section in order to perform the experiment.

Construction of *B. cenocepacia flrR* mutant

Construction of an allelic replacement plasmid for inactivating chromosomal *flrR*

To make marked gene knockout mutants in *B. cenocepacia*, a suicide plasmid such as pSHAFT2 is required. It was decided to use this plasmid to inactivate the *flrR* gene with a trimethoprim resistance (Tp) cassette. For constructing pSHAFT2-*flrR*::Tp, pSHAFT2 was digested with restriction enzymes *Xho*I and *Bgl*II while pBBR2-*flrR*::Tp was digested with *Xho*I and *Bam*HI (Figure 4.6). pBBR2-*flrR*::Tp is pBBR1MCS-2 containing the entire *flrR* gene into which was inserted a trimethoprim-resistance cassette in opposite orientation. The digested products were checked by electrophoresis in a 0.8% agarose gel (result not shown). The resulting products were ligated overnight at room temperature. (15 µl) of ligation mixture was used to transform *E. coli* strain CC118(*λpir*) competent cells, and the transformant colonies were selected on IST plates containing 50 µg/ml chloramphenicol and 25 µg/ml trimethoprim. Obtained colonies were patched onto three different plates containing different antibiotics, LB 100 µg/ml ampicillin, LB 50 µg/ml kanamycin and IST 25 µg/ml trimethoprim. The required plasmid would confer trimethoprim and ampicillin resistance but kanamycin sensitivity on the host strain. Such colonies were screened by plasmid miniprep, and the sizes of the plasmid clones were checked by electrophoresis in a 0.8% agarose gel. The expected size of required plasmid was 6.4 kb, which corresponds to the size of pSHAFT2 (4.5 kb) (result not shown) and the *flrR*::Tp DNA fragment (1.8 kb). Thus, pSHAFT2-*flrR*::Tp was successfully constructed.

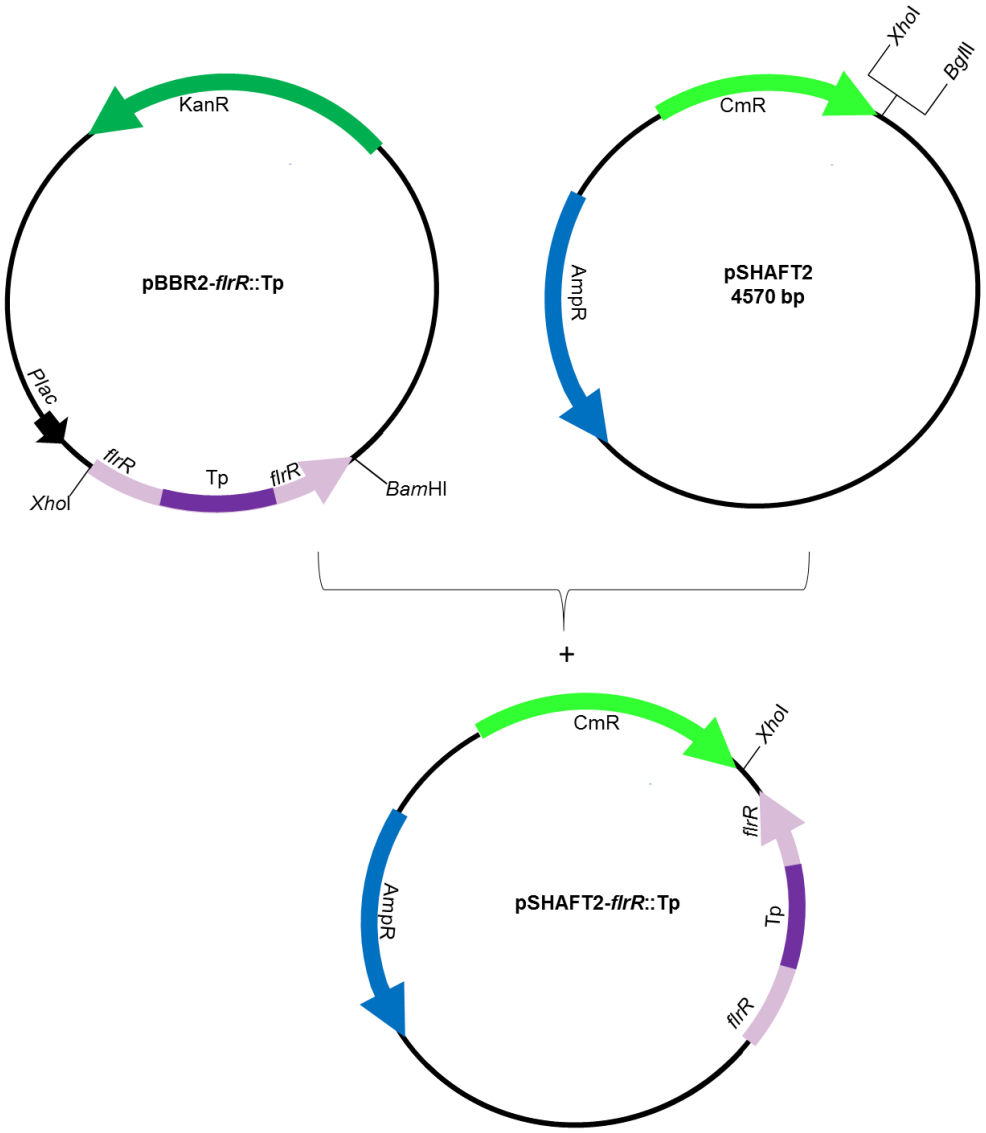

Figure 4-6: Construction of pSHAFT2-*flrR*::Tp.

pSHAFT2 and pBBR2-*flrR*::Tp were digested with *Xho*I and *Bgl*II, and *Xho*I and *BamH*I, respectively. The digested plasmids were ligated to give pSHAFT2-*flrR*::Tp.

Inactivation of chromosomal *flrR* by allelic replacement

pSHAFT2-*flrR*::Tp was used to transform the *E. coli* conjugal donor strain SM10(*λpir*). By conjugation, the SM10(*λpir*) transformant cells were then used to introduce pSHAFT2-*flrR*::Tp into *B. cenocepacia* HIII. As pSHAFT2-*flrR*::Tp cannot replicate in the absence of the *pir* gene, it functions as a suicide plasmid in *B. cenocepacia*. Acquisition of resistance to the antibiotics to which the plasmid encodes resistance can only occur if the plasmid integrates into the HIII genome due to recombination between regions of homology present on the plasmid and the chromosome. Rare double crossover recombinants were obtained by applying selection for trimethoprim resistance following conjugation and screening candidate recombinants for chloramphenicol sensitivity (Figure 4.7). To do this, M9 agar plates containing 25 µg/ml trimethoprim were used initially to select for recombinants following conjugation. Approximately 100 of the trimethoprim-resistant ex-conjugants were patched on IST agar plates containing 25 µg/ml trimethoprim and LB plates containing 50 µg/ml chloramphenicol. Six of the trimethoprim-resistant clones were found to be chloramphenicol sensitive, suggesting that they were double crossover recombinants. All six candidate double crossover recombinants were screened by PCR using boiled cell lysates as template DNA. The expected size of PCR product for the *flrR*::Tp mutant was 1.85 kb obtained with the FlrRforOut and pFlrArev2 pair of primers that anneal to genomic sequences located outside the region contained on the plasmid (Figure 4.8). In contrast, the WT strain HIII was expected to give a PCR product of ~1.25 kb using the same pair of primers.

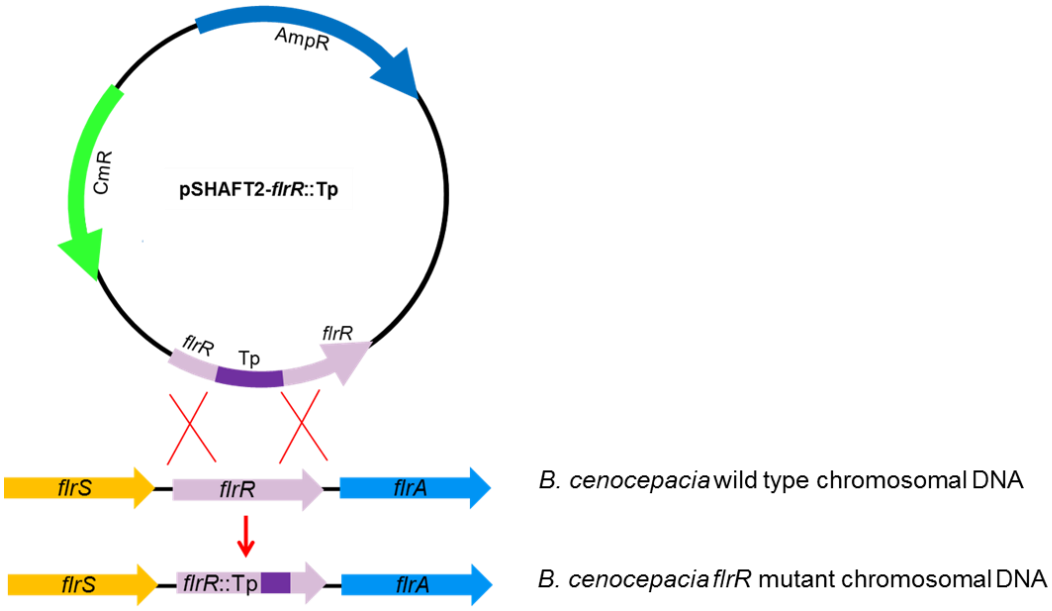

Figure 4-7: Construction of HIII-*flrR*::Tp.

pSHAFT2-*flrR*::Tp was introduced into *B. cenocepacia* HIII by conjugation. The allelic replacement shown in the diagram is a result of a double crossover between the mutated gene *flrR*::Tp on the plasmid and the WT *flrR* gene on the chromosome. The trimethoprim resistance gene was inserted in the opposite orientation to *flrR*.

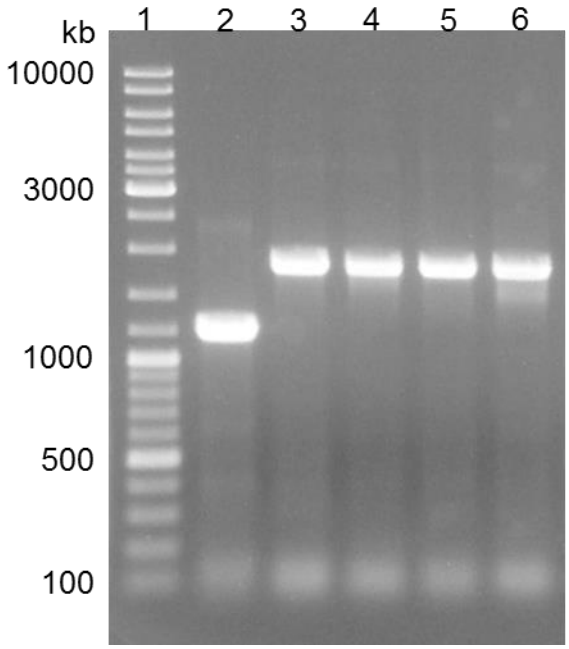

Figure 4-8: PCR screening of candidate HIII-*flrR*::Tp mutants using *flrR* outside primers.

Lane 1, Qstep4 ladder; lane 2, HIII WT control; lanes, 3-6, candidate HIII-*flrR*::Tp mutants.

FlrS-dependent P_{flrA} activity in *B. cenocepacia*

Full-length P_{flrA} promoter activity was assayed in *B. cenocepacia flrR* mutant and compared to the promoter activity in the WT HIII strain, in the presence and absence of additional copies of *flrS*. Plasmid pKAGd4-P_{flrA} with or without pBBR1MCS-2 and pBBR2-FlrS were introduced into S17-1(*λpir*) competent cells and the transformants were used to introduce the plasmids into HIII and HIII-*flrR*::Tp by conjugation. The exconjugants were selected on LB agar plates containing 50 µg/ml chloramphenicol and 50 µg/ml kanamycin and stored on M9 plates containing the same antibiotics. β-galactosidase assays were conducted by growing the bacterial cells in LB under iron-limiting conditions using 175 µM dipyridyl.

As before, the results of β-galactosidase assays in the WT HIII showed an extremely low level of P_{flrA} promoter activity in the presence of chromosomal *flrS* but absence of plasmid copy of *flrS*. When pBBR2-FlrS was also present the activity of P_{flrA} increased approximately 6 fold although it was still relatively low (~300 Mu) (Figure 4.9). Also, the effect of FlrS on the full-length P_{flrA} promoter activity was measured in HIII-*flrR*::Tp mutant. In this situation, the activity observed for the P_{flrA} promoter in the presence of pBBR2-FlrS was lower than that observed in the WT strain containing pBBR2-FlrS (Figure 4.9). This result suggests that FlrR does not inhibits FlrS activity.

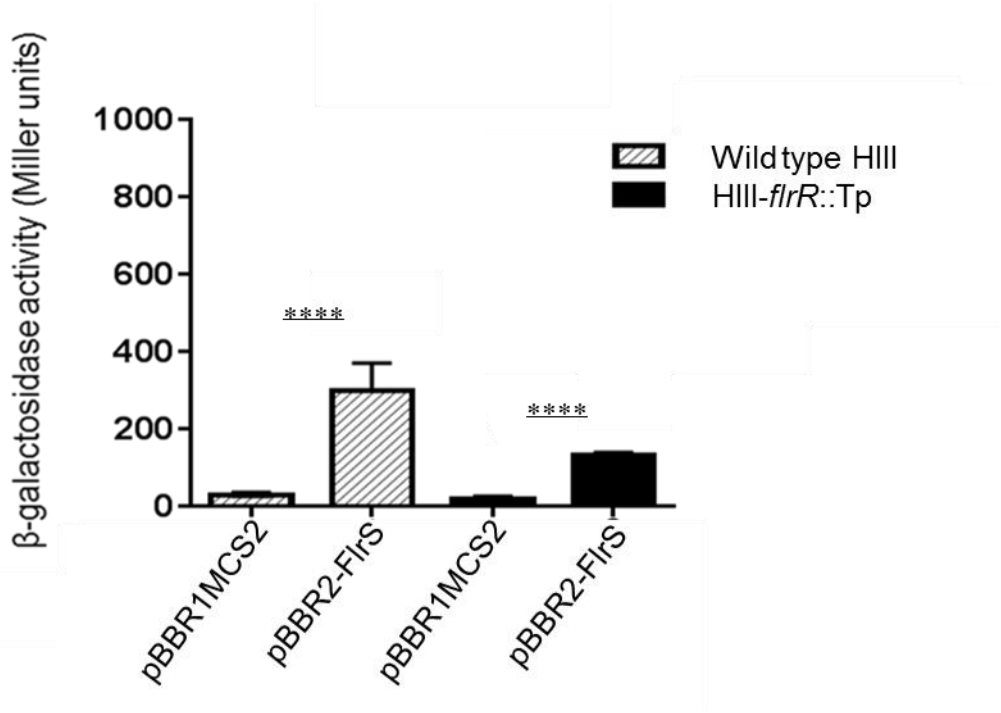

Figure 4-9: Effect of FlrS on P_{flrA} promoter activity in *B. cenocepacia* HIII and HIII-*flrR*::Tp mutant.

pBBR1MCS-2 or pBBR2-FlrS and pKAGd4-P_{flrA} were introduced into HIII and HIII-*flrR*::Tp by conjugation. The β-galactosidase assays were carried out in LB medium supplemented with 50 µg/ml kanamycin and 50 µg/ml chloramphenicol. The bacterial cells were grown under low iron conditions by adding 175 µM of dipyridyl. Activities were corrected by subtraction of the background pKAGd4 activity. Error bars represent the standard deviation of three replicates assayed. The results were analysed using one-way analysis (ANOVA) ****P < 0.0001.

Effect of pBBR2-FlrR$_{NTD}$ on FlrS activity in *B. cenocepacia*

The activity of full-length P_{flrA} promoter was also assayed in the *flrR* mutant in the presence of pBBR2-FlrR$_{NTD}$ and in the presence of pBBR2-FlrSR$_{NTD}$ with the additional copies of *flrS* (Figure 4.10). The results obtained from β-galactosidase assay of the HIII-*flrR*::Tp mutant indicated low level of P_{flrA} promoter activity in the absence of *flrR* as previously observed (Figure 4.9). Introducing the full length *flrR* indicate low level of P_{flrA} promoter activity. However, when introducing pBBR2-FlrR$_{NTD}$ and pBBR2-FlrSR$_{NTD}$ the activity of the full-length P_{flrA} promoter increased significantly, pBBR2-FlrSR$_{NTD}$ showed increase in the activity by almost 30% compared to the activity in the presence of pBBR2-FlrR$_{NTD}$ (Figure 4.10). This result indicates that the pBBR2-FlrSR$_{NTD}$ is the best construct to use for further copies of P_{flrA} in *B. cenocepacia.*

4.5 Effect of iron availability on FlrS-dependent P_{flrA} activity

The effect of iron on full-length P_{flrA} promoter activity in *B. cenocepacia* HIII-*flrR*::Tp was assayed in the presence of pBBR2-FlrSR$_{NTD}$. HIII-*flrR*::Tp containing pKAGd4-P_{flrA} and pBBR2-FlrSR$_{NTD}$ were grown in LB medium under low iron condition and high iron conditions, in which the β-galactosidase activities were measured (Figure 4.11). In comparison, the activity of full-length P_{flrA} under high iron conditions was less active and decreased by almost 5 fold. This result indicates that the σ factor gene *flrS* not transcribed as Fur binds to P_{flrS} promoter thus no FlrS being synthesised and the rest of FlrS in the cell is being inactivated by FlrR (Figure 4.11). To conclude, these experiments showed that the optimal system for analyzing the P_{flrA} promoter in *B. cenocepacia* is to use the HIII-*flrR*::Tp mutant with a plasmid expressing FlrS and FlrR$_{NTD}$.

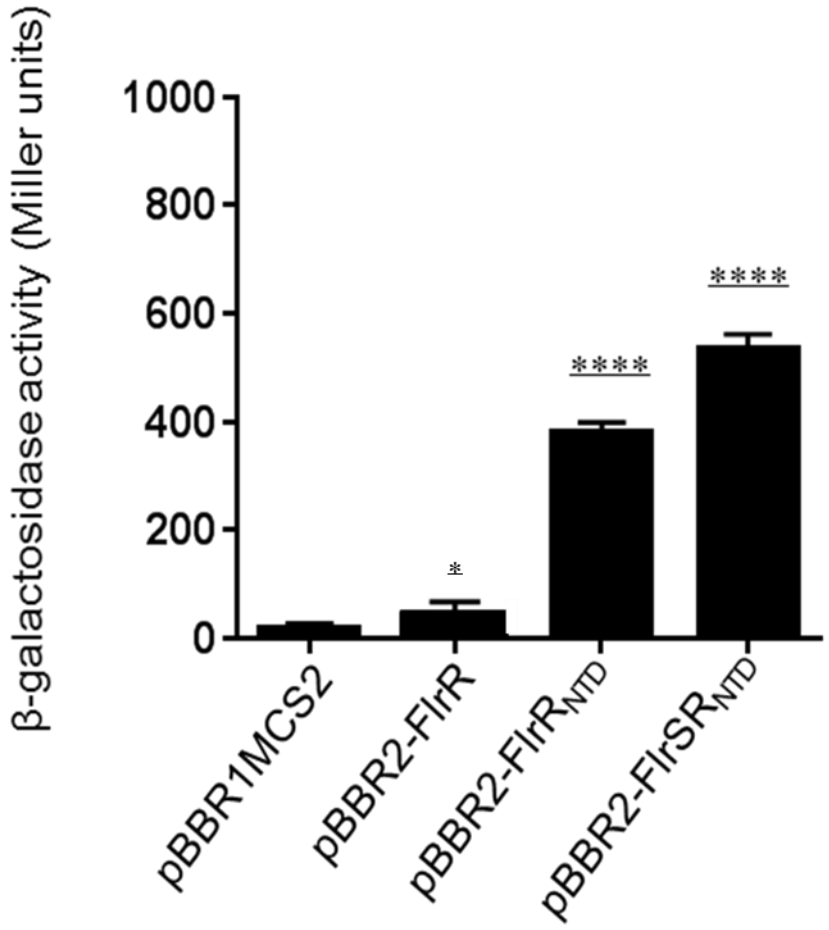

Figure 4-10: Effect of FlrR, FlrR$_{NTD}$ and FlrSR$_{NTD}$ on P$_{flrA}$ activity in *B. cenocepacia* HIII-*flrR*::Tp mutant.

P$_{flrA}$ promoter activity was assayed in *B. cenocepacia* HIII-*flrR*::Tp containing pKAGd4-P$_{flrA}$ in the presence of the indicated pBBR2-FlrR, pBBR2-FlrR$_{NTD}$ and pBBR2-FlrSR$_{NTD}$ plasmids and compared to the activity of cells harbouring pBBR1MCS-2. The activities shown are after the subtraction of pKAGd4 basal activity in cells containing the corresponding pBBR1MCS-2 (pBBR2) derivative. Error bars represent the standard deviation of three replicates assayed. The results were analysed using one-way analysis (ANOVA) ****P < 0.0001, *P < 0.05.

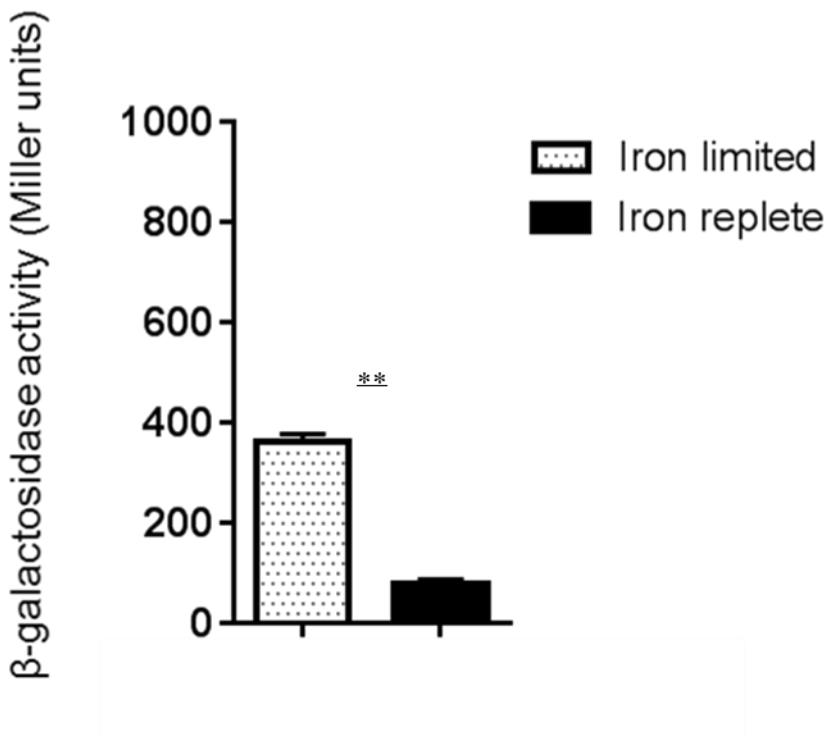

Figure 4-11: Effect of iron on P_{flrA} activity in *B. cenocepacia* HIII-*flrR*::Tp mutant expressing FlrS and $FlrR_{NTD}$.

β-galactosidase activity was measured in HIII-*flrR*::Tp containing pKAGd4-P_{flrA} and pBBR2-$FlrSR_{NTD}$ growing in LB at 37°C in the presence of 175 µM dipyridyl or 50 µM FeCl3. Error bars represent the standard deviation of three replicates assayed. The results were analysed using T-test ** $P < 0.01$.

4.6 Bioinformatic analysis of the *flrR-flrA* intergenic region

The *flrR-flrA* intergenic region was compared to the region downstream of '*flrR'* in other bacterial species that habour *flrS* and *flrR* homologues as they may share some common sequences that may indicate the location of the FlrS-dependent promoters. These species include other members of *B. cenocepacia* genes and some *Pseudomonas*. In each case, the *flrR* homologue is located upstream of a gene encoding a TBDR (Figure 4.12). These sequences are TGAGC and TCGCGTGACA. Second motif could be the -10 region as it contains the CGTG motif found in ECF σ-dependent promoters. Between these two conserved motifs is a conserved TTT triad. Downstream of the putative -10 region it has been noticed that there is a region, which is rich in A and G residues. Upstream of putative -35 region shows an AT rich region. The *flrR-flrA* intergenic region seems to contain conserved sequences element that are likely to be -35 and -10 elements which were investigated further in this study.

.

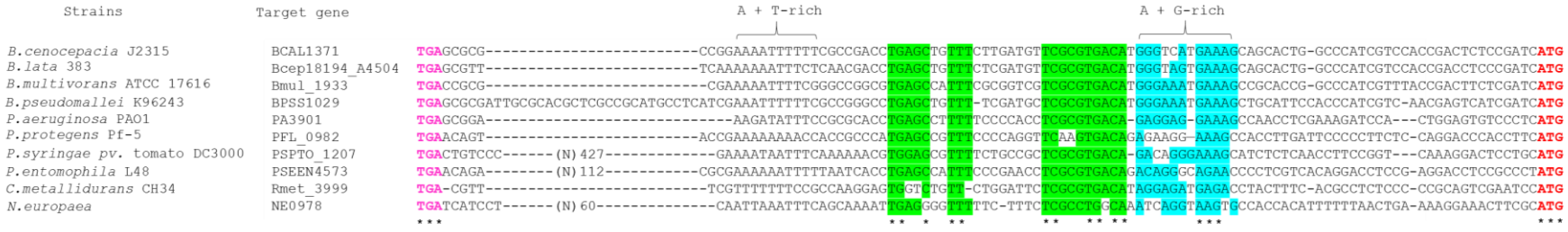

Figure 4-12: Sequence alignment of the *flrR-flrA* intergenic region from *B. cenocepacia* and other bacterial species.

The green highlighted regions show highly conserved sequence motifs that may act as the FlrS-dependent promoter core elements. The blue highlight region indicates an A+G-rich region located downstream from the core elements in these bacterial species. Upstream of the putative promoter core elements there is an A+T-rich region. The *flrR* translation stop codon is shown in magenta and *flrA* or alternative TBDR gene translation start codon is shown in red.

4.7 Determination of a 'minimal' P_{flrA} promoter sequence

To determine the minimum promoter sequence required for recognition by FlrS a series of shorter DNA fragments which contained one or both promoter elements predicted by the bioinformatic analysis (Section 4.6) were fused to *lacZ* in the promoter-probe vector pKAGd4 (Figure 4.13). All plasmid derivatives were transformed into *E. coli* Δ*lacZ* MC1061 competent cells containing pBBR2-$FlrSR_{NTD}$ and transformants were selected on LB agar supplemented with 50 µg/ml kanamycin and 100 µg/ml ampicillin. The activities of all P_{flrA} derivatives were measured by conducting β-galactosidase assays on cells growing in LB medium under iron starvation conditions using 175 µM dipyridyl.

The results showed that the P_{flrA} vvshort and P_{flrA} short DNA fragments had negligible levels of FlrS-dependent promoter activity. These fragments lack part of the predicted -10 region and all of the -35 region, respectively, consistent with the idea that these conserved regions are likely to serve as the putative core elements. P_{flrA} core showed some FlrS-dependent activity but it was only ~15% of the activity of full-length P_{flrA}. P_{flrA} vshort, P_{flrA}ds1, P_{flrA} intermediate and P_{flrA} up, specified progressively higher levels of full-length P_{flrA} β-galactosidase activity, demonstrating that these DNA fragments have the important elements for promoter recognition by σ factor FlrS (Figure 4.14).

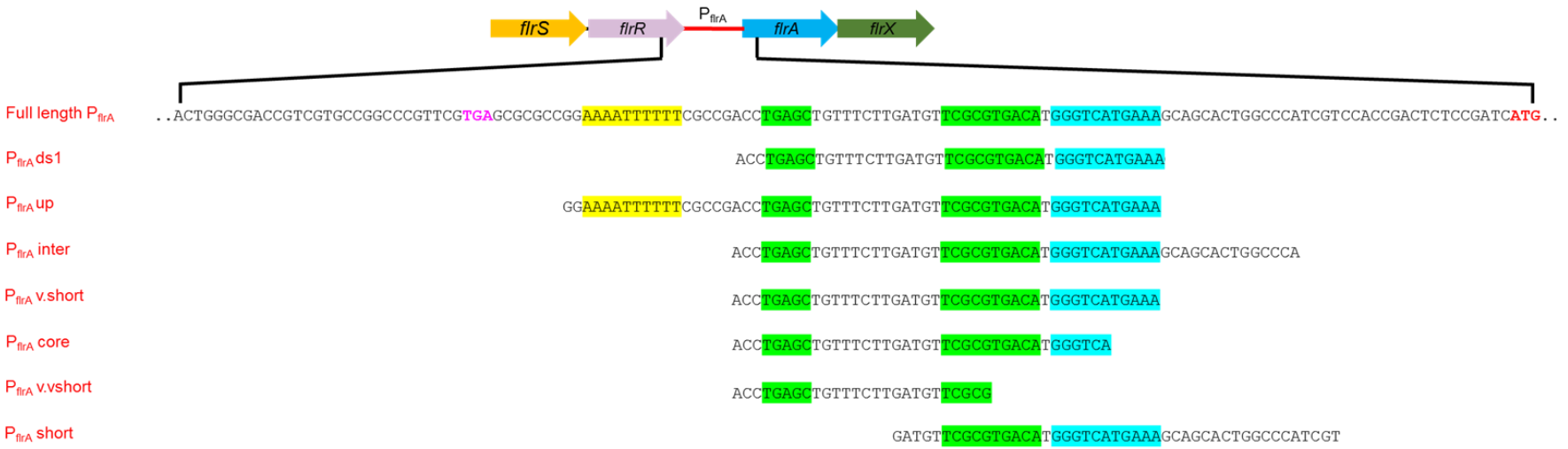

Figure 4-13: Promoter deletion derivatives for determination of a minimal P_{flrA} promoter.

P_{flrA} promoter is contained the full-length P_{flrA} promoter fragment that includes 48 bp of *flrR* coding sequence located upstream of the *flrR* stop codon, the entire *flrR* and *flrA* intergenic region, and 10 bp of *flrA* following the start codon. The green highlighted regions show the location of the putative -35 and -10 elements. Yellow and blue highlighted regions indicated the A-T-rich and A-G-rich regions, respectively.

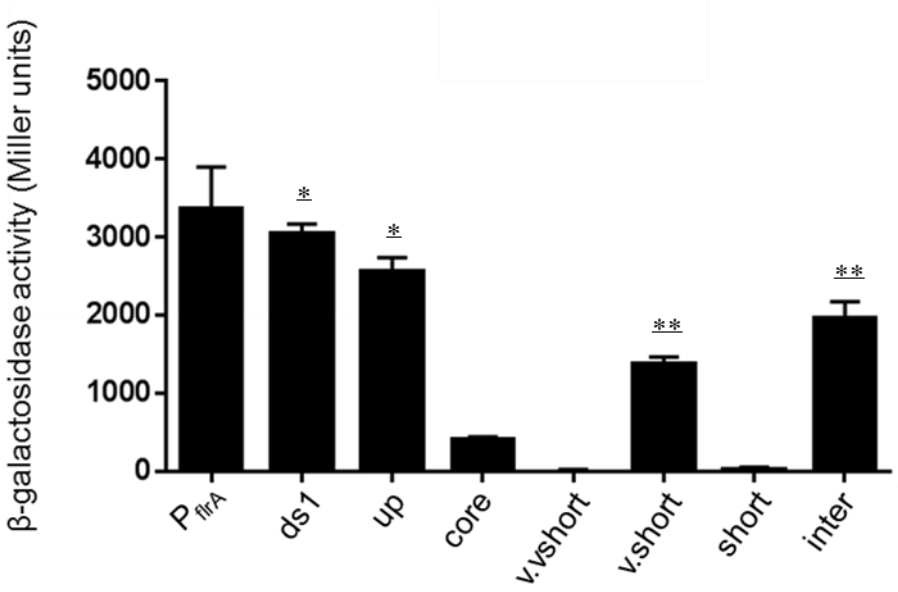

Figure 4-14: Activities of P_{flrA} deletion derivatives in *E. coli*.

P_{flrA} promoter activities were assayed in *E. coli* MC1061 harbouring pBBR2-$FlrSR_{NTD}$ and pKAGd4 containing the indicated P_{flrA} derivatives. P_{flrA} corresponds to the full-length P_{flrA} promoter and includes the entire *flrR-flrA* intergenic region (Figure 4.13). Cells were grown in LB medium supplemented with 50 µg/ml kanamycin, 100 µg/ml ampicillin and 175 µM dipyridyl at 37°C to generate iron-limited conditions. Activities were corrected by subtraction of the background pKAGd4 basal activity. The error bars represent the standard deviation activities of three replicates assayed. The results were analysed using one-way analysis (ANOVA) ** $P < 0.01$, * $P < 0.05$.

4.8 Analysis of DNA sequence requirements for promoter recognition by the FlrS σ factor

The results from the previous section show that the P_{flrA} promoter is localized to a 38 bp DNA fragment known as P_{flrA} core although the activity is not as high as for some longer promoter derivatives. Therefore, it was decided to use P_{flrA}ds1. P_{flrA}ds1 is a 44 bp DNA fragment that includes the A+G rich region and show higher promoter activity compare to the activity observed when using P_{flrA} core.

In order to determine the promoter sequence of P_{flrA} that can be recognized by σ factor FlrS the sequence corresponding to P_{flrA}ds1 and P_{flrA}ds2 to P_{flrA}ds44 were previously fused to *lacZ* in pKAGd4 (Paleja, MSC dissertation, 2009; Yunrui, MSC dissertation, 2010). P_{flrA}ds2 to P_{flrA}ds44 contain a single base substitution at each position of P_{flrA}ds1 where purine is replaced by the non-base pairing pyrimidine and *vice versa* (i.e. A is substituted by C, G by T, C by A and T by G). All P_{flrA}ds derivatives were generated by annealing complementary oligonucleotides designed to generate *Bam*HI and *Hin*dIII compatible ends, which were ligated into the vector pKAGd4 cut with the same enzymes. These plasmids were transformed into *E. coli* MC1061 and HIII-*flrR*::Tp both containing pBBR2-$FlrSR_{NTD}$. All P_{flrA} derivatives were subjected to the β-galactosidase assay in order to establish the effect of each mutation on the activity of the P_{flrA} promoter. The β-galactosidase assay was carried out on cells growing in iron-limiting conditions using 175 µM dipyridyl.

The results of the β-galactosidase activity measurements in *E. coli* harbouring the single substitution mutations indicated that substitution at certain positions significantly affects the activity of P_{flrA} promoter (Figure 4.15). The β-galactosidase activity of P_{flrA} containing substitution at positions 4-8 (predicted -35 element, TGAGC) showed approximately 85-90% decrease in activity compared to the WT ds1. Similarly, substitution mutations at positions 28-31 (within the predicted -10 element, GACA) caused a decline of about 95% of the β-galactosidase activity, which was the most severe at positions 29-31(~95% decrease (Figure 4.15).

The β-galactosidase activity in the *B. cenocepacia flrR* mutant demonstrate a similar overall pattern of results as observed in *E. coli* suggesting that the TGAGC and GACA motifs might be the core elements for recognition of P_{flrA} by σ FlrS (Figure 4.16). It was also observed that P_{flrA}ds1 in the *B. cenocepacia flrR* mutant is significantly more active than the full-length P_{flrA} promoter. In both species, the single substitution at the middle base of the conserved TTT tract (position 13) decreased the β-galactosidase activity by 10 fold relative to the WT promoter activity. The role of this T tract was investigated further in this study (Section 4.9).

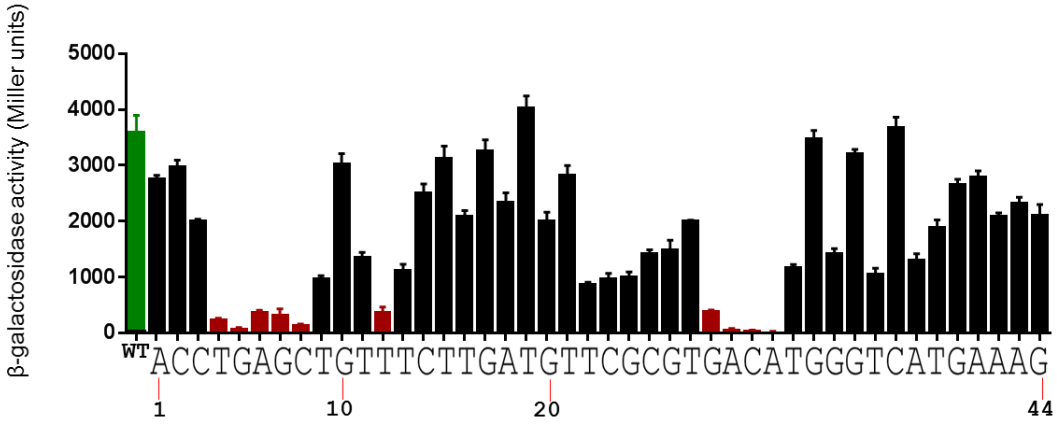

Figure 4-15: Effect of single base pair substitutions on P_{flrA} activity in *E. coli*.

P_{flrA}ds1 derivatives containing a single base substitution at each position of the promoter (P_{flrA}ds2-ds44 (numbers indicate the positions of some P_{flrA}ds1 derivatives)) were cloned into the *lacZ* reporter vector pKAGd4 and introduced into *E. coli* strain MC1061 containing pBBR2-$FlrSR_{NTD}$. The transformants were grown under iron-limited conditions by adding 175 µM 2,2'-dipyridyl to LB medium and promoter activities measured using the β-galactosidase assay. Dark green colour represents WT sequence (ds1), the red colour represents the putative -35 and -10 regions and the T residue positions where the activity of P_{flrA} has decreased by more than 90%. The error bars represent the standard deviation activities of three replicates assayed. Promoters activities at -35, -10 regions and T residue were significantly decresed ****P < 0.0001.

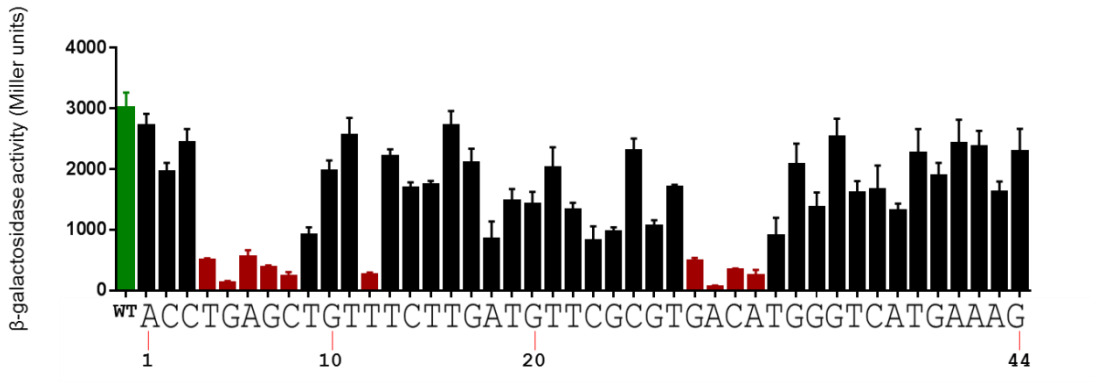

Figure 4-16: Effect of single base pair substitutions on P_{flrA} activity in *B. cenocepacia* HIII-*flrR*::Tp.

P_{flrA}ds1 derivatives containing a single base substitution at each position of the promoter (P_{flrA}ds2-ds44 (numbers indicate the positions of some P_{flrA}ds1 derivatives~)) introduced into *B. cenocepacia* HIII-*flrR*::Tp containing pBBR2-FlrSR$_{NTD}$. The transformants were grown under iron-limited conditions by adding 175 μM 2,2'-dipyridyl to LB medium and promoter activates measured using the β-galactosidase assay. Dark green colour represents WT sequence (ds1), the red colour represents the putative -35 and -10 regions and the T residue positions where the activity of P_{flrA} has decreased by more than 90%. The error bars represent the standard deviation activities of three replicates assayed. Promoters activities at -35, -10 regions and T residue were significantly decresed ****P < 0.0001.

4.9 Investigation the role of the T residue triad in the P_{flrA} spacer region

The T residue at position 13 that is sensitive to substitutions is located in the middle of a T triad that is conserved in the same location relative to the putative -35 element in the sequence located downstream of *flrR* orthologues in other bacterial species. In order to further explore the role of T residue triad in the P_{flrA} spacer region located 2 bp downstream of the -35 element, different P_{flrA}ds1 promoter derivatives were constructed with alteration within and adjacent to the TTT tract. Oligonucleotides were designed to generate dinucleotide and trinucleotide substitutions of all 3 T residues in the triad. In addition, the T triad was extended to a hexa-T tract by substituting the base at position 14 with a T (P_{flrA}triTX). As some putative promoters for FlrR orthologues in other bacteria have a spacer region that is a single bp shorter (Figure 4.12), it was decided to construct a promoter derivative that contains a single bp deletion in the spacer (P_{flrA}dsSP) (Figure 4.17). In some cases, as in *B. pseudomallei*, putative promoters with a shorter spacer have a T tetrad rather than a triad (Figure 4.12). Therefore, another promoter derivative was tested (P_{flrA}triTXSP) which contained a shorter spacer and a longer T tract. All promoter-constructed were ligated and transformed into *E. coli* MC1061 competent cells. The resulting transformants were selected on 100 µg/ml ampicillin LB agar plates. Vector specific primers AP10 and AP11 were used to screen transformant colonies and to identify the presence of pKAGd4 containing the double-stranded oligonucleotide. pKAGd4 gives rise to ~282 bp PCR products with these primers whereas the promoter-containing derivatives will generate an amplicon that is ~20 bp longer (result not shown).

The effect of each mutation in the T tract and the spacer was determined using the β-galactosidase assay to measure the promoter activities in *E. coli* MC1061 cells growing under low iron conditions. The effect of all six different mutations on promoter activity were compared to the activity of the WT ds1 promoter and the promoters containing single point mutations located in the TTT tract (P_{flrA}ds12, P_{flrA}ds13 and P_{flrA}ds14). The data obtained for investigating the TTT tract confirmed that the single point mutation in the middle of the T tract exerts a strong negative effect on the promoter activity (Figure 4.17). Dinucleotide substitutions in the TTT tract

unexpectedly showed an increased in the promoter activity relative to P_{flrA}ds1 and was almost 40 fold higher when compared with the promoter containing the single point mutation at position 12 (numbering according to Figure 4.15). Substitutions of all three T residues in the TTT triad showed a significantly higher β-galactosidase activity compared to the single point mutation.

Deletion of one residue in the spacer region as in the case of P_{flrA}dsSP and P_{flrA}triTXSP did not show a significant different when compare to the WT. In fact, P_{flrA}dsSP was significantly active than the WT promoters. Moreover, extending the T triad to a hexa T tract (P_{flrA}triTX) still gave high level of β-galactosidase activity but it was similar to that of the WT (Figure 4.17).

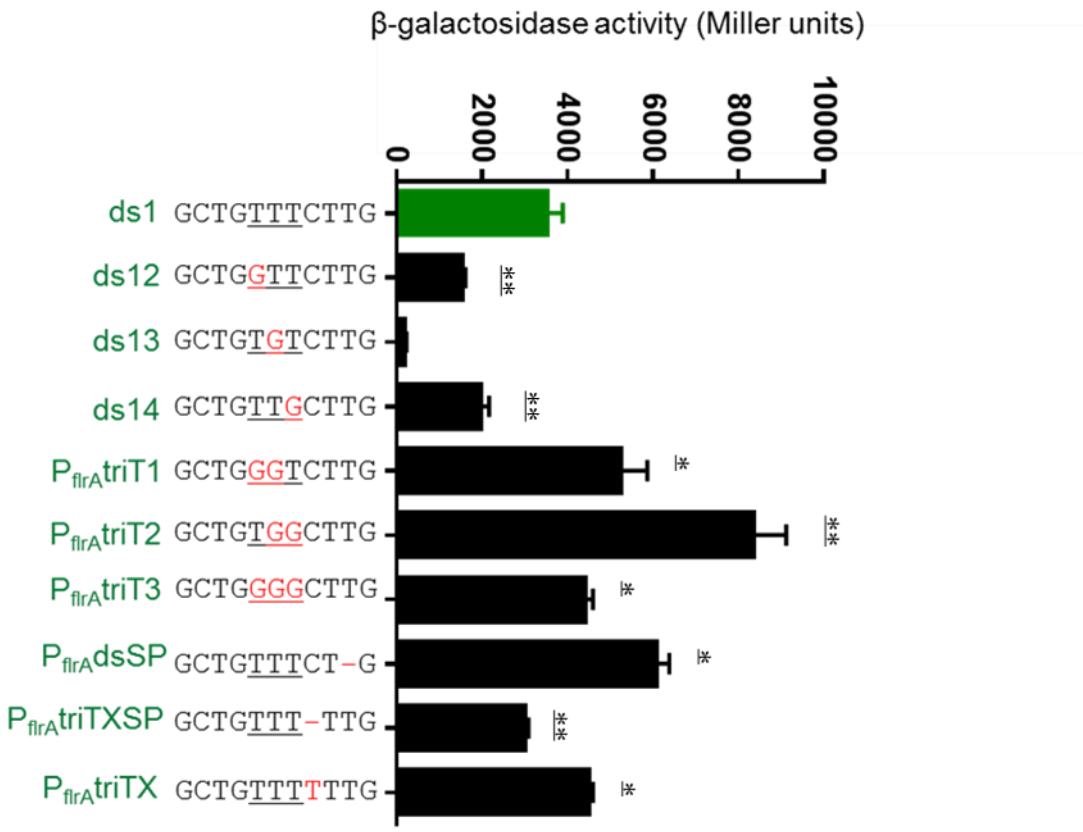

Figure 4-17: Mutations analysis of the T residue triad in the P_{flrA} spacer region.

The sequence at positions 7-17 of P_{flrA}ds1 and a series of derivatives containing base substitutions or deletions in or adjacent to conserved T triad is shown 'below' the x axis. The location of the T triad is underlined. The positions of each mutation are shown in red font. The activity of all promoters containing T residue tract mutations were cloned in pKAGd4 were assayed in *E. coli* MC1061 in the presence of pBBR2-$FlrSR_{NTD}$. The cells were grown in LB supplemented with 100 µg/ml ampicillin, 50 µg/ml kanamycin and 175 µM dipyridyl. The activity of the WT P_{flrA}ds1 is shown in dark green colour. Error bars represent the standard deviation of the activities of the three cultures assayed. The results were analysed using one-way analysis (ANOVA) ** $P < 0.01$, * $P < 0.05$.

4.10 Bioinformatic search for additional FlrS-dependent promoters

In order to identify other potential FlrS-dependent promoters in the Burkholderia genomes a program called FUZZNUC was used. This program can specify a search for an exact sequence and can allow various ambiguities and matches to variable lengths of sequence. Aprosite pattern, TGAGCnnnnnnnnnnnnnnnnnnGACA, was use where the putative -35 and -10 regions of P_{flrA} were spreated by (19 n, the n represents the 19 nucleotides of P_{flrA} spacer region. The FUZZNUC analysis for potential FlrS-dependent promoters was carried out on the *B. cenocepacia* genome was found 12 matching sequences incuding P_{flrA}. However, these scand sequences did not indicate any promsing matching promoter sequences as most of them were located in the middle of the gene.

4.11 RT-PCR analysis of *flr* gene transcripts

In order to determine whether the genes of the *flr* operon are organized as units, two reverse transcriptase PCR (RT-PCR) assay was carried out. Two pairs of primers were designed in order to amplify the DNA spanning each intergenic region. RNA from *B. cenocepacia* HIII was extracted as described in Section 2.6. The bacterial culture was grown under two conditions: iron-limited condition and iron sufficiency, thus allowing us to compare transcription of *flr* operon genes under both conditions. RNA was used to generate cDNA using the reverse primer and RT-PCR was carried out using the pairs of primers as shown in Figure 4.18. The PCR products obtained were analyzed on agarose gel (result not shown). Negative controls were also included where there was no reverse transcriptase added to the reaction.

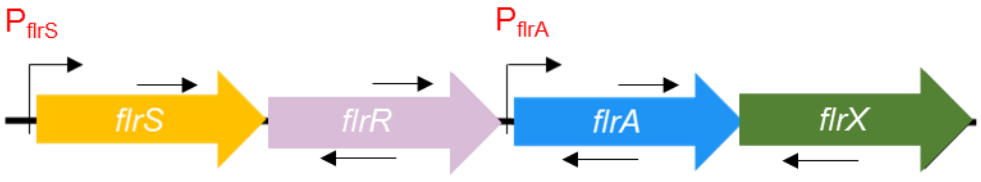

Figure 4-18: Illustration of RT-PCR primers located in the *flr* operon.

4.12 Preparation of purified FlrS

Construction of a plasmid for expression of His_6-FlrS

The reason for purifying FlrS is to confirm that FlrS is a σ factor by carrying out an *in vitro* transcription experiment. To purify FlrS it was decided to overproduce it as an N-terminal His_6-tag protein in *E. coli*. To do this, the *flrS* gene was PCR amplified from pBBR2-FlrSR DNA template using His_6-FlrSfor and His_6-FlrSrev. The amplified PCR product was digested with *Bam*HI and *Pst*I followed by cloning into the first MCS of pACYCDuet-1 which added the His_6-tag at the N-terminus of FlrS (result not shown). The resulting plasmid, pACYCDuet-His_6-FlrS was transformed into *E. coli* BL21(λDE3).

To induce His_6-FlrS expression IPTG was added to a final concentration of 0.1 mM to a log phase culture (OD_{600} ~0.5-0.7) and the cells were cultured for further 3 hours at 37°C. To test the solubility of His_6-FlrS, the cells were harvested by centrifugation and sonicated as described in Section 2.14.1. Lysis of the cells taken before and after inductions of His_6.FlrS as well as samples of the soluble and insoluble fractions were resolved in a 15% SDS polyacrylamide gel and stained with coomassie blue (Figure 4.19A). The results show that His_6-FlrS was overproduced based on the presence of a protein of ~22 kDa in cells that were induced with IPTG. However, most of overproduced His_6-FlrS was insoluble. In an attempt to increase the solubility of overproduced His_6-FlrS, the induction was performed in the cells growing at 22°C and 30°C using a lower concentration of IPTG (0.5 mM). However, the attempt to overproduce His_6-FlrS at the lower temperatures was unsuccessful (Figure 4.19B and C). Thus the purification of His_6-FlrS was carried out by using the insoluble protein produced at 37°C (Figure 4.20).

Purifcation of His_6-FlrS

Insoluble His_6-FlrS from a 200 ml induced culture was resuspended in TGED buffer (50 mM Tris-HCl, 5% glycerol, 0.1 mM EDTA, 0.1 mM DTT (pH 7.9) and 50 mM NaCl) containing 0.25% N-lauroylsarcosine and incubated at 4°C overnight. The supernatant fraction obtained following centrifugation was used for the purification using nickel affinity chromatography as described in Section 2.14.3. The first attempt at purifying His_6-FlrS was unsuccessful as most of the FlrS protein bound to the column and could not be eluted (Figure 4.20).

In the second purification attempt following a fresh induction at 37°C and solubility test (Figure 4.21A). The IMAC protocol was modified by increasing the incubation time with the resin and fresh DTT was added to all buffers used for purification. The insoluble His_6-FlrS was attempted to solublise by resuspending the pellet in 0.25% N-lauroylsarcosine before applied to nickel-column (1 ml, GE Healthcare). Binding buffer with fresh DTT was used to wash the nickel-column with 20 volumes which allows the removel of non-specifically bound proteins. The protein was eluted with 500 mM imidazole. A 1 ml fraction size was collected in order to be analysed by SDS-PAGE gel (Figure 4.21B). The result showed the successful purification of His_6-FlrS where a small amount of purify protein was visible on a coomassie blue-stained SDS-PAGE gel. The overproduced His_6-FlrS protein was confirmed by Western blotting using anti-His_6 antibody (Figure 4.22).

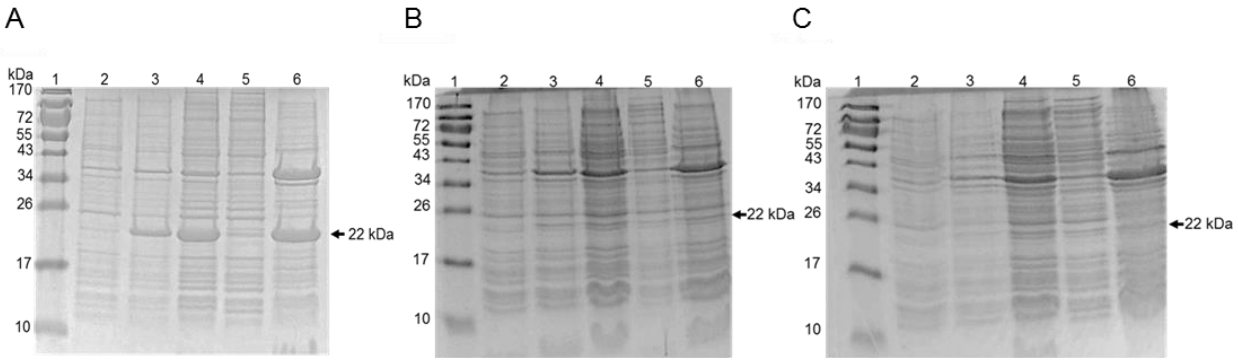

Figure 4-19: Analysis of His_6-FlrS expression and solubility test.

A. His_6-FlrS was overproduced in *E. coli* BL21(λDE3) 37°C.

B. His_6-FlrS was overproduced in *E. coli* BL21(λDE3) 22°C.

C. His_6-FlrS was overproduced in *E. coli* BL21(λDE3) 30°C.

The induction was carried out by adding IPTG to final concentration of 0.1 mM. The cells were collected by centrifugation, and the solubility of His_6-FlrS following inductions were determined by sonication. A, B and C. Lane 1, EZ-Run Rec unstained protein ladder; lane 2, sample of uninduced cells; lane 3, sample of induced cells; lane 4, whole cell extracts, total; lane 5, soluble fraction; lane 6, insoluble fraction. The black arrow indicates the expected size of His_6-FlrS.

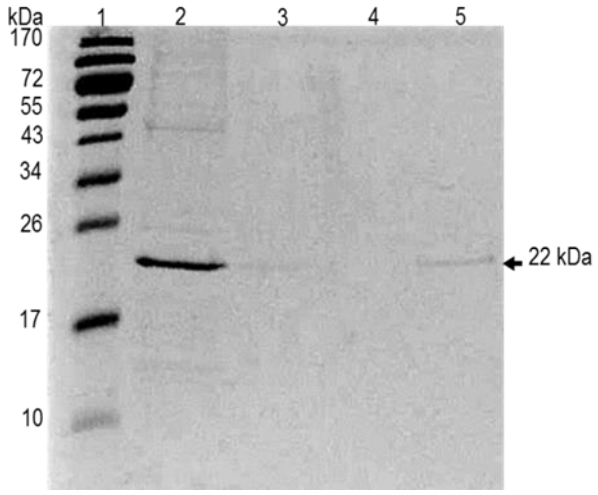

Figure 4-20: Purification of insoluble His_6-FlrS using nickel affinity chromatography.

Coomassie blue-stained 15% SDS-PA gel showing the purification of His_6-FlrS. Lane 1, EZ-Run Rec unstained protein ladder; lane 2, flow-through of the cell extract; lane 3, first wash; lane 4, second wash; lane 5, eluate following elution with 500 mM imidazole. The black arrow indicates the expected size of His_6-FlrS.

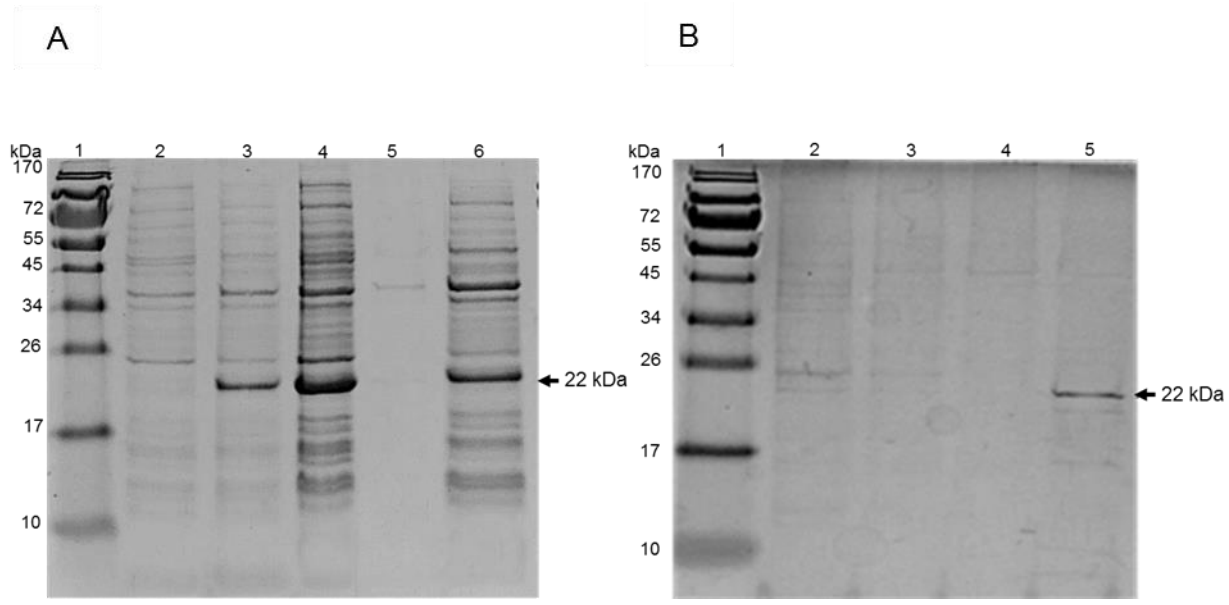

Figure 4-21: Solubility and purification of insoluble His_6-FlrS using nickel affinity chromatography.

A. His_6-FlrS was overproduced in *E. coli* BL21(λDE3) containing pACYCDuet-His_6-FlrS at 37°C. The induction was carried out by adding IPTG to final concentration of 0.1 mM. The cells were collected by centrifugation, and the solubility of His_6-FlrS following inductions was determined by sonication. Lane 1, EZ-Run Rec unstained protein ladder; lane 2, sample of uninduced cells; lane 3, sample of induced cells; lane 4, whole cell extracts, total; lane 5, soluble fraction; lane 6, insoluble fraction.

B. His_6-FlrS was purified by adding fresh DTT in all buffers used for purification process. Lane 1, EZ-Run Rec unstained protein ladder; lane 2, flow-through of the cell extract; lane 3, first wash; lane 4, second wash; lane 5, eluate following elution with 500 mM imidazole. The black arrow indicates the expected size of His_6-FlrS.

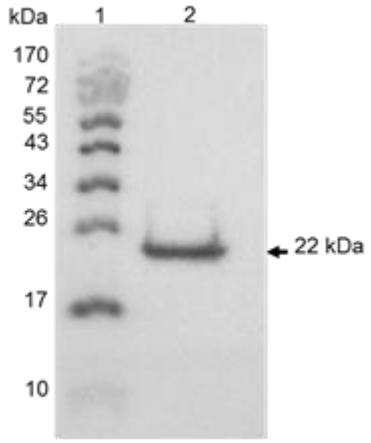

Figure 4-22: Western blot detection of His_6-FlrS produced in *E. coli* BL21(λDE3).

Insoluble fraction containing His_6-FlrS was resolved by SDS-PAGE and transferred onto PVDF membrane. Purified protein was detected with anti-His_6 antibody. Lane 1, EZ-Run Rec unstained protein ladder; lane 2, insoluble fraction containing His_6-FlrS. The black arrow indicates the expected size of His_6-FlrS.

Cloning the P_{flrA} promoter region into pRLG770

To carry out an *in vitro* transcription reaction, a template containing the promoter of interest (P_{flrA}) needs to be designed. One way of doing this, is using a linear DNA fragment, which is called 'run-off' transcription. In this method, RNAP initiates transcription from the promoter and progressed to the end of the DNA fragment where it 'falls off'. However, the method used in this study involves the use of supercoiled plasmid DNA. In this method a transcription terminator is located downstream of the promoter cloning site in the *in vitro* transcription assay plasmid. The presence of a strong transcription terminator ensures that all transcripts are short and are the same size (resolvable and measurable in gels). Therefore, it was decided to clone the putative P_{flrA} promoter region into plasmid pRLG770 (Figure 4.23). This plasmid uses the pair of strong Rho-independent transcription terminators that are located downstream of the *E. coli* 5S rRNA gene. As the location of the P_{flrA} promoter is known, complementary oligonucleotide nucleotides corresponding to the P_{flrA} promoter region were designed and annealed as described in Section 2.5.9. The resulting double-stranded oligonucleotide is 50 bp in length. pRLG770 was digested with *Eco*RI and *Hin*dIII. The P_{flrA} oligonucleotide and pRLG770 were ligated and transformed into *E. coli* MC1061. The correct clone was confirmed by sequencing using primers ApRG7702_1204 and ApRG7702_1204. Using this construct, transcripts of ~160 nts nucleotides would be generated, the vector itself will provide about 150 nts from the *Hin*dIII site to the transcription terminator as a promoter fragment has a downstream endpoint of +10 with respect to the transcription start site (+1).

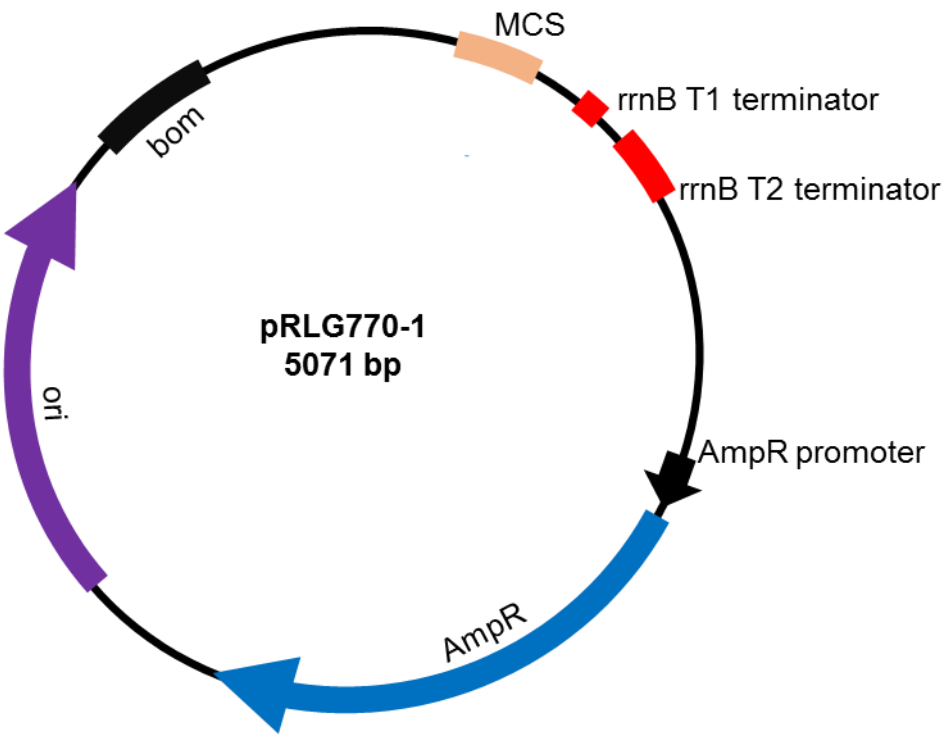

Figure 4-23: Diagrammatic illustration of pRLG770 *E. coli* vector.

rrnB T1 and rrnB T2 terminator are shown in red colour.

Construction of a plasmid expressing $FlrR_{NTD}$-His_6

The reason to construct and purifiy $FlrR_{NTD}$-His_6 is to determine whether $FlrR_{NTD}$ activates FlrS *in vitro*. A DNA fragment encoding the N-terminal domain of FlrR was amplified form pBBR2-FlrSR template. The pair of primers used for amplification were FlrRNTDHis-for and FlrRNTDHis-rev. The FlrRNTDHis-rev contains a hexa-histidine coding sequence followed by a stop codon which result in addition of a His-tag to the C-terminus of $FlrR_{NTD}$. Amplified PCR product was ligated into the first MCS of pETDuet-1 between *Nco*I and *Bam*HI (Figure 4.24). PCR products and pETDuet-1 were digested with *Nco*I and *Bam*HI restriction site. The products were ligated and transformed into *E. coli* MC1061. The resulting plasmid construct pETDuet-$FlrR_{NTD}$-His_6 was introduced into *E. coli* BL21(λDE3) and a transformant was grown in LB medium containing 100 µg/ml ampicillin at 37°C. When the culture reached OD_{600}~ 0.5–0.7, 0.1 mM of IPTG was added to induce protein expression. After 3 hours of induction the cells were harvested by centrifugation. The protein expression was analyzed by electrophoresis in 15% polyacrylamide gel (Figure 4.25A). However, $FlrR_{NTD}$-His_6 did not appear to be expressed. The same issue was observed when attempted to overproduced $FlrR_{NTD}$-VSVg into pACYCDuet-1 (Section 3.4).

Another way to overexpress $FlrR_{NTD}$-His_6 is a MBP fusion protein by cloning it into pMAL-c5X. To do this, pETDuet-$FlrR_{NTD}$-His_6 and pMAL-c5X were cut with *Nde*I and *Bam*HI. The products of the digestions were then ligated and transformed into *E. coli* MC1061. pMAL-c5X-$FlrR_{NTD}$-His_6 was transferred to *E. coli* BL21(λDE3) to test protein expression and solubility. After 3 hours of IPTG induction of the *lac* promoters at 37°C SDS-PAGE analysis showed that both pMAL-c5X and pMAL-c5X-$FlrR_{NTD}$-His_6 were overproduced (the expected molecular weight of MBP-$FlrR_{NTD}$-His_6 is 58 kDa). The sonicated protein samples showed that most of the expressed MBP-$FlrR_{NTD}$-His_6 was present in the insoluble and the soluble fraction (Figure 4.25B). MBP-$FlrR_{NTD}$-His_6 was purified from cleared cell lysate using amylose affinity chromatography as described in Section 2.14.4. SDS-PAGE analysis showed that most of MBP-$FlrR_{NTD}$-His_6 bound to the amylose column and it was detectable in the maltose elution fraction by anti-MBP antibody (Figure 4.26).

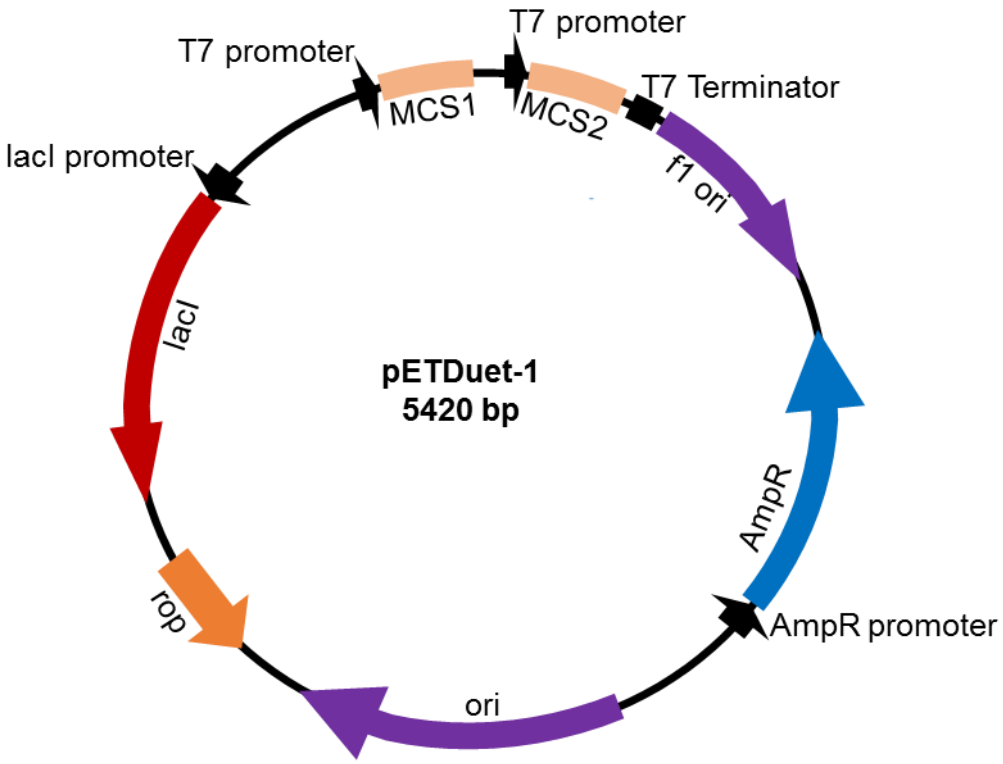

Figure 4-24: Diagrammatic illustration of T7 expression vector pETDuet-1.

The purple colour represents the origin of replication of plasmid ColE1. The two multiple cloning sites (MCS) sites of this overexpression vector are shown in nude colour. The *lacI* gene shown in red encodes Lac repressor.

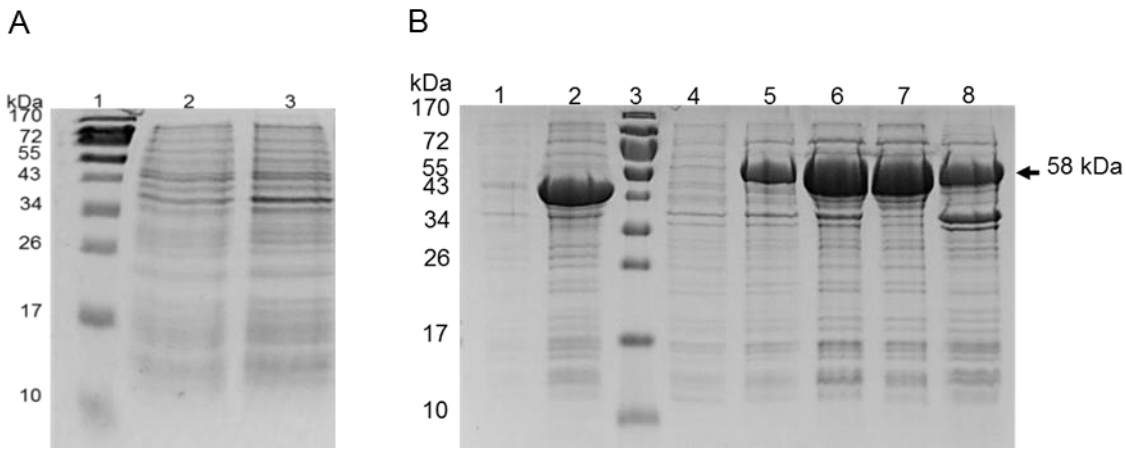

Figure 4-25: Analysis of His_6-$FlrR_{NTD}$ expression and solubility test in *E. coli* BL21(λDE3) strain.

A. pETDuet-$FlrR_{NTD}$-His_6 was expressed in *E. coli* BL21(λDE3).

B. pMAL-c5X empty vector and pMAL-c5X-$FlrR_{NTD}$-His_6 was expressed in *E. coli* BL21(λDE3).

In A and B the cells were grown at 37°C in LB medium supplemented with 100 µg/ml ampicillin until they reached an OD_{600} 0.5. Protein synthesis was induced by adding IPTG to final concentration of 0.1 mM. The pre-induction and induced samples were electrophoresed in a 15% SDS-PAGE. A. Lane 1, EZ-Run Rec unstained protein ladder; lane 2, uninduced pETDuet-$FlrR_{NTD}$-His_6; lane 3, induced pETDuet-$FlrR_{NTD}$-His_6. B. Lane 1, uninduced pMAL-c5X; lane 2, induced pMAL-c5X; lane 3, EZ-Run Rec unstained protein ladder; lane 4, uninduced MBP-$FlrR_{NTD}$-His_6; lane 5, induced MBP-$FlrR_{NTD}$-His_6; lane 6, whole cell extracts, total containing MBP-$FlrR_{NTD}$-His_6; lane 7, insoluble fraction containing MBP-$FlrR_{NTD}$-His_6; lane 8, soluble fraction containing MBP-$FlrR_{NTD}$-His_6. The black arrow indicates the expected size of MBP-$FlrR_{NTD}$-His_6.

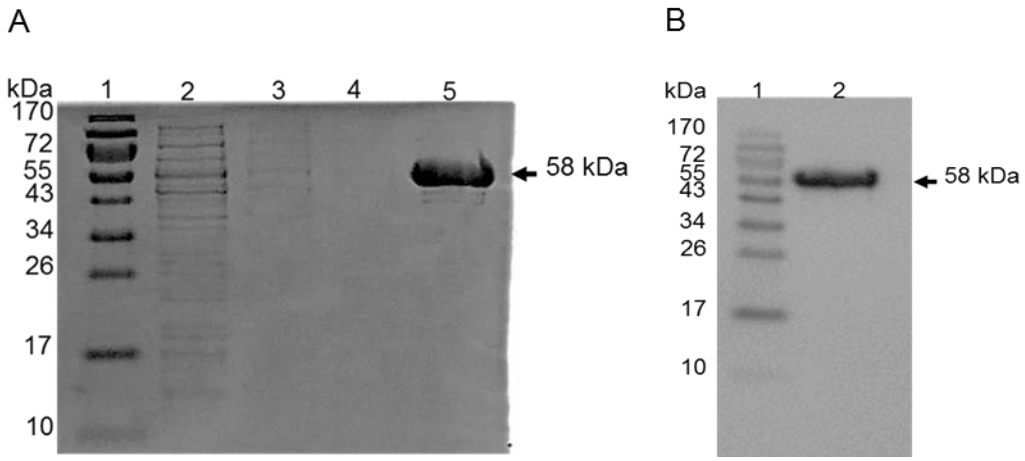

Figure 4-26: Purification of MBP-FlrR$_{NTD}$-His$_6$ by amylase affinity chromatography.

A. SDS-PAGE analysis of purification of MBP-FlrR$_{NTD}$-His$_6$ by amylase chromatography. Lane 1, EZ-Run Rec unstained protein ladder; lane 2, flow-through of the cell extract; lane 3, first wash; lane 4, second wash; lane 5, soluble fraction of MBP-FlrR$_{NTD}$-His$_6$ eluted by 10 mM maltose. The black arrow indicates the expected size of MBP-FlrR$_{NTD}$-His$_6$.

B. Western blot detection of MBP-FlrR$_{NTD}$-His$_6$ by anti-MBP anitbody. Lane 1, EZ-Run Rec unstained protein ladder; lane 2, fraction of MBP-FlrR$_{NTD}$-His$_6$. The black arrow indicates the expected size of MBP-FlrR$_{NTD}$-His$_6$.

4.13 Investigation of the utilisation of *B. cenocepacia* P_{flrA} by FlrS-like *Pseudomonas* ECF σ factors and the utilization of *Pseudomonas* P_{flrA}-like sequence by FlrS

Genes that are highly similar to *flrS, flrR* and *flrA* are present in other *Burkholderia* species and several species of Gram-negative bacteria that are closely related to *Burkholderia* such as *Cupriavidus* and *Delftia* as well as in some *Pseudomonas* species, which are not members of the β-proteobacteria. However, in the pseudomonads, the *flrA* homologue (i.e *PA0151* in *P. aeruginosa* strain PAO1) is not located adjacent to the *flrS-flrR* homologues (*PA3899-PA3900 P. aeruginosa* PAO1 and *PSPTO1209-PSPTO1208* of *P. syringae* DC3000 but rather it is adjacent to a different ECF σ factor: anti-σ factor gene pair (*PA0149-PA0150*) or not there at all (as in the case with *P. syringae*) (Figure 4.27). Accordingly, there is not a sequence that matches the *Burkholderia* P_{flrA} sequence promoters located upstream of the *P. aeruginosa flrA* gene (*PA0151*), but there is one located upstream of the *PA3901* TBDT gene and *PSPTO1207* (Figure 4.28). Thus, it would appear that *flrA* is regulated by a different σ factor: anti-σ factor pair in *P. aeruginosa* and FlrS-FlrR regulates a different TBDT gene in several species of *Pseudomonas*. The *PA3901* TBDT gene that is presumed to be regulated by the FlrS-FlrR orthologous in *P. aeruginosa* PAO1 is annotated as *fecA,* and the PA3899-PA3901 system has been proposed to be involved in ferric dicitrate uptake in the *pseudomonads* (Banin *et al*., 2005).

To determine whether FlrS could recognise the P_{flrA}-like sequences located upstream of *PA3901* and *PSPTO1209,* they were first analysed by amino acid alignment to find the identical conserved regions within their amino acid sequence as well as the amino acid sequence of PA0149 (Figure 4.29). To determine whether PA3899 and PSPTO1209 are FlrS orthologues it was decided to clone their coding sequences into pBBR1MCS-2 and measure the effect of their expression on P_{flrA} activity. It was also decided to include the PA0149 σ factor located upstream of the *P. aeruginosa flrA* homologue in this analysis.

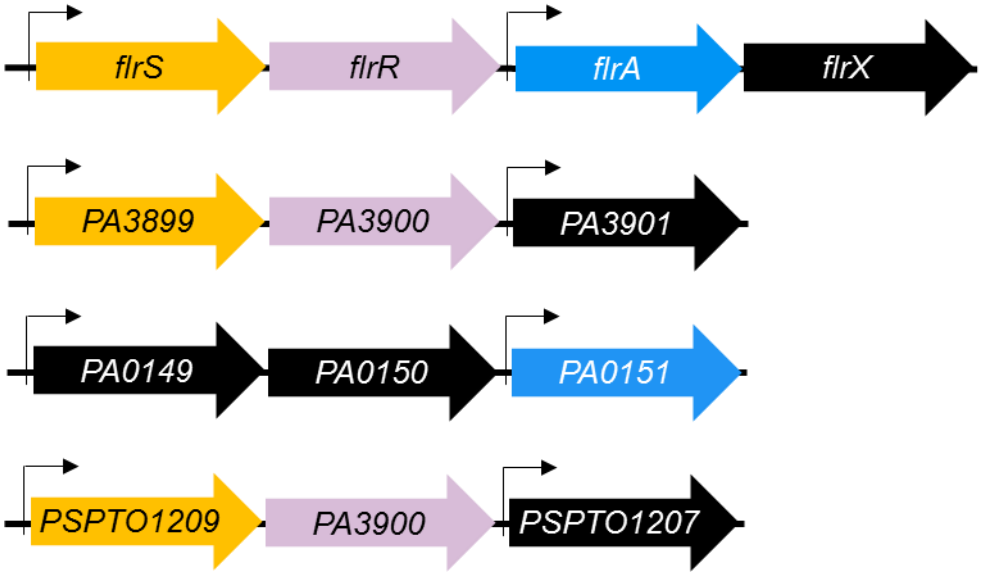

Figure 4-27: *flrS-flrR-flrA* operons in *B. cenocepacia* and *P. aeruginosa* and *P. syringae*.

Homologous gene *flrS*, *flrR* and *flrA* of *B. cenocepacia*, *P. aeruginosa* and *P. syringae* are shown in yellow, light pruple and blue colour, respectively. Black colour indicates non-homologous genes in these species.

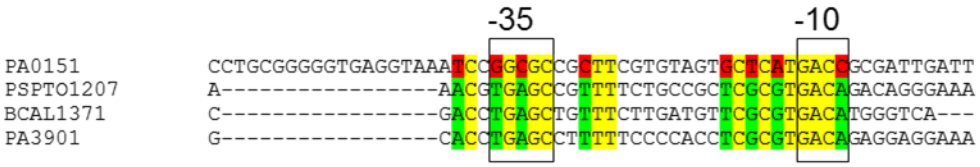

Figure 4-28: Alignment of *B. cenocepacia* P_{flrA} with predicted FlrS-dependent promoters from *P. aeruginosa* and *P. syringae*.

Sequences located downstream of *B. cenocepacia flrR*, *flrR* homologues of *P. aeruginosa* PAO1 (PA3900) and *P. syringae* DC3000 (PSPTO1208) that contains P_{flrA} and P_{flrA}-like sequences are shown. Identical bases within the FlrS-dependent promoter (P_{flrA}), PSPTO1207 and PA3901 promoter sequences are highlighted in green. The yellow colour indicates the conserved region in all four promoter sequences. The red colour indicates bases different within the PA0151. The -10 and -35 regions of all promoters have been boxed.

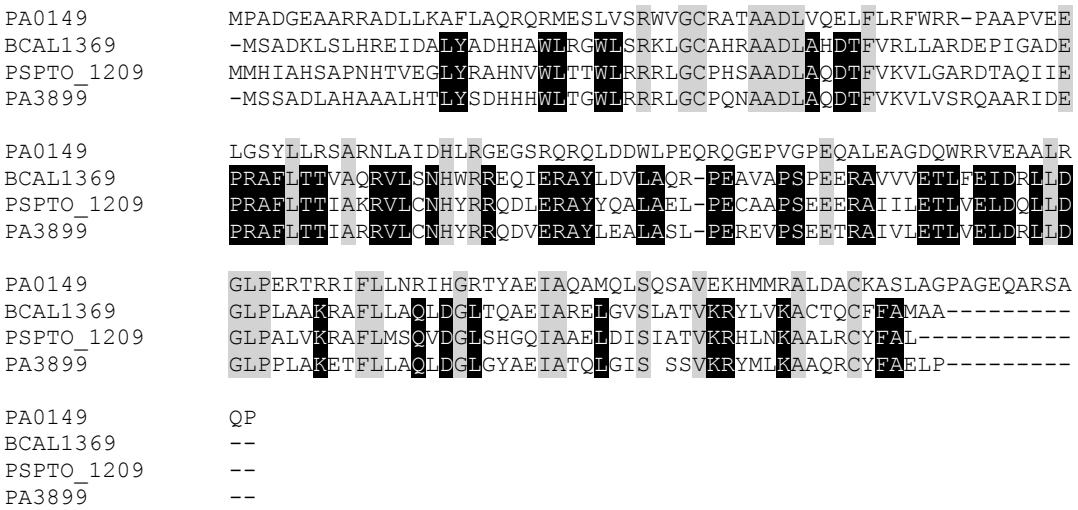

Figure 4-29: Amino acid sequence alignment of *B. cenocepacia*; BCAL1369 (FlrS) with other iron starvation σ factors (*P. aeruginosa*; PA0149, *P. syringae*; PSPTO1209 and *P. aeruginosa*; PA3899).

Amino acid shown in black font with grey shading are conserved in all four-iron starvation σ factors. Those in white font with black highlight are conserved within BCAL1369, PSPTO1209 and PA3899, and are predicted to be FlrS orthologous.

Construction of plasmids for expressing ECF σ factors PA0149 and PSPTO1209

In order to study the effect of other σ factors on P_{flrA} it was important to clone σ factors PA0149 from *P. aeruginosa* and PSPTO1209 from *P. syringae* into pBBR1MCS-2 (*PA3899* was already cloned in this plasmid (Yunrui, MSC dissertation, 2010)). The cloning process started by preparing genomic DNA from *P. aeruginosa* strain PAO1 and from *P. syringae* pv. tomato str. DC3000 in the form of a boiled lysate. Cloning *PA0149* and *PSPTO1209* into pBBR1MCS-2 was carried out as described in Section 4.4.1 (result not shown).

Construction of a reporter plasmid containing the $P_{PSPTO1207}$ promoter

The gene encoding promoter sequence of *P. syringae PSPTO1207* was cloned into pKAGd4 (P_{PA3901} and P_{PA0151} were already cloned in this plasmid (Yunrui, MSC dissertation, 2010)). The P_{flrA}-like promoter sequence located upstream of *P. syringae PSPTO1207* was created by annealing of the oligonucleotides known as pPSPTO1207dsfor and pPSPTO1207dsRev. These two oligonucleotides generate a 50 bp double stranded DNA fragment with *Bam*HI and *Hin*dIII compatible sticky ends. The resulting product was subjected for ligation into pKAGd4 which was also cut with *Bam*HI and *Hin*dIII. The ligation products were transformed into *E. coli* JM83 competent cells. PCR was used to screen for positive clones. As the size of inserted DNA fragment was very small the positive clones were confirmed by DNA sequencing.

By constructing these three plasmids, pBBR2-PA3899, pKAGd4-P_{PA3901} and pKAGd4-P_{PA0151}, all σ factors and promoters were transformed into *E. coli* MC1061 competent cells in order to assay them. The whole set of σ factors and promoters were subjected to determine promoter activities by performing β-galactosidase assay. The promoter activities of P_{flrA}, P_{PA3901}, $P_{PSPTO1207}$ and P_{PA0151} in *E. coli* MC1061 growing under iron starvation conditions were investigated and compared with each other. All four promoters were assay in presence of these σ factors; FlrS, PSPTO1209, PA3899 and PA0149.

The activity of P_{flrA} assay in the presence of its own σ factor show an increase in its activities. P_{flrA} activity in response to the two FlrS orthologous, PSPTO120 and

PA3899 compared to FlrS and PSPTO1209 showed a decrease in P_{flrA} activity that was almost 5 fold less than the activity of P_{flrA} in the presence of FlrS. This indicates that both σ factors can utilise P_{flrA}, although less efficiently than FlrS, and that PA3899 utilised P_{flrA} more efficiently than PSPTO1209. P_{flrA} activity was extremely low when assayed in the presence of PA0149 (Figure 4.30A).

PA3899 efficiently utilised its own promoter P_{PA3901} as shown by the high level of β-galactosidase activity. FlrS and PSPTO1209 could also utilize P_{PA3901} efficiently. The activity of P_{PA3901} in the presence of PA0149 was as low as the activity of background control (Figure 4.30B).

P. syringae $P_{PSPTO1207}$ promoter activity in the presence of its own σ factor PSPTO1209 showed high response. Assaying the activity of $P_{PSPTO1207}$ in the presence of FlrS also give a high response of β-galactosidase activity. The ability of PA3899 in regulating the activity of $P_{PSPTO1207}$ was investigated and the result showed that its activity repressed by 2 fold in comparable to its own σ factor and with FlrS (Figure 4.30C). PA0149 σ factor showed no response on the activity of $P_{PSPTO1207}$ and indicate extreme low activity comparable to control experiment.

PA0149 σ factor is only efficient in utilising its own promoter, P_{PA0151}. This assay showed that P_{PA0151} give the highest activity among all promoter's assay in the presence of their own σ factors (Figure 4.30D). To confirm that these promoter's activity is due to σ factor utalisation the activity of all σ factors were assayed in the presence of pBBR1MC-2 empty vector as a control. The activities obtained in the presence of these σ factors showed low level of β-galactosidase activity that comparable to the background activity (result not shown). The results of these experiments indicate that these σ factor FlrS, PA3899 and PSPTO1209 are able to recognize these promoters P_{flrA}, $P_{PSPTO1207}$, P_{PA3901}. However, PA0149 was unsuccessful in utilising any of these promoters.

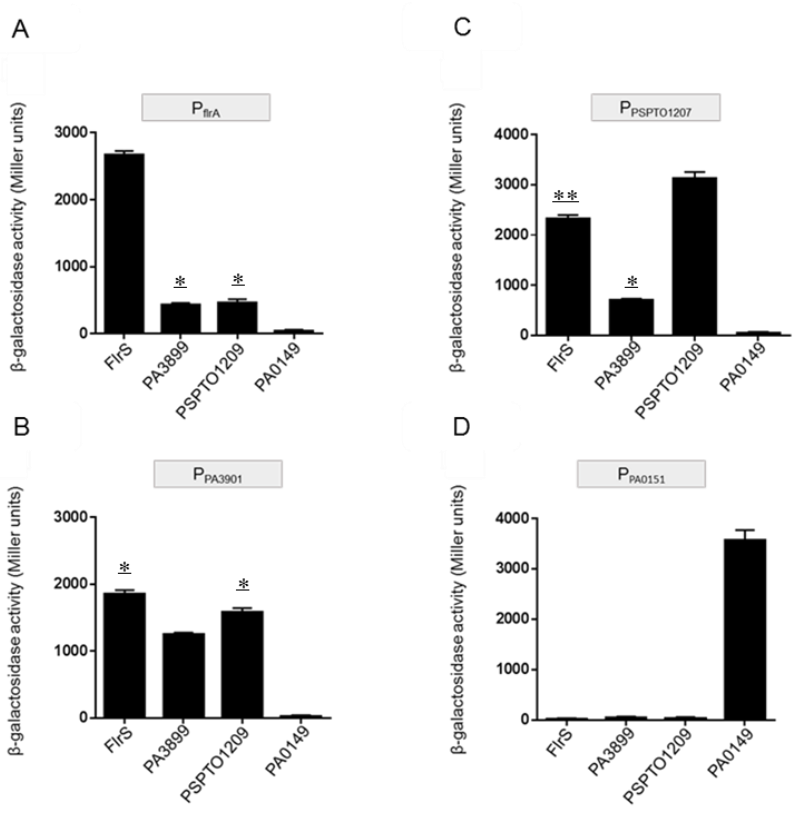

Figure 4-30: Promoters activity in response to FlrS, PA3899, PSPTO1209 and PA0149 σ factors.

Effect of *flrS*, *PA3899*, *PSPTO1209* and *PA0149* on the activity of $P_{flrA,}$ P_{PA3901}, $P_{PSPTO1207}$ and P_{PA0151}, respectively. These putative promoters were cloned into pKAGd4 for *lacZ*-fusion analysis.

A. FlrS dependent activity on $P_{flrA,}$ P_{PA3901}, $P_{PSPTO1207}$ and P_{PA0151}.

B. PA3899 dependent activity on P_{flrA}, P_{PA3901}, $P_{PSPTO1207}$ and P_{PA0151}.

C. PSPTO1209 dependent activity on P_{flrA}, P_{PA3901}, $P_{PSPTO1207}$ and P_{PA0151}.

D. PA0149 dependent activity on P_{flrA}, P_{PA3901}, $P_{PSPTO1207}$ and P_{PA0151}.

The activities of these promoters were analysed in *E. coli* MC1061 competent cells grown under iron-limited conditions and were carried out in LB broth supplemented with 50 µg/ml kanamycin, 50 µg/ml chloramphenicol and 175 µM 2'2-dipyridyl. The assays were carried out in triplicate. The result shown after subtracting of pKAGd4 background activity. The mean values are shown and the standard deviation of the three culture activities are represented by the error bars. The results were analysed using one-way analysis (ANOVA) ** P value <0.01 and ***** P value <0.1.

4.14 Discussion

It is very well known that the σ factor subunits are the main primarily contact with the specific sequence of promoter DNA. Previous studies on *E. coli* showed that there is specific amino acid at regions 2.4 and 4.2 of σ factors are responsible for the direct contact with the -10 and -35, respectively (Barne *et al*., 1997). In this study we have investigated the role of putative ECF σ factor FlrS and its association with putative anti-σ factor FlrR and with the P_{flrA} promoter region located between the anti-σ factor gene, *flrR* and *flrA*.

It has been demonstrated that the activity of ECF σ factors is controlled by anti-σ factors (Hughes and Mathee, 1998**;** Helmann, 1999). External signal is able to activate and inactive σ factors, which in many cases may occur because of dissociation of the anti-σ factors from the σ factors. The ECF σ factors can than initiate transcription in the absence of anti-σ factor and in the absence of extracytoplasmic signals (Mahren *et al*., 2002)

We hypothesised that FlrR is the anti-σ factor for FlrS. Under non-inducing conditions, the σ factor remain bound to their anti-σ factor and because of this binding the σ factor will not be activated. In this study, the role of FlrR on the FlrS activity was monitored through measuring the activity of the FlrS-dependent promoter P_{flrA}. The role of FlrR on FlrS activity has been investigated by using *E. coli* and *B. cenocepacia* as host systems. The β-galactosidase results obtained using *E. coli* as a host system indicates that there is no P_{flrA} promoter activity when there was no FlrS present. When the full-length FlrR was present there was detectable change in P_{flrA} activity. If FlrR is the anti-σ factor for FlrS then it would be expected that FlrR acts as an inhibitor of FlrS activity in the absence of the inducing signal (ferric-siderophore complex), and it is expected to cause some decrease in P_{flrA} activity because there is no signal, but it did not. In fact, there was a small increased in promoter activity. Therefore, FlrR does not behave as a classical anti-σ factor. This suggests the role of FlrR might be to activate FlrS in the presence of signal. Moreover, it has been found that the anti-σ factor is responsible for controlling the activity of iron starvation σ factors post-translationally in order to inhibit its interaction with core RNA polymerase (Osterberg *et al.*, 2011; Tabib-Salazar., 2013). Accordantly, P_{flrA} promoter

activity increased significantly in the presence of $FlrR_{NTD}$ and $FlrSR_{NTD}$ compared to the activity observed when FlrR was present. Suggest the the N-terminal domain has an important role in actviting σ FlrS. Similar to FecR, the higher promoter activity cuased by the N-terminal domain of FlrR induce the transcrption of *flr* genes in the absence of ferric siderophore thus its should be located in the cytopiasm (Ochs *et al*., 1995). This suggests that FlrR is stimulatory in the presence of signal and without it FlrS is not active. Overall, the activity of FlrS is regulated by the anti-σ factor FlrR via its cytoplasmic domain.

The β-galactosidase results from *B. cenocepacia* strain HIII indicates slight increase in P_{flrA} activity when FlrS was introduced. This result might be due to the inhibition of FlrS by FlrR and adding more copies of FlrS might increase the level of P_{flrA} activity. Also, the activity of pKAGd4-P_{flrA} and pBBR2-FlrS were assayed in the HIII-*flrR*::Tp indcating a small increase in P_{flrA} activity. In addition, the activity of P_{flrA} was assayed in HIII and in HIII-*flrR*::Tp in the presence of a plasmid expressing $FlrR_{NTD}$, FlrR and FlrS. When both proteins were provided there was an increase in P_{flrA} activity compared to the $FlrR_{NTD}$ alone. To conclude, adding more copies of *flrS* cause increased in P_{flrA} activity but the activities were still not particularly high.

The effect of iron concentration on P_{flrA} activity in *B. cenocepacia flrR*::Tp mutant expressing $FlrSR_{NTD}$ was investigated in this study. The use of low iron concentration led to an increased in P_{flrA} promoter activity while a high concentration gave rise to a low level of promoter activity. This is likely due to the binding of the Fur repressor to the P_{flrS} promoter which result in decreased level of FlrS (Chapter 5).

CSS in bacteria has been described into two different classes. The first one consists of proteins that function solely as anti-σ factors such as FpvR of *P. aeruginosa* (Mettrick and Lamont, 2009). The second class contains proteins that not only inhibit the activity of σ factors but also activates them in response to the signal (FecR of *E. coli* and FiuR and FoxR of *P. aeruginosa*) (Koster *et al*., 1994; Ochs *et al*., 1995; Stiefel *et al*., 2001; Mettrick and Lamont, 2009). Self-cleavage of anti-σ factors likely occurs in the periplasm. FoxR self-cleavage produces two domains, N-terminal and C-terminal domain. It has been reported that ferrioxamine induced CSS pathway through two separate domains of FoxR. In the periplasm, most of FoxR is autocleavaed once it

transports across the cytoplasmic membrane and producing the N-terminal and C-terminal domains. In the absence of the signal, the N-terminal domain is attached to the cytoplasmic membrane through its transmembrane domain and sequesters FoxI σ factor via its cytosolic tail, causing the interaction of the C-terminal domain with the N-terminal domain and presumably prevent proteolysis (Bastiaansen *et al*., 2015).

Based on analogy to *P. aeruginosa* FoxR and *E. coli* FecR system, FlrR is a transmembrane protein and it is likely to be responsible for signal transmission. This might occur through proteolysis of FlrR that involves the presence of a specific protease. As a result of FlrR proteolysis, the σ factor FlrS is consequently released in order to direct transcription of *flrA*.

In the present work, we have identified important elements for recognition of the P_{flrA} promoter. This was firstly done by comparing the corresponding regions of the P_{flrA} promoter in different species of *Burkholderia* and *pseudomonas.* The important elements promoter was identified by introducing single point mutation at each base of the promoter sequence, P_{flrA}ds1. The β-galactosidase assay results conducted for each mutation revealed that there was a marked decreasein the activity of P_{flrA} promoter when mutations occurred in two regions correspond to -35 and -10 regions. The -35 region was recognized as TGAGC while -10 region recognized as GACA. This analysis suggest that these two sequences are the regions where σ factor FlrS (bound to core RNAP). From this promoter analysis we have also found a significant decrease in the activity at position 13 of TTT triad, 4 bp downstream from the -35 elements. β-galactosidase assay was conducted to study the role of T residue (13) by making different mutations in the TTT triad. The data obtained from β-galactosidase assay indicate very high level of promoter activity when multiple base substitution was introduced into the TTT triad. The results obtained for the TTT triad were surprising results as this might be a result for generating unkown important region recognize by other factors in *E. coli* strain.

In addition, the base substitution analysis indicates that the length of the spacer region between the -35 and -10 regions is 19 basepairs. In *E. coli* strain, the -35 and -10 regions of σ^{70}-dependent promoters are separated by a spacer region which usually consist of 17 base-pairs. The length of the spacer region is important for the promoter

function. It allow the two conserved regions -35 and -10 to be at the correct position (Auble *et al*., 1986; Beutel and Record, 1990; Chiang *et al*., 2006). It has been reported that 17 bp spacer region is the most frequent length. As the length of the spacer region varies from 15 to 21 bp (Aoyama *et al*., 1983).

Determination of the activity of *B. cenocepacia* P_{flrA}, *P. aeruginosa* P_{PA3901} and *P. syringae* $P_{PSPTO1207}$ dependent promoters in *E. coli* strain using *lacZ*-fusion vector, showed that FlrS is efficiently able to utilize promoters of other bacteria that are located between the *flrR* homologous gene and the TBDR gene located downstream. These results suggest that FlrS σ factor of *B. cenocepacia*, PA3899 of *P. aeruginosa* and PSPTO1209 of *P. syringae* can assemble with *E. coli* core RNA polymerase. Data from this study support that FlrS is a class of σ factor.

Chapter 5 Characterization of the P_{flrS} promoter

5.1 Introduction

Iron is an essential element for bacterial cell growth. However, excess iron is harmful to the cells as it catalyses the formation of toxic superoxides. As a result, the process of iron uptake is tightly regulated in order to maintain the intracellular level of iron at appropriate concentrations (Escolar *et al.*, 1999). An important mechanism for maintaining the intracellular level of iron in bacteria is by the regulatory protein, Fur. Under iron-replete conditions Fur represses genes involved in high affinity iron uptake (Section 1.12) (Escolar *et al.*, 1999). The promoter regions of Fur-regulated genes contain specific motifs for Fur binding that are referred to as Fur boxes. These motifs have the consensus sequence GATAATGATAATCATTATC (Baichoo and Helmann, 2002). Upstream of *flrS* is proposed to be a σ^{70}-dependent promoter that is under the control of Fur. By analogy with other iron starvation σ factor regulated system, the putative P_{flrS} promoter, P_{flrS} is proposed to be under the control of Fur. The work in this chapter focuses on the identification of P_{flrS} and its regulation.

5.2 Objectives

- To identify the putative σ^{70}-dependent promoter P_{flrS} located upstream of *flrS*.

- To investigate whether the activity of P_{flrS} is regulated by Fur.

5.3 Identification of a σ^{70}-dependent promoter upstream of *flrS*

To investigate the presence of a σ^{70}-dependent promoter located upstream of *flrS,* a 279 bp DNA fragment, containing 259 bp of sequence upstream of *flrS* translation initiation codon, was tested. This DNA fragment is refered to as $P_{flrSlong}$. $P_{flrSlong}$ was previously fused to the *lacZ* reporter gene in pKAGd4ΔAp plasmid (Jithu, MSC dissertation, 2007). pKAGd4ΔAp and pKAGd4ΔAp-$P_{flrSlong}$ were transformed into *E. coli* QC771 (Δ*lac*) and the resulting transformants were grown on LB agar plates containing 50 mg/ml chloramphenicol. The β-galactosidase activity of this candidate promoter region was measured in cells growing in LB medium supplemented with 50 mg/ml chloramphenicol and 175 μM dipyridyl in order to subject the cells to low iron conditions. The result of the β-galactosidase assay indicated a promoter activity present on $P_{flrSlong}$ as the activity was ~4 times higher than that specified by pKAGd4ΔAp (Figure 5.1). As the promoter was active in *E. coli* it suggested that it was most likely to be σ^{70}-dependent although it is possible that one of the other *E. coli* σ factors could be responsible.

5.4 Investigation of the role of iron and Fur in the regulation of the P_{flrS} promoter

The region upstream of *flrS* shows a predicted Fur box sequence that overlaps a sequence resembling a σ^{70}-dependent promoter (Figure 5.2). This suggests that gene transcription of the *flr* operon in *B. cenocepacia* is controlled by iron in a Fur dependent manner. The protein sequence alignment of Fur from *E. coli* and *B. cenocepacia* showed the conserved amino acid sequence in both strains indicating ~72% of protein similarity (Figure 5.3A). To investigate whether the activity of the P_{flrS} promoter is regulated by Fur, the activity of the promoter was measured in the presence and absence of the *fur* gene. Shorter P_{flrS} fragments $P_{flrSinter}$ and $P_{flrSshort}$ were previously cloned into pKAGd4ΔAp (Jithu, MSC dissertation, 2007) in order to establish the location of the promoter and to confirm that they are iron-regulated and controlled by Fur. These different lengths of P_{flrS} promoter fragments are $P_{flrSinter}$ and $P_{flrSshort}$ an even shorter promoter fragment called $P_{flrSvshort}$ was also constructed and cloned into pKAGd4ΔAp (Figure 5.2). The DNA sequence of putative *fur* box within

the $P_{flr}S$ promoter was compared with *E. coli fur* box DNA seqecance in order to determind sequence similarity between them (Figure 5.3B).

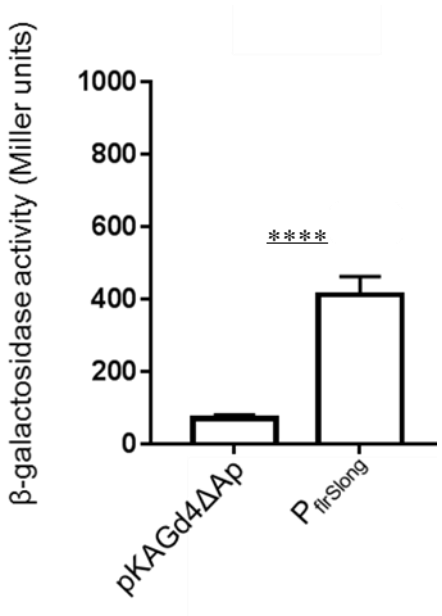

Figure 5-1: Activity of pKAGd4ΔAp and pKAGd4ΔAp-$P_{flrSlong}$ in *E. coli*.

E. coli QC771 containing pKAGd4ΔAp and pKAGd4ΔAp-$P_{flrSlong}$ were grown in LB broth supplemented with 50 mg/ml chloramphenicol and 175 μM dipyridyl. Error bars represent the standard deviation of the mean of the activities of the three cultures assayed. The results were analysed using T-test ****$P < 0.0001$.

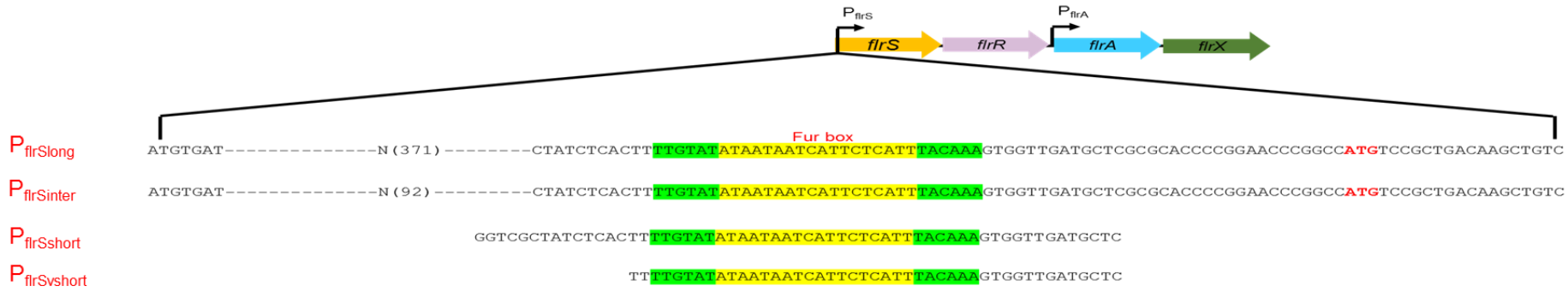

Figure 5-2: P_{flrS} σ^{70}-dependent promoter derivatives.

The putative -35 and -10 elements are highlighted in green. The proposed Fur box sequence is yellow highlighted. The *flrS* start codon is shown in red font.

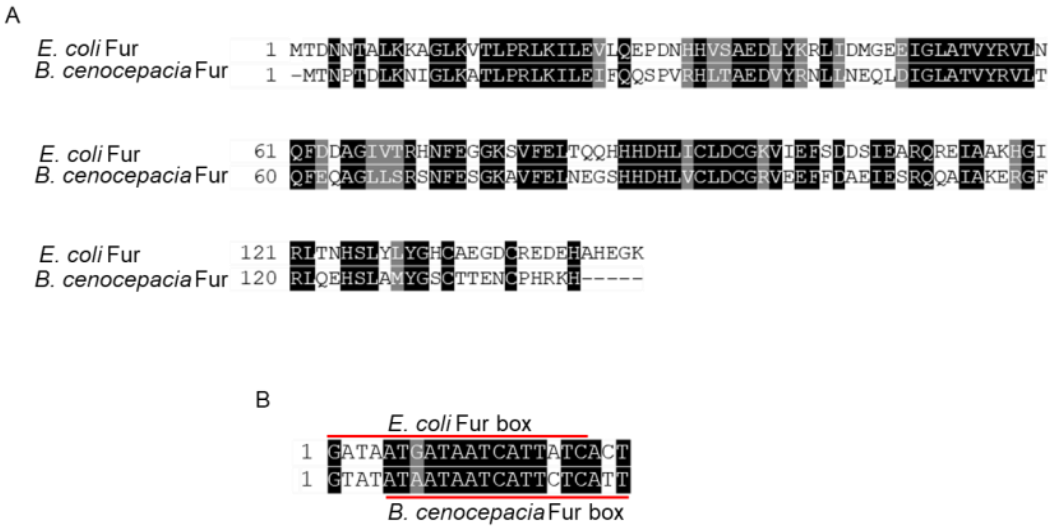

Figure 5-3: Sequence alignment of *E. coli* Fur box consensus sequence with *B. cenocepacia* putative Fur box sequence.

A. Fur amino acid sequences from *E. coli* and *B. cenocepacia*.

B. DNA consensus sequences of Fur box from *E. coli* and *B. cenocepacia* Fur box region within P_{flrS} promoter. Red lines indicate DAN consensus sequences of Fur box from *E. coli* and *B. cenocepacia*.

Fur amino acids and DNA consensus Fur box sequences identical or similar in both sequences are shown in white font and shaded by black or grey, respectively.

Construction of pKAGd4ΔAp-$P_{flrSvshort}$

In order to construct $P_{flrSvshort}$ a DNA fragment was generated by annealing complementary oligonucleotides PflrSvshortdsFor and PflrSvshortdsRev as described in Section 2.5.9. The double stranded fragment was ligated to pKAGd4ΔAp following the digestion of the plasmid with *Hin*dIII and *Bam*HI. The ligation products were transformed into *E. coli* MC1061 and plated onto LB agar plates containing 50 mg/ml chloramphenicol. Colony PCR was carried out using the primers AP10 and AP11 to screen for positive candidates for pKAGd4ΔAp-$P_{flrSvshort}$.

Comparison of $P_{flrSlong}$ activitiy with $P_{flrSinter}$, $P_{flrSvshort}$ and $P_{flrSvshort}$

To identify the location of P_{flrS} and to investigate whether the activity of P_{flrS} promoter derivatives are dependent on Fur, pKAGd4ΔAp derivatives bearing $P_{flrSlong}$, $P_{flrSinter}$, $P_{flrSshort}$ and $P_{flrSvshort}$ were introduced into *E. coli* WT (QC771) and *E. coli fur* mutant (QC1732) strains. The activities of all derivatives were measured by growing the cells in LB under iron-limited and iron-replete conditions. The results showed that $P_{flrSshort}$ activity in QC771 was the highest among all P_{flrS} derivatives under iron-limited conditions (Figure 5.4A). Also, these results indicate that all P_{flrS} promoters are iron-regulated and the highest degree of iron regulation was obsereved with $P_{flrSshort}$. In the absence of *fur*, there is no longer regulation by iron suggestion that the promoter is under control of Fur. The activities of P_{flrS} promoters in the *fur* mutant were higher than the WT (Figure 5.4B).

The activities of $P_{flrSlong}$, $P_{flrSinter}$, $P_{flrSshort}$ and $P_{flrSvshort}$ promoters were also assayed in *B. cenocepacia* 715j WT and 715jΔ*fur* mutant. pKAGd4ΔAp bearing P_{flrS} derivatives: $P_{flrSlong}$, $P_{flrSinter}$, $P_{flrSshort}$ and $P_{flrSvshort}$ were introduced into *B. cenocepacia* 715j WT and 715jΔ*fur* mutant by conjugation. The bacterial cells were grown in LB broth in low and high iron conditions and the activities of P_{flrS} promoter derivatives were measured by performing β-galactosidase assays. In *B. cenocepacia* 715j WT, the activity of $P_{flrSshort}$ was observed to be highest activity of all promoter derivatives and also showed that this promoter is highly regulated by iron. The activities were obsreved with all promoter derivatives, indicating they are iron-regulated (Figure 5.5A). In 715jΔ*fur* mutant, the activities of P_{flrS} promoter indicate that this promoter is iron-regulated (Figure 5.5B). The obsreved results from the FURTA and the β-

galactosidase assays indicate that the P_{flrS} region contains a *fur* binding region and its responsible for regulating the activity of this region.

Construction of pKAGd4ΔAp-$P_{flrSvshort-11G}$

$P_{flrSvshort-11G}$ is a mutant version of the P_{flrS} promoter, it has on A to G substitution at the second position of the predicted -10 element (-11). pKAGd4ΔAp-$P_{flrSvshort-11G}$ was constructed by annealing complementary oligonucleotides PflrSvshort-11GdsFor and PflrSvshort-11GdsRev as described in Section 2.5.9. The double stranded fragment was ligated and transformed into *E. coli* MC1061 in order to clone it into pKAGd4ΔAp.

Comparison of $P_{flrSvshort}$ activities and $P_{flrSvshort-11G}$

The activities $P_{flrSvshort}$ and $P_{flrSvshort-11G}$ were compared by conducting a β-galactosidase assay in *E. coli* strain QC771. The result showed that the promoter with the mutation $P_{flrSvshort-11G}$ had low activity as expected (Figure 5.6).

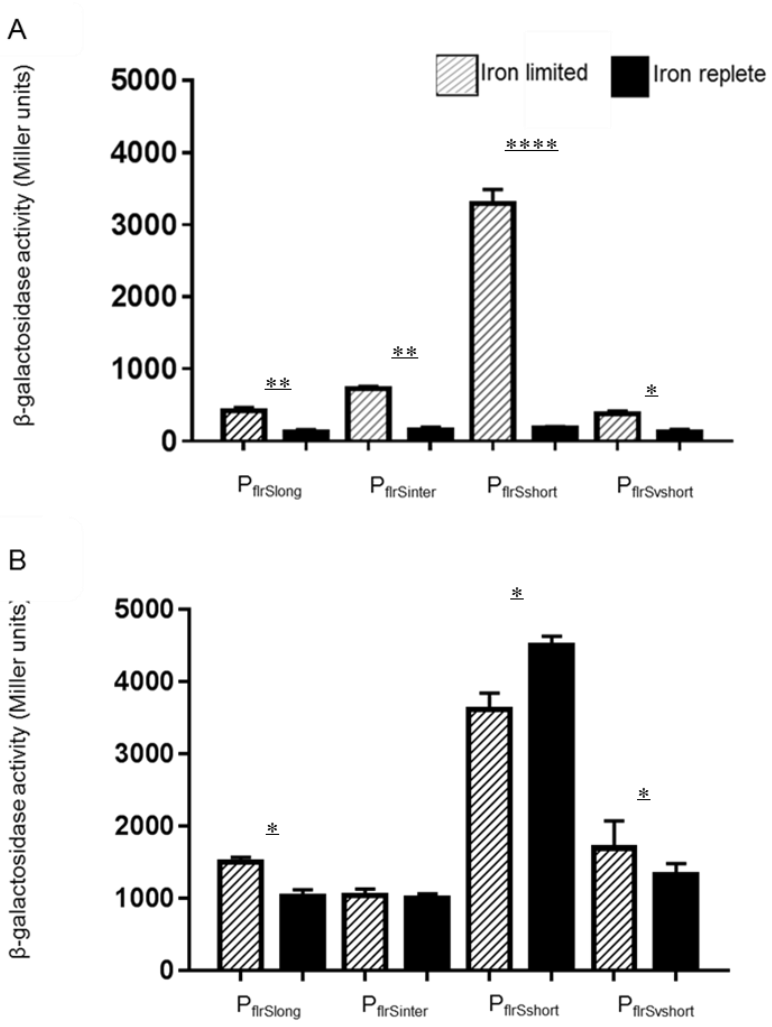

Figure 5-4: Iron-regulation of the P_{flrS} promoter is dependent on Fur in *E. coli*.

A. pKAGd4ΔAp bearing P_{flrS} derivatives: $P_{flrSlong}$, $P_{flrSinter}$, $P_{flrSshort}$ and $P_{flrSvshort}$ activities in *E. coli* QC771 (fur^+).

B. pKAGd4ΔAp bearing P_{flrS} derivatives: $P_{flrSlong}$, $P_{flrSinter}$, $P_{flrSshort}$ and $P_{flrSvshort}$ activities in *E. coli* QC1732 (fur^-).

Bacterial cells containing P_{flrS} derivatives were grown in LB broth under iron-limited and iron-replete conditions. The activities were measured by β-galactosidase assay, and the activities shown after subtraction of the basal activity of pKAGd4ΔAp. Error bars represent the standard deviation of the mean of the activities of the three cultures assayed. The results were analysed using one-way analysis (ANOVA) ****$P < 0.0001$, ** $P < 0.01$, * $P < 0.05$.

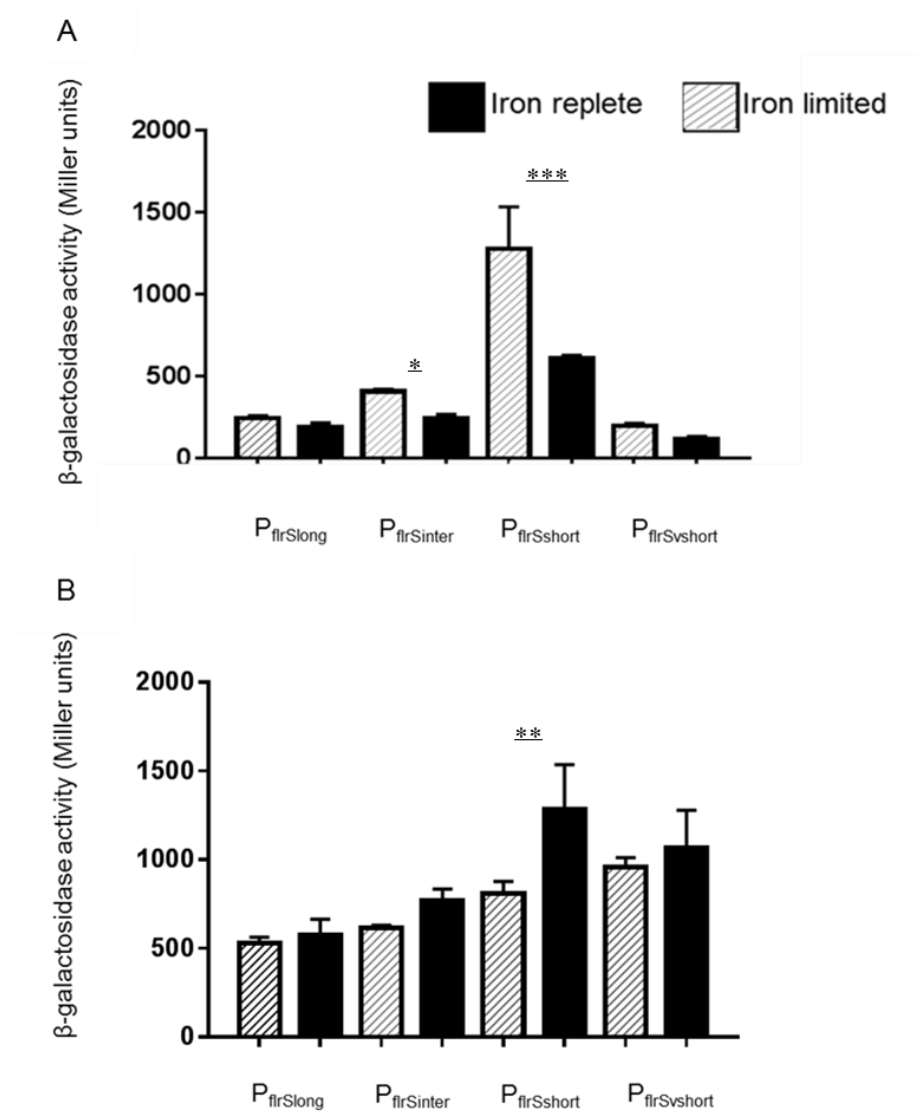

Figure 5-5: Iron-regulation of the P_{flrS} promoter is dependent on Fur in *B. cenocepacia*.

A. pKAGd4ΔAp bearing P_{flrS} derivatives: $P_{flrSlong}$, $P_{flrSinter}$, $P_{flrSshort}$ and $P_{flrSvshort}$ activities in *B. cenocepacia* 715j WT.

B. pKAGd4ΔAp bearing P_{flrS} derivatives**:** $P_{flrSlong}$, $P_{flrSinter}$, $P_{flrSshort}$ and $P_{flrSvshort}$ activities in 715jΔ*fur*

P_{flrS} derivatives introduced into *B. cenocepacia* 715j WT and 715jΔ*fur* by conjugation. Bacterial cells were grown in LB broth under iron-limited and iron-replete conditions. The activities were measured by β-galactosidase assay, the activities shown after subtraction of the basal activity of pKAGd4ΔAp. Error bars represent the standard deviation of the mean of the activities of the three cultures assayed. The results were analysed using one-way analysis (ANOVA) ***P < 0.001, ** P < 0.01, * P < 0.05.

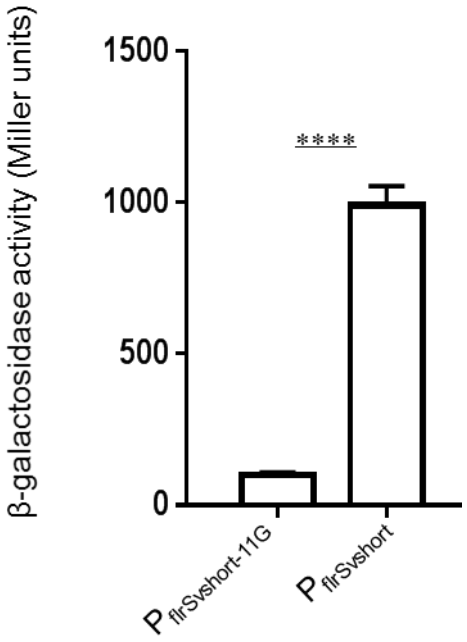

Figure 5-6: Activity of $P_{flrSvshort}$ and $P_{flrSvshort-11G}$ in *E. coli* QC771.

pKAGd4ΔAp-$P_{flrSvshort}$ and pKAGd4ΔAp-$P_{flrSvshort-11G}$ were transformed into *E. coli* QC771. The cultures were grown in LB broth supplemented with 50 mg/ml chloramphenicol and 175 μM dipyridyl. The assays were performed in triplicate and the activities were corrected by subtracting the activity of cells containing pKAGd4ΔAp. Error bars represent the standard deviation of the mean of the activities of the three cultures assayed. The results were analysed using T-test ****$P < 0.0001$.

5.5 The Fur titration assay (FURTA)

The results from all β-galactosidase assays indicate that the activities of P_{flrS} promoter derivatives are Fur regulated. However, it is not clear yet if these activities are because of the binding of Fur at the predicted Fur binding site on these promoter derivatives. The regulation of the P_{flrS} promoter by Fur might be a result for another factor which Fur regulates its transcription. As P_{flrS} promoter derivatives are regulated by Fur in *E. coli* and *B. cenocepacia* thus this factor would be common to both strains. Therefore, it was important to confirm that these activities were the result of direct binding between Fur and the P_{flrS} promoter. Thus, the Fur titration assay was included to confirm that these regulations is due to Fur binding.

FURTA (Fur-titration assay), is a method used to identify Fur regulated genes. It is based on using multiple plasmid bearing Fur boxes that derepress chromosomal Fur-regulated genes by titrating the Fur protein. FURTA employs an *E. coli* strain called H1717 which has a chromosomal *fhuF-lacZ* fusion and a Fur box located at the *fhuF* promoter. High iron concentration result in repression of *lacZ* transcription and thus a negative Lac phenotype would be observed. Using a high copy number plasmid in the cell such as pBluescript IIKS bearing a Fur box would titrate Fur away from the single chromosomal Fur box. As a result of Fur titration, the Fur repression would be relieved permitting increased utilisation of lactose even at high iron concentration (Stojiljkovic *et al*., 1994). The result of the Fur-titration assay can be visualised using MacConkey lactose agar medium. This medium allows screening for the lactose phenotype as it contains the pH indicator neutral red. The fermentation of lactose by bacteria causes the production of lactic acid that decreases the pH in the surrounding medium and results in red colour colonies. Bacteria unable to ferment lactose give rise to white colonies. Thus, introducing a high copy number plasmid bearing a Fur box in H1717 relieves the repression effect of Fur and results in the production of red colonies in high iron conditions (Stojiljkovic *et al*., 1994).

The upstream region of the *flrS* gene shows a putative Fur box sequence (Figure 5.2). This suggests that the transcription of *flr* operon of *B. cenocepacia* might be regulated by Fur. Therefore, it has been decided to test this promoter region as well as P_{flrA} promoter region in order to confirm the presence of the consensus Fur box. To

demonstrate that the P_{flrS} promoter region contains a Fur box, pBluescript IIKS containing long $P_{flrSlong}$ promoter, intermediate P_{flrS} promoter, short P_{flrS} promoter and very short P_{flrS} promoter were included in FURTA assay. Also, P_{flrA} promoter was included in this assay.

Construction of pBluescript-$P_{flrSvshort}$

Annealing of $P_{flrSvshort}$ complementary oligonucleotides pBluescript-PflrSvshortFor and pBluescript-PflrSvshortRev was performed as described in Section 2.5.9. The resulting fragment was ligated into pBluescript II KS which was previously digested with *Hin*dIII and *Bam*HI and purified using a PCR purification column. The ligations were transformed into *E. coli* strain JM83 and colonies were selected on LB agar plates supplemented with 100 μg/ml ampicillin, 40 μg/ml X-gal and 0.2 mM IPTG. The transformants that give rise to white colonies were streaked onto fresh LB plates containing 100 μg/ml ampicillin.

Determination of the location of the Fur binding site at the P_{flrS} promoter by FURTA

In order to perform the FURTA assay it was necessary to optimize the conditions for this experiment. Therefore, p3ZFBS, a plasmid containing the consensus *E. coli* Fur box, was introduced into H1717 as a positive control, and pBluescript II KS was introduced into H1717 as a negative control. pBluescript II KS containing the different promoter fragments were also transformed into *E. coli* H1717. Cells were spread on MacConkey lactose agar plates supplemented with increasing concentrations (20-40 μM) of theferrous ammonium sulphate ($Fe(NH_4)_2(SO_4)_2$). The optimization experiment showed that $Fe(NH_4)_2(SO_4)_2$ at 40 μM gave the best colour definition for colonies harbouring p3ZFBS (Lac^+) and those harbouring pBluescript II KS (Lac^-). The result for each of the P_{flrS} clones were observed for their phenotype after 24 hours' incubation at 37ºC (Figure 5.7). The Lac^- phenotype observed for the $P_{flrSlong}$ and the P_{flrA} promoter fragments. In contrast, a Lac^+ phenotype was observed for H1717 bearing the intermediate, short and very short P_{flrS} promoters as they gave rise to red

colonies. These results showed that these P_{flrS} promoter regions contain Fur box.

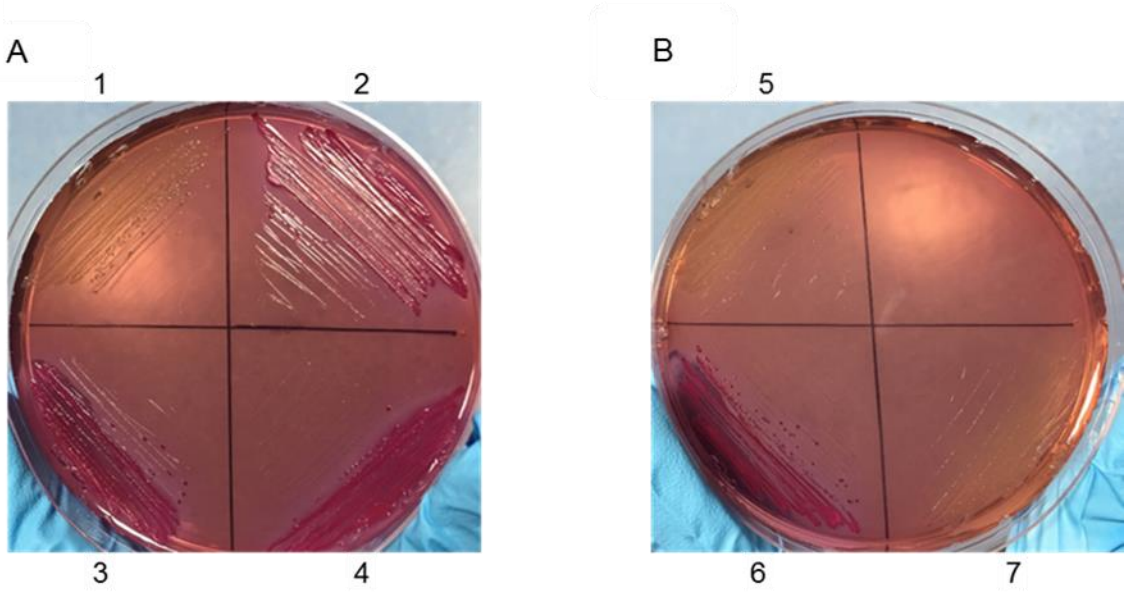

Figure 5-7: Fur titration assay (FURTA) with P_{flrS} derivatives and P_{flrA} promoter.

A. 1-4, pBluescript II KS-$P_{flrSlong}$, p3ZFBS, pBluescript II KS-$P_{flrSinter}$ and pBluescript II KS-$P_{flrSvshort}$ promoters, respectively.

B. 5-7, pBluescript II KS, pBluescript II KS-$P_{flrSshort}$ and pBluescript II KS-P_{flrA} promoters, respectively.

p3ZFBS and pBluescript II KS were introduced into *E. coli* strain H1717 as positive (Lac^+) and negative (Lac^-), controls respectively.

5.6 Discussion

The iron starvation σ factor FlrS in *B. cenocepacia* is regulated by the anti-σ factor FlrR. One hypothesis associated with this study is that Fur, the global suppressor, might regulate *flrS*. Therefore, the effect of Fur on P_{flrS} promoter activity was investigated in both *E. coli* and *B. cenocepacia fur* mutant and WT strains in the presence and absence of iron. It has been observed that *B. cenocepacia* lacking the *fur* gene were grown slowly and colonies on plates were smaller than in the case of WT. In the presence of high iron concentration, the P_{flrS} promoter derivative activities were lower in the WT strains than the *fur* mutant strains. The results obtained from the WT suggest that iron has a role in regulating *flrS* activity.

The FURTA assay was carried out to confirm that the Fur regulator interacts with the Fur box on the promoter derivatives which were assayed in this study. The assays were performed using promoter derivatives cloned into pBluescript II KS. The P_{flrA} promoter clone did not show red colonies suggesting that the P_{flrA} promoter sequence has no Fur box sequence. All P_{flrS} derivatives promoters cloned into pBluescript II KS were found to give rise to intense pinkish red colonies. However, the $P_{flrSlong}$ clone did not give rise to intense pinkish red colonies even though few pinkish red colonies were observed. The strain containing the $P_{flrSlong}$ clone into pBluescript II KS result showed no obvious Fur regulation. This might be as a result for streaking unhealthy candidate that effect the bacterial growth. Overall, the data obtained in this study demonstrate that the region of P_{flrS} promoter is a regulatory region.

Chapter 6 Xenosiderophore utilization in *B. cenocepacia*

6.1 Introduction

Under iron starvation conditions, many bacteria are able to synthesize and secrete low molecular weight iron-chelating compounds termed siderophores. The ferric-siderophore complexes are transported across the outer-membrane of Gram-negative bacteria through TonB-dependent receptors. It has been demonstrated that bacteria are also able to utilize non-endogenous siderophores: xenosiderophores (D'Onofrio *et al.,* 2010; Strange *et al.,* 2011). *B. cenocepacia* is an opportunistic pathogen that produces two siderophores, ornibactin and pyochelin (Darling *et al*., 1998). This bacterium not only utilizes its own siderophores but also has the ability to utilize xenosiderophores such as ferrichrome and ferrioxamine B (Sofoluwe, MSC dissertation, 2014). At least 20 TonB-dependent siderophore receptors have been reported in *B. cenocepacia* through BLASTP search (Thomas unpublished observations) in addition to the OrbA and FptA receptors for ornibactin and pyochelin, respectively. The specific receptors for the two xenosiderophores have also been identified (Hussein, Sofoluwe and Thomas, unpublished results) but the rest of the other TonB-dependent receptors, including FlrA, have not been determined. Studying xenosiderophore uptake by Flr system in *B. cenocepacia* maybe an important step in understanding the pathogenicity of *B. cenocepacia*.

6.2 Objective

- To identify the siderophore transported by the TonB-dependent outer-membrane receptor FlrA.

6.3 Siderophore utilization assay

To analyse the role of FlrA, it would not be possible to use a *B. cenocepacia* WT strain, such as 715j because of other systems that present in this strain which may involved in siderophore biosynthesis and uptake. Therefore, it was decided to use a modified strain called AHA27 in which mini-Tn5Cm*lacZ* (a transposons) is inserted in the *pobA* gene of strain 715j (Asghar *et al.*, 2011). The *pobA* gene encodes the enzyme Sfp-type phosphopantetheinyltransferases (PPTases). This enzyme is responsible for activation of NRPSs by the covalent attachment of the 4′-phosphopantetheine (P-pant) moiety of coenzyme A (Asghar *et al*., 2011). The *pobA* gene is therefoure required for siderophore biosysnthesis. However, knocking out/inactivating the *pobA* gene does not inhibit the mechanism of siderophore uptake and would allow the bacteria to transport any supplied siderophores for which a receptor is present.

An overnight culture of AHA27 was used to test the ability of *B. cenocepacia* to utilise supplied siderophores. AHA27 culture was mixed with 0.65% of molten agar and poured over LB agar containing 50 mg/ml chloramphenicol and an iron chelator (40 μM EDDHA) to establish iron starvation conditions. The plates were allowed to dry for 10 minutes and the siderophore to be tested was spotted on a filter paper discs and placed on the agar. Utilization of siderophore by this bacterium was observed by growth around the filter paper. In this study, eight siderophores were used: nicotianamine, coprogen, rhodotorulic acid, rhizoferrin, enterobactin, bacillibactin, arthrobactin and schizokinen. Also, these siderophores were assayed with the AHA27-*flrA*::Tp mutant in order to test its ability to uptake any of them. The siderophore utilization bioassay was carried out by using ferrichrome as a positive control and H_2O as the negative control.

As expected, the ferrichrome showed a growth around the filter discs while water showed no growth. Four siderophores, nicotianamine, coprogen, rhodotorulic acid and rhizoferrin, did not give rise to haloes of growth around the filter discs (the results for rhodotorulic acid and rhizoferrin) are shown in Figure 6.1A and B. Because of the negative results of the four siderophores, it was decided to test these siderophores with strains that are known to utilize them. *E. coli* JC28 strain was used to test the ability of *B. cenocepacia* to utilize coprogen and rhodotorulic acid (Figure 6.2A). Both

coprogen and rhodotorulic acid showed haloes of growth around the filter discs. However, the utilization of coprogen is much more obvious compared to rhodotorulic acid that showed small haloes around the filter. No growth around the filter discs was observed when adding 1 μM at an amount of 15 μl of rhodotorulic acid but increasing the amount of rhodotorulic acid to 5 μM showed small haloes around the filter discs. To confirm that the other two siderophores are effective in this type of bioassay, *P. aeruginosa* was used as a second control strain to test utilization of nicotianamine and rhizoferrin. As expected *P. aeruginosa* showed utilization of nicotianamine but rhizoferrin unexpectedly do not promote growth of *P. aeruginosa* (Figure 6.2B). In addition, positive control ferrichrome and the negative control H_2O were included in the siderophore bioassay when using *E. coli* JC28 and *P. aeruginosa* (Figure 6.2). Filter discs impregnated with 1 μM at an amount of 15 μl of siderophores: schizokinen and enterobactin showed little growth of *B. cenocepacia*, AHA27 (results not shown). In contrast, the growth around the filter discs impregnated with arthrobactin and bacillibactin gave rise to strong haloes around the filter discs (Figure 6.1A and B).

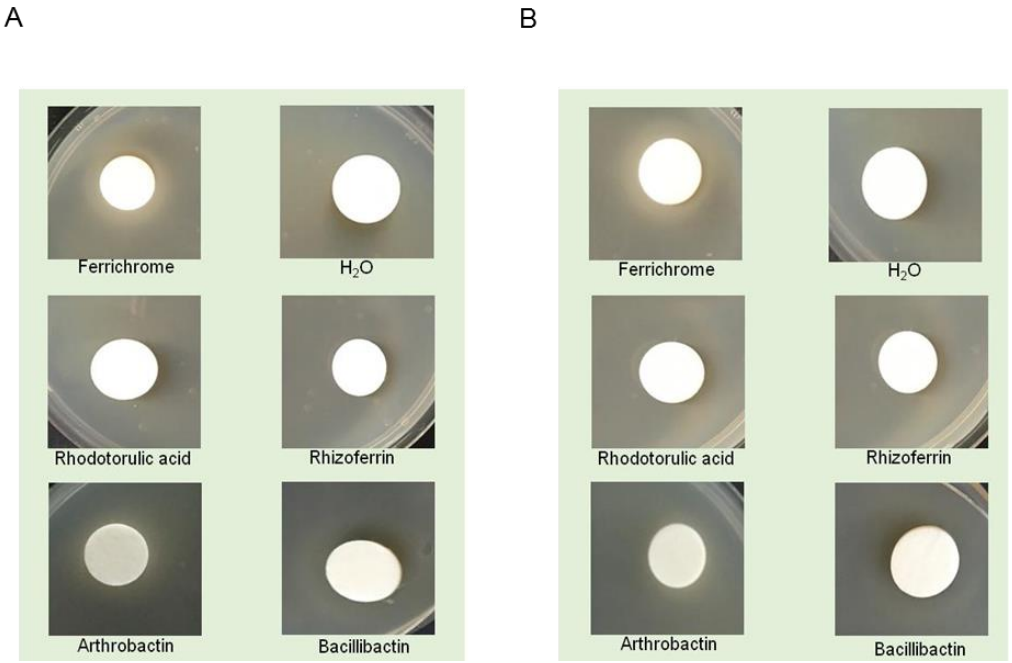

Figure 6-1: *B. cenocepacia* xenosiderophore utilization bioassay.

A. Bioassay of AHA27.

B. Bioassay of AHA27-*flrA*::Tp.

The ability of AHA27 and AHA27-*flrA*::Tp to uptake different xenosiderophores was tested on LB plates containing 40 μM EDDHA and their growth were observed around the filter discs. AHA27-*flrA*::Tp assays showed no effect on the uptake of siderophores. Ferrichrome was used as positive control while H_2O was used as negative control. Not all siderophores assayed are included in this Figure.

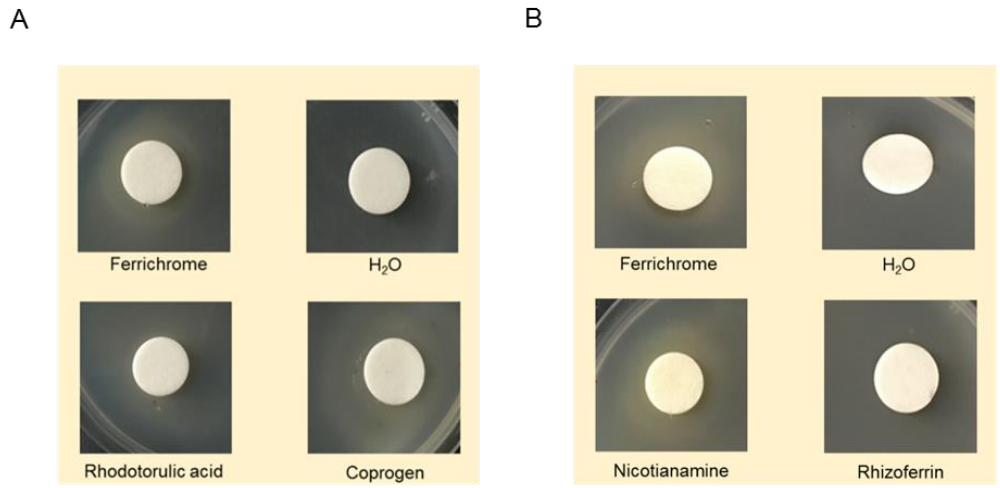

Figure 6-2: Siderophore utilization bioassay of *E. coli* JC28 strain and *P. aeruginosa*.

A. Utilization of rhodotorulic acid and coprogen by *E. coli* JC28.

B. Utilization of nicotianamine and rhizoferrin by *P. aeruginosa*.

Ferrichrome was used as a positive control and H_2O as a negative control.

6.4 Analysis of xenosiderophore utilization of *B. cenocepacia BCAM1371* (*flrA*) mutant in the presence of non-functional *BCAM2439*

As mentioned, *B. cenocepacia* was found to be able to utilize two siderophores: ferrichrome and ferrioxamine B as well as other xenosiderophores for iron acquisition (Paleja, Sofoluwe and Thomas, unpublished results). BCAL0116 is a TonB-dependent receptor that was found to be involved in the uptake of both siderophores (Sofoluwe and Thomas, unpublished results). BCAL2281 is a phylogenetically similar TonB-dependent receptor that is associated with the uptake of ferrichrome. Inactivation of both *BCAL0116* and *BCAL2281* results in the loss of *B. cenocepacia* ability to take up ferrichrome (Hussein and Thomas, unpublished result). Likewise, FlrA and BCAM2439 are closely related TBDRs, they share about 39% of identitiy and 57% of similarity while the BCAL0116 and BCAL2281 share about 30% and 44% of identitiy and similarity respectively (Figure 6.3). It was hypothesized that FlrA and BCAM2439 may be involved in the uptake of the same siderophore, thus it was decided to construct a double mutant by inactivating both corresponding genes locus. To make the double mutant, HIIIΔ*pobA* strain was used as it lacks the chloramphenicol-resistance marker of the AHA27 strain and this would allow the use of a chloramphenicol cassette to inactivate *BCAM2439* gene locus.

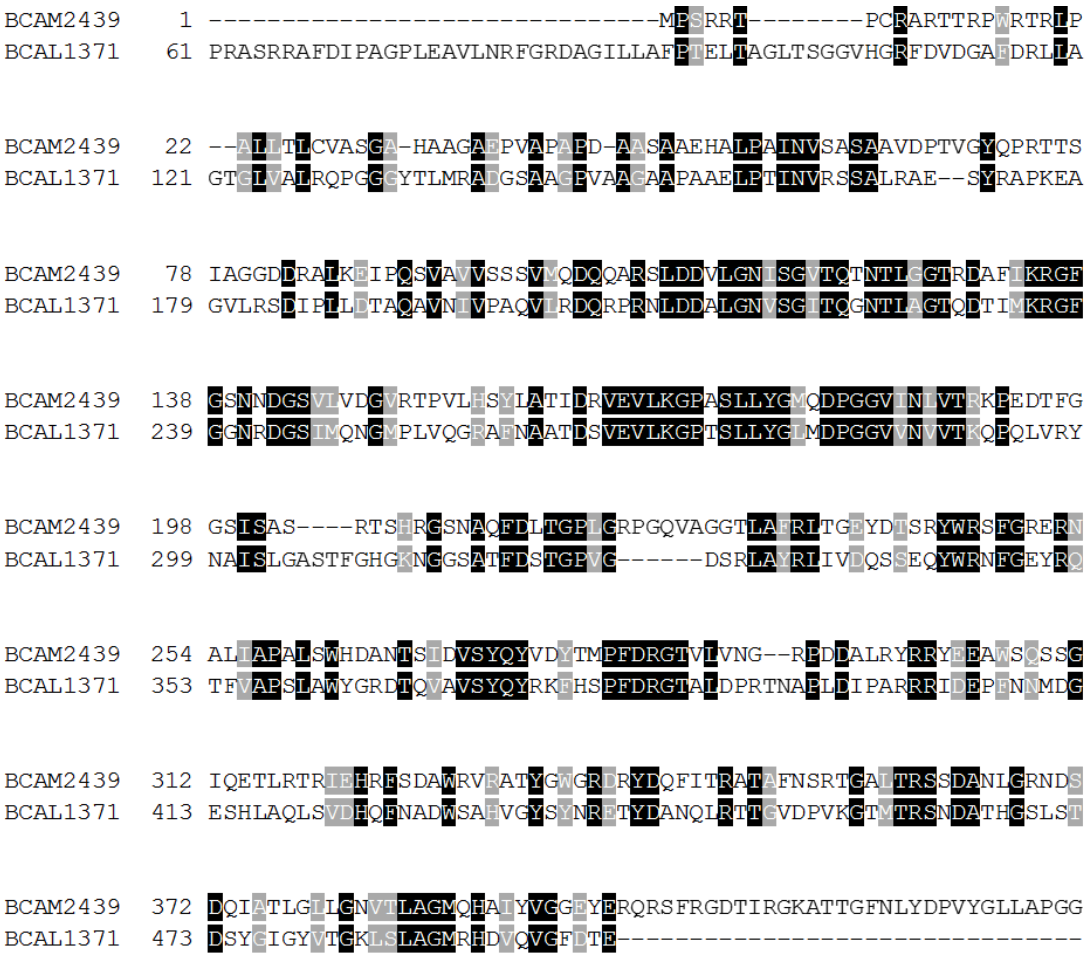

Figure 6-3: Amino acid sequence alignment of BCAM2439 and BCAL1371 (FlrA) TonB-dependent receptors.

Alignment was carried out using Clustal Omega and the identical amino acids of BCAM2439 and BCAL1371 TBDRs are shown in white font and shaded by black or grey.

Construction of HIII∆*pobA*/*flrA*::Tp

To construct HIII∆*pobA*/*flrA*::Tp, pSHAFT.GFP-*flrA*::Tp plasmid was introduced into *E. coli* SM10 donor strain. Consequently, pSHAFT.GFP-*flrA*::Tp was introduced into HIII∆*pobA* by conjugation. Clones were selected on M9-glucose CAA (0.1%) agar containing 10 mg/ml tetracycline and 25 mg/ml trimethoprim. 100 trimethoprim-resistant colonies were patched in duplicates on IST-trimethoprim plates and on the same selection medium. The patches on IST plates were viewed under UV light. The non-fluorescent candidates were screened by PCR using the bacteria that were not exposed to UV light. To screen for candidate *flrA*::Tp mutants, the flrAforout and flrArevout pair of primers were used for PCR screening of non-fluorescent recombinants. The expected PCR product for the candidate clone of *flrA*::Tp is 2.16 kb. The boiled lysate of HIII WT was used as a template for a negative control which should give a WT PCR product of 1.54 kb with the outside primers. The result showed that two HIII∆*pobA*/*flrA*::Tp mutants were obtained (Figure 6.4).

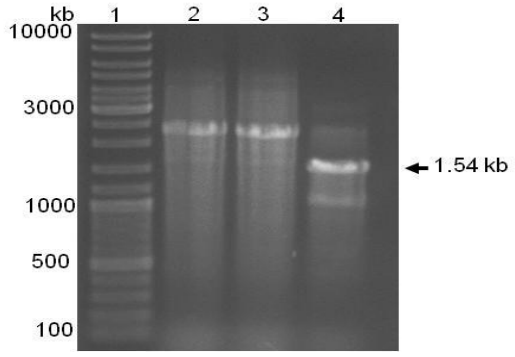

Figure 6-4: PCR screening of candidate HIII∆*pobA*/*flrA*::Tp mutants.

Outside primers flrAforout and flrArevout were used to screen non-fluorescent recombinants following introducing of pSHAFT.GFP-*flrA*::Tp into HIII∆*pobA*. Lane 1; GeneRuler DNA ladder; lanes 2-3, PCR products of candidate *flrA*::Tp mutants; lane 4, boiled cell lysate of HIII used as control.

Construction of pSHAFT.GFP-*BCAM2439*::Cm

In order to introduce a mutant BCAM2439 allele into the HIIIΔ*pobA*/*flrA*::Tp mutant, a plasmid called pSHAFT.GFP-*BCAM2439*::Cm was constructed. To make pSHAFT.GFP-*BCAM2439*::Cm, a previously constructed plasmid called pSHAFT.GFP-*BCAM2439* and another plasmid called p34E-Cm2 were used (Sofoluwe, 2014). The latter plasmid was cut with *Eco*53kI which recognised the *Sac*I sites flanking the *cat* cassette but generates blunt ends. The released *cat* cassette was ligated into the *Zra*I site of *BCAM2439* located on pSHAFT.GFP-*BCAM2439* plasmid and transformed into CC118 (*λpir*). The transformants containing the correct size were screened by PCR using primer pair BCAM2439forOut and BCAM2439revOut. The PCR products of the corrected clones gave expected size of 1388 bp (result not shown).

Construction of HIIIΔ*pobA/flrA*::Tp/*BCAM2439*::Cm double TBDR mutant

After confirmation of pSHAFT.GFP-*BCAM2439*::Cm integrity, the plasmid was introduced onto *E. coli* S17-1(*λpir*) donor strain in order to transfer it to HIIIΔ*pobA*/*flrA*::Tp by conjugation. The colonies were selected on LB plates containing 50 mg/ml chloramphenicol and 10 mg/ml tetracycline. Following conjugation colonies were patched in duplicates on an IST plate and onto the selection medium and one set was screened for fluorescence under UV. The non-fluorescent colonies were candidate *BCAM2439* mutants. To confirm the candidates HIIIΔ*pobA*/*flrA*::Tp/*BCAM2439*::Cm mutants colony PCR was carried out and six positive candidates gave expected PCR products of 2998 bp (Figure 6.5).

Analysis of xenosiderophore utilization by *B. cenocepacia BCAL1371* and *BCAM2439* double mutant

Once the BCAL1371 and BCAM2439 TBDR double mutant had been made, the siderophore utilisation bioassay was carried out as described in Section 2.12. A variety of xenosiderophores were tested for their ability to allow growth of HIIIΔ*pobA*/*flrA*::Tp-*BCAM2439*::Cm and HIIIΔ*pobA*/*flrA*::Tp, the latter strain was used as control. The siderophores tested on both strains were rhizoferrin, rhodotorulic acid, coprogen, nicotianamine, enterobactin, bacillibactin, schizokinen and arthrobactin. The siderophore assays were performed by plating the overnight culture

on LB agar plate containing 40 µM EDDHA. Coprogen, nicotianamine and bacillibactin did not lead to any growth around the filter discs for either strains. As observed previously rhodotorulic acid gave rise to a little growth for both strains when adding 5 µM at an amount of 15 µl of rhodotorulic acid (Table 6.1A and Table 6.1B). Enterobactin and arthrobactin exhibited very strong haloes around the filter discs while growth around the schizokinen filter was not that strong for both strains. Coprogen, nicotianamine, bacillibactin and rhizoferrin did not allow for any growth in all siderophore utilisation bioassay indicating undetectable growth on the filter for both strains suggesting that none of the inactivated TBDR genes *BCAL1371* and *BCAM2439* were identified to be involved in coprogen, nicotianamine, bacillibactin and rhizoferrin uptake (Table 6.2A and Table 6.2B). The positive control ferrichrome and the negative control H_2O were included in all assays.

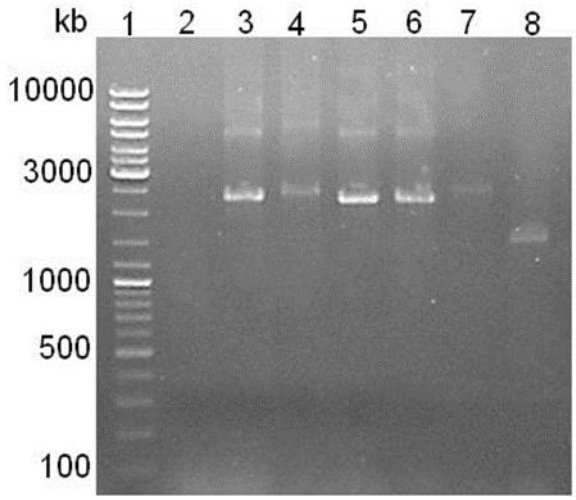

Figure 6-5: Gradient PCR screening of candidate HIIIΔ*pobA*/*flrA*::Tp-*BCAM2439*::Cm mutants.

Colony PCR of candidate HIIIΔ*pobA*/*flrA*::Tp-*BCAM2439*::Cm mutant. Lane 1, GeneRuler DNA ladder; lanes 2-7, PCR products of candidate HIIIΔ*pobA*/*flrA*::Tp-BCAM2439::Cm mutant at annealing temperatures 61, 63, 66, 67, 68 and 70^{o}C; lane 8, HIII strain was used as control.

Table 6-1: A. Ability of siderophores to promote growth of HIII∆*pobA*/*flrA*::Tp-BCAM2439::Cm

Siderophores	Growth in presence of siderophore	Degree of growth with 1 mM of siderophore	Degree of growth with 5 mM siderophore
Ferrichrome	Yes	++++	++++
Coprogen	No	-	n/a
Bacillibactin	No	-	n/a
Nicotianamine	No	-	n/a
Rhodotorulic acid	Yes	-	++

Table 6-1: B. Ability of siderophores to promote growth of HIII∆*pobA*/*flrA*::Tp

Siderophores	Growth in presence of siderophore	Degree of growth with 1 mM of siderophore	Degree of growth with 5 mM siderophore
Ferrichrome	Yes	++++	++++
Coprogen	No	-	n/a
Bacillibactin	No	-	n/a
Nicotianamine	No	-	n/a
Rhodotorulic acid	Yes	-	++

++++, very large diameter of growth; +++, large diameter of growth; ++, medium diameter of growth; +, slight growth.

Table 6-2: A. Ability of siderophores to promote growth of HIII*ΔpobA/flrA*::Tp-*BCAM2439*::Cm

Siderophores	Growth in presence of siderophore	Degree of growth with 1 mM of siderophore
Ferrichrome	Yes	++++
Arthrobactin	Yes	+++
Enterobactin	Yes	+++
Rhizoferrin	No	-
Schizokinen	Yes	+

Table 6-2: B. Ability of siderophores to promote growth of HIII*ΔpobA/flrA*::Tp

Siderophores	Growth in presence of siderophore	Degree of growth with 1 mM of siderophore
Ferrichrome	Yes	++++
Arthrobactin	Yes	+++
Enterobactin	Yes	+++
Rhizoferrin	No	-
Schizokinen	Yes	+

++++, very large diameter of growth; +++, large diameter of growth; ++, medium diameter of growth; +, slight growth.

6.5 Discussion

The production of siderophores is one of the virulence factors associated with infection and pathogenesis of *B. cenocepacia* (Uehlinger *et al.,* 2009). Currently, the studies on drug design dealing with siderophore-conjugated antimicrobials are on the rise (Wencewicz *et al*., 2009). It has been shown that antimicrobial molecules attached to siderophore compounds inhibit the growth of multi-drug resistant in Gram-negative bacteria such as the members of *Pseudomonas spp* and *Burkholderia cepacia* complex. Examples of these compounds are the catechol-conjugates of aminopenicillin and conjugates of BAL30072 and PTX2466 (Livermore *et al.,* 2010; Page, 2013)**.** Unlike non-conjugated antimicrobials, the siderophore-conjugated antimicrobial compounds have a great advantage that is associated with iron uptake systems. Uptake of these compounds is facilitated by the TonB-dependent outer membrane receptors which allow drug access and evasion of the pathogen's resistance mechanisms. Also, it has been observed that the cognate siderophores loaded with iron are preferable and selected by the TBDRs (Tomaras *et al.,* 2013).

In iron-limited conditions, competition increases among pathogens associated with infection of the lung of CF patients, and because of this, an adaptive approach such as a siderophore piracy can be used by bacterial pathogens. Determining the xenosiderophores and the receptors of *B. cenocepacia* for ferric-siderophore complex uptake would increase the potential of antimicrobial drug design and support a cure for pathogens diseases in the future.

One hypothesis associated with this study is that the Flr system of *B. cenocepacia* can uptake xenosiderophores. In this study, we aimed to identify the xenosiderophore utilized by *B. cenocepacia* Flr system. Also, the study aimed to determine whether the FlrA and BCAL2439 outer-membrane receptors recognize the same siderophore. In order to identify xenosiderophores utilised by *B. cenocepacia,* the production of native siderophore are essential to be inactivated. It has been previously identified that the *pobA* gene encodes the enzyme Sfp-type phosphopantetheinyl transferase which is responsible for activation of the non-ribosomal peptide synthetases required for pyochelin and ornibactin production (Asghar *et al.,* 2011).

Inactivating the *pobA* gene prevents the production of endogenous siderophores which facilitates the use of xenosiderophore utilisation bioassays to verify xenosiderophore utilisation. Therefore, *B. cenocepacia* with an inactivated *pobA* gene was used in this study.

Most of the siderophores used in this study did not suggest growth of *B. cenocepacia* on the filter papers discs and a few of them that did supported equal growth in AHA27, AHA27-*flrA*::Tp, HIIIΔ*pobA*/*flrA*::Tp and HIIIΔ*pobA*/*flrA*::Tp/*BCAM2439*::Cm strains suggesting that the FlrA TBDRs were not involved in the uptake of the siderophores used in this study. This might be due to gene redundancy in the regulation of siderophores uptake that has been suggested by Llamas *et al.*, 2006. The case of gene redundancy occurs when two or more genes encode proteins with the same function as an example for that is the two TBDR genes encoding receptors that recognize ferrichrome. Inactivation of a single gene has no effect on siderophore utilisation because it depends on another TBDR encoded by a duplicate gene. However, using a double receptor mutatnt involving the *flrA* and *BCAM2439* gene locus for screeing also do not show uptake of the siderophore teasted. To conclude, this study was unable to confirm that FlrA is a TBDR.

Chapter 7 General discussion

In order for bacteria to survive in stressed conditions a rapid and appropriate response is required. The essential global regulators that can be used to establish this priority are alternative σ factors. Because of the critical role of these σ factors, they are tightly controlled. There are several mechanisms of controlling these σ factors and one of them is regulation of σ factor activity by anti-σ factors (Benson and Haldenwang, 1993; Duncan and Losick, 1993).

How anti-σ factors modulate cognate alternate σ factors in response to stress signals is an emerging theme. This study investigated Flr system of *B. cenocepacia* and how FlrR regulates FlrS in response to the binding of an unknown ferric-siderophore complex to FlrA. It has been shown that several ECF σ factors interact with anti-σ factors via the N-terminal cytoplasmic domain of the anti-σ factor (Yoshimura *et al.*, 2004). These include *E. coli* σ^E and its anti-σ factor RseA, and FecI and its anti-σ factor FecR (Enz *et al*., 2000; Campbell *et al*., 2003). In this study, we demonstrate that the 48 amino acid residues of the N-terminal domain of the anti-σ factor FlrR are sufficient for interaction with FlrS. The interaction between $FlrR_{NTD}$ and $FlrS_{CTD}$ was assigned by using bacterial BACTH assay and pull-down assay. These results suggest that σ_4 of σ factor is specific for the binding with the N-terminal domain of FlrR and this binding seems to be important for FlrS to function as a σ factor. It is not clear yet if the inducing signal is responsible for a conformational change which occurs in FlrR and whether the altered FlrR causes activation of FlrS by conformational change. FlrS might be regulated in a similar way to the regulation of allosteric enzymes. Another possible explanation that is closely related to the anti-σ factor concept, is that the binding between FlrR and FlrS prevents activation of FlrS because of precipitation or proteolytic degradation. This study demonstrates similar findings observed in *E. coli* for the interaction between FecR and FecI (Mahren *et al*., 2002). Unknown siderophore activite FecR which then activites FlrS in order to allow transcription of *flr* genes (Ochs *et al*., 1995).

Furthermore, BACTH assay showed that the C-terminal region of the anti-σ factor FlrR interacts with the N-terminal region of the outer-membrane receptor, FlrA which was confirmed by the pull-down assay. Similarly, the N-terminal region of FecA has been showed to interact with the C-terminal domain of FecR. Removing the N-terminal has no effect on the FecA transport activity but it cannot be an independent

domain from the rest of the FecA as it is responsible for communicating structural changes that occur by binding of ferric citrate to FecA. The extra-long N-terminus acts in signalling ferric citrate occupation of FecA into the periplasm. The periplasmic location of the N-terminus brings it into position where it interacts with the C-terminus of FecR (Kim *et al*., 1997).

In addition, the β-galactosidase assay results from *E. coli* and *B. cenocepacia* suggests that $FlrR_{NTD}$ acts as an activator for FlrS. In the absence of external signal, specifically when no siderophore binds to the outer-membrane receptor, FlrR may inhibit the activity of FlrS. If this is the case, FlrS would show a high level of promoter activity in the absence of FlrR. However, the observed activity of FlrS in the absence of FlrR was extremely low which proposed that FlrR is unable to purely function as an inhibitor. A study by Braun *et al*. (2003) suggested that the anti-σ factor FecR is responsible for activating σ factor FecI in iron-limited conditions. This might be as a result for spontaneous induction of the σ factor's active conformation. Data obtained from this study showed that the presence of $FlrR_{NTD}$ has a significant effect on FlrS-dependent promoter activity as it showed a high level of promoter activity when compared with the absence of $FlrR_{NTD}$ and full-length FlrR. This clearly suggests that $FlrR_{NTD}$ must have a crucial role in activating FlrS.

In this study, sequence analysis of P_{flrA} promoter region revealed similar promoter regions among different species of bacteria. The P_{flrA} promoter activity at this highly conserved region was tested by creating point mutations at each base. One novel finding of this study is the important promoter features of P_{flrA} for recognition by FlrS that have been determined. These are a -35 element composed of TGAGC and the -10 element that consists of GACA.

The alternative FlrS-like σ factors of *P. aeruginosa* and *P. syringae*, PA3899 and PSPTO1209 respectively, are able to recognise FlrS-dependent promoter sequences. Also, FlrS was found to be able to recognise PA3899 and PSPTO1209-dependent promoters. However, none of these σ factor-dependent promoters were able to fulfil the requirements for recognition by σ factor PA0149.

One of the aims of this study was to investigate the region upstream of *flrS*. The activities of different P_{flrS} promoter derivatives indicate that this promoter region are regulatory regions as they showed high level of β-galactosidase in low iron conditions compared with high iron conditions. There is a high possibility that the P_{flrS} promoter is σ^{70}-dependant. The involvement of Fur in P_{flrS} promoter was investigated further by performing FURTA. The use of the FURTA assay has highlighted the efficiency of the P_{flrS} region to bind to Fur. However, in the case of the P_{flrA} promoter there was no detected binding by Fur suggestion that P_{flrA} promoter region has no Fur box sequance.

Completion of genomic sequencing projects for a broad range of pathogens, including *B.cenocepacia*, will enable differentiation between pathogenic and non-pathogenic strains at the genetic level. Along with this, a vast amount of information is potentially becoming available regarding virulence, host immune evasion, stress response systems and other regulatory systems (in pathogenic bacteria).

Given the problems of drug targets affecting hosts adversely and increased resistance of pathogens to antibiotics, further knowledge of (*B. cenocepacia*) ECF σ factors could yield new prospective drug targets specific to the organism. Detailed study of ECF σ factors could reveal the relationship between their gene sequence and pathogenesis. The ECF regulon itself could also be modified to generate attenuated strains of pathogens and thus vaccines.

The relative importance of the various iron acquisition mechanisms (potentially) active during Burkholderia infection of a human host is still poorly understood. A number of studies of *B. cenocepacia* addressing this question have generated apparently conflicting results. Whether high affinity iron acquisition systems are essential for successful colonization of the CF lung and which mechanisms are the most significant requires further study.

Future work

Due to the time limitation, the *in vitro* transcription experiment could not be accomplished. So far, all the constructs used for these experiments were made as described in Section 4.12. There are two reasons for carrying out an *in vitro* transcription experiment: the first is to confirm that FlrS is a σ factor. The second reason is to determine whether $FlrR_{NTD}$ activates FlrS *in vitro*. To confirm that FlrS is a σ factor the assay would be carried out using candidate σ FlrS-dependent promoter P_{flrA}, *E. coli* core RNAP and *E. coli* core RNAP + FlrS. To determine whether $FlrR_{NTD}$ activates FlrS the *E. coli* core RNAP, FlrS and $FlrR_{NTD}$ will be included in the assay. Also, assay would be carried out in the presence of candidate σ^{70}-dependent promoter P_{flrS}. The σ^{70}-dependent promoter P_{lacUV5}, *E. coli* core RNAP and FlrS or σ^{70} will be included as a separate control for this experiment. Moreover, as orthologues of *Pseudomonas* FlrS have been tested at the P_{flrA} promoter *in vivo* it would be necessary to test them at P_{flrA} *in vitro*.

During this study, several unsuccessful attempts were made to identify the transcription start site of P_{flrA} and P_{flrS} promoters. It would be extremely essential to perform the experiment using the same methods, ART-TSS, as the unexpected result may be due to technical error. It could also be possible to use a different approach, such as primer extension, to determine the transcription start site of both promoter regions.

Appendix

8.1 P_{flrA} deletion derivatives:

P_{flrA} full-length	GTCCACTACCTGACGCGTTACTGGGCGACCGTCGTGCCGGC CCGTTCG**TGA**GCGCGCCGGAAAATTTTTTCGCCGACCTGAG CTGTTTCTTGATGTTCGCGTGACATGGGTCATGAAAGCAGC ACTGGCCCATCGTCCACCGACTCTCCGATC**ATG**GCTTCCAT CC
P_{flrA}long	GCGCGCCGGAAAATTTTTTCGCCGACCTGAGCTGTTTCTTG ATGTTCGCGTGACATGGGTCATGAAAGCAGCACTGGCCCAT CGT
P_{flrA}inter	ACCTGAGCTGTTTCTTGATGTTCGCGTGACATGGGTCATGA AAGCAGCACTGGCCCA
P_{flrA}short	GATGTTCGCGTGACATGGGTCATGAAAGCAGCACTGGCCCA TCGT
P_{flrA}UP	GGAAAATTTTTTCGCCGACCTGAGCTGTTTCTTGATGTTCG CGTGACATGGGTCATGAAAG
$P_{flrAds1}$	ACCTGAGCTGTTTCTTGATGTTCGCGTGACATGGGTCATGA AAG
P_{flrA}vshort	ACCTGAGCTGTTTCTTGATGTTCGCGTGACATGGGTCATGA AA
P_{flrA}core	ACCTGAGCTGTTTCTTGATGTTCGCGTGACATGGGTCA
P_{flrA}vvshort	ACCTGAGCTGTTTCTTGATGTTCGCG

8.2 All P_{flrA} deletion derivatives:

ds1	AGCTTACCTGAGCTGTTTCTTGATGTTCGCGTGACATGGGTCATGAAAGG GATCCCTTTCATGACCCATGTCACGCGAACATCAAGAAACAGCTCAGGTA
ds2	AGCTT**C**CCTGAGCTGTTTCTTGATGTTCGCGTGACATGGGTCATGAAAGG GATCCCTTTCATGACCCATGTCACGCGAACATCAAGAAACAGCTCAGG**G**A
ds3	AGCTT**A**ACTGAGCTGTTTCTTGATGTTCGCGTGACATGGGTCATGAAAGG GATCCCTTTCATGACCCATGTCACGCGAACATCAAGAAACAGCTCAG**T**TA
ds4	AGCTTAC**A**TGAGCTGTTTCTTGATGTTCGCGTGACATGGGTCATGAAAGG GATCCCTTTCATGACCCATGTCACGCGAACATCAAGAAACAGCTCA**T**GTA

ds5	AGCTTACCGGAGCTGTTTCTTGATGTTCGCGTGACATGGGTCATGAAAGG GATCCCTTTCATGACCCATGTCACGCGAACATCAAGAAACAGCTCCGGTA
ds6	AGCTTACCTTAGCTGTTTCTTGATGTTCGCGTGACATGGGTCATGAAAGG GATCCCTTTCATGACCCATGTCACGCGAACATCAAGAAACAGCTAAGGTA
ds7	AGCTTACCTGCGCTGTTTCTTGATGTTCGCGTGACATGGGTCATGAAAGG GATCCCTTTCATGACCCATGTCACGCGAACATCAAGAAACAGCGCAGGTA
ds8	AGCTTACCTGATCTGTTTCTTGATGTTCGCGTGACATGGGTCATGAAAGG GATCCCTTTCATGACCCATGTCACGCGAACATCAAGAAACAGATCAGGTA
Ds9	AGCTTACCTGAGATGTTTCTTGATGTTCGCGTGACATGGGTCATGAAAGG GATCCCTTTCATGACCCATGTCACGCGAACATCAAGAAACATCTCAGGTA
Ds10	AGCTTACCTGAGCGGTTTCTTGATGTTCGCGTGACATGGGTCATGAAAGG GATCCCTTTCATGACCCATGTCACGCGAACATCAAGAAACCGCTCAGGTA
Ds11	AGCTTACCTGAGCTTTTTCTTGATGTTCGCGTGACATGGGTCATGAAAGG GATCCCTTTCATGACCCATGTCACGCGAACATCAAGAAAAAGCTCAGGTA
Ds12	AGCTTACCTGAGCTGGTTCTTGATGTTCGCGTGACATGGGTCATGAAAGG GATCCCTTTCATGACCCATGTCACGCGAACATCAAGAACCAGCTCAGGTA
Ds13	AGCTTACCTGAGCTGTGTCTTGATGTTCGCGTGACATGGGTCATGAAAGG GATCCCTTTCATGACCCATGTCACGCGAACATCAAGACCACAGCTCAGGTA
Ds14	AGCTTACCTGAGCTGTTGCTTGATGTTCGCGTGACATGGGTCATGAAAGG GATCCCTTTCATGACCCATGTCACGCGAACATCAAGCAACAGCTCAGGTA
Ds15	AGCTTACCTGAGCTGTTTAATTGATGTTCGCGTGACATGGGTCATGAAAGG GATCCCTTTCATGACCCATGTCACGCGAACATCAATAAACAGCTCAGGTA
Ds16	AGCTTACCTGAGCTGTTTCGTGATGTTCGCGTGACATGGGTCATGAAAGG GATCCCTTTCATGACCCATGTCACGCGAACATCACGAAACAGCTCAGGTA
Ds17	AGCTTACCTGAGCTGTTTCTGGATGTTCGCGTGACATGGGTCATGAAAGG GATCCCTTTCATGACCCATGTCACGCGAACATCCAGAAACAGCTCAGGTA
Ds18	AGCTTACCTGAGCTGTTTCTTTATGTTCGCGTGACATGGGTCATGAAAGG GATCCCTTTCATGACCCATGTCACGCGAACATAAAGAAACAGCTCAGGTA
Ds19	AGCTTACCTGAGCTGTTTCTTGCTGTTCGCGTGACATGGGTCATGAAAGG GATCCCTTTCATGACCCATGTCACGCGAACAGCAAGAAACAGCTCAGGTA
Ds20	AGCTTACCTGAGCTGTTTCTTGAGGTTCGCGTGACATGGGTCATGAAAGG GATCCCTTTCATGACCCATGTCACGCGAACCTCAAGAAACAGCTCAGGTA
Ds21	AGCTTACCTGAGCTGTTTCTTGATTTTCGCGTGACATGGGTCATGAAAGG

	GATCCCTTTCATGACCCATGTCACGCGAA**A**ATCAAGAAACAGCTCAGGTA
Ds22	AGCTTACCTGAGCTGTTTCTTGATG**G**TCGCGTGACATGGGTCATGAAAGG GATCCCTTTCATGACCCATGTCACGCGAC**C**ATCAAGAAACAGCTCAGGTA
Ds23	AGCTTACCTGAGCTGTTTCTTGATGT**G**CGCGTGACATGGGTCATGAAAGG GATCCCTTTCATGACCCATGTCACGCG**C**ACATCAAGAAACAGCTCAGGTA
Ds24	AGCTTACCTGAGCTGTTTCTTGATGTT**A**GCGTGACATGGGTCATGAAAGG GATCCCTTTCATGACCCATGTCACGC**T**AACATCAAGAAACAGCTCAGGTA
Ds25	AGCTTACCTGAGCTGTTTCTTGATGTTC**T**CGTGACATGGGTCATGAAAGG GATCCCTTTCATGACCCATGTCACG**A**GAACATCAAGAAACAGCTCAGGTA
Ds26	AGCTTACCTGAGCTGTTTCTTGATGTTCG**A**GTGACATGGGTCATGAAAGG GATCCCTTTCATGACCCATGTCAC**T**CGAACATCAAGAAACAGCTCAGGTA
Ds27	AGCTTACCTGAGCTGTTTCTTGATGTTCGC**T**TGACATGGGTCATGAAAGG GATCCCTTTCATGACCCATGTCA**A**GCGAACATCAAGAAACAGCTCAGGTA
Ds28	AGCTTACCTGAGCTGTTTCTTGATTTCGCG**G**GACATGGGTCATGAAAGG GATCCCTTTCATGACCCATGTC**C**CGCGAACATCAAGAAACAGCTCAGGTA
Ds29	AGCTTACCTGAGCTGTTTCTTGATGTTCGCGT**T**ACATGGGTCATGAAAGG GATCCCTTTCATGACCCATGT**A**ACGCGAACATCAAGAAACAGCTCAGGTA
Ds30	AGCTTACCTGAGCTGTTTCTTGATGTTCGCGTG**C**CATGGGTCATGAAAGG GATCCCTTTCATGACCCATG**G**CACGCGAACATCAAGAAACAGCTCAGGTA
Ds31	AGCTTACCTGAGCTGTTTCTTGATGTTCGCGTGA**A**ATGGGTCATGAAAGG GATCCCTTTCATGACCCAT**T**TCACGCGAACATCAAGAAACAGCTCAGGTA
Ds32	AGCTTACCTGAGCTGTTTCTTGATGTTCGCGTGAC**C**TGGGTCATGAAAGG GATCCCTTTCATGACCCA**G**GTCACGCGAACATCAAGAAACAGCTCAGGTA
Ds33	AGCTTACCTGAGCTGTTTCTTGATGTTCGCGTGACA**G**GGGTCATGAAAGG GATCCCTTTCATGACCC**C**TGTCACGCGAACATCAAGAAACAGCTCAGGTA
Ds34	AGCTTACCTGAGCTGTTTCTTGATGTTCGCGTGACAT**T**GGTCATGAAAGG GATCCCTTTCATGACC**A**ATGTCACGCGAACATCAAGAAACAGCTCAGGTA
Ds35	AGCTTACCTGAGCTGTTTCTTGATGTTCGCGTGACATG**T**GTCATGAAAGG GATCCCTTTCATGACACATGTCACGCG**A**ACATCAAGAAACAGCTCAGGTA
Ds36	AGCTTACCTGAGCTGTTTCTTGATGTTCGCGTGACATGG**T**TCATGAAAGG GATCCCTTTCATGA**A**CCATGTCACGCGAACATCAAGAAACAGCTCAGGTA
Ds37	AGCTTACCTGAGCTGTTTCTTGATGTTCGCGTGACATGGG**G**CATGAAAGG GATCCCTTTCATG**C**CCCATGTCACGCGAACATCAAGAAACAGCTCAGGTA

Ds38	AGCTTACCTGAGCTGTTTCTTGATGTTCGCGTGACATGGGT**A**ATGAAAGG GATCCCTTTCAT**T**ACCCATGTCACGCGAACATCAAGAAACAGCTCAGGTA
Ds39	AGCTTACCTGAGCTGTTTCTTGATGTTCGCGTGACATGGGTC**C**TGAAAGG GATCCCTTTCA**G**GACCCATGTCACGCGAACATCAAGAAACAGCTCAGGTA
Ds40	AGCTTACCTGAGCTGTTTCTTGATGTTCGCGTGACATGGGTCA**G**GAAAGG GATCCCTTTC**C**TGACCCATGTCACGCGAACATCAAGAAACAGCTCAGGTA
Ds41	AGCTTACCTGAGCTGTTTCTTGATGTTCGCGTGACATGGGTCAT**T**AAAGG GATCCCTTT**A**ATGACCCATGTCACGCGAACATCAAGAAACAGCTCAGGTA
Ds42	AGCTTACCTGAGCTGTTTCTTGATGTTCGCGTGACATGGGTCATG**C**AAGG GATCCCTT**G**CATGACCCATGTCACGCGAACATCAAGAAACAGCTCAGGTA
Ds43	AGCTTACCTGAGCTGTTTCTTGATGTTCGCGTGACATGGGTCATGA**C**AGG GATCCCT**G**TCATGACCCATGTCACGCGAACATCAAGAAACAGCTCAGGTA
Ds44	AGCTTACCTGAGCTGTTTCTTGATGTTCGCGTGACATGGGTCATGAA**C**GG GATCCC**G**TTCATGACCCATGTCACGCGAACATCAAGAAACAGCTCAGGTA
Ds45	AGCTTACCTGAGCTGTTTCTTGATGTTCGCGTGACATGGGTCATGAAA**T**G GATCC**A**TTTCATGACCCATGTCACGCGAACATCAAGAAACAGCTCAGGTA

8.3 Primers used in this study:

Primer names	Sequences (5' to 3')
FlrRNTDKTfor	GCGCCTGCAGCGGTGCCGCCGCACGTTGCACG
FlrRNTDfor2	GCGCCTGCAGCGTGCCGCCGCACGTTGCACG
FlrSCTDfor2	GCGCCTGCAGCGCCGTCGTCGTCGAGACGCT
FlrSCTDrev	GCGCGGATCCCTCAGGCCGCCATCGCGAAAA
$FlrR_{CTD}$for	GCGCTCTAGAGATGGCCGAACCCGCGCGGCG
$FlrR_{CTD}$rev	GCGCGGATCCGTCACGAACGGGCCGGCACG
$FlrR_{CTD}$rev2	CCGGGGATCCGACGAACGGGCCGGCACGACGG
$FlrA_{NTD}$for	GCGCTCTAGAGAATGTGCCGCGCGCGTCGCGCCCG
$FlrA_{NTD}$rev1	GCGCGGATCCGGCGGGCCGGCCGGAATGTCGTGA
$FlrA_{NTD}$rev1	GCGCGGATCCGGCGGGCCGGCCGGAATGTCG
M13for	GTAAAACGACGGCCAGT
FlrRforOut	GAACTCGGCGTATCGCTCGC
pFlrArev2	GACGGCGCCGATACGTGAGA

FlrRNTDforVSV-G	GCGCCATATGGTGCCGCCGCACGTTGCACGT
FlrRNTDrevVSV-G	GCGCAGATCTTAACTTACCCAGGCGGTTCATTTCG ATATCAGTGTACTTCGCGGCCGCGCGGCGGCC
FlrSCTDforHis	GCGCGGATCCGGTAGTGGCGCCGTCGCCGGAA
FlrSCTDrevHis	GCGCCTGCAGTCAGGCCGCCATCGTGAAAAA
FlrANTDforVSV-G	GCGCCATATGGACACCGACGCCGATGCGGC
FlrANTDREVVSV-G	GcgcAGATCTTTACTTACCCAGGCGGTTCATTTCG ATATCAGTGTAGAGCAGCGGAATGTCCGAGC
FlrRCTDforHis	GCGCGGATCCGGAACCCGCGCGGCGCGCGG
FlrRCTDrevHis	GCGCCTGCAGTCACGAACGGGCCGGCACGA
pACYC-T7-1for	GGATCTCGACGCTCTCCCT
pACYC-T7-1rev	TTGTACACGGCCGCATAATC
pACYC-T7-2for	TTGTACACGGCCGCATAATC
T7rev	GCTAGTTATTGCTCAGCGGT
PA0149for	GCGCAAGCTTAACTTCCATGCCTTGCAGCA
PA0149rev	GCGCGGATCCTATCGGGTCGAGTCATGGCT
AP10	GAACGCTCTCCTGAGTA
AP11	CCGACTCACTATAGAGG
pMALMC5Xfor	GGTCGTCAGACTGTCGATGAAGCC
pMALMC5Xrev	TGTCCTACTCAGGAGAGCGTTCAC
PSPTO1209For	GCGCAAGCTTATAGAGTCCCCGTGGATTGTTCTC
PSPTO1209Rev	GCGCGGATCCTCATAAGGCGAAGTAGCAGC
FullFlrSFor	GCGCGGATCCGATGTCCGCTGACAAGCTGTCC
FullFlrSrev	GCGCCTGCAGTCAGGCCGCCATCGCGAAAAA
FlrRNTD-Hisfor	CCATGGGCGTGCCGCCGCACGTTGCACGT
FlrRNTD-Hisrev	GGATCCTCAGTGGTGATGATGGTGATGCTTCGCGG CCGCGCGGCGGCC
BCAM2439forOut	TCGATCCAACCGTCGGCTAT
BCAM2439revOut	GCGCTTGTCGATCTGGTACA
PA0149for	GCGCAAGCTTAACTTCCATGCCTTGCAGCA
PA0149rev	GCGCGGATCCTATCGGGTCGAGTCATGGCT
ApRG7702_1204for	GAAGTGAAACGCCGTAGCG
ApRG7702_1204Rev	GTATCACGAGGCCCTTTCG

8.3 Sequences of oligonucleotides used in this study:

Oligonucleotide names	Sequences (5' to 3')
flrRstopfor2	GCGGCCGCGAAGTAAGGATCCGAGCT
flrRstoprev2	CGCGCCGGCGCTTCATTCCTAGGC
pPSPTO1207dsfor	AGCTTAAACGTGAGCCGTTTTCTGCCGCTCGCGT GACAGACAGGGAAAGCATCTCG
pPSPTO1207dsRev	GATCCGAGATGCTTTCCCTGTCTGTCACGCGAGC GGCAGAAAACGGCTCACGTTTA
PflrSvshortdsFor	AGCTTTTTTGTATATAATAATCATTCTCATTTAC AAAGTGGTTGATGCTCG
PflrSvshortdsRev	GATCCGAGCATCAACCACTTTGTAAATGAGAATG ATTATTATATACAAAAA
PflrSvshort (-11G)dsFor	AGCTTTTTTGTATATAATAATCATTCTCATTTGC AAAGTGGTTGATGCTCG
PflrSvshort (-11G)dsRev	GATCCGAGCATCAACCACTTTGCAAATGAGAATG ATTATTATATACAAAAA
pflrAtriT1For	AGCTTACCTGAGCTGGGTCTTGATGTTCGCGTGA CATGGGTCATGAAAGG
pflrAtriT1Rev	GATCCCTTTCATGACCCATGTCACGCGAACATCA AGACCCAGCTCAGGTA
pflrAtriT2For	AGCTTACCTGAGCTGTGGCTTGATGTTCGCGTGA CATGGGTCATGAAAGG
pflrAtriT2Rev	GATCCCTTTCATGACCCATGTCACGCGAACATCA AGCCACAGCTCAGGTA
pflrAtriT3For	AGCTTACCTGAGCTGGGGCTTGATGTTCGCGTGA CATGGGTCATGAAAGG
pflrAtriT3Rev	GATCCCTTTCATGACCCATGTCACGCGAACATCA AGCCCCAGCTCAGGTA
pflrAdsSP-1For	AGCTTACCTGAGCTGTTTCTGATGTTCGCGTGAC ATGGGTCATGAAAGG
pflrAdsSP-1Rev	GATCCCTTTCATGACCCATGTCACGCGAACATCA GAAACAGCTCAGGTA
pflrAtriTXFor	AGCTTACCTGAGCTGTTTTTTGATGTTCGCGTGA CATGGGTCATGAAAGG
pflrAtriTXRev	GATCCCTTTCATGACCCATGTCACGCGAACATCA AAAAACAGCTCAGGTA
pflrAtriTXSP-1For	AGCTTACCTGAGCTGTTTTTGATGTTCGCGTGAC ATGGGTCATGAAAGG
pflrAtriTXSP-1Rev	GATCCCTTTCATGACCCATGTCACGCGAACATCA AAAACAGCTCAGGTA
pflrAvFor	AATTCACCTGAGCTGTTTCTTGATGTTCGCGTGA CATGGGTCATGAAAGCAGCACA

pflrAvRev	AGCTTGTGCTGCTTTCATGACCCATGTCACGCGA ACATCAAGAAACAGCTCAGGTG
PflrAApRG7702for	AATTCACCTGAGCTGTTTCTTGATGTTCGCGTGA CATGGGTcATGAAAGCAGCACG
PflrAApRG7702Rer	GATCCGTGCTGCTTTCATGACCCATGTCACGCGA ACATCAAGAAACAGCTCAGGTA
pBlue-PflrSvshortdsFor	AGCTTTTTTGTATATAATAATCATTCTCATTTAC AAAGTGGTTGATGCTCG
pBlue-PflrSvshortdsRor	GATCCGAGCATCAACCACTTTGTAAATGAGAATG ATTATTATATACAAAAA

8.4 Transcription start site primers:

P_{flrS}startR1	ACGAACGTGTCGTGCGCGAGG
P_{flrS}startR2	CGCAACCACGCGTGGTGGTCG
P_{flrS}startF3	TCGGGTGCGCGCACCGCGCCG
P_{flrA}startR1	GGCAGCAGTGCCGACAGCAGG
P_{flrA}startR2	CGCGACGCGCGCGGCAGATGA
P_{flrA}startF3	TTGCCCGCCGGCTCGCCGGCG

8.5 RT-PCR primers:

FlrSRTFor	GAGCCGCGCGCGTTCCTGACG
FlrRRTRev	AGGTCGGCCGGCCAGATCGCC
FlrRRTFor	TGGCCGATCTCGTCGCCGAGC
FlrARTRev	AGGCCCGCCGTCAGCTCGGCC
FlrARTFor	ACAGCTTCACGCTGCCGTCGT
FlrXRTRev	TGGCCGATGCGTTCGTCGACC

8.6 pBBR2-FlrR$_{NTD}$

NNNNNNNNNNNNNCCCTCACTAAAGGGAACAAAAGCTGGGTACCGGGCCCCCCCTCGAGG
TCGACGGTATCGATAAGCTTGAAGCGCTATCTCGTGAAGGCCGGCACGCAGTGCTTTTTC
ACGATGGCGGCCTGACCGATGGCCGCCCCGGGAGCGCCGGCGGTGCCGCCGCACGTTGCA
CGTCGCGCGGTCGAATGGTGGGTCGACCGGCAATCCGGCCGTACCGACGACGCATTCGTC
GCCGCGCTCGCGCGCTGGCGCGCGGAAGATCCGGCGCACGACGCGGCGTGGCGTCACATC
GAAGCGATGCAGGGCCGGTTCGGCCGGCTGGCGGCCGGGCTCGATGCGCAGGCCGCGCAC
GCGGCGCTGTTGCCGAAGCGGGCAGGCCGCCGCGGGCGCGAAGTAAGGATCCACTAGTTC
TAGAGCGGCCGCCACCGCGGTGGAGCTCCAATTCGCCCTATAGTGAGTCGTATTACGCGC
GCTCACTGGCCGTCGTTTTACAACGTCGTGACTGGGAAAACCCTGGCGTTACCCAACTTA
ATCGCCTTGCAGCACATCCCCCTTTCGCCAGCTGGCGTAATAGCGAAGAGGCCCGCACCG
ATCGCCCTTCCCAACAGTTGCGCAGCCTGAATGGCGAATGGAAATTGTAAGCGTTAATAT
TTTGTTAAAATTCGCGTTAAATTTTTGTTAAATCAGCTCATTTTTTAACCAATAGGCCGT
ACTGCGATGAGTGGCAGGGCGGGGCGTAATTTTTTTAAGGCAGTTATTGGTGCCCTTAAA

The change of *flrR* DNA sequence and amino acids sequence is shown sequence in the table below:

WT	ggccgccgcgcggccgcgaagTAAggatccactagttctaga	GRRAAAK*
clone 2	gGCCGCCGCG-GG-CGCGAAGTAAggatccactagttctaga	GRRGREVRIH*

8.7 DNA and protein ladders used in this study:

DNA ladders:

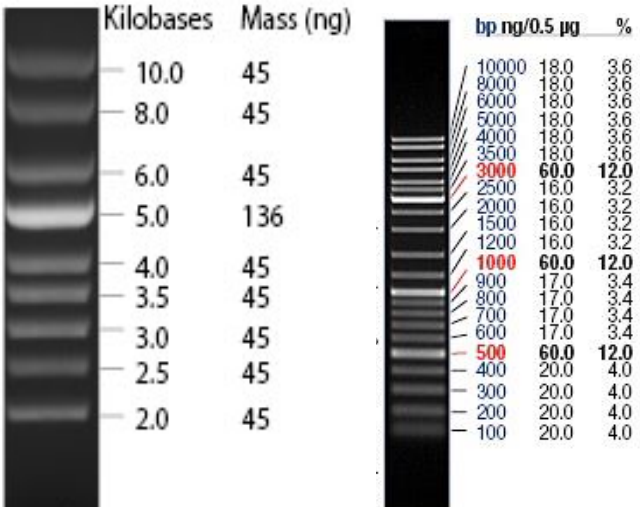

Supercoiled DNA ladder GeneRuler DNA ladder mix

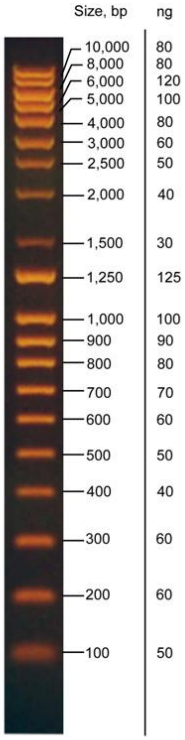

Q-Step 4Quantitative DNA Ladder

Proteins ladders:

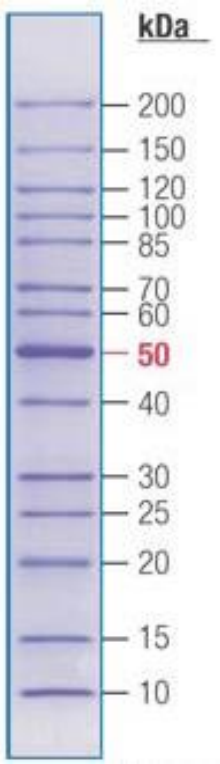

EZ-Run *Rec* Protein Ladder

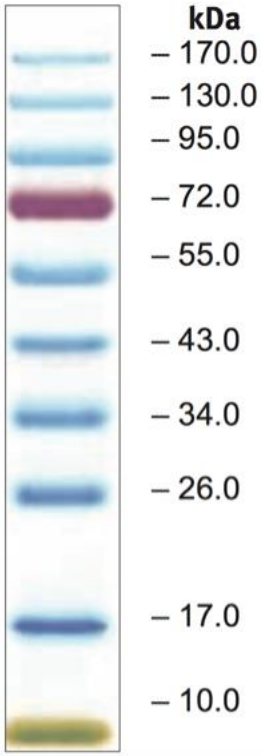

EZ-Run Prestained *Rec* Protein Ladder

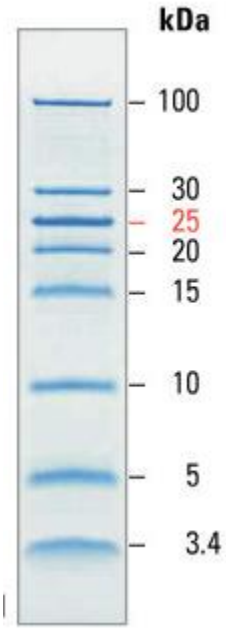

PageRuler Unstained Low Range Protein Ladder

References

ABI-KHALIL, E., SEGOND, D., TERPSTRA, T., ANDRE-LEROUX, G., KALLASSY, M., LERECLUS, D., BOU-ABDALLAH, F. & NIELSEN-LEROUX, C. 2015. Heme interplay between IlsA and IsdC: Two structurally different surface proteins from Bacillus cereus. Biochim Biophys Acta, 1850, 1930-41.

AGNOLI, K., LOWE, C. A., FARMER, K. L., HUSNAIN, S. I. & THOMAS, M. S. 2006. The ornibactin biosynthesis and transport genes of Burkholderia cenocepacia are regulated by an extracytoplasmic function sigma factor which is a part of the Fur regulon. J Bacteriol, 188, 3631-44.

ALBA, B. M., ZHONG, H. J., PELAYO, J. C. & GROSS, C. A. 2001. degS (hhoB) is an essential Escherichia coli gene whose indispensable function is to provide sigma (E) activity. Mol Microbiol, 40, 1323-33.

ALLEN, C. E. & SCHMITT, M. P. 2009. HtaA is an iron-regulated hemin binding protein involved in the utilization of heme iron in Corynebacterium diphtheriae. J Bacteriol, 191, 2638-48.

ANDREWS, S. C., ROBINSON, A. K. & RODRIGUEZ-QUINONES, F. 2003. Bacterial iron homeostasis. FEMS Microbiol Rev, 27, 215-37.

ANKENBAUER, R. G., TOYOKUNI, T., STALEY, A., RINEHART, K. L., JR. & COX, C. D. 1988. Synthesis and biological activity of pyochelin, a siderophore of Pseudomonas aeruginosa. J Bacteriol, 170, 5344-51.

ANZALDI, L. L. & SKAAR, E. P. 2010. Overcoming the heme paradox: heme toxicity and tolerance in bacterial pathogens. Infect Immun, 78, 4977-89.

AOYAMA, T., TAKANAMI, M., OHTSUKA, E., TANIYAMA, Y., MARUMOTO, R., SATO, H. & IKEHARA, M. 1983. Essential structure of E. coli promoter: effect of spacer length between the two consensus sequences on promoter function. Nucleic Acids Res, 11, 5855-64.

ASGHAR, A. H., SHASTRI, S., DAVE, E., WOWK, I., AGNOLI, K., COOK, A. M. & THOMAS, M. S. 2011. The pobA gene of Burkholderia cenocepacia encodes a

group I Sfp-type phosphopantetheinyltransferase required for biosynthesis of the siderophores ornibactin and pyochelin. Microbiology, 157, 349-61.

AUBLE, D. T., ALLEN, T. L. & DEHASETH, P. L. 1986. Promoter recognition by Escherichia coli RNA polymerase. Effects of substitutions in the spacer DNA separating the -10 and -35 regions. J Biol Chem, 261, 11202-6.

BAGG, A. & NEILANDS, J. B. 1987a. Molecular mechanism of regulation of siderophore-mediated iron assimilation. Microbiol Rev, 51, 509-18.

BAICHOO, N. & HELMANN, J. D. 2002. Recognition of DNA by Fur: a reinterpretation of the Fur box consensus sequence. J Bacteriol, 184, 5826-32.

BAKER, H. M. & BAKER, E. N. 2004. Lactoferrin and iron: structural and dynamic aspects of binding and release. Biometals, 17, 209-16.

BALDWIN, A., SOKOL, P. A., PARKHILL, J. & MAHENTHIRALINGAM, E. 2004. The Burkholderia cepacia epidemic strain marker is part of a novel genomic island encoding both virulence and metabolism-associated genes in Burkholderia cenocepacia. Infect Immun, 72, 1537-47.

BAMFORD, S., RYLEY, H. & JACKSON, S. K. 2007a. Highly purified lipopolysaccharides from Burkholderia cepacia complex clinical isolates induce inflammatory cytokine responses via TLR4-mediated MAPK signalling pathways and activation of NFkappaB. Cell Microbiol, 9, 532-43.

BANIN, E., VASIL, M. L. & GREENBERG, E. P. 2005. Iron and Pseudomonas aeruginosa biofilm formation. Proc Natl Acad Sci U S A, 102, 11076-81.

BARELMANN, I., J. M. MEYER, K. TARAZ, AND H. BUDZIKIEWICZ 1996. Cepaciachelin, a new catecholate siderophore from

BARNE, K. A., BOWN, J. A., BUSBY, S. J. & MINCHIN, S. D. 1997. Region 2.5 of the Escherichia coli RNA polymerase sigma70 subunit is responsible for the recognition of the 'extended-10' motif at promoters. Embo j, 16, 4034-40.

BARNES, C. M., THEIL, E. C. & RAYMOND, K. N. 2002. Iron uptake in ferritin is blocked by binding of [Cr(TREN)(H(2)O)(OH)](2+), a slow dissociating model for [Fe(H(2)O)(6)](2+). Proc Natl Acad Sci U S A, 99, 5195-200.

BASHYAM, M. D. & HASNAIN, S. E. 2004. The extracytoplasmic function sigma factors: role in bacterial pathogenesis. Infect Genet Evol, 4, 301-8.

BASTIAANSEN, K. C., OTERO-ASMAN, J. R., LUIRINK, J., BITTER, W. & LLAMAS, M. A. 2015. Processing of cell-surface signalling anti-sigma factors prior to signal recognition is a conserved autoproteolytic mechanism that produces two functional domains. Environ Microbiol, 17, 3263-77.

BATTESTI, A. & BOUVERET, E. 2012. The bacterial two-hybrid system based on adenylate cyclase reconstitution in Escherichia coli. Methods, 58, 325-34.

BENSON, A. K. & HALDENWANG, W. G. 1993. Bacillus subtilis sigma B is regulated by a binding protein (RsbW) that blocks its association with core RNA polymerase. Proc Natl Acad Sci U S A, 90, 2330-4.

BEUTEL, B. A. & RECORD, M. T., JR. 1990. E. coli promoter spacer regions contain nonrandom sequences which correlate to spacer length. Nucleic Acids Res, 18, 3597-603.

BIEMANS-OLDEHINKEL, E., DOEVEN, M. K. & POOLMAN, B. 2006. ABC transporter architecture and regulatory roles of accessory domains. FEBS Lett, 580, 1023-35.

BILLINGS, N., MILLAN, M., CALDARA, M., RUSCONI, R., TARASOVA, Y., STOCKER, R. & RIBBECK, K. 2013. The extracellular matrix Component Psl provides fast-acting antibiotic defense in Pseudomonas aeruginosa biofilms. PLoS Pathog, 9, e1003526.

BOBROV, A. G., KIRILLINA, O., VADYVALOO, V., KOESTLER, B. J., HINZ, A. K., MACK, D., WATERS, C. M. & PERRY, R. D. 2015. The Yersinia pestis HmsCDE regulatory system is essential for blockage of the oriental rat flea (Xenopsylla cheopis), a classic plague vector. Environ Microbiol, 17, 947-59.

BOCHKAREVA, A. & ZENKIN, N. 2013. The sigma70 region 1.2 regulates promoter escape by unwinding DNA downstream of the transcription start site. Nucleic Acids Res, 41, 4565-72.

BONYHADY, R. E., HENDRY, I. A., HILL, C. E. & MCLENNAN, I. S. 1982. Effects of haemin on neurones derived from the neural crest. Dev Neurosci, 5, 125-9.

BORTHS, E. L., LOCHER, K. P., LEE, A. T. & REES, D. C. 2002. The structure of Escherichia coli BtuF and binding to its cognate ATP binding cassette transporter. Proc Natl Acad Sci U S A, 99, 16642-7.

BORUKHOV, S. & NUDLER, E. 2003. RNA polymerase holoenzyme: structure, function and biological implications. Curr Opin Microbiol, 6, 93-100.

BOUCHER, R. C. 2007. Evidence for airway surface dehydration as the initiating event in CF airway disease. J Intern Med, 261, 5-16.

BRAUD, A., GEOFFROY, V., HOEGY, F., MISLIN, G. L. & SCHALK, I. J. 2010. Presence of the siderophores pyoverdine and pyochelin in the extracellular medium reduces toxic metal accumulation in Pseudomonas aeruginosa and increases bacterial metal tolerance. Environ Microbiol Rep, 2, 419-25.

BRAUD, A., HANNAUER, M., MISLIN, G. L. & SCHALK, I. J. 2009a. The Pseudomonas aeruginosa pyochelin-iron uptake pathway and its metal specificity. J Bacteriol, 191, 3517-25.

BRAUD, A., HOEGY, F., JEZEQUEL, K., LEBEAU, T. & SCHALK, I. J. 2009b. New insights into the metal specificity of the Pseudomonas aeruginosa pyoverdine-iron uptake pathway. Environ Microbiol, 11, 1079-91.

BRAUD, A., JEZEQUEL, K., BAZOT, S. & LEBEAU, T. 2009. Enhanced phytoextraction of an agricultural Cr- and Pb-contaminated soil by bioaugmentation with siderophore-producing bacteria. Chemosphere, 74, 280-6.

BRAUN, V., MAHREN, S. & OGIERMAN, M. 2003. Regulation of the FecI-type ECF sigma factor by transmembrane signalling. Curr Opin Microbiol, 6, 173-80.

BREIDENSTEIN, E., MAHREN, S. & BRAUN, V. 2006. Residues involved in FecR binding are localized on one side of the FecA signaling domain in Escherichia coli. J Bacteriol, 188, 6440-2.

BRICKMAN, T. J. & ARMSTRONG, S. K. 2012. Iron and pH-responsive FtrABCD ferrous iron utilization system of Bordetella species. Mol Microbiol, 86, 580-93.

BROWN, J. S. & HOLDEN, D. W. 2002. Iron acquisition by Gram-positive bacterial pathogens. Microbes Infect, 4, 1149-56.

BROWNING, D. F. & BUSBY, S. J. 2004. The regulation of bacterial transcription initiation. Nat Rev Microbiol, 2, 57-65.

BURGESS, R. R., TRAVERS, A. A., DUNN, J. J. & BAUTZ, E. K. 1969. Factor stimulating transcription by RNA polymerase. Nature, 221, 43-6.

BURKHOLDER & W.H 1950. Sour skin, a bacterial rot of onion bulbs phytopathology. 40, 115-11.

BURNS, J. L., WADSWORTH, C. D., BARRY, J. J. & GOODALL, C. P. 1996. Nucleotide sequence analysis of a gene from Burkholderia (Pseudomonas) cepacia encoding an outer membrane lipoprotein involved in multiple antibiotic resistance. Antimicrob Agents Chemother, 40, 307-13.

BUTCHER, B. G., BRONSTEIN, P. A., MYERS, C. R., STODGHILL, P. V., BOLTON, J. J., MARKEL, E. J., FILIATRAULT, M. J., SWINGLE, B., GABALLA, A., HELMANN, J. D., SCHNEIDER, D. J. & CARTINHOUR, S. W. 2011. Characterization of the Fur regulon in Pseudomonas syringae pv. tomato DC3000. J Bacteriol, 193, 4598-611.

BYERS, B. R. & ARCENEAUX, J. E. 1998. Microbial iron transport: iron acquisition by pathogenic microorganisms. Met Ions Biol Syst, 35, 37-66.

CADIEUX, N., BAREKZI, N. & BRADBEER, C. 2007. Observations on the calcium dependence and reversibility of cobalamin transport across the outer membrane of Escherichia coli. J Biol Chem, 282, 34921-8.

CAMPBELL, E. A., MASUDA, S., SUN, J. L., MUZZIN, O., OLSON, C. A., WANG, S. & DARST, S. A. 2002a. Crystal structure of the Bacillus stearothermophilus anti-sigma factor SpoIIAB with the sporulation sigma factor sigmaF. Cell, 108, 795-807.

CAMPBELL, E. A., MUZZIN, O., CHLENOV, M., SUN, J. L., OLSON, C. A., WEINMAN, O., TRESTER-ZEDLITZ, M. L. & DARST, S. A. 2002b. Structure of

the bacterial RNA polymerase promoter specificity sigma subunit. Mol Cell, 9, 527-39.

CAMPBELL, E. A., TUPY, J. L., GRUBER, T. M., WANG, S., SHARP, M. M., GROSS, C. A. & DARST, S. A. 2003. Crystal structure of Escherichia coli sigmaE with the cytoplasmic domain of its anti-sigma RseA. Mol Cell, 11, 1067-78.

CAO, J., WOODHALL, M. R., ALVAREZ, J., CARTRON, M. L. & ANDREWS, S. C. 2007. EfeUOB (YcdNOB) is a tripartite, acid-induced and CpxAR-regulated, low-pH Fe2+ transporter that is cryptic in Escherichia coli K-12 but functional in E. coli O157:H7. Mol Microbiol, 65, 857-75.

CARPENTER, B. M., WHITMIRE, J. M. & MERRELL, D. S. 2009. This is not your mother's repressor: the complex role of fur in pathogenesis. Infect Immun, 77, 2590-601.

CARSON, M. R., TRAVIS, S. M. & WELSH, M. J. 1995. The two nucleotide-binding domains of cystic fibrosis transmembrane conductance regulator (CFTR) have distinct functions in controlling channel activity. J Biol Chem, 270, 1711-7.

CELIA, H., NOINAJ, N., ZAKHAROV, S. D., BORDIGNON, E., BOTOS, I., SANTAMARIA, M., BARNARD, T. J., CRAMER, W. A., LLOUBES, R. & BUCHANAN, S. K. 2016. Structural insight into the role of the Ton complex in energy transduction. Nature, 538, 60-65.

CESCUTTI, P., IMPALLOMENI, G., GAROZZO, D., STURIALE, L., HERASIMENKA, Y., LAGATOLLA, C. & RIZZO, R. 2003. Exopolysaccharides produced by a clinical strain of Burkholderia cepacia isolated from a cystic fibrosis patient. Carbohydr Res, 338, 2687-95.

CEZAIRLIYAN, B. O. & SAUER, R. T. 2007. Inhibition of regulated proteolysis by RseB. Proc Natl Acad Sci U S A, 104, 3771-6.

CHALLIS, G. L. 2005. A widely distributed bacterial pathway for siderophore biosynthesis independent of nonribosomal peptide synthetases. Chembiochem, 6, 601-11.

CHIANG, D. Y., NIX, D. A., SHULTZABERGER, R. K., GASCH, A. P. & EISEN, M. B. 2006. Flexible promoter architecture requirements for coactivator recruitment. BMC Mol Biol, 7, 16.

CHIMENTO, D. P., KADNER, R. J. & WIENER, M. C. 2005. Comparative structural analysis of TonB-dependent outer membrane transporters: implications for the transport cycle. Proteins, 59, 240-51.

CHIPPERFIELD, J. R. & RATLEDGE, C. 2000. Salicylic acid is not a bacterial siderophore: a theoretical study. Biometals, 13, 165-8.

CHU, B. C., GARCIA-HERRERO, A., JOHANSON, T. H., KREWULAK, K. D., LAU, C. K., PEACOCK, R. S., SLAVINSKAYA, Z. & VOGEL, H. J. 2010. Siderophore uptake in bacteria and the battle for iron with the host; a bird's eye view. Biometals, 23, 601-11.

CHUA, K. L., CHAN, Y. Y. & GAN, Y. H. 2003. Flagella are virulence determinants of Burkholderia pseudomallei. Infect Immun, 71, 1622-9.

COENYE, T., VANDAMME, P., GOVAN, J. R. & LIPUMA, J. J. 2001. Taxonomy and identification of the Burkholderia cepacia complex. J Clin Microbiol, 39, 3427-36.

CORREA, N. E., PENG, F. & KLOSE, K. E. 2005. Roles of the regulatory proteins FlhF and FlhG in the Vibrio cholerae flagellar transcription hierarchy. J Bacteriol, 187, 6324-32.

COSTERTON, J. W., STEWART, P. S. & GREENBERG, E. P. 1999. Bacterial biofilms: a common cause of persistent infections. Science, 284, 1318-22.

COX, C. D. & GRAHAM, R. 1979. Isolation of an iron-binding compound from Pseudomonas aeruginosa. J Bacteriol, 137, 357-64.

COX, C. D., RINEHART, K. L., JR., MOORE, M. L. & COOK, J. C., JR. 1981. Pyochelin: novel structure of an iron-chelating growth promoter for Pseudomonas aeruginosa. Proc Natl Acad Sci U S A, 78, 4256-60.

CROSA, J. H. 1997. Signal transduction and transcriptional and posttranscriptional control of iron-regulated genes in bacteria. Microbiol Mol Biol Rev, 61, 319-36.

CROSA, J. H. & WALSH, C. T. 2002. Genetics and assembly line enzymology of siderophore biosynthesis in bacteria. Microbiol Mol Biol Rev, 66, 223-49.

CROWLEY DE, W. Y. 1991. Mechanisms of iron acquisition from siderophores by microorganisms and

plants. Plant and Soil, 130, 179-198.

CULLEN, L. & MCCLEAN, S. 2015. Bacterial Adaptation during Chronic Respiratory Infections. Pathogens, 4, 66-89.

D'ONOFRIO, A., CRAWFORD, J. M., STEWART, E. J., WITT, K., GAVRISH, E., EPSTEIN, S., CLARDY, J. & LEWIS, K. 2010. Siderophores from neighbouring organisms promote the growth of uncultured bacteria. Chem Biol, 17, 254-64.

DANESE, P. N., SNYDER, W. B., COSMA, C. L., DAVIS, L. J. & SILHAVY, T. J. 1995. The Cpx two-component signal transduction pathway of Escherichia coli regulates transcription of the gene specifying the stress-inducible periplasmic protease, DegP. Genes Dev, 9, 387-98.

DARLING, P., CHAN, M., COX, A. D. & SOKOL, P. A. 1998. Siderophore production by cystic fibrosis isolates of Burkholderia cepacia. Infect Immun, 66, 874-7.

DAS, A. 1993. Control of transcription termination by RNA-binding proteins. Annu Rev Biochem, 62, 893-930.

DAVIS, P. B. 2006. Cystic fibrosis since 1938. Am J Respir Crit Care Med, 173, 475-82.

DELANY, I., SPOHN, G., RAPPUOLI, R. & SCARLATO, V. 2001. The Fur repressor controls transcription of iron-activated and -repressed genes in Helicobacter pylori. Mol Microbiol, 42, 1297-309.

DENMAN, C. C., ROBINSON, M. T., SASS, A. M., MAHENTHIRALINGAM, E. & BROWN, A. R. 2014. Growth on mannitol-rich media elicits a genome-wide transcriptional response in Burkholderia multivorans that impacts on multiple virulence traits in an exopolysaccharide-independent manner. Microbiology, 160, 187-97.

DRAPER, R. C., MARTIN, L. W., BEARE, P. A. & LAMONT, I. L. 2011. Differential proteolysis of sigma regulators controls cell-surface signalling in Pseudomonas aeruginosa. Mol Microbiol, 82, 1444-53.

DRAZEK, E. S., HAMMACK, C. A. & SCHMITT, M. P. 2000. Corynebacterium diphtheriae genes required for acquisition of iron from haemin and haemoglobin are homologous to ABC haemin transporters. Mol Microbiol, 36, 68-84.

DRUMM, M. L., ZIADY, A. G. & DAVIS, P. B. 2012. Genetic variation and clinical heterogeneity in cystic fibrosis. Annu Rev Pathol, 7, 267-82.

DUNCAN, L. & LOSICK, R. 1993. SpoIIAB is an anti-sigma factor that binds to and inhibits transcription by regulatory protein sigma F from Bacillus subtilis. Proc Natl Acad Sci U S A, 90, 2325-9.

EAVES-PYLES, T., MURTHY, K., LIAUDET, L., VIRAG, L., ROSS, G., SORIANO, F. G., SZABO, C. & SALZMAN, A. L. 2001. Flagellin, a novel mediator of Salmonella-induced epithelial activation and systemic inflammation: I kappa B alpha degradation, induction of nitric oxide synthase, induction of proinflammatory mediators, and cardiovascular dysfunction. J Immunol, 166, 1248-60

EISENHAUER, H. A., SHAMES, S., PAWELEK, P. D. & COULTON, J. W. 2005. Siderophore transport through Escherichia coli outer membrane receptor FhuA with disulfide-tethered cork and barrel domains. J Biol Chem, 280, 30574-80.

ELHASSANNY, A. E., ANDERSON, E. S., MENSCHER, E. A. & ROOP, R. M., 2ND 2013. The ferrous iron transporter FtrABCD is required for the virulence of Brucella abortus 2308 in mice. Mol Microbiol, 88, 1070-82.

ENZ, S., MAHREN, S., MENZEL, C. & BRAUN, V. 2003. Analysis of the ferric citrate transport gene promoter of Escherichia coli. J Bacteriol, 185, 2387-91.

ENZ, S., MAHREN, S., STROEHER, U. H. & BRAUN, V. 2000. Surface signaling in ferric citrate transport gene induction: interaction of the FecA, FecR, and FecI regulatory proteins. J Bacteriol, 182, 637-46.

ERNST, F. D., BERESWILL, S., WAIDNER, B., STOOF, J., MADER, U., KUSTERS, J. G., KUIPERS, E. J., KIST, M., VAN VLIET, A. H. & HOMUTH, G.

2005. Transcriptional profiling of Helicobacter pylori Fur- and iron-regulated gene expression. Microbiology, 151, 533-46.

ESCOLAR, L., PEREZ-MARTIN, J. & DE LORENZO, V. 1999. Opening the iron box: transcriptional metalloregulation by the Fur protein. J Bacteriol, 181, 6223-9.

FALLER, M., MATSUNAGA, M., YIN, S., LOO, J. A. & GUO, F. 2007. Heme is involved in microRNA processing. Nat Struct Mol Biol, 14, 23-9.

FEKLISTOV, A. & DARST, S. A. 2011. Structural basis for promoter-10 element recognition by the bacterial RNA polymerase sigma subunit. Cell, 147, 1257-69.

FERENCI, T. & KLOTZ, U. 1978. Affinity chromatographic isolation of the periplasmic maltose binding protein of Escherichia coli. FEBS Lett, 94, 213-7.

FERGUSON, A. D., CHAKRABORTY, R., SMITH, B. S., ESSER, L., VAN DER HELM, D. & DEISENHOFER, J. 2002. Structural basis of gating by the outer membrane transporter FecA. Science, 295, 1715-9.

FERGUSON, A. D., HOFMANN, E., COULTON, J. W., DIEDERICHS, K. & WELTE, W. 1998. Siderophore-mediated iron transport: crystal structure of FhuA with bound lipopolysaccharide. Science, 282, 2215-20.

FLANNAGAN, R. S., AUBERT, D., KOOI, C., SOKOL, P. A. & VALVANO, M. A. 2007. Burkholderia cenocepacia requires a periplasmic HtrA protease for growth under thermal and osmotic stress and for survival in vivo. Infect Immun, 75, 1679-89.

FLEMMING, H.-C. 1993. BIOFLMS A ENVIRONMENTAL PROTECTION. Wat Sci. Tech, 27, 1-10.

FLYNN, J. M., LEVCHENKO, I., SAUER, R. T. & BAKER, T. A. 2004. Modulating substrate choice: the SspB adaptor delivers a regulator of the extracytoplasmic-stress response to the AAA+ protease ClpXP for degradation. Genes Dev, 18, 2292-301.

FLYNN, J. M., NEHER, S. B., KIM, Y. I., SAUER, R. T. & BAKER, T. A. 2003. Proteomic discovery of cellular substrates of the ClpXP protease reveals five classes of ClpX-recognition signals. Mol Cell, 11, 671-83.

FUQUA, C., WINANS, S. C. & GREENBERG, E. P. 1996. Census and consensus in bacterial ecosystems: the LuxR-LuxI family of quorum-sensing transcriptional regulators. Annu Rev Microbiol, 50, 727-51.

GAO, H., ZHOU, D., LI, Y., GUO, Z., HAN, Y., SONG, Y., ZHAI, J., DU, Z., WANG, X., LU, J. & YANG, R. 2008. The iron-responsive Fur regulon in Yersinia pestis. J Bacteriol, 190, 3063-75.

GAVRILIN, M. A., ABDELAZIZ, D. H., MOSTAFA, M., ABDULRAHMAN, B. A., GRANDHI, J., AKHTER, A., ABU KHWEEK, A., AUBERT, D. F., VALVANO, M. A., WEWERS, M. D. & AMER, A. O. 2012. Activation of the pyrin inflammasome by intracellular Burkholderia cenocepacia. J Immunol, 188, 3469-77.

GINGUES, S., KOOI, C., VISSER, M. B., SUBSIN, B. & SOKOL, P. A. 2005. Distribution and expression of the ZmpA metalloprotease in the Burkholderia cepacia complex. J Bacteriol, 187, 8247-55.

GOLDSTEIN, R., SUN, L., JIANG, R. Z., SAJJAN, U., FORSTNER, J. F. & CAMPANELLI, C. 1995. Structurally variant classes of pilus appendage fibers coexpressed from Burkholderia (Pseudomonas) cepacia. J Bacteriol, 177, 1039-52.

GOVAN, J. R. & DERETIC, V. 1996. Microbial pathogenesis in cystic fibrosis: mucoid Pseudomonas aeruginosa and Burkholderia cepacia. Microbiol Rev, 60, 539-74.

GROSS, C. A., CHAN, C., DOMBROSKI, A., GRUBER, T., SHARP, M., TUPY, J. & YOUNG, B. 1998. The functional and regulatory roles of sigma factors in transcription. Cold Spring Harb Symp Quant Biol, 63, 141-55.

GRUBER, T. M. & GROSS, C. A. 2003. Multiple sigma subunits and the partitioning of bacterial transcription space. Annu Rev Microbiol, 57, 441-66.

GUERIN, M., ROBICHON, N., GEISELMANN, J. & RAHMOUNI, A. R. 1998. A simple polypyrimidine repeat acts as an artificial Rho-dependent terminator in vivo and in vitro. Nucleic Acids Res, 26, 4895-900.

GUERINOT, M. L. 1994. Microbial iron transport. Annu Rev Microbiol, 48, 743-72.

DOROTHY H. ANDERSEN, M. D. 1938. CYSTIC FIBROSIS OF THE PANCREAS AND ITS RELATION TO CELIAC DISEASEA CLINICAL AND PATHOLOGIC STUDY. Am J Dis Child, 56, 344-399.

HARTNEY, S. L., MAZURIER, S., KIDARSA, T. A., QUECINE, M. C., LEMANCEAU, P. & LOPER, J. E. 2011. TonB-dependent outer-membrane proteins and siderophore utilization in Pseudomonas fluorescens Pf-5. Biometals, 24, 193-213.

HAUGEN, S. P., ROSS, W. & GOURSE, R. L. 2008. Advances in bacterial promoter recognition and its control by factors that do not bind DNA. Nat Rev Microbiol, 6, 507-19.

HEINRICHS, D. E. & POOLE, K. 1996. PchR, a regulator of ferripyochelin receptor gene (fptA) expression in Pseudomonas aeruginosa, functions both as an activator and as a repressor. J Bacteriol, 178, 2586-92.

HEINRICHS, D. E., YOUNG, L. & POOLE, K. 1991. Pyochelin-mediated iron transport in Pseudomonas aeruginosa: involvement of a high-molecular-mass outer membrane protein. Infect Immun, 59, 3680-4.

HELMANN, J. D. 2002. The extracytoplasmic function (ECF) sigma factors. Adv Microb Physiol, 46, 47-110.

HELMANN, J. D. & DEHASETH, P. L. 1999. Protein-nucleic acid interactions during open complex formation investigated by systematic alteration of the protein and DNA binding partners. Biochemistry, 38, 5959-67.

HERASIMENKA, Y., CESCUTTI, P., IMPALLOMENI, G., CAMPANA, S., TACCETTI, G., RAVENNI, N., ZANETTI, F. & RIZZO, R. 2007. Exopolysaccharides produced by clinical strains belonging to the Burkholderia cepacia complex. J Cyst Fibros, 6, 145-52.

HERASIMENKA, Y., CESCUTTI, P., SAMPAIO NOGUERA, C. E., RUGGIERO, J. R., URBANI, R., IMPALLOMENI, G., ZANETTI, F., CAMPIDELLI, S., PRATO, M. & RIZZO, R. 2008. Macromolecular properties of cepacian in water and in dimethylsulfoxide. Carbohydr Res, 343, 81-9.

HIDER, R. C. & KONG, X. 2010. Chemistry and biology of siderophores. Nat Prod Rep, 27, 637-57.

HOLLOWAY, B. W. 1969. Genetics of Pseudomonas. Bacteriol Rev, 33, 419-43.

HOOK-BARNARD, I. G. & HINTON, D. M. 2007. Transcription initiation by mix and match elements: flexibility for polymerase binding to bacterial promoters. Gene Regul Syst Bio, 1, 275-93.

HUANG, S. H., WANG, C. K., PENG, H. L., WU, C. C., CHEN, Y. T., HONG, Y. M. & LIN, C. T. 2012. Role of the small RNA RyhB in the Fur regulon in mediating the capsular polysaccharide biosynthesis and iron acquisition systems in Klebsiella pneumoniae. BMC Microbiol, 12, 148.

HUBER, B., RIEDEL, K., HENTZER, M., HEYDORN, A., GOTSCHLICH, A., GIVSKOV, M., MOLIN, S. & EBERL, L. 2001. The cep quorum-sensing system of Burkholderia cepacia H111 controls biofilm formation and swarming motility. Microbiology, 147, 2517-28.

HUGHES, K. T. & MATHEE, K. 1998. The anti-sigma factors. Annu Rev Microbiol, 52, 231-86.

HUNT, G. M., OAKESHOTT, P. & KERRY, S. 1999. Link between the CSF shunt and achievement in adults with spina bifida. J Neurol Neurosurg Psychiatry, 67, 591-5.

HUSE, H. K., KWON, T., ZLOSNIK, J. E., SPEERT, D. P., MARCOTTE, E. M. & WHITELEY, M. 2013. Pseudomonas aeruginosa enhances production of a non-alginate exopolysaccharide during long-term colonization of the cystic fibrosis lung. PLoS One, 8, e82621.

ISLES, A., MACLUSKY, I., COREY, M., GOLD, R., PROBER, C., FLEMING, P. & LEVISON, H. 1984. Pseudomonas cepacia infection in cystic fibrosis: an emerging problem. J Pediatr, 104, 206-10.

KAELIN, W. G., JR., PALLAS, D. C., DECAPRIO, J. A., KAYE, F. J. & LIVINGSTON, D. M. 1991. Identification of cellular proteins that can interact

specifically with the T/E1A-binding region of the retinoblastoma gene product. Cell, 64, 521-32.

KANEHARA, K., ITO, K. & AKIYAMA, Y. 2002. YaeL (EcfE) activates the sigma(E) pathway of stress response through a site-2 cleavage of anti-sigma(E), RseA. Genes Dev, 16, 2147-55.

KAPUST, R. B. & WAUGH, D. S. 1999. Escherichia coli maltose-binding protein is uncommonly effective at promoting the solubility of polypeptides to which it is fused. Protein Sci, 8, 1668-74.

KARIMOVA, G., DAUTIN, N. & LADANT, D. 2005. Interaction network among Escherichia coli membrane proteins involved in cell division as revealed by bacterial two-hybrid analysis. J Bacteriol, 187, 2233-43.

KARIMOVA, G., PIDOUX, J., ULLMANN, A. & LADANT, D. 1998. A bacterial two-hybrid system based on a reconstituted signal transduction pathway. Proc Natl Acad Sci U S A, 95, 5752-6.

KAZMIERCZAK, M. J., WIEDMANN, M. & BOOR, K. J. 2005. Alternative sigma factors and their roles in bacterial virulence. Microbiol Mol Biol Rev, 69, 527-43.

KELLERMANN, O. K. & FERENCI, T. 1982. Maltose-binding protein from Escherichia coli. Methods Enzymol, 90 Pt E, 459-63.

KIM, D. Y. & KIM, K. K. 2005. Structure and function of HtrA family proteins, the key players in protein quality control. J Biochem Mol Biol, 38, 266-74.

KIM, I., STIEFEL, A., PLANTOR, S., ANGERER, A. & BRAUN, V. 1997. Transcription induction of the ferric citrate transport genes via the N-terminus of the FecA outer membrane protein, the Ton system and the electrochemical potential of the cytoplasmic membrane. Mol Microbiol, 23, 333-44.

KLEINE, B., FREUDENBERG, M. A. & GALANOS, C. 1985. Excretion of radioactivity in faeces and urine of rats injected with 3H,14C-lipopolysaccharide. Br J Exp Pathol, 66, 303-8.

KLUMPP, C., BURGER, A., MISLIN, G. L. & ABDALLAH, M. A. 2005. From a total synthesis of cepabactin and its 3:1 ferric complex to the isolation of a 1:1:1 mixed

complex between iron (III), cepabactin and pyochelin. Bioorg Med Chem Lett, 15, 1721-4.

KOEBNIK, R. 2005. TonB-dependent trans-envelope signalling: the exception or the rule? Trends Microbiol, 13, 343-7.

KOOI, C., CORBETT, C. R. & SOKOL, P. A. 2005. Functional analysis of the Burkholderia cenocepacia ZmpA metalloprotease. J Bacteriol, 187, 4421-9.

KOOI, C., SUBSIN, B., CHEN, R., POHORELIC, B. & SOKOL, P. A. 2006. Burkholderia cenocepacia ZmpB is a broad-specificity zinc metalloprotease involved in virulence. Infect Immun, 74, 4083-93.

KOSTER, M., VAN KLOMPENBURG, W., BITTER, W., LEONG, J. & WEISBEEK, P. 1994. Role for the outer membrane ferric siderophore receptor PupB in signal transduction across the bacterial cell envelope. Embo j, 13, 2805-13.

KOSTER, W. 2001. ABC transporter-mediated uptake of iron, siderophores, heme and vitamin B12. Res Microbiol, 152, 291-301.

KRAEPIEL, A. M., BELLENGER, J. P., WICHARD, T. & MOREL, F. M. 2009. Multiple roles of siderophores in free-living nitrogen-fixing bacteria. Biometals, 22, 573-81.

KREWULAK, K. D. & VOGEL, H. J. 2008a. Structural biology of bacterial iron uptake. Biochim Biophys Acta, 1778, 1781-804.

KREWULAK, K. D. & VOGEL, H. J. 2008. Structural biology of bacterial iron uptake. Biochim Biophys Acta, 1778, 1781-804.

KREWULAK, K. D. & VOGEL, H. J. 2011. TonB or not TonB: is that the question? Biochem Cell Biol, 89, 87-97.

KUHNAU, S., REYES, M., SIEVERTSEN, A., SHUMAN, H. A. & BOOS, W. 1991. The activities of the Escherichia coli MalK protein in maltose transport, regulation, and inducer exclusion can be separated by mutations. J Bacteriol, 173, 2180-6.

KUMAR, B. & CARDONA, S. T. 2016. Synthetic Cystic Fibrosis Sputum Medium Regulates Flagellar Biosynthesis through the flhF Gene in Burkholderia cenocepacia. Front Cell Infect Microbiol, 6, 65.

KUZNEDELOV, K., MINAKHIN, L., NIEDZIELA-MAJKA, A., DOVE, S. L., ROGULJA, D., NICKELS, B. E., HOCHSCHILD, A., HEYDUK, T. & SEVERINOV, K. 2002. A role for interaction of the RNA polymerase flap domain with the sigma subunit in promoter recognition. Science, 295, 855-7.

LADANT, D. 1988. Interaction of Bordetella pertussis adenylate cyclase with calmodulin. Identification of two separated calmodulin-binding domains. J Biol Chem, 263, 2612-8.

LADANT, D. & ULLMANN, A. 1999. Bordatella pertussis adenylate cyclase: a toxin with multiple talents. Trends Microbiol, 7, 172-6.

LAMONT, I. L., BEARE, P. A., OCHSNER, U., VASIL, A. I. & VASIL, M. L. 2002. Siderophore-mediated signaling regulates virulence factor production in Pseudomonasaeruginosa. Proc Natl Acad Sci U S A, 99, 7072-7.

LEONI, L., ORSI, N., DE LORENZO, V. & VISCA, P. 2000. Functional analysis of PvdS, an iron starvation sigma factor of Pseudomonas aeruginosa. J Bacteriol, 182, 1481-91.

LETAIN, T. E. & POSTLE, K. 1997. TonB protein appears to transduce energy by shuttling between the cytoplasmic membrane and the outer membrane in Escherichia coli. Mol Microbiol, 24, 271-83.

LETOFFE, S., GHIGO, J. M. & WANDERSMAN, C. 1994. Iron acquisition from heme and hemoglobin by a Serratia marcescens extracellular protein. Proc Natl Acad Sci U S A, 91, 9876-80.

LEWENZA, S., CONWAY, B., GREENBERG, E. P. & SOKOL, P. A. 1999. Quorum sensing in Burkholderia cepacia: identification of the LuxRI homologs CepRI. J Bacteriol, 181, 748-56.

LEWENZA, S. & SOKOL, P. A. 2001. Regulation of ornibactin biosynthesis and N-acyl-L-homoserine lactone production by CepR in Burkholderia cepacia. J Bacteriol, 183, 2212-8.

LEWENZA, S., VISSER, M. B. & SOKOL, P. A. 2002. Interspecies communication between Burkholderia cepacia and Pseudomonas aeruginosa. Can J Microbiol, 48, 707-16.

LIMA, S., GUO, M. S., CHABA, R., GROSS, C. A. & SAUER, R. T. 2013. Dual molecular signals mediate the bacterial response to outer-membrane stress. Science, 340, 837-41.

LIPUMA, J. J. 1998. Burkholderia cepacia. Management issues and new insights. Clin Chest Med, 19, 473-86, vi.

LIPUMA, J. J., SPILKER, T., GILL, L. H., CAMPBELL, P. W., 3RD, LIU, L. & MAHENTHIRALINGAM, E. 2001. Disproportionate distribution of Burkholderia cepacia complex species and transmissibility markers in cystic fibrosis. Am J Respir Crit Care Med, 164, 92-6.

LIVERMORE, D. M., MUSHTAQ, S. & WARNER, M. 2010. Activity of BAL30376 (monobactam BAL19764 + BAL29880 + clavulanate) versus Gram-negative bacteria with characterized resistance mechanisms. J Antimicrob Chemother, 65, 2382-95.

LLAMAS, M.A., AND, BITTER & W 2010. Cell-surface signalling in Pseudomonas. In

Pseudomonas: Molecular Microbiology. Springer Science, 59-95.

LLAMAS, M. A., IMPERI, F., VISCA, P. & LAMONT, I. L. 2014. Cell-surface signaling in Pseudomonas: stress responses, iron transport, and pathogenicity. FEMS Microbiol Rev, 38, 569-97.

LLAMAS, M. A., SPARRIUS, M., KLOET, R., JIMENEZ, C. R., VANDENBROUCKE-GRAULS, C. & BITTER, W. 2006. The heterologous siderophores ferrioxamine B and ferrichrome activate signaling pathways in Pseudomonas aeruginosa. J Bacteriol, 188, 1882-91.

LONETTO, M., GRIBSKOV, M. & GROSS, C. A. 1992. The sigma 70 family: sequence conservation and evolutionary relationships. J Bacteriol, 174, 3843-9.

LYCZAK, J. B., CANNON, C. L. & PIER, G. B. 2002. Lung infections associated with cystic fibrosis. Clin Microbiol Rev, 15, 194-222.

MADEIRA, A., DOS SANTOS, S. C., SANTOS, P. M., COUTINHO, C. P., TYRRELL, J., MCCLEAN, S., CALLAGHAN, M. & SA-CORREIA, I. 2013. Proteomic profiling of Burkholderia cenocepacia clonal isolates with different virulence potential retrieved from a cystic fibrosis patient during chronic lung infection. PLoS One, 8, e83065.

MAHENTHIRALINGAM, E., BALDWIN, A. & DOWSON, C. G. 2008. Burkholderia cepacia complex bacteria: opportunistic pathogens with important natural biology. J Appl Microbiol, 104, 1539-51.

MAHENTHIRALINGAM, E., SIMPSON, D. A. & SPEERT, D. P. 1997. Identification and characterization of a novel DNA marker associated with epidemic Burkholderia cepacia strains recovered from patients with cystic fibrosis. J Clin Microbiol, 35, 808-16.

MAHENTHIRALINGAM, E., URBAN, T. A. & GOLDBERG, J. B. 2005. The multifarious, multireplicon Burkholderia cepacia complex. Nat Rev Microbiol, 3, 144-56.

MAHENTHIRALINGAM, E. & VANDAMME, P. 2005. Taxonomy and pathogenesis of the Burkholderia cepacia complex. Chron Respir Dis, 2, 209-17.

MAHENTHIRALINGAM, E., VANDAMME, P., CAMPBELL, M. E., HENRY, D. A., GRAVELLE, A. M., WONG, L. T., DAVIDSON, A. G., WILCOX, P. G., NAKIELNA, B. & SPEERT, D. P. 2001. Infection with Burkholderia cepacia complex genomovars in patients with cystic fibrosis: virulent transmissible strains of genomovar III can replace Burkholderia multivorans. Clin Infect Dis, 33, 1469-75.

MAHREN, S., ENZ, S. & BRAUN, V. 2002. Functional interaction of region 4 of the extracytoplasmic function sigma factor FecI with the cytoplasmic portion of the FecR transmembrane protein of the Escherichia coli ferric citrate transport system. J Bacteriol, 184, 3704-11.

MANNO, G., DALMASTRI, C., TABACCHIONI, S., VANDAMME, P., LORINI, R., MINICUCCI, L., ROMANO, L., GIANNATTASIO, A., CHIARINI, L. & BEVIVINO, A. 2004. Epidemiology and clinical course of Burkholderia cepacia complex infections, particularly those caused by different Burkholderia cenocepacia strains, among patients attending an Italian Cystic Fibrosis Center. J Clin Microbiol, 42, 1491-7.

MASSE, E., ESCORCIA, F. E. & GOTTESMAN, S. 2003. Coupled degradation of a small regulatory RNA and its mRNA targets in Escherichia coli. Genes Dev, 17, 2374-83.

MATHEW, A., EBERL, L. & CARLIER, A. L. 2014. A novel siderophore-independent strategy of iron uptake in the genus Burkholderia. Mol Microbiol, 91, 805-20.

MATZANKE, B. F., ANEMULLER, S., SCHUNEMANN, V., TRAUTWEIN, A. X. & HANTKE, K. 2004. FhuF, part of a siderophore-reductase system. Biochemistry, 43, 1386-92.

MATZANKE, B. F., BOHNKE, R., MOLLMANN, U., REISSBRODT, R., SCHUNEMANN, V. & TRAUTWEIN, A. X. 1997. Iron uptake and intracellular metal transfer in mycobacteria mediated by xenosiderophores. Biometals, 10, 193-203.

MCCLURE, W. R. 1985. Mechanism and control of transcription initiation in prokaryotes. Annu Rev Biochem, 54, 171-204.

MCKEON, S. A., NGUYEN, D. T., VITERI, D. F., ZLOSNIK, J. E. & SOKOL, P. A. 2011. Functional quorum sensing systems are maintained during chronic Burkholderia cepacia complex infections in patients with cystic fibrosis. J Infect Dis, 203, 383-92.

MENARD, A., DE LOS SANTOS, P. E., GRAINDORGE, A. & COURNOYER, B. 2007. Architecture of Burkholderia cepacia complex sigma70 gene family: evidence of alternative primary and clade-specific factors, and genomic instability. BMC Genomics, 8, 308.

METTRICK, K. A. & LAMONT, I. L. 2009. Different roles for anti-sigma factors in siderophore signalling pathways of Pseudomonas aeruginosa. Mol Microbiol, 74, 1257-71.

MEYER, J. M. 1992. Exogenous siderophore-mediated iron uptake in Pseudomonas aeruginosa: possible involvement of porin OprF in iron translocation. J Gen Microbiol, 138, 951-8.

MEYER, J. M., HOHNADEL, D. & HALLE, F. 1989. Cepabactin from Pseudomonas cepacia, a new type of siderophore. J Gen Microbiol, 135, 1479-87.

MEYER, J. M., VAN, V. T., STINTZI, A., BERGE, O. & WINKELMANN, G. 1995. Ornibactin production and transport properties in strains of Burkholderia vietnamiensis and Burkholderia cepacia (formerly Pseudomonas cepacia). Biometals, 8, 309-17.

MIETHKE, M. & MARAHIEL, M. A. 2007. Siderophore-based iron acquisition and pathogen control. Microbiol Mol Biol Rev, 71, 413-51.

MILLS, S. A. & MARLETTA, M. A. 2005. Metal binding characteristics and role of iron oxidation in the ferric uptake regulator from Escherichia coli. Biochemistry, 44, 13553-9.

MISLIN, G. L., HOEGY, F., COBESSI, D., POOLE, K., ROGNAN, D. & SCHALK, I. J. 2006. Binding properties of pyochelin and structurally related molecules to FptA of Pseudomonas aeruginosa. J Mol Biol, 357, 1437-48.

MIYAZAKI, H., KATO, H., NAKAZAWA, T. & TSUDA, M. 1995. A positive regulatory gene, pvdS, for expression of pyoverdin biosynthetic genes in Pseudomonas aeruginosa PAO. Mol Gen Genet, 248, 17-24.

MULVEY, M. R. & LOEWEN, P. C. 1989. Nucleotide sequence of katF of Escherichia coli suggests KatF protein is a novel sigma transcription factor. Nucleic Acids Res, 17, 9979-91.

MURAKAMI, K. S. 2013. X-ray crystal structure of Escherichia coli RNA polymerase sigma70 holoenzyme. J Biol Chem, 288, 9126-34.

MURAKAMI, K. S., MASUDA, S., CAMPBELL, E. A., MUZZIN, O. & DARST, S. A. 2002. Structural basis of transcription initiation: an RNA polymerase holoenzyme-DNA complex. Science, 296, 1285-90.

MURAKAMI, K. S. & DARST, S. A. 2003. Bacterial RNA polymerases: the whole story. Curr Opin Struct Biol, 13, 31-9.

MURRAY, T. S. & KAZMIERCZAK, B. I. 2006. FlhF is required for swimming and swarming in Pseudomonas aeruginosa. J Bacteriol, 188, 6995-7004.

NEILANDS, J. B. 1995. Siderophores: structure and function of microbial iron transport compounds. J Biol Chem, 270, 26723-6.

NG, W. L. & BASSLER, B. L. 2009. Bacterial quorum-sensing network architectures. Annu Rev Genet, 43, 197-222.

N. MORRAL, J. BERTRANPETIT, X. ESTIVILL, V. NUNES, T. CASALS, J. GIMENEZ, A. REIS, R. VARON-MATEEVA, M. MACEK JR., L. KALAYDJIEVA, D. ANGELICHEVA, R. DANCHEVA, G. ROMEO, M.P. RUSSO, S. GARNERONE, G. RESTAGNO, M. FERRARI, C. MAGNANI, M. CLAUSTRES, M. DESGEORGES, M. SCHWARTZ, M. SCHWARZ, B. DALLAPICCOLA, G. NOVELLI, C. FEREC, M. DE ARCE, M. NEMETI, J. KERE, M. ANVRET, N. DAHL & L. KADASI. The origin of the major cystic fibrosis mutation (ΔF508) in European populations. Nature Genetics,7, 169–175

NOINAJ, N., GUILLIER, M., BARNARD, T. J. & BUCHANAN, S. K. 2010. TonB-dependent transporters: regulation, structure, and function. Annu Rev Microbiol, 64, 43-60.

OCHS, M., VEITINGER, S., KIM, I., WELZ, D., ANGERER, A. & BRAUN, V. 1995. Regulation of citrate-dependent iron transport of Escherichia coli: fecR is required for transcription activation by FecI. Mol Microbiol, 15, 119-32.

OCHSNER, U. A. & VASIL, M. L. 1996. Gene repression by the ferric uptake regulator in Pseudomonas aeruginosa: cycle selection of iron-regulated genes. Proc Natl Acad Sci U S A, 93, 4409-14.

OCHSNER, U. A., WILDERMAN, P. J., VASIL, A. I. & VASIL, M. L. 2002. GeneChip expression analysis of the iron starvation response in Pseudomonas aeruginosa: identification of novel pyoverdine biosynthesis genes. Mol Microbiol, 45, 1277-87.

OLLIS, A. A., KUMAR, A. & POSTLE, K. 2012. The ExbD periplasmic domain contains distinct functional regions for two stages in TonB energization. J Bacteriol, 194, 3069-77.

OLLIS, A. A. & POSTLE, K. 2012. ExbD mutants define initial stages in TonB energization. J Mol Biol, 415, 237-47.

ORSI, G. B., SCORZOLINI, L., FRANCHI, C., MONDILLO, V., ROSA, G. & VENDITTI, M. 2006. Hospital-acquired infection surveillance in a neurosurgical intensive care unit. J Hosp Infect, 64, 23-9.

OSTERBERG, S., DEL PESO-SANTOS, T. & SHINGLER, V. 2011. Regulation of alternative sigma factor use. Annu Rev Microbiol, 65, 37-55.

PAGE, M. G. 2013. Siderophore conjugates. Ann N Y Acad Sci, 1277, 115-26.

PAGET, M. S. 2015. Bacterial Sigma Factors and Anti-Sigma Factors: Structure, Function and Distribution. Biomolecules, 5, 1245-65.

PAGET, M. S. & HELMANN, J. D. 2003. The sigma70 family of sigma factors. Genome Biol, 41, 203.

PALLERONI, N. J., KUNISAWA, R., CONTOPOULOU, R. & DOUDOROFF, M. 1973. Nucleic Acid Homologies in the Genus Pseudomonas. INTERNATIONAL JOURNAL of SYSTEMATIC BACTERIOLOGY, 23, 333-339.

PARKE, J. L. & GURIAN-SHERMAN, D. 2001. Diversity of the Burkholderia cepacia complex and implications for risk assessment of biological control strains. Annu Rev Phytopathol, 39, 225-58.

PARKER, W. L., RATHNUM, M. L., SEINER, V., TREJO, W. H., PRINCIPE, P. A. & SYKES, R. B. 1984. Cepacin A and cepacin B, two new antibiotics produced by Pseudomonas cepacia. J Antibiot (Tokyo), 37, 431-40.

PEETERS, C., ZLOSNIK, J. E., SPILKER, T., HIRD, T. J., LIPUMA, J. J. & VANDAMME, P. 2013. Burkholderia pseudomultivorans sp. nov., a novel Burkholderia cepacia complex species from human respiratory samples and the rhizosphere. Syst Appl Microbiol, 36, 483-9.

Pi, H., JONES, S. A., MERCER, L. E., MEADOR, J. P., CAUGHRON, J. E., JORDAN, L., NEWTON, S. M., CONWAY, T. & KLEBBA, P. E. 2012. Role of catecholate siderophores in gram-negative bacterial colonization of the mouse gut. PLoS One, 7, e50020.

POHL, E., HALLER, J. C., MIJOVILOVICH, A., MEYER-KLAUCKE, W., GARMAN, E. & VASIL, M. L. 2003. Architecture of a protein central to iron homeostasis: crystal structure and spectroscopic analysis of the ferric uptake regulator. Mol Microbiol, 47, 903-15.

QUAIL, M. A., JORDAN, P., GROGAN, J. M., BUTT, J. N., LUTZ, M., THOMSON, A. J., ANDREWS, S. C. & GUEST, J. R. 1996. Spectroscopic and voltammetric characterisation of the bacterioferritin-associated ferredoxin of Escherichia coli. Biochem Biophys Res Commun, 229, 635-42.

RAIVIO, T. L. & SILHAVY, T. J. 2001. Periplasmic stress and ECF sigma factors. Annu Rev Microbiol, 55, 591-624.

RATJEN, F. A. 2009. Cystic fibrosis: pathogenesis and future treatment strategies. Respir Care, 54, 595-605.

RATLEDGE, C. & DOVER, L. G. 2000. Iron metabolism in pathogenic bacteria. Annu Rev Microbiol, 54, 881-941.

REDLY, G. A. & POOLE, K. 2005. FpvIR control of fpvA ferric pyoverdine receptor gene expression in Pseudomonas aeruginosa: demonstration of an interaction between FpvI and FpvR and identification of mutations in each compromising this interaction. J Bacteriol, 187, 5648-57.

REIMMANN, C., PATEL, H. M., SERINO, L., BARONE, M., WALSH, C. T. & HAAS, D. 2001. Essential PchG-dependent reduction in pyochelin biosynthesis of Pseudomonas aeruginosa. J Bacteriol, 183, 813-20.

REIMMANN, C., SERINO, L., BEYELER, M. & HAAS, D. 1998. Dihydroaeruginoic acid synthetase and pyochelin synthetase, products of the pchEF genes, are induced by extracellular pyochelin in Pseudomonas aeruginosa. Microbiology, 144 (Pt 11), 3135-48.

RICHARME, G. & CALDAS, T. D. 1997. Chaperone properties of the bacterial periplasmic substrate-binding proteins. J Biol Chem, 272, 15607-12.

RIEDEL, K., AREVALO-FERRO, C., REIL, G., GORG, A., LOTTSPEICH, F. & EBERL, L. 2003. Analysis of the quorum-sensing regulon of the opportunistic pathogen Burkholderia cepacia H111 by proteomics. Electrophoresis, 24, 740-50.

ROOSENBERG, J. M., 2ND, LIN, Y. M., LU, Y. & MILLER, M. J. 2000. Studies and syntheses of siderophores, microbial iron chelators, and analogs as potential drug delivery agents. Curr Med Chem, 7, 159-97.

ROSALES-REYES, R., AUBERT, D. F., TOLMAN, J. S., AMER, A. O. & VALVANO, M. A. 2012. Burkholderia cenocepacia type VI secretion system mediates escape of type II secreted proteins into the cytoplasm of infected macrophages. PLoS One, 7, e41726.

RYAN, R. P. & DOW, J. M. 2008. Diffusible signals and interspecies communication in bacteria. Microbiology, 154, 1845-58.

RYDER, C., BYRD, M. & WOZNIAK, D. J. 2007. Role of polysaccharides in Pseudomonas aeruginosa biofilm development. Curr Opin Microbiol, 10, 644-8.

SAHA, R., SAHA, N., DONOFRIO, R. S. & BESTERVELT, L. L. 2013. Microbial siderophores: a mini review. J Basic Microbiol, 53, 303-17.

SAJJAN, U., ACKERLEY, C. & FORSTNER, J. 2002. Interaction of cblA/adhesin-positive Burkholderia cepacia with squamous epithelium. Cell Microbiol, 4, 73-86.

SAJJAN, U. S. & FORSTNER, J. F. 1993. Role of a 22-kilodalton pilin protein in binding of Pseudomonas cepacia to buccal epithelial cells. Infect Immun, 61, 3157-63.

SALDIAS, M. S. & VALVANO, M. A. 2009. Interactions of Burkholderia cenocepacia and other Burkholderia cepacia complex bacteria with epithelial and phagocytic cells. Microbiology, 155, 2809-17.

SCHALK, I. J., HANNAUER, M. & BRAUD, A. 2011. New roles for bacterial siderophores in metal transport and tolerance. Environ Microbiol, 13, 2844-54.

SCHNEIDER, E. & HUNKE, S. 1998. ATP-binding-cassette (ABC) transport systems: functional and structural aspects of the ATP-hydrolyzing subunits/domains. FEMS Microbiol Rev, 22, 1-20.

SCHRYVERS, A. B. & STOJILJKOVIC, I. 1999. Iron acquisition systems in the pathogenic Neisseria. Mol Microbiol, 32, 1117-23.

SCHWYN, B. & NEILANDS, J. B. 1987. Universal chemical assay for the detection and determination of siderophores. Anal Biochem, 160, 47-56.

SEBULSKY, M. T. & HEINRICHS, D. E. 2001. Identification and characterization of fhuD1 and fhuD2, two genes involved in iron-hydroxamate uptake in Staphylococcus aureus. J Bacteriol, 183, 4994-5000.

SEGAL, B. H., LETO, T. L., GALLIN, J. I., MALECH, H. L. & HOLLAND, S. M. 2000. Genetic, biochemical, and clinical features of chronic granulomatous disease. Medicine (Baltimore), 79, 170-200.

SHEIKH, M. A. & TAYLOR, G. L. 2009. Crystal structure of the Vibrio cholerae ferric uptake regulator (Fur) reveals insights into metal co-ordination. Mol Microbiol, 72, 1208-20.

SHELVER, D., KERBY, R. L., HE, Y. & ROBERTS, G. P. 1997. CooA, a CO-sensing transcription factor from Rhodospirillum rubrum, is a CO-binding heme protein. Proc Natl Acad Sci U S A, 94, 11216-20.

SHEN, J., MELDRUM, A. & POOLE, K. 2002. FpvA receptor involvement in pyoverdine biosynthesis in Pseudomonas aeruginosa. J Bacteriol, 184, 3268-75.

SILAR, R., HOLATKO, J., RUCKA, L., RAPOPORT, A., DOSTALOVA, H., KADERABKOVA, P., NESVERA, J. & PATEK, M. 2016. Use of In Vitro

Transcription System for Analysis of Corynebacterium glutamicum Promoters Recognized by Two Sigma Factors. Curr Microbiol, 73, 401-8.

SILIPO, A., MOLINARO, A., IERANO, T., DE SOYZA, A., STURIALE, L., GAROZZO, D., ALDRIDGE, C., CORRIS, P. A., KHAN, C. M., LANZETTA, R. & PARRILLI, M. 2007. The complete structure and pro-inflammatory activity of the lipooligosaccharide of the highly epidemic and virulent gram-negative bacterium Burkholderia cenocepacia ET-12 (strain J2315). Chemistry, 13, 3501-11.

SMITH, A. D. & WILKS, A. 2015. Differential contributions of the outer membrane receptors PhuR and HasR to heme acquisition in Pseudomonas aeruginosa. J Biol Chem, 290, 7756-66.

SOKOL, P. A. 1986. Production and utilization of pyochelin by clinical isolates of Pseudomonas cepacia. J Clin Microbiol, 23, 560-2.

SOKOL, P. A., DARLING, P., WOODS, D. E., MAHENTHIRALINGAM, E. & KOOI, C. 1999. Role of ornibactin biosynthesis in the virulence of Burkholderia cepacia: characterization of pvdA, the gene encoding L-ornithine N(5)-oxygenase. Infect Immun, 67, 4443-55.

SOUSA, S. A., RAMOS, C. G. & LEITAO, J. H. 2011. Burkholderia cepacia Complex: Emerging Multihost Pathogens Equipped with a Wide Range of Virulence Factors and Determinants. Int J Microbiol, 2011.

SPEERT, D. P. 2002. Advances in Burkholderia cepacia complex. Paediatr Respir Rev, 3, 230-5.

SPENCER, M. R., BEARE, P. A. & LAMONT, I. L. 2008. Role of cell surface signaling in proteolysis of an alternative sigma factor in Pseudomonas aeruginosa. J Bacteriol, 190, 4865-9.

STEPHAN, H., FREUND, S., BECK, W., JUNG, G., MEYER, J. M. & WINKELMANN, G. 1993. Ornibactins--a new family of siderophores from Pseudomonas. Biometals, 6, 93-100.

STERN, R. C. 1997. The diagnosis of cystic fibrosis. N Engl J Med, 336, 487-91.

STEWART, P. S. & COSTERTON, J. W. 2001. Antibiotic resistance of bacteria in biofilms. Lancet, 358, 135-8.

STIEFEL, A., MAHREN, S., OCHS, M., SCHINDLER, P. T., ENZ, S. & BRAUN, V. 2001. Control of the ferric citrate transport system of Escherichia coli: mutations in region 2.1 of the FecI extracytoplasmic-function sigma factor suppress mutations in the FecR transmembrane regulatory protein. J Bacteriol, 183, 162-70.

STINTZI, A., JOHNSON, Z., STONEHOUSE, M., OCHSNER, U., MEYER, J. M., VASIL, M. L. & POOLE, K. 1999. The pvc gene cluster of Pseudomonas aeruginosa: role in synthesis of the pyoverdine chromophore and regulation by PtxR and PvdS. J Bacteriol, 181, 4118-24.

STOJILJKOVIC, I., BAUMLER, A. J. & HANTKE, K. 1994. Fur regulon in gram-negative bacteria. Identification and characterization of new iron-regulated Escherichia coli genes by a fur titration assay. J Mol Biol, 236, 531-45.

STRANGE, H. R., ZOLA, T. A. & CORNELISSEN, C. N. 2011. The fbpABC operon is required for Ton-independent utilization of xenosiderophores by Neisseria gonorrhoeae strain FA19. Infect Immun, 79, 267-78.

STRAUCH, K. L., JOHNSON, K. & BECKWITH, J. 1989. Characterization of degP, a gene required for proteolysis in the cell envelope and essential for growth of Escherichia coli at high temperature. J Bacteriol, 171, 2689-96.

STRAUS, D. C., LONON, M. K., WOODS, D. E. & GARNER, C. W. 1989. Production of an extracellular toxic complex by various strains of Pseudomonas cepacia. J Med Microbiol, 30, 17-22.

STRAUS, D. C., LONON, M. K., WOODS, D. E. & GARNER, C. W. 1990. 3-deoxy-D-manno-2-octulosonic acid in the lipopolysaccharide of various strains of Pseudomonas cepacia. J Med Microbiol, 33, 265-9.

STRAUS, D. C., WOODS, D. E., LONON, M. K. & GARNER, C. W. 1988. The importance of extracellular antigens in Pseudomonas cepacia infections. J Med Microbiol, 26, 269-80.

SUBRAMONI, S. & VENTURI, V. 2009. LuxR-family 'solos': bachelor sensors/regulators of signalling molecules. Microbiology, 155, 1377-85.

TABIB-SALAZAR, A., LIU, B., DOUGHTY, P., LEWIS, R. A., GHOSH, S., PARSY, M. L., SIMPSON, P. J., O'DWYER, K., MATTHEWS, S. J. & PAGET, M. S. 2013. The actinobacterial transcription factor RbpA binds to the principal sigma subunit of RNA polymerase. Nucleic Acids Res, 41, 5679-91.

THOMAS, M. S. 2007. Iron acquisition mechanisms of the Burkholderia cepacia complex. Biometals, 20, 431-52.

TOMARAS, A. P., CRANDON, J. L., MCPHERSON, C. J., BANEVICIUS, M. A., FINEGAN, S. M., IRVINE, R. L., BROWN, M. F., O'DONNELL, J. P. & NICOLAU, D. P. 2013. Adaptation-based resistance to siderophore-conjugated antibacterial agents by Pseudomonas aeruginosa. Antimicrob Agents Chemother, 57, 4197-207.

TOMICH, M., HERFST, C. A., GOLDEN, J. W. & MOHR, C. D. 2002. Role of flagella in host cell invasion by Burkholderia cepacia. Infect Immun, 70, 1799-806.

TSENG, C. F., BURGER, A., MISLIN, G. L., SCHALK, I. J., YU, S. S., CHAN, S. I. & ABDALLAH, M. A. 2006. Bacterial siderophores: the solution stoichiometry and coordination of the Fe(III) complexes of pyochelin and related compounds. J Biol Inorg Chem, 11, 419-32.

UDINE, C., BRACKMAN, G., BAZZINI, S., BURONI, S., VAN ACKER, H., PASCA, M. R., RICCARDI, G. & COENYE, T. 2013. Phenotypic and genotypic characterisation of Burkholderia cenocepacia J2315 mutants affected in homoserine lactone and diffusible signal factor-based quorum sensing systems suggests interplay between both types of systems. PLoS One, 8, e55112.

UEHLINGER, S., SCHWAGER, S., BERNIER, S. P., RIEDEL, K., NGUYEN, D. T., SOKOL, P. A. & EBERL, L. 2009. Identification of specific and universal virulence factors in Burkholderia cenocepacia strains by using multiple infection hosts. Infect Immun, 77, 4102-10.

URBAN, T. A., GOLDBERG, J. B., FORSTNER, J. F. & SAJJAN, U. S. 2005. Cable pili and the 22-kilodalton adhesin are required for Burkholderia cenocepacia binding to and transmigration across the squamous epithelium. Infect Immun, 73, 5426-37.

URBAN, T. A., GRIFFITH, A., TOROK, A. M., SMOLKIN, M. E., BURNS, J. L. & GOLDBERG, J. B. 2004. Contribution of Burkholderia cenocepacia flagella to infectivity and inflammation. Infect Immun, 72, 5126-34.

VALGARD JONSSON. 1970. Proposal of a new species Pseudomonas kingii. International Journal of Systematic and Evolutionary Microbiology, 20, 255-257.

VALVANO, M. A., KEITH, K. E. & CARDONA, S. T. 2005. Survival and persistence of opportunistic Burkholderia species in host cells. Curr Opin Microbiol, 8, 99-105.

VAN DEN BERG, J. M., VAN KOPPEN, E., AHLIN, A., BELOHRADSKY, B. H., BERNATOWSKA, E., CORBEEL, L., ESPANOL, T., FISCHER, A., KURENKO-DEPTUCH, M., MOUY, R., PETROPOULOU, T., ROESLER, J., SEGER, R., STASIA, M. J., VALERIUS, N. H., WEENING, R. S., WOLACH, B., ROOS, D. & KUIJPERS, T. W. 2009. Chronic granulomatous disease: the European experience. PLoS One, 4, e5234.

VANDAMME, P. & DAWYNDT, P. 2011. Classification and identification of the Burkholderia cepacia complex: Past, present and future. Syst Appl Microbiol, 34, 87-95.

VANDAMME, P., HOLMES, B., COENYE, T., GORIS, J., MAHENTHIRALINGAM, E., LIPUMA, J. J. & GOVAN, J. R. 2003. Burkholderia cenocepacia sp. nov.--a new twist to an old story. Res Microbiol, 154, 91-6.

VANDAMME, P., HOLMES, B., VANCANNEYT, M., COENYE, T., HOSTE, B., COOPMAN, R., REVETS, H., LAUWERS, S., GILLIS, M., KERSTERS, K. & GOVAN, J. R. 1997. Occurrence of multiple genomovars of Burkholderia cepacia in cystic fibrosis patients and proposal of Burkholderia multivorans sp. nov. Int J Syst Bacteriol, 47, 1188-200.

VISCA, P., IMPERI, F. & LAMONT, I. L. 2007. Pyoverdine siderophores: from biogenesis to biosignificance. Trends Microbiol, 15, 22-30.

VISCA, P., LEONI, L., WILSON, M. J. & LAMONT, I. L. 2002. Iron transport and regulation, cell signalling and genomics: lessons from Escherichia coli and Pseudomonas. Mol Microbiol, 45, 1177-90.

VISSER, M. B., MAJUMDAR, S., HANI, E. & SOKOL, P. A. 2004. Importance of the ornibactin and pyochelin siderophore transport systems in Burkholderia cenocepacia lung infections. Infect Immun, 72, 2850-7.

WANDERSMAN, C. & DELEPELAIRE, P. 2004. Bacterial iron sources: from siderophores to hemophores. Annu Rev Microbiol, 58, 611-47.

WANG, C., LEE, J., DENG, Y., TAO, F. & ZHANG, L. H. 2012. ARF-TSS: an alternative method for identification of transcription start site in bacteria. Biotechniques, 52.

WANG, Q. P. & KAGUNI, J. M. 1989. A novel sigma factor is involved in expression of the rpoH gene of Escherichia coli. J Bacteriol, 171, 4248-53.

WENCEWICZ, T. A., MOLLMANN, U., LONG, T. E. & MILLER, M. J. 2009. Is drug release necessary for antimicrobial activity of siderophore-drug conjugates? Syntheses and biological studies of the naturally occurring salmycin "Trojan Horse" antibiotics and synthetic desferridanoxamine-antibiotic conjugates. Biometals, 22, 633-48.

WHITBY, P. W., VANWAGONER, T. M., SPRINGER, J. M., MORTON, D. J., SEALE, T. W. & STULL, T. L. 2006. Burkholderia cenocepacia utilizes ferritin as an iron source. J Med Microbiol, 55, 661-8.

WIENER, M. C. 2005. TonB-dependent outer membrane transport: going for Baroque? Curr Opin Struct Biol, 15, 394-400.

WILDERMAN, P. J., VASIL, A. I., JOHNSON, Z., WILSON, M. J., CUNLIFFE, H. E., LAMONT, I. L. & VASIL, M. L. 2001. Characterization of an endoprotease (PrpL) encoded by a PvdS-regulated gene in Pseudomonas aeruginosa. Infect Immun, 69, 5385-94.

WILKS, A. & SCHMITT, M. P. 1998. Expression and characterization of a heme oxygenase (Hmu O) from Corynebacterium diphtheriae. Iron acquisition requires oxidative cleavage of the heme macrocycle. J Biol Chem, 273, 837-41.

WOZNIAK, D. J., WYCKOFF, T. J., STARKEY, M., KEYSER, R., AZADI, P., O'TOOLE, G. A. & PARSEK, M. R. 2003. Alginate is not a significant component of

the extracellular polysaccharide matrix of PA14 and PAO1 Pseudomonas aeruginosa biofilms. Proc Natl Acad Sci U S A, 100, 7907-12.

YABUUCHI, E., KOSAKO, Y., OYAIZU, H., YANO, I., HOTTA, H., HASHIMOTO, Y., EZAKI, T. & ARAKAWA, M. 1992. Proposal of Burkholderia gen. nov. and transfer of seven species of the genus Pseudomonas homology group II to the new genus, with the type species Burkholderia cepacia (Palleroni and Holmes 1981) comb. nov. Microbiol Immunol, 36, 1251-75.

YARNELL, W. S. & ROBERTS, J. W. 1999. Mechanism of intrinsic transcription termination and antitermination. Science, 284, 611-5.

YOSHIMURA, M., ASAI, K., SADAIE, Y. & YOSHIKAWA, H. 2004. Interaction of Bacillus subtilis extracytoplasmic function (ECF) sigma factors with the N-terminal regions of their potential anti-sigma factors. Microbiology, 150, 591-9.

YOSHIHISA, H., Z ENJI, S., F UKUSHI, H., K ATSUHIRO, K., H ARUHISA, S. & T AKAHITO, S. 1989. Production of antibiotics by Pseudomonas cepacia as an agent for biological control of soilborne plant pathogens. Soil Biology and Biochemistry, 21, 723–728.

YOUNG, B. A., ANTHONY, L. C., GRUBER, T. M., ARTHUR, T. M., HEYDUK, E., LU, C. Z., SHARP, M. M., HEYDUK, T., BURGESS, R. R. & GROSS, C. A. 2001. A coiled-coil from the RNA polymerase beta' subunit allosterically induces selective nontemplate strand binding by sigma (70). Cell, 105, 935-44.

YOUNG, B. A., GRUBER, T. M. & GROSS, C. A. 2004. Minimal machinery of RNA polymerase holoenzyme sufficient for promoter melting. Science, 303, 1382-4.

YU, C. & GENCO, C. A. 2012. Fur-mediated activation of gene transcription in the human pathogen Neisseria gonorrhoeae. J Bacteriol, 194, 1730-42.

ZHANG, J., KUMAR, A., WHEATER, M. & YU, F. S. 2009. Lack of MD-2 expression in human corneal epithelial cells is an underlying mechanism of lipopolysaccharide (LPS) unresponsiveness. Immunol Cell Biol, 87, 141-8.